ResearchOnline@JCU

JAMES COOK UNIVERSITY AUSTRALIA

This file is part of the following work:

Yan, Helen F. (2025) ***The growth and productivity of fishes through space and time.*** **PhD Thesis, James Cook University.**

Access to this file is available from:

https://doi.org/10.25903/ty4y%2D2z23

Copyright © 2025 Helen F. Yan

The author has certified to JCU that they have made a reasonable effort to gain permission and acknowledge the owners of any third party copyright material included in this document. If you believe that this is not the case, please email researchonline@jcu.edu.au

The growth and productivity of fishes through space and time

Submitted by

Helen F. Yan, B.Sc. (Hons.)

In fulfilment of the requirements for the degree of

Doctor of Philosophy

College of Science and Engineering

James Cook University

January 2025



Acknowledgements

While it seems conventional to acknowledge and highlight the invaluable support that I have received over the last three-and-a-half years of forming this thesis, there is an insurmountable amount of support that I have received that led me to this PhD journey for which I will try to do justice within the span of a few pages. For some (if not most), grad school can feel like a seemingly lonely and competitive journey to stand out, but I cannot believe how lucky I am to have worked with (and continue to work with) some of the most amazing and supportive people in the world.

First and foremost, I must thank my PhD supervisor, David Bellwood. Dave, I know it took some convincing from a number of people (i.e. Sterling and Simon) but thank you for taking a chance on the random shark imposter from Canada. Even though I was continually delayed from the pandemic, I still felt your support via conversations about lockdowns and everyday life from 12,000 km away. And while I feel like the majority of my degree was spent whingeing instead of actually working, those numerous complaints always transpired into fruitful conversations. Thank you for imparting your mad-scientist wisdom on me and allowing me the freedom to pave my own academic path. Even though I had a shark-infested final chapter, you still provided me with endless guidance and support over the years. For cultivating a creative and supportive PhD experience, while also embracing mediocrity, thank you.

To Orpha Bellwood, thank you for being our lab mum. Your bubbly personality and smile always brought cheerful energy into the lab, even on the cloudiest of days. Whether it was a new pack of sour squirms or foreign European chocolates, you always thought of us poor, hungry grad students. Thank you for fostering such a warm lab environment and making JCU our home-away-from-home.

To the various staff at JCU who helped me cross the finish line. To Garry Russ, thank you for being on my advisory team and helping me navigate university bureaucracies. Thank you to all the JCU staff who supported me through my candidature, especially Debbie Berry, Greg Suosaari, Glenn Ewels, Jodie Wilson, Janet Swanson, and Vivian Doherty. Also, a big thank you to the College of Science and Engineering for providing me with funding support and opportunities to present my work at multiple international conferences. While neither projects made it into this final thesis, I wanted to thank those that helped me with the logistics of conducting field work. From Lizard Island, I wanted to thank Dr Anne Hoggett and Dr Lyle Vail for all your help and support. To Jenni Calcraft from Orpheus Island, thank you for your support and for the fun chats.

To the Reef Function Hub past and present. I often reflect on how unbelievably lucky I was to go from one enigmatically supportive group to another. And yet, here I am. This group, that is, Christopher Hemingson, Alexandre Siqueira, Renato Morais, Sterling Tebbett, Robert Streit, Juliano Morais, Mike Mihalitsis, Isabelle Ng, William Collins, Pooven Muruga, James Gahan, Lucas Lutzenkirchen, Victor Huertas, Sam Swan, Casey Bowden, Caitlin Philipps, and Sam Crisp, is truly special. Thank you all for the coffee breaks, the scientific chats, the Friday beers, and much, much more. I need to give a special thanks to a handful of individuals from this group who were pivotal to my thesis over the last few years. To

Renato, thank you for all the insightful conversations around growth, productivity, biodiversity, and modelling. To Ale, thank you for flipping tables with me and teaching me about the black magic that is phylogenetic comparative methods. Here's to flipping more tables in the future. To Bert, thank you for the insightful conversations about biodiversity and life. To Mike, thank you for being my rock music/ABBA buddy and making my first trip to Lizard so memorable. To Victor, thank you for elevating my presentations from "mediocre" to "mediocre with great photos". To Sterling, I really owe you a lot. You convinced Dave to take me into his lab, you took me on my first trip to Lizard, you're one of the first people I turn to when I learn new and exciting stats, and you (almost) convinced me that looking at dirt is cool. Thank you for being a wonderful collaborator and an even better academic friend. To everyone, thank you for putting the *fun* in *Fun*ction Hub.

There are some specific people who have made Townsville really feel like home over the last few years. To Isabelle Ng, from drooling over delicious food to hanging out with your cats, thank you for all your love and support over the years. To Sam Swan, thank you for always loving a piping hot cup of tea and all your generosity. To Jess Cheok, thank you for bringing Singapore chili crab into my life and letting me hangout with Pacha. To Juliano, Dailanne, and Ben Morais, obrigado por todo o seu amor. To Olivia Lindsay and Paul Atteridge, thank you for all the nights of DnD. To Shannon and Luke Calleja, thank you for all the running and volleyball shenanigans. To the rest of my Monsoons family, thank you for bringing this washed-up player out of retirement for a few more years of glory.

When I finally started my PhD, I hit the ground running, but I could only run because others arduously had to hold my hand and teach me to walk. To my first academic mentors, Isabelle Côté and Nick Dulvy. Isa, you are my academic origin story. What started as me drunkenly telling you that you were (and still are, by the way) the coolest person that I've ever met in the world back in 2015, turned into nearly a decade of personal and academic growth. Although I didn't have the best grades in undergrad, you still gave me a chance and opened the door to an academic path for me. You kickstarted my career in so many ways, I am and will be forever grateful to you. Thank you.

Nick, you pushed me to be the scientist that I am today. From converting me into a shark person, to convincing me to give my first- and second-ever conference talks, to exposing me to the international conservation scene, to pushing me to learn difficult analytical techniques, you gave me the support and opportunities to learn how to be a scientist. Here's to more Smirnoff Ices, laughs, and collaborations in the future. Thank you.

To the rest of the Earth2Ocean research group, thank you for setting the bar so high for what a supportive and collaborative research group can be. From allowing me to deliver an epic monologue at IDEAS, to all the wonderful discussions in Statsbeerz, to all the lunchtime/brewery chats, thank you. Each and every one of you played pivotal roles in shaping my experience as a pseudo-grad student, that is: Brett Howard, Fiona Francis, Nicola Smith, Jillian Dunic, Melissa Orobko, Steven Brownlee, Jessica Edwards, Crystal McRae, Manon Picard, Rachel Munger, Lindsay Davidson, Serena Wong, Jessica Cheok, Nathan Pacoureau, Jenny Bigman, Rachel Walls, Wade VanderWright, Samm Sherman, Colin Bailey, Debora

Obrist, Allison Dennert, Kyle Wilson, Griffin Dare, Anna Potapova, Julian Gan, Jordan Hollarsmith, Rylee Murray, Nico Muñoz, and Dan Greenberg. I could go on and describe how each of these people have made my time and experience in E2O so unforgettable, but I'll limit it to just a few. Nicola, thank you for all the laughs and inspiration. Jill, thank you for showing me how soft of a scientific diver I am and for making my coding practices exponentially better. Steven, thank you for being my co-bully of Hannah. Lindsay, thank you for introducing me to the world of GIS and holding my hand through writing my first scientific paper. Serena, thank you for all the laughs and adventures we've had. Wade, thank you for being one of the funniest people I know. Kyle, thank you for opening the door to Stan for me. Also, thank you to both Christopher Brown and Sean Anderson whose big, analytical brains have helped me be a better quantitative scientist.

There are a few people that I met from E2O who have not only been wonderful colleagues, but even better friends: Simon Brandl, Danielle Derrick, and Hannah Watkins. Simon, thank you for being the first robot role model in my life and (also) convincing Dave to take me into his group. I know I can always count on you. From spirited conversations around ecological theory to nuking cryptos in Mo'orea to making the best gin and tonics I've ever had, thank you. Danielle, even when navigating the world of shark conservation and spatial statistics together, you always brought such a positive and loving energy throughout our time in E2O and in my life. I can always count on you to brighten up my day and always make me feel loved. Thank you for being such a great friend and (almost) sister.

Oh Hannah. Of course you need your own paragraph (really perhaps your own chapter). It's actually hard to describe how important you've been for just my thesis – the fact that you're in almost all of my acknowledgement sections (or authorship list) says it all really. I've built a bit of a reputation of being pretty good at statistics around here, but little does everyone know this is all because of you. Realistically, the only reason why I understand statistics and coding in Stan to the level that I do is because you've had to explain it to me. So, realistically my entire quantitative reputation and prowess comes from you – thank you. As for everything else, well, if you skip to the second-last paragraph of my general discussion, I think it really highlights what I think about you. Your view on life and nature is inspiring, especially to me. Thank you for both allowing me to be my most narcissistic self, while also grounding me when my head is getting too big (which happens all too often). I wouldn't be the human/robot that I am today if it weren't for you, my academic soul mate. Thank you. To the other Watkii, thank you for loving me more than your actual daughter.

To Ellen, Max, Myles, and Mackenzie Barkeley, and the entire Kett family, thank you for always making Australia feel like home, even 12,000 km away. You will always be my Australian family. Thank you.

To my childhood friends who have loved and supported me through the years and into our 30's regardless of which hemisphere I am living in: Tamara Donoghue, Brady Yano, Agata Kowalska, and Olivia Aguiar. To Nana, even though you're still the only friend to have ever sued me, thank you for always being that much crazier and more Type A than me through all these years. To Brades, from

peppering in the gym at Banting, to foam parties in Mexico, to memorising obscure facts in History 130, thank you for supporting me through every step of the way. To Aga, we've lived rather parallel lives – from studying together in undergrad, to avoiding the tap water in Bali, to moving to Australia for postgrad, to living in Sydney together, to having our weddings in 2024 – I am so grateful for you and your constant support. Thank you. To BB Livs, even from our early Math 154 days, you've always been an academic and athletic powerhouse, and I've always looked up to you. Thank you. Tam, Brades, Aga, and Liv: thank you for everything, I love you all. And, to all of your families: Paige, Peter, Kiera, Keely, Jordan, Lee, Susan, Lauren, Sam, Marty, Matt, Samia, Luis, and Veronica, thank you for making me a part of your families for all these years.

To the Beaudry family. Luc, Nathalie, Marc, and Patrick: thank you for welcoming me into your family and for always embracing curiosity.

To my actual family. To my dad, Sam, thank you for instilling a sense of pride in pursuing a career in science from a young age. To my mom, Yichun, you are the light of my life. Even through all your wonderful silliness, you've supported me in more ways than you know, through every step of the way. You have the biggest heart out of anyone that I know. Thank you. To my sister, Joyce, the first person I knew who wanted to be a marine biologist. Thank you for being my best friend along the way and my number one cheerleader. You are an incredibly fierce woman and I am so proud of you. To my brother, Art: thank you for being the big brother that I never had. To Callie and Nathan, you've made my Grinch heart grow two sizes larger. Thank you for showing me I had the ability to love more than just dogs – I hope you both continue to be curious about the natural world.

To my husband, Phil. It's impossible to put into words the endless support you've given me while I pursue my career dreams – even in a country full of spiders. You were willing to drop everything and move to all parts of the world for me to follow this crazy academic path. For that, and everything else that you do, I am eternally grateful. Thank you.

To all the people who love me unconditionally and continue to support me and my dreams, thank you.

Statement of the Contribution of Others

Throughout my candidature, I was supported by an Australian Research Council (ARC) Laureate PhD Scholarship and a Natural Sciences and Engineering Research Council of Canada Postgraduate Doctoral Scholarship. I also thank James Cook University and the College of Science and Engineering for providing additional financial support with a tuition waiver, SSA funds, and Competitive Research Grants. Field and research activities were also supported by an Orpheus Island Research Station Morris Family Trust Student Research Grant and an International Coral Reef Society Graduate Fellowship. While the projects were regrettably excluded from this thesis, I acknowledge and thank the Orpheus Island Research Station and the Lizard Island Research Station for providing field support throughout my candidature.

Supervision throughout my candidature was predominately provided by my primary supervisor, Prof. David Bellwood. The final chapter of my thesis (Chapter 5), however, was supervised by my collaborator Dr Alexandre Siqueira. Additionally, Chapter 2 titled: *The evolution of fast-growing coral reef fishes* was jointly written with Dr Alexandre Siqueira. As co-first authors, we contributed equally to this project. I collected the majority of the growth data with our collaborator Dr Renato Morais and ran all the models validating and predicting growth; Dr Siqueira ran the phylogenetic models. We wrote the first draft of the paper together and both contributed to the editing and response to reviewers.

Throughout my candidature, I was fortunate to work with so many wonderful collaborators. As mentioned above, Dr Alexandre Siqueira and I worked equally on Chapter 2; Dr Morais contributed to the conceptualization, data collection, and revisions of the manuscript; Prof. Bellwood contributed to the conceptualization and supervision of the project. In Chapter 3, Dr Hannah Watkins provided statistical support, while Dr Siqueira provided a genus-level phylogenetic tree. This project also benefited by comments from Dr Sean Anderson. I acknowledge the support from Sam Swan and Sophie Douglas who assisted with processing lab samples for Chapter 4. In Chapter 5, Dr Morais provided additional comments and edits to the manuscript. For chapters 2-5, Prof. Bellwood was the primary supervisor of the project and contributed substantially to the supervision, conceptualization,

funding acquisition, and revisions of the manuscript. Chapter 6 was done in collaboration with the primary investigators of the Global FinPrint Project, who have provided data on shark abundances: Drs. Colin Simpfendorfer, Demian Chapman, Euan Harvey, Michael Heithaus, Michelle Heupel, Aaron MacNeil, and Mark Meekan. This project also included the primary investigators of the Reef Life Survey project, Drs. Rick Stuart-Smith and Graham Edgar; previous members of the International Union of Conservation of Nature Species Survival Commission Shark Specialist Group, Dr Nicholas Dulvy and Wade VanderWright; and coral reef fisheries expert Dr Joshua Cinner. Finally, this project was conceived by Drs. Colin Simpfendorfer, Sterling Tebbett, Alexandre Siqueira, Prof. David Bellwood, and me. I collated the data, ran the models, and wrote the first draft of the manuscript. All authors have provided valuable comments and edits to improve the manuscript.

Statistical support throughout my candidature was predominantly provided by Dr Hannah Watkins. Additional statistical support was also provided by Dr Murray Logan through a two-week intensive statistics course and the Statsbeerz Group from the Earth2Ocean Research Group (specifically Drs. Dan Greenberg, Jennifer Bigman, Kyle Wilson, Sean Anderson, and Christopher Brown).

Abstract

Our industrialisation has fundamentally reshaped marine ecosystems. Dominant stressors of the Anthropocene are continuously reshuffling biological systems and impacting the energetic fluxes of marine communities. Human-driven impacts can negatively impact both the ecosystem functions and services provided by our oceans. Marine fishes lie at the forefront of delivering valuable these ecosystem functions and services. As major conduits of energy and matter, fishes simultaneously provide a wide range of valuable ecological functions, while also supporting the livelihoods of people via fisheries. Therefore, evaluating the environmental and socioeconomic impacts of human activities on fishes will be imperative if we wish to understand the future of marine ecosystems across human-dominated landscapes.

In this thesis, I have evaluated the energetic dynamics of fishes across three levels of functional organisation: the expression of life-history traits that underpin functioning, the expected function delivery via demographic processes, and the interactions among species when functions are lost. **Chapters 2** and **3** of my thesis addressed the ecological and socioeconomic drivers of growth, a fundamental life-history trait underpinning the productivity of marine fishes. The following two chapters (**Chapters 4** and **5**) applied estimates of growth in a demographic modelling framework to evaluate the ecological factors affecting the productivity of coastal fishes. Here, I applied a fisheries-independent method to estimate productivity (defined as the biomass arising via somatic growth of all surviving individuals in a community). The final chapter of my thesis (**Chapter 6**) evaluated the energetic consequences of human-altered predator-prey dynamics on coral reefs.

The first data chapter of my thesis (**Chapter 2**) laid the foundation by using a macroevolutionary approach to assess the evolution of growth across coral reef fishes. This chapter revealed that the evolutionary patterns towards faster growth trajectories were much more common than the evolution of slow growth trajectories, with the former largely concentrated in the Eocene (56-33.9 million years ago). The high global temperatures of the Eocene, paired with the subsequent habitat reconfigurations across coral reefs, were likely the primary factors leading to the evolution of faster growth rates across coral reef fishes.

While **Chapter 2** examined the growth of coral reef fishes across evolutionary time, **Chapter 3** drilled in on this theme to assess the global impacts of fishing and climate change on the growth performance of marine fishes over the last century. Here, I found a global pattern of decline in the growth performance of marine fishes, with the greatest declines in commercially valuable fishes. Across geographic regions, this pattern was only apparent in temperate regions, pointing to the dominance of commercially valuable fishes at higher latitudes. This chapter illustrated that the declines in growth performance likely reflect the legacy effects shaped by overfishing, which may mask the potential impacts of climate change.

By applying estimates of growth in a demographic modelling framework, **Chapters 4** and **5** measured the productivity of fishes across two different scales. In **Chapter 4**, I used a 26-year dataset of benthic reef fishes to identify multi-decadal trends in productivity on a degraded coral reef. Following the first mass coral bleaching event in 1998, there was a decline in species richness and a shift in community composition. Yet, the productivity of small benthic fishes remained remarkably constant through time, despite multiple environmental disturbances. Indeed, this newly formed community was able to maintain a steady level of fish biomass production for nearly three decades.

In **Chapter 5**, I applied ecological theory to assess whether biodiversity could bolster communities to produce higher levels of ecosystem functioning. By expanding the productivity framework from **Chapter 4**, I quantified the biomass production of fishes across roughly 3,000 sites around the world. In this chapter, I showed that Hill diversity emphasizing abundance effects outpaced the effects of species richness and community evenness. Indeed, abundance-emphasised diversity had a positive relationship with biomass production, that was characterised by a shift towards higher abundances and lower per-capita productivity with increasing diversity. This suggests that community productivity is metabolically limited by warmer temperatures.

Finally, **Chapter 6** explores the premise that species abundances are the primary drivers of ecosystem functions. The widespread depletion of sharks across the world's coral reefs suggests that sharks may no longer be capable of delivering ecosystem functions at biologically relevant levels. In this chapter, I assessed how the ecological structuring of coral reef communities was related to both

human pressure and shark abundances. Here, I found evidence of strong negative relationships between human pressures and reef fish biomass and abundance. Conversely, reef communities harbouring higher shark abundances were characterised by inverted biomass structures (i.e. disproportionally higher biomasses in larger size classes). Fisheries-induced declines in the abundance of sharks and fishes indicate that fisheries have fundamentally reshaped the biomass distribution of marine fish communities.

Throughout my thesis, I have highlighted the contrasting roles of environmental and anthropogenic impacts on the functioning of marine fish communities. From altering the expression of life histories to community-scale patterns of biomass distributions, my work has shown that human pressures are outpacing environmental factors by fundamentally reshaping the energetic fluxes of marine fishes. While the oceans are becoming increasingly impacted by multiple stressors, it appears that the prioritisation of conserving ecosystem functions in the Anthropocene is critical and will require the effective management of marine fisheries.

Table of Contents

Acknowledgements i
Statement of the Contribution of Others v
Abstract vii
Table of Contents x
List of Figures xiii
Chapter 1: General Introduction 2
1.1 The oceans of the Anthropocene 2
1.2 Fishes and functions 3
1.3 The renaissance of productivity 4
1.4 A game of growth 5
1.5 Thesis outlines and aims 7
Chapter 2: The evolution of fast-growing coral reef fishes 2
2.1 Introduction 11
2.2 Methods 13
2.2.1 Foundations of fish growth 13
2.2.2 Collating a dataset of reef fish growth 13
2.2.3 Predicting reef fish growth 14
2.2.4 Evolutionary regimes of reef fish growth 16
2.2.5 Evolution of allometry (growth and size) 19
2.3 Results 20
2.3.1 Evolutionary shifts in growth 20
2.3.2 Shifts in size and allometry 25
2.4 Discussion 27
2.4.1 Novelty in reef fish growth and size 27
2.4.2 A new energetic regime on coral reefs 29
2.4.3 Conclusions 31
Chapter 3: Over a century of global decline in growth performance of commercially valuable fishes 26
3.1 Introduction 35
3.2 Methods 36
3.2.1 Data collation and growth performance 36
3.2.2 Spatial and management regimes 38
3.2.3 Analyses 39
3.3 Results and Discussion 42
3.3.1 Global decline of growth performance 42
3.3.2 Overfishing is driving global declines 44
3.3.3 Geographic patterns reflect overfishing 48

3.3.4 Conclusion 51
Chapter 4: Multi-decadal stability of fish productivity despite increasing coral reef degradation 46
4.1 Introduction 55
4.2 Methods 57
4.2.1 Sampling protocol 57
4.2.2 Productivity calculations 58
4.2.3 Analysis 60
4.3 Results 62
4.3.1 Changes in productivity and proxies 62
4.3.2 Ecological thresholds 67
4.4 Discussion 70
Chapter 5: Species abundances surpass richness effects in global biodiversity-ecosystem function relationships 65
5.1 Introduction 75
5.2 Methods 76
5.2.1 Data collation 77
5.2.2 Predicting growth 79
5.2.3 Calculating productivity 80
5.2.4 Quantifying biodiversity 81
5.2.5 Analyses 82
5.3 Results and Discussion 84
5.3.1 Abundances skew global BEF 84
5.3.2 Mechanistic patterns of community productivity 90
Chapter 6: Humans outpace sharks as dominant predators on coral reefs 88
6.1 Introduction 98
6.2 Methods 100
6.2.1 Data collation 100
6.2.2 Spatially explicit models 102
6.2.3 Catch per unit effort 104
6.3 Results and Discussion 106
6.3.1 Human gravity outweighs shark abundances 106
6.3.2 Overfishing through coral reefs 113
Chapter 7: General discussion 108
7.1 Growth in an era of relentless change 117
7.2 Biodiversity and productivity: two sides of two different coins? 119
7.3 More data, more problems 122
7.4 The ghost of functions past: shifts without a baseline 123
7.5 The growth of a failed fish 126

References 119
Appendix A – Supplementary materials for Chapter 2 155
Appendix B – Supplementary materials for Chapter 3 169
Appendix C – Supplementary materials for Chapter 4 174
Appendix D – Supplementary materials for Chapter 5 180
Appendix E – Supplementary materials for Chapter 6 190

List of Figures

Figure 1-1. Theoretical descriptions of standardised growth parameters. 7
Figure 2-1. Phylogenetic reconstruction of reef fish growth. 22
Figure 2-2. The location and magnitude of growth regime shifts in the reef fish phylogeny. 24
Figure 2-3. Evolutionary regime shifts in the allometry between growth and maximum body length in reef fishes. 26
Figure 3-1. Distribution of 7,683 growth curves indicate a global decline in fish growth performance. 43
Figure 3-2. Changes in growth performance through time by management status. 47
Figure 3-3. Changes in growth performance and increasing ocean temperatures. 49
Figure 3-4. Global distribution of fisheries management. 50
Figure 4-1. Patterns of benthic reef fish productivity. 64
Figure 4-2. Patterns of abundance, standing biomass, and species richness. 66
Figure 4-3. The detection of ecological thresholds. 68
Figure 4-4. The effect of the 1998 bleaching event on community composition. 69
Figure 5-1. Variation in Hill diversity metrics on ecosystem function. 86
Figure 5-2. Global biodiversity-ecosystem function relationship (BEF) across marine fishes. 89
Figure 5-3. Deconstructing the BEF across geographic regions. 92
Figure 5-4. Temperature limits the BEF. 95
Figure 6-1. Anthropogenic impacts on reef fishes. 108
Figure 6-2. The dichotomy between sharks and human gravity on reef fishes. 112
Figure 6-3. Fishing down coral reef communities. 114

It is a curious situation that the sea, from which life first arose, should now be threatened by the activities of one form of that life. But the sea, though changed in a sinister way, will continue to exist; the threat is rather to life itself.

Rachel Carson
The Sea Around Us, 1961

Chapter 1: General Introduction

1.1 The oceans of the Anthropocene

Despite controversies surrounding the acceptance of the Anthropocene as a geological epoch (Lewis and Maslin 2015), it is indisputable that industrialised human activities have greatly impacted every ecosystem on Earth (Dirzo et al. 2014; McCauley et al. 2015). The world's oceans, which harbour 99.8% of the habitable volume on Earth (Dawson 2012), are at the forefront of modern industrialised change. From alterations in the geophysical properties of the water due climate change (Frölicher et al. 2009) to the elevated risk of fisheries-induced extinctions (Dulvy et al. 2003; Halpern et al. 2015), human impacts are manifesting throughout entire orders of ecological organisation. Indeed, anthropogenic climate change has caused shifts in the temporal synchrony of plankton blooms in the open ocean (Defriez et al. 2016), while simultaneously driving mass coral bleaching events across the world's coastal tropics (Hughes et al. 2017b; Sully et al. 2019). Despite many management efforts, some of which have been relatively successful (e.g. Hilborn et al. 2020; Pacoureau et al. 2023), many of the world's fisheries are still considered unsustainable, with the first recorded marine extinction due to unregulated fishing and coastal development announced just two years ago (Constance et al. 2023). With the universal reach of our destructive impacts on the marine environment, we as ecologists need to ask ourselves: are the oceans still functional?

Ecosystem functions are defined as the movement or storage of energy/materials through a system (Bellwood et al. 2019b). While resource pool metrics, or proxies of functioning, have been used to infer the state of various ecosystems (e.g. coral cover, standing biomass), functions describe the processes by which ecosystems arise and/or persist (e.g. calcium carbonate accretion, biomass production). Proxies rose in popularity due to the availability and relative simplicity in calculation, but they are often poorly linked to of their respective functions (Bellwood et al. 2019b; Morais and Bellwood 2020; Schiettekatte et al. 2022). For example, standing biomass has long been used as a measure of productivity, yet the two are often decoupled across numerous ecological systems (e.g. Bardach 1959; Morais et al. 2023). The mismatch between proxies and functions are likely due to their underlying design: proxies are a static measure of the resource pool at a specific time, whereas

functions measure the rates of accumulation and dissipation (Brandl et al. 2019b; Streit and Bellwood 2022). Because ecosystem functions quantify the underlying energetic fluxes in a system, they are the underpinning mechanisms that give rise to the valuable ecosystem services that people derive from the marine environment.

1.2 Fishes and functions

Across marine habitats, fishes are major conduits of energy and matter, making them critical contributors to ecosystem functioning (Bellwood et al. 2019b; Brandl et al. 2019b). For example, fishes play valuable roles in the bioerosion of calcium carbonate on coral reefs (Bellwood et al. 2003), nutrient provisioning via excretion (Francis and Côté 2018; Schiettekatte et al. 2020a), and are dominant contributors to predator-prey dynamics with high rates of biomass consumption (Mihalitsis et al. 2022) and mortality (Goatley and Bellwood 2016). The diversity of functions that fishes deliver likely owes to the even greater diversity in life-history traits expressed. Fishes' body sizes span many orders of magnitude, from < 5 cm for dwarf gobies (genus *Eviota*) to 8 m for the Giant Oarfish (*Regalecus glesne*) and 17 m for the world's biggest fish, the whale shark (*Rhincodon typus*). While the smallest fishes on coral reefs disproportionally support the functioning of reef communities (Brandl et al. 2019c), the largest fishes are globally targeted by fishers. Indeed, fisheries support the livelihoods of billions of people around the world by providing food and livelihood security. Given their ecological and socioeconomic importance, understanding the functioning of fishes will be critical in understanding how the oceans function in a human-dominated world.

While fishes perform a multitude of functions across seascapes, our ability to measure and quantify functions across large geographic regions is limited. For many functions, such as piscivory or herbivory, simply observing an individual on a survey does not necessarily equate to function delivery. For example, the spatial distribution of herbivory provided by fishes on a coral reef is highly concentrated within < 20% of the reef surface (Streit et al. 2019). Therefore, simply combining the abundance of herbivores with species-specific grazing rates, which are variable under different environmental and socioeconomic gradients (e.g. Fox and Bellwood 2007; Carlson et al. 2017; Price et

al. 2021), can disproportionally over- or under-estimate herbivory rates across coral reefs. There are other functions, however, that are under constant production, such as those relating to metabolic or demographic processes (Brandl et al. 2022). Indeed, the indeterminate nature of fishes' growth would imply that productivity-related functions are constantly transpiring and could be effectively measured and assessed across macroecological scales.

1.3 The renaissance of productivity

Ecological productivity is defined as the net gain of new biomass (West et al. 2001; Gillooly et al. 2002; Rogers et al. 2018a; Morais and Bellwood 2020). Given the inherent extractive nature of fisheries, understanding and quantifying the productivity of fish stocks has been the central dogma of fisheries science since the genesis of common stock assessment models (Hilborn and Walters 1992), such as surplus production models (Schaefer 1954, 1957) and age-structured population models (Beverton and Holt 1957). Simply put, stock assessment models are attempting to quantify the exploitation rates that maximise fisheries yields without driving fished stocks towards collapse (Hilborn and Walters 1992; Medley et al. 1993). These methods are analytically complex and economically costly; therefore, stock assessments are relatively concentrated across the world's wealthiest nations (Pauly et al. 2013), whereby each assessment is tailored towards a single species or subpopulation. Consequently, conducting stock assessments is outside the socioeconomic reach of many of the world's developing nations. The use of fisheries production models is further complicated across the world's tropics: coral reef fisheries target multiple species and are overwhelmingly data poor compared to temperate fisheries (Worm and Branch 2012). For the last half century, there was essentially no cost-effective method of implementing a universal method to calculate the productivity of all fishes across the globe.

In 2020, while the world (and my PhD journey) came to an abrupt halt from the COVID-19 pandemic, advancements in the quantification of fish community productivity soared. Two widely applicable methods were developed, each converting a suite of ecological and/or physiological traits into estimates of productivity from fisheries-independent surveys. The first method, developed by

(Schiettekatte et al. 2020a), used elemental stoichiometry and bioenergetics to quantify the elemental fluxes mediated by fishes across coral reefs. The authors defined productivity as the grams of carbon produced by the community. The second method, developed by (Morais and Bellwood 2020), used demographic models of growth and mortality to measure productivity as the biomass accumulated via somatic growth of surviving individuals in a given community. Although other methods to estimate productivity existed, such as using size-structured trophic models (e.g. Rogers et al. 2018b, 2018a) or individual age models (e.g. Depczynski et al. 2007), they were relatively context limited (Morais and Bellwood 2020). Therefore, the near-universal utility of bioenergetics or demographic modelling provided ecologists with new tools to quantify the productivity of fishes without extensive fisheries protocols.

Although both methods, that is, bioenergetics and demographic modelling, can provide insights into how individual traits scale up to community-wide processes, the latter holistically quantifies biomass, whereas the former only measures a single element. Indeed, the biomass production of fishes via demographic modelling has revealed that energetic shifts may be triggered by the loss of scleractinian corals (Morais et al. 2020). The biomass production of coral reef fishes has also been shown to buffer coral reef fisheries with more biomass than expected, providing a compensatory mechanism to sustain relatively overfished reefs and, thus, providing a direct link from systems to consumption by humans (Morais et al. 2023). Therefore, productivity measured as biomass production has both ecological and socioeconomic implications. The focus of my thesis was therefore centred around defining productivity as the biomass production arising via somatic growth and mortality (Morais and Bellwood 2020). With this new framework in hand, we can begin to disentangle the underlying drivers of this iconic ecosystem function.

1.4 A game of growth

Fishes exhibit an enormous range of life-history traits, all of which contribute to their capacities to deliver ecosystem functions. The productivity of fishes, however, is largely predicated on one trait in particular: growth (Morais and Bellwood 2018). Individual somatic growth, or the increase in body

mass throughout ontogeny, is a fundamental life-history trait that is linked with other traits such as body size, fecundity, and age at maturity (Healy et al. 2019; Wong et al. 2021). By balancing antagonistic metabolic processes (i.e. catabolism and anabolism), the growth of ectotherms, like fishes, is highly sensitive to changes in biotic and abiotic conditions (Sebens 1987; Arendt 1997; Heino and Kaitala 1999). Indeed, the growth rates between conspecifics has been relatively plastic to changes in biotic interactions, such as predator-prey dynamics or food availability (Abrams et al. 1996; Arendt 1997), and abiotic environmental conditions, such as rising temperatures (Gillooly et al. 2002). Growth rates are intrinsically linked with maximum body size, which is considered as a universal trait (Bellwood et al. 2019b), whereby a negative allometric relationship exists; consequently, changes in growth rates can also occur as a by-product of changes in body sizes (Gillooly et al. 2002; Brown et al. 2004). For example, the size-selective nature of fisheries has artificially induced selection pressures against larger body sizes in some fished stocks (Law and Grey 1989; Olsen et al. 2004; Jørgensen et al. 2007), resulting in populations truncated towards smaller body sizes and faster growth rates (Hutchings and Reynolds 2004; Anderson et al. 2008). There therefore appears to be two levels of functional organisation that are vulnerable to stressors: the expression of function-performing life-history traits and the function delivery themselves.

The interdependency between somatic growth and body size highlights a fundamental challenge in evaluating growth across scales. While von Bertalanffy equations are useful in distilling demographic characteristics into a handful of parameters, they are population/sub-population/stock specific and are thus difficult to compare across groups. However, standardising the von Bertalanffy growth parameter K against a uniform body size has allowed scientists to circumvent the co-dependencies between growth and body size to generate cross-scale comparisons. Regressing the $\log_{10}$ relationship between L_∞ and $\log_{10} K$ towards a common body size (where L_∞ = 1 cm) generates the growth performance index (sensu Munro and Pauly 1983; ϕ), which can be interpreted as the growth of populations constrained to a minimum body size. Conversely, extending the same linear relationship of $\log_{10} L_\infty$ and $\log_{10} K$ towards a species' maximum recorded body size would generate K_{max}, which can be interpreted as the growth trajectory of a population if the population grew to the

species' maximum reported size (sensu Morais and Bellwood 2018; Fig. 1-1). Although both growth performance and K_{max} are effectively different points along the same line, the two are decoupled from one another (Morais and Bellwood 2018), because of the different way each metric standardises for body size.

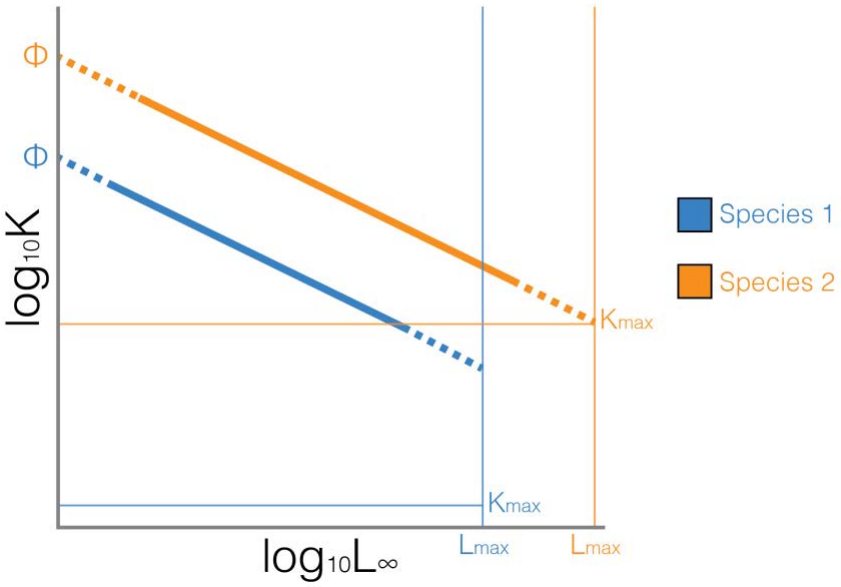

Figure 1-1. Theoretical descriptions of standardised growth parameters. *Growth curves from different species (blue and orange) that vary in their von Bertalanffy growth parameters K and L_{∞}. Regressing the line towards the y axis produces the growth performance index (ϕ), whereas regressing the line to the species' maximum reported body size (L_{max}) generates K_{max}. This figure has been adapted from (Morais and Bellwood 2018).*

1.5 Thesis outlines and aims

The productivity of fishes is a critical ecosystem function, representing the underlying energetic fluxes across the entire community with direct links to a valuable ecosystem service: fisheries. Therefore, the aims of my thesis were to explore the extrinsic and intrinsic factors affecting the productivity of the world's fishes. By leveraging large datasets, I have drawn evolutionary and macroecological insights to the functioning of fishes across three levels of ecological organisation: the expression of somatic growth (**Chapter 2** and **3**), the biomass production (**Chapter 4** and **5**), and the consequences when functions are lost (**Chapter 6**). In **Chapter 2**, I combined machine learning algorithms with

phylogenetic comparative methods to assess the evolution of growth rates across coral reef fishes using a measure of growth that standardises for body size. I also assessed changes in the allometric scaling relationship between growth and body size across the phylogeny. In **Chapter 3**, I conducted a systematic literature review comprising 2,886 growth studies performed on marine teleost fishes over the last century. I extracted all von Bertalanffy growth parameters to generate a standardised measure of growth, then used multivariate autoregressive state-space models to evaluate changes in growth over time across different geographic regions and management regimes. In **Chapter 4**, I applied demographic models of growth and mortality into estimates of productivity to evaluate the changes in productivity, abundance, standing biomass, and species richness of small benthic fishes over the last 26 years. Due to the non-linearities of time series, I also quantified ecological thresholds to detect significant shifts in functioning and related those shifts with large environmental disturbances. In **Chapter 5**, I expanded on the methods from **Chapter 4** to calculate the productivity of all fishes and evaluate whether there were internal regulatory mechanisms that could bolster functioning. I applied ecological theory with different measures of biodiversity to assess the biodiversity-ecosystem function relationship across geographic regions. Finally, in **Chapter 6**, I combined two of the largest reef-censusing programs in the world to assess the functional consequences of the loss of predators on reef fishes. In this chapter, I used size spectra analyses to compare the differences in the biomass distribution across reef fishes under different predator gradients.

Man selects only for his own good; Nature only for that of the being which she tends.

Charles Darwin
The Origin of Species, 1859

Chapter 2: The evolution of fast-growing coral reef fishes

Published as: Siqueira, A.C., Yan, H.F., Morais, R.A., Bellwood, D.R. (2023). The evolution of fast-growing coral reef fishes. Nature, 618 (7964), 322-327.

Abstract

Individual growth is a fundamental life history trait, yet its macroevolutionary trajectories have rarely been investigated for entire animal assemblages. Here, we analyse the evolution of growth in a highly diverse vertebrate assemblage, coral reef fishes. We combined state-of-the-art extreme gradient boosted regression trees with phylogenetic comparative methods to detect the timing, number, location, and magnitude of shifts in the adaptive regime of somatic growth. We also explored the evolution of the allometric relationship between body size and growth. Our results show that the evolution of fast growth trajectories in reef fishes has been considerably more common than the evolution of slow growth trajectories. Many reef fish lineages shifted towards faster growth and smaller body size evolutionary optima in the Eocene (56-33.9 Ma), pointing to a major expansion of life history strategies in this Epoch. Of all lineages examined, the small-bodied, high-turnover cryptobenthic fishes shifted most towards extremely high growth optima, even after accounting for body size allometry. In concert, these results suggest that the high global temperatures of the Eocene and subsequent habitat reconfigurations might have been critical for the rise and retention of the highly productive, high-turnover fish faunas that characterise modern coral reef ecosystems.

Keywords: evolutionary optima, fish growth, Ornstein–Uhlenbeck, productivity, Von Bertalanffy Growth Model, XGBoost

2.1 Introduction

Somatic growth, the increase in muscle-skeletal tissues during ontogeny, is a fundamental trait that drives animal life history (Healy et al. 2019; Wong et al. 2021). The variation in somatic growth rates across populations results from the allocation of finite resources to competing life history traits (i.e. growth, reproduction and survival) with the goal of maximising fitness (Stearns 1989; Charnov and Berrigan 1991; Dmitriew 2011; Healy et al. 2019). Because growth rates are optimized rather than maximized, suites of life history strategies evoking several solutions to the same problem co-evolved with one another and are thus correlated. These clustered traits place species along a fast-slow axis of variation in life histories, whereby species at one extreme exhibit faster growth and reproductive rates, smaller sizes, and earlier ages at maturity compared to species at the slow end of the axis (Ricklefs and Wikelski 2002). Consequently, growth trajectories are intrinsically linked with other life history parameters, most notably with maximum body size (Brown et al. 2004). Species tend to grow quickly to a smaller maximum size compared to those that grow slowly to a larger maximum size (e.g. Jennings et al. 1999). These composite life history traits (i.e. life history traits correlated with other life history traits), such as growth, can thus be good proxies to characterise a species' life history strategy, which is crucial for ecosystem and population assessments (Reynolds 2003; Thygesen et al. 2005; Wong et al. 2021).

Life history strategies likely co-evolved in response to local biotic and abiotic conditions (Arendt 1997; Heino and Kaitala 1999). Therefore, the evolutionary trajectories of composite life history traits can be indicative of both the underlying processes that shaped past ecosystems and the impacts of these ecosystems on modern taxa. Somatic growth rates have been shown to be relatively plastic between distinct populations of conspecifics, changing in response to the duration of growth seasons (e.g. Caley and Schwarzkopf 2004; Lindgren and Laurila 2005), food availability (e.g. Arendt 1997), and predator-prey interactions (e.g. Abrams et al. 1996; Arendt 1997). Consequently, large-scale changes in environmental and ecological conditions should be mirrored by the expression of different growth strategies. Coral reefs, which are highly productive ecosystems, exhibited a drastic compositional change 33.9-5.3 million years ago (Ma) during the Oligocene–Miocene with the

diversification of both corals and reef-associated fishes (Santodomingo et al. 2015; Bellwood et al. 2017; Siqueira et al. 2020). As fishes expanded into new habitats and exploited new food resources, faster life histories arose with the diversification of small, high-turnover reef fishes (Bellwood et al. 2017). Given the disproportionately large energetic contribution of these fishes to modern coral reefs, specifically the cryptobenthic and planktivorous taxa (Brandl et al. 2019c; Morais et al. 2021), it appears that the iconic productivity of today's reefs may have arisen, at least in part, from the expansion of faster reef fish growth trajectories.

Although many studies have assessed the evolutionary patterns of specific life history trade-offs that included growth (e.g. Charnov and Berrigan 1991), as well as the evolution of certain growth strategies (e.g. Frýdlová et al. 2020), none have directly addressed the evolution of growth trajectories for an entire animal assemblage. Here, we assess the evolution of growth trajectories across a diverse assemblage of vertebrates displaying a wide range of life histories: coral reef fishes (Bellwood and Wainwright 2002; Depczynski and Bellwood 2006). Despite sharing a common habitat, coral reef fishes span over seven orders of magnitude in body mass (Morais and Bellwood 2019) and thus exhibit a large diversity of growth trajectories (Morais and Bellwood 2018). Unsurprisingly, growth is a dominant life history trait for fishes and has been used to explain variations in physiological processes (Wong et al. 2021), large-scale spatial distributions (Beukhof et al. 2019), and relative extinction risks (Denney et al. 2002). Given its key role for determining the critical ecosystem process and service of biomass production on coral reefs (Morais and Bellwood 2020), we mostly focus our analyses on growth, but we also explore its intrinsic correlation with body size. To assess coral reef fish growth from an evolutionary perspective, we first calculate a standardised, composite metric summarising growth trajectories at the species level and apply a robust, predictive framework to estimate values for unsampled species. We then use a comparative phylogenetic framework to assess how growth rates and body sizes have evolved through time across coral reef fish lineages. We hypothesise that the evolution of faster life histories would have coincided with the expansion of lineages during the Oligocene–Miocene (Bellwood et al. 2017) and that this was essential for the energetic composition of today's coral reef fish assemblages.

2.2 Methods

2.2.1 Foundations of fish growth

To calculate the growth in coral reef fishes, we adopted the framework developed by Morais and Bellwood (2018), standardising parameters derived from the Von Bertalanffy Growth Model (VBGM; Von Bertalanffy 1949). The VBGM has been applied to thousands of fish species and has been used in both ecology- and fisheries-related studies to model the ontogenetic growth of fishes. In short, the VBGM reflects a balance between the two metabolic processes affecting growth: anabolism, the production of body materials, and catabolism, the consumption of body materials. By integrating both anabolic and catabolic processes into the VBGM, we can derive the growth parameters L_∞, which reflects the average asymptotic size of the population, and the von Bertalanffy growth coefficient K ($year^{-1}$), which is indicative of the mean rate at which the population approaches the population asymptotic size (L_∞). Both L_∞ and K are sensitive to the methodology used and can have different interpretations at the individual or population level, which can be problematic for cross-scale studies such as this one (Morais and Bellwood 2018). To circumvent these issues, we standardised K to the maximum body size (i.e. length) recorded for each species to generate theoretical projections of fish growth that are comparable across species. This process then generates a composite, standardised life history trait, which encapsulates the trade-off between maximum size and growth. Following Morais and Bellwood (2018), we also directly considered the ageing 'method' used to collect the size-at-age data fitted by the VBGM in each case as a variable in our predictive model (see below).

2.2.2 Collating a dataset of reef fish growth

We first conducted a systematic review of the recent, published literature (from 2019 to June 2021) on coral reef fish growth to build upon the dataset created by Morais and Bellwood (2018). Our search mirrored the same criteria as Morais and Bellwood (2018), including 49 different families, 46 of which are listed as reef fishes in Bellwood and Wainwright (2002). For each species, we recorded the maximum length, the method by which length was measured [i.e. total length (TL), standard length (SL), or fork length (FL)], the aging method, the von Bertalanffy growth parameters L_∞ and K, and,

when available, the length-weight conversion factors *a* and *b*. We converted all estimates of maximum size and L_∞ to TL using the length-length conversion factors from FishBase (Froese and Pauly 2021). Using the same quality checks as Morais and Bellwood (2018; see Supplementary methods), we added an additional 58 growth curves to the dataset for a total of 1,979 growth curves, belonging to 596 species.

We used collated values of L_∞ and K to calculate standardised, theoretical projections of growth for each species (cf. Morais and Bellwood 2018). We calculated K_{max} (unit year^{-1}) as the rate that fishes would reach their asymptotic size L_∞ if they grew to the maximum reported size for that species (L_{max}; see Morais and Bellwood (2018) and supplementary methods for equations). This metric can thus be intuitively thought of as the number of maximum body lengths attainable via growth in a year. Unlike the growth performance index (ϕ; Pauly 1979; Morais and Bellwood 2018) that offers a similar standardisation solution, K_{max} is readily interpretable biologically, and therefore will be the focus of this work. We used the same procedures to model K_{max} as a function of environmental and ecological variables as Morais and Bellwood (2018), which included georeferencing the growth curve and extracting mean sea surface temperature for each new record and classifying each new recorded species according to their diet and relationship to the reef. We also recorded the aging methods used to obtain the size-at-age data used to fit the VBGM in each study. The detailed procedures used to assert geographical coordinates and extract temperature data, as well as the exact definitions of each categorical variable can be found in Morais and Bellwood (2018).

2.2.3 Predicting reef fish growth

We used temperature, maximum size, diet, position, and method in an extreme gradient Boosted Regression Tree (BRT) to predict K_{max} for all the species in the molecular phylogeny of Rabosky et al. (2018) for which there are no empirically measured growth data. Data from these predictors have been obtained from Morais and Bellwood (2018), and were originally sourced from literature sources and FishBase (Froese and Pauly 2021). BRTs are a form of machine learning that combines multiple

decision trees with a boosting algorithm and can achieve a high predictive accuracy (Elith et al. 2008). Unlike other statistical models, BRTs are not restricted by nonlinear relationships, complex interactions, nor missing data and can handle collinear variables (Elith et al. 2008). We used the `XGBoost` (v.1.4.1.1) package (Chen et al. 2018) in R (v.4.1.0) due to its superior performance in controlling for overfitting and faster speed compared to other packages (Chen and Guestrin 2016; Mitchell and Frank 2017).

Using a Gamma distribution to model K_{max}, we selected hyperparameters mirroring the two-step tuning method done by Morais and Bellwood (2018). We first selected hyperparameters by varying the learning rate (eta), the regularizing parameter gamma, the maximum tree depth, and the subsample rate by choosing the combination of values which minimized the negative log likelihood. We then varied the values from the first step by drawing values from a normal distribution, truncated to ± 10% of each hyperparameter value. Using this two-step approach, we were able to reduce the negative log likelihood from 2.0 to 1.77 using the following hyperparameter values: eta = 0.19, gamma = 0.46, maximum tree depth = 5, and subsample rate = 0.75.

To model and predict K_{max}, we used a cross-validation approach by building the model on a training set (= 80% of the data) and assessing the model's performance on the remaining test set (20%). We assessed model performance by measuring the average bias of the model by subtracting the predicted K_{max} values from the observed in the test set, whereby a well-fitted model should have a bias close to zero. We also measured model performance by fitting a linear model through the log-log transformed predicted-observed K_{max} values and extracted the corresponding R^2. Finally, we used the model to predict the K_{max} values for fishes that were found in the phylogeny but were missing empirically measured von Bertalanffy growth parameters. Overall, empirical and estimated values were evenly distributed across taxonomic groups (**Appendix A**: Fig. A1a), body sizes (**Appendix A**: Fig. A1b), and temperatures (**Appendix A**: Fig. A1c). Due to the stochastic model-building process of BRTs, we bootstrapped each iteration 1,000 times and used the mean predicted K_{max} value across all iterations. Model diagnostics can be found in **Appendix A**: Fig. A2-A3.

2.2.4 Evolutionary regimes of reef fish growth

From the total of 596 species with empirical growth data, 525 were present in the phylogenetic tree of Rabosky et al. (2018). Another 1,949 species from the selected reef-associated fish families were also present in the tree but had no associated growth data. After adding the K_{max} values predicted by the BRTs for these species, we ended up with a dataset containing 2,474 species for which we had both phylogenetic and growth data (empirical and predicted). We only used the time-calibrated phylogeny of Rabosky et al. (2018) that was built using genetic data in the main results to minimize issues with topological uncertainty in the ancestral state reconstructions. However, we repeated the analyses using the backbone (see details below) of the most recent phylogenomic tree of spiny-rayed fishes by Ghezelayagh et al. (2022; findings presented in the **Appendix A**: Extended Data). Our first goal with the phylogenetic reconstructions was to detect the location, timing, number, and magnitude of shifts in the adaptive optima of K_{max} values along the reef fish phylogenetic tree. To that end, we used the `bayou` R package v.2.2.0 (Uyeda and Harmon 2014) to fit multi-optima Ornstein–Uhlenbeck (OU) models of continuous trait evolution. This package uses a Bayesian reversible-jump method to identify significant shifts in the evolutionary regime of a continuously distributed trait, without the need to specify any *a priori* hypotheses about the location of these shifts in the phylogeny (Uyeda and Harmon 2014). The main parameters estimated for the OU regime describe the rate of adaptation (α), the magnitude of uncorrelated diffusion per unit of time (σ^2), and the optimum trait value (θ) associated with each regime shift (Uyeda and Harmon 2014). For our models, we set half-Cauchy priors for α and σ^2, and a normal prior for θ (with mean and standard deviation defined by the full dataset of K_{max} values). In addition, we assigned a conditional Poisson prior for the number of shifts, with the maximum number of possible regime shifts equal to half the number of tips in the phylogeny. We also used the average bias estimated by the BRTs as an indication of the potential measurement error associated with K_{max} values in the models. Finally, we set a maximum of one shift allowed per branch, and equal probability of shifts across all branches in the tree. We ran two independent Markov Chain Monte Carlo (MCMC) chains, each with a random starting point, to assess whether models were converging toward similar solutions. Each chain was run for ten million generations, sampling

parameters every 1,000 generations. Convergence was evaluated through the effective sample sizes of all parameters, after discarding the first 30% samples of each chain as burn-in. All K_{max} values were $\log_{10}$ transformed before the analyses to reduce the extreme skew towards low growth values.

We combined the results from both MCMC chains to assess the locations of the most likely shifts in the evolutionary optima of K_{max}. Only shifts detected with 75% posterior probability were considered in our main results. Typically, studies applying this model use a lower threshold for the detection of shifts, around 30% posterior probability, which already represents thirty times the set prior probability. However, we used the conservative approach of 75% to reduce the chance of finding spurious regime shifts given the large size of our phylogenetic tree. Using an extremely conservative posterior probability of 90% reduces the number of shifts detected but does not change our overall temporal patterns (**Appendix A**: Fig. A4). We also excluded three branches that passed the posterior probability criteria, but had three or fewer descendant species, which can also produce spurious regime shifts. Although the MCMC chains were very consistent in identifying which branches had regime shifts in the evolutionary optima of K_{max}, the precise location of the shift along the branch is hard to estimate. Therefore, to standardise across regime shifts, here we report shift locations as the nodes representing the most recent common ancestor of all descendants of the branch identified by the model. In other words, we consider specific locations as the crown age of regime shifts. After detecting these shifts, we calculated their probabilities after accounting for the span of possible locations where they could occur along the tree at each geologic Epoch. We did this by dividing the sum of shifts found per Epoch by the total branch length in the same time period, calculated using the `phytools` R package v.1.0.3 (Revell 2012).

After applying the necessary filters to the multi-optima OU model derived from `bayou`, we compared it against a single evolutionary optimum (single-optimum OU) model or a Brownian motion (BM) model to assess whether these simpler models might represent a better fit to our data. This analysis was performed using the `mvMORPH` R package v.1.1.4 (Clavel et al. 2015), which requires an *a priori* definition of regime shift locations in multi-optima OU models. Therefore, we used the shifts detected through `bayou` in the maximum likelihood framework of `mvMORPH` to perform our model

comparison. The multi-optima OU model was detected as having a far better fit when compared to the single-optimum OU and the BM models ($\Delta AICc > 20$; **Appendix A**: Table A1).

We followed the exact same modelling procedures described above to run the `bayou` model with species maximum body length (body size) as input instead of the growth coefficient. This was done to assess whether the results found for growth would be similar to the ones found for body size (**Appendix A**: Extended Data Fig. 4). Importantly, our intention here was not to tease apart the effects of growth independent of body size, given how strongly correlated these traits are. In addition, we assessed the sensitivity of our growth results against an alternative dating scheme based on the recent phylogenomic analysis of Ghezelayagh et al. (2022). This tree was inferred using ultraconserved elements and sampled the majority of spiny-rayed fish families, including the ones analysed herein. However, it had a substantially lower species level sampling when compared to Rabosky et al. (2018). Therefore, to be able to have the same dense sampling as the latter, we used the congruification (Eastman et al. 2013) approach, as implemented in the `geiger` R package v.2.0.9 (Harmon et al. 2008). This method uses a reference phylogeny to time-calibrate a target tree based on shared nodes of higher taxa. We thus selected all nodes that were concordant between the Rabosky et al. (2018) and the Ghezelayagh et al. (2022) trees at the genus level to generate our reference chronogram. We then applied the method of congruification to include all the tips from the target tree (Rabosky et al. 2018) and generate an input with time calibration points for subsequent use in treePL (Smith and O'Meara 2012). Through this algorithm, we finally estimated divergence times in the target tree based on the reference calibration points from Ghezelayagh et al. (2022), using its penalized likelihood approach. Importantly, although we followed the best practices for this type of analysis (i.e. performing priming to select the best optimization parameters and selecting the best smoothing value from a cross-validation analysis; Smith and O'Meara 2012), the calibration scheme generated divergence times that are at odds with the fossil record. For example, the origin of Apogonidae in the new chronogram is estimated at ~43 Ma, however, there are fossil apogonids described from ~50 Ma (Bannikov 2008). The family Chaetodontidae has its crown estimated at ~17 Ma, while the oldest fossil within this family is ~33 Ma (Marramà et al. 2016). The crown Pomacentridae gets dated at ~28 Ma, which is far

from the oldest described fossil from the Paleocene or from multiple examples from the Eocene (Cantalice et al. 2022). Because of these inconsistencies, we kept the phylogeny of Rabosky et al. (2018) as our main chronogram of analysis and we used the sensitivity analysis described herein as a likely representation of the youngest possible limit of uncertainty around the estimated timing of shifts in our main results.

2.2.5 Evolution of allometry (growth and size)

As expected by theoretical models (Brown et al. 2004), the growth coefficient K_{max} is strongly correlated with species maximum body size in reef fishes (Morais and Bellwood 2018). Therefore, we were also interested in assessing whether there is any evidence of shifts in the evolutionary regime of the allometric relationship between these two variables. We approached this question by applying the recently developed mixed Gaussian phylogenetic model (MGPM; Mitov et al. 2019). This model accounts for the heterogeneity of the evolutionary processes operating in different parts of the tree and jointly infers different types of Gaussian models (i.e. BM and OU) to each of the distinct evolutionary regimes detected (Mitov et al. 2019). The MGPM represents a state-of-the-art phylogenetic model of trait evolution and was specifically designed to detect changes in evolutionary regimes of allometric relationships (Mitov et al. 2019). However, given its computational complexity, it is difficult to achieve convergence for this model when using large phylogenetic trees, such as the one used here.

To be able to run the MGPM with our dataset, we first pruned our reef fish tree to the genus level, which resulted in a phylogeny contained 602 tips. We then summarised both maximum body length and K_{max} as the $\log_{10}$ transformed values at the most recent common ancestor node of each genus, calculated through ancestral state reconstructions. These reconstructions were performed using the *fastAnc* function from `phytools`. For monotypic genera we used the trait values from the only species within each genus. We then used the `PCMBase` (v.1.2.12) and `PCMFit` (v.1.1.0) libraries in R (Mitov et al. 2019, 2020) to fit the six default models of allometric trait evolution to our data. These models are detailed in Mitov et al. (2019), but in short, they include combinations of global BM and OU models in which traits are either uncorrelated or correlated in different ways (for more details, see

Appendix A: Table A2). After fitting these six models, we fit the MGPM model, which was built to detect nodes along the tree with shifts in the evolutionary regime of the allometric relationship between maximum body size and K_{max}. Finally, we performed model comparisons, which demonstrated strong support for the MGPM when compared to the six default models ($\Delta AICc > 20$; **Appendix A**: Table A2). After finding the MGPM as the best-fit evolutionary model for the relationship between maximum body length and K_{max} in reef fishes, we assessed the location of regime shifts along the phylogenetic tree (**Appendix A**: Extended Data Fig. 5). Each shift is associated with a specific Gaussian process, from which we extracted the respective slopes and the intercepts for the allometric relationship from the MGPM model output.

2.3 Results

2.3.1 Evolutionary shifts in growth

Our boosted regression tree analysis had a high predictive accuracy and was used to predict the standardised growth coefficient K_{max} for reef fish species without empirically measured data (see **Appendix A**: Supplementary results). Derived from the Von Bertalanffy growth coefficient K, K_{max} represents the rate at which individual fishes would reach their asymptotic size if they grew to the maximum reported size for that species (unit $year^{-1}$; Morais and Bellwood 2018). By placing K_{max} values in a phylogenetic context (Rabosky et al. 2018), we found a striking pattern of regime shifts throughout reef fish evolution. Our multi-optima Ornstein–Uhlenbeck (OU) models (Uyeda and Harmon 2014) detected 20 evolutionary regime shifts with high confidence (i.e. occurring in 75% of posterior samples; see Methods) across the reef fish phylogeny. Of the 20 shifts detected, 19 occurred toward higher (i.e. faster) growth evolutionary optima, and in only one instance did it shift towards a lower optimum K_{max} value (**Fig. 2-1**). Using a less conservative threshold of detection (50% of posterior samples), we found two additional shifts toward lower K_{max} values, however, ten more shifts toward high growth are also identified (**Appendix A**: Extended Data Fig. 1). In combination with the ancestral state reconstruction (**Fig. 2-1**), these results suggest that the evolution of growth coefficients in reef fishes had a strong directionality towards faster growth rates (**Appendix A**: Extended Data Fig.

2). Although extant species cover a large range of growth coefficient values, evolutionary novelty mainly occurred at the higher end of the spectrum. In other words, departures from the ancestral evolutionary regimes in reef fish growth almost always happened toward faster growth rates.

The timing of evolutionary regime shifts in growth is also disproportionally concentrated, with most occurring in the Eocene (56-33.9 Ma), peaking at about 47 Ma (**Fig. 2-1**). When controlling for the total branch length per Epoch, we found more positive shifts on the Paleocene/Eocene (**Fig. 2-1** inset). We also found similar patterns when we used an alternative chronogram (Ghezelayagh et al. 2022; see Methods), with a higher probability of shifts occurring in the Eocene, despite some shifts being found in more recent times in the Oligocene/Miocene (**Appendix A**: Extended Data Fig. 3). Most remarkably, in our main analysis, we detected only one shift in the entire Neogene (i.e. Miocene, Pliocene, and Pleistocene, from 23 to 2.6 Ma) a period when most lineages appeared and when the confidence of phylogenetic reconstructions and inference is maximal. There were no detectable changes in the last 18 million years. The only regime shift towards a lower growth optimum in reef fishes was detected well before the Cretaceous-Paleogene (K/Pg, 66 Ma) boundary, at about 100 Ma (**Fig. 2-1**).

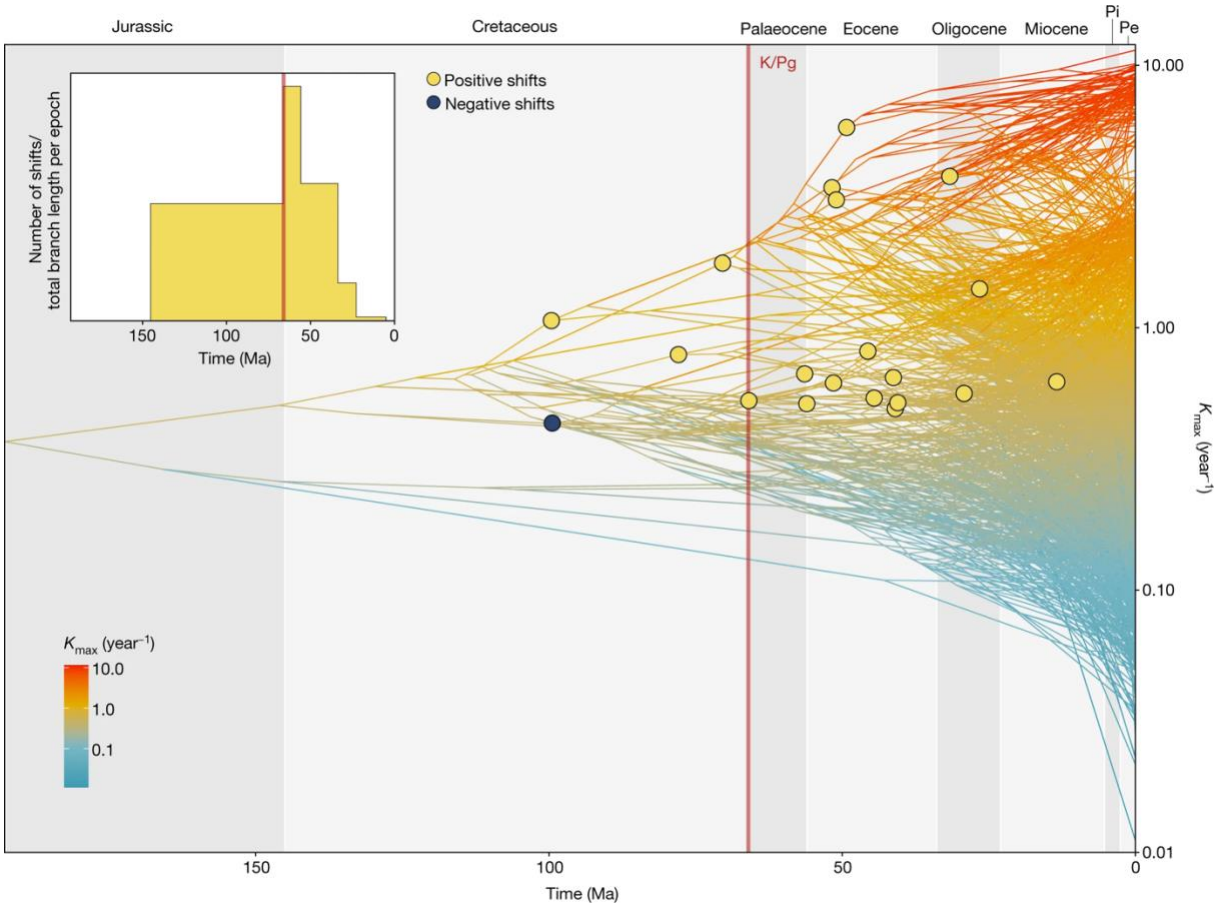

Figure 2-1. Phylogenetic reconstruction of reef fish growth. *Standardised growth coefficient (K_{max}) reconstructed through time across the phylogenetic tree of coral reef-associated fishes (n = 2,474). The points represent estimated shifts in the evolutionary regime of growth detected through multi-optima OU models. The light-yellow points represent shifts towards higher values of evolutionary optima (faster growth rates), whereas the dark blue point represents the opposite. Note that the y axis is shown as a log_{10} scale. Inset: the number of positive shifts divided by the total branch length in the phylogeny per geological epoch (y axis) through time (x axis). This metric gives an indication of the probability of shifts controlled by the availability of locations for them to occur. The red line represents the K/Pg boundary. Pe, Pleistocene; Pi, Pliocene.*

From a taxonomic perspective, evolutionary regime shifts in growth are spread throughout the reef fish phylogeny. Although some species-rich families, like Acanthuridae, Labridae (without Julidini), Carangidae, and Mullidae, were found to retain the root evolutionary growth regime (**Fig. 2-2**), many other speciose groups displayed regime shifts. The oldest shifts occurred at the base of larger clades, such as the Gobiaria (Gobiiformes and Apogonidae), and the crown group that now encompasses typical coral reef families like Serranidae, Lutjanidae, Chaetodontidae, and Pomacanthidae. Interestingly, this latter evolutionary shift was towards a lower evolutionary optimum growth value. Multiple groups nested within this large, slower-growing clade subsequently exhibited a secondary shift towards higher growth optima, such as the Chaetodontidae, the Nemipteridae, and the Anthiinae serranids (**Fig. 2-2**). However, the highest magnitude of change in growth evolutionary trajectories occurred at the base of clades that contain small-bodied, cryptobenthic reef fish groups. Both the Gobiaria, and the Ovalentaria (including Blenniidae, Tripterygiidae, and Pomacentridae), presented shifts toward extremely high median evolutionary optima in K_{max} (**Fig. 2-2**). Subsequent shifts within gobies cumulatively led to the highest growth optimum detected in the reef fish tree, with an over 20-fold estimated increase from the root optimum in the clade containing the genera *Eviota*, *Gobiodon*, and *Paragobiodon*.

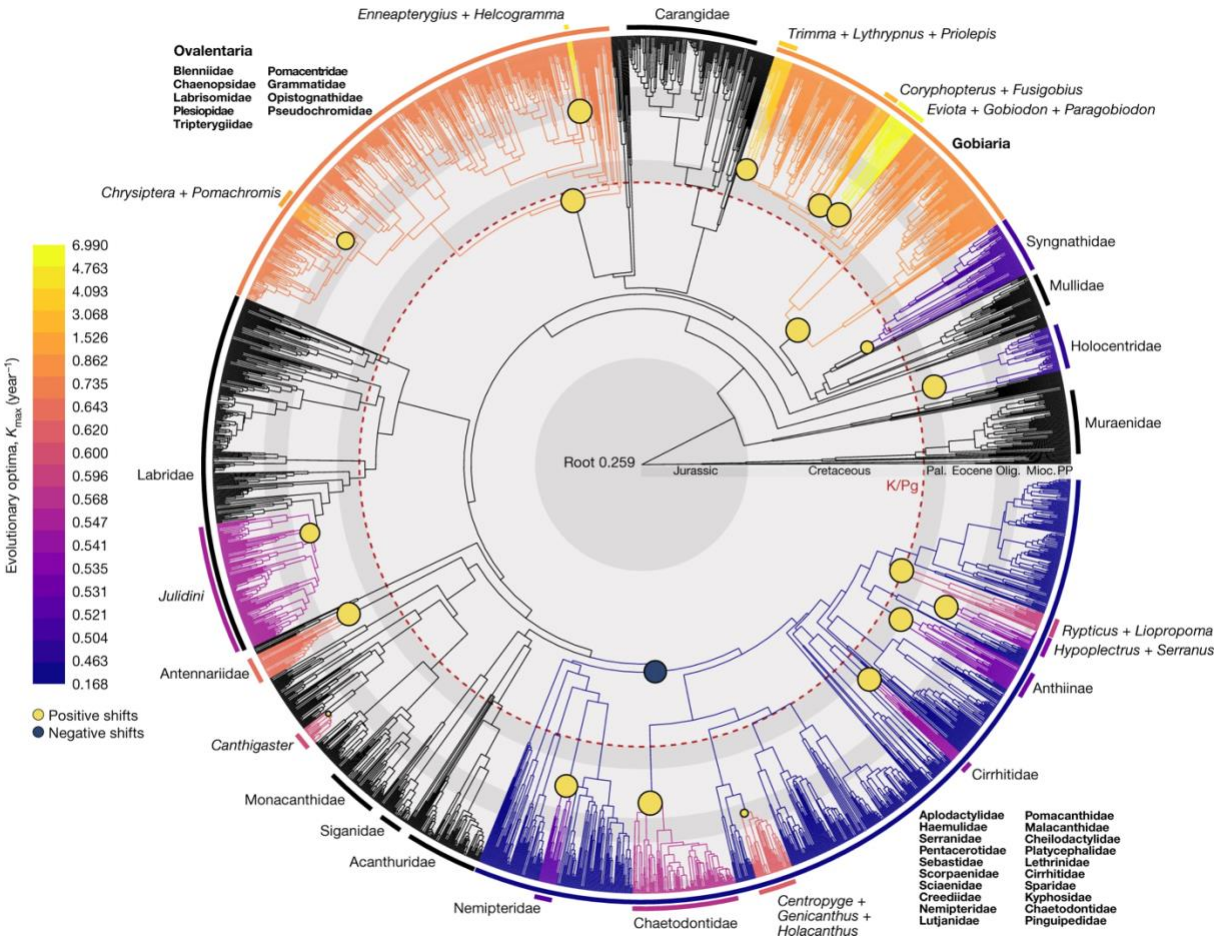

Figure 2-2. The location and magnitude of growth regime shifts in the reef fish phylogeny. *Branches and external arcs are discretely coloured according to the estimated value of the median evolutionary optimum in growth that clades shifted towards. The black branches represent lineages without any detectable shift in evolutionary optimum of growth. The points on the nodes represent the same shifts depicted in* ***Fig. 2-1****; that is, shifts towards higher K_{max} values (light yellow) and shifts towards a lower K_{max} values (dark blue). The size of the points is scaled according to the posterior probability of the shift. The red dashed line represents the K/Pg boundary. Mioc, Miocene; Olig, Oligocene; Pal, Palaeocene; PP, Pliocene–Pleistocene.*

2.3.2 Shifts in size and allometry

After finding frequent and strong shifts in growth coefficients throughout reef fish evolution, we investigated whether these shifts would also be observed in body size (measured here as maximum body length) and in the allometric scaling relationship between growth and size among species. Our multi-optima OU model using body size revealed an inverse reflection of the growth results (**Appendix A**: Extended Data Fig. 4), i.e. there was an accumulation of shifts toward smaller body sizes in the Eocene, highlighting the inversely correlated nature of these two life history traits. In the case of size, however, we found more shifts toward higher values spread throughout the tree (**Appendix A**: Extended Data Fig. 4), indicating that not all instances of evolution of larger body sizes were accompanied by the evolution of slower growth rate optima.

To explore the allometric relationship between size and growth, we applied a mixed Gaussian phylogenetic model (Mitov et al. 2019) using the genus-level reef fish phylogeny (see Methods). This model detected a total of five evolutionary regime shifts in the allometric growth scaling through time (**Appendix A**: Extended Data Fig. 5). All regimes were associated with distinct OU models, therefore, each shift had different evolutionary optima for the coefficients of the relationship between growth and size. The root allometric scaling state was retained through time in families like Carangidae, Mugillidae, Holocentridae, and Mullidae (**Fig. 2-3a**; **Appendix A**: Extended Data Fig. 5). All subsequent shifts from that root allometry detected by the model represented a steepening of the slope (i.e. becoming more negative **Fig. 2-3b-f**). In alignment with the ancestral-state reconstruction results, two of the most extreme allometric shifts happened in the main cryptobenthic clades: the Gobiaria (slope = -1.4), and the Ovalentaria (slope = -1.31; **Fig. 2-3d** and **f**). Hence, these two non-related reef fish lineages represent major evolutionary departures from the typical allometry, with species growing substantially faster than predicted by their maximum body length. Interestingly, although the clade containing the families Lethrinidae, Nemipteridae, Sparidae, and Malacanthidae is generally composed of larger-sized species, it has also been identified as having a substantially steep allometry (slope = -1.37; **Fig. 2-3e**).

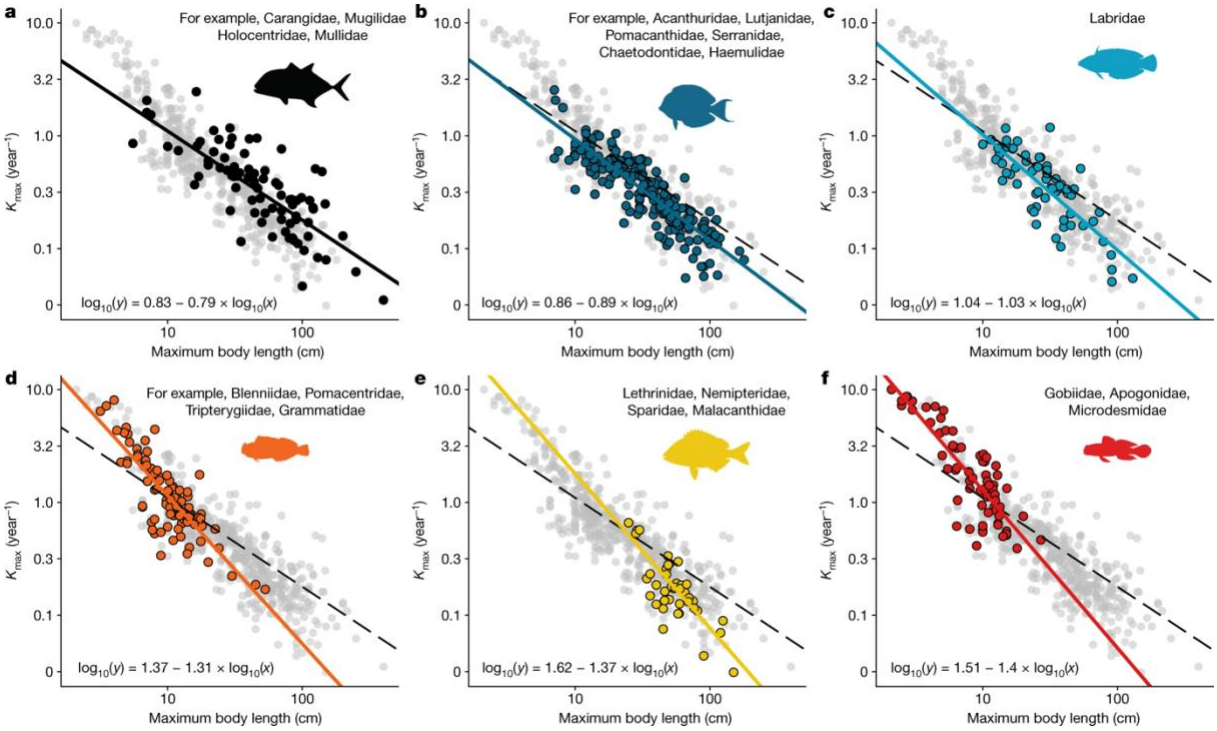

Figure 2-3. Evolutionary regime shifts in the allometry between growth and maximum body length in reef fishes. a–f*, Reconstructed values (points) of K_{max} and maximum body length at the most recent common ancestor of each genus (n = 602) of the reef fish phylogeny. The black lines (solid in* ***a****, dashed in* ***b–f****) represent the root state coefficients for the reef fish tree, estimated by a mixed Gaussian phylogenetic model. For* ***b–f****, each subsequent panel shows an evolutionary regime shift detected in the relationship between the traits along the phylogeny, with respective slopes and intercepts (coloured lines), and all tips that display that relationship in the present (coloured points). The panels are organized in order of the steepness of the slopes. The root allometry is shown in* ***a****, and the other plots show an increase in growth relative to body size (steeper allometry). Both axes are on a log_{10} scale. The names in each panel refer to extant families that retained that evolutionary regime through time. Fish silhouettes were sourced from fishualize (Schiettekatte et al. 2020b).*

2.4 Discussion

By applying a robust predictive framework within a phylogenetic context, we reveal recurrent departures in life history regimes throughout coral reef fish evolution. Surprisingly, these evolutionary regime shifts occurred predominantly toward increased growth optima (i.e. faster growth trajectories) and smaller body sizes. This suggests either an asymmetrical exploration or selection/retention, of this fast life history dynamics in the evolution of reef-associated fish lineages. While the slower growth trajectory regimes remained relatively constant through time, the high end of the reef fish growth spectrum has been a constant source of evolutionary novelty. As a result, extant coral reef fishes display faster growth rates, on average, when compared with non-reef associated species (**Appendix A**: Extended Data Fig. 6). These accelerations in growth and reductions in size optima, however, were not homogeneously distributed over time. Shifts toward a higher growth and lower size optima were concentrated in the Eocene (56-33.9 Ma). Thus, at the time of the highest recorded reef fish diversification in the Oligocene-Miocene (33.9-5.3 Ma; Cowman and Bellwood 2011; Bellwood et al. 2017), most of the shifts in life history had already taken place millions of years before. Hence, our results call for a reinterpretation of the evolutionary events shaping one of the most diverse vertebrate radiations in the world.

2.4.1 Novelty in reef fish growth and size

Extant coral reef fish faunas are largely a product of key historical and evolutionary developments that took place throughout the Cenozoic Era. To characterise these developments, this Era was split into three major phases: the Paleocene–Eocene (66-34 Ma), the Oligocene–Miocene (34-5.3 Ma), and the Pliocene–Pleistocene (5.3-0 Ma; Bellwood et al. 2015). The Paleocene–Eocene was marked by the origins of most typical coral reef fish families (e.g. Labridae, Apogonidae, Pomacentridae), while the Oligocene–Miocene was regarded as the most important time for reef fish functional differentiation, including the rise and expansion of small-bodied and fast-growing species (Bellwood et al. 2017). Although the Miocene seems to have indeed been an important time for trophic innovations in reef fishes (e.g. Cowman et al. 2009; Bellwood et al. 2014; Siqueira et al. 2020), our results suggest that

this was not necessarily mirrored by growth and body size. Most evolutionary novelty in reef fish size and growth trajectories appears to have occurred at an earlier age, in the Eocene, which highlights this Epoch as a fundamental time for the evolution of fast-paced life histories. However, the Eocene shifts in growth evolutionary optima were not limited to small-bodied cryptobenthic species. These cryptobenthic lineages did indeed shift toward more extreme, high values of growth optima, but growth accelerations were widespread throughout the phylogeny (**Fig. 2-2**). This temporal congruence and phylogenetic spread in evolutionary regime shifts suggest that the Eocene might have been a time that indiscriminately favoured high growth rates across several reef fish lineages. But what factors could have driven the accumulation of growth shifts in the Eocene?

Generally, the best predictors of patterns in individual growth for vertebrate populations are body size and temperature (e.g. Gillooly et al. 2001; Brown et al. 2004), underscored by the high relative importance of these factors in our predictive models (see **Appendix A**). Maximum body length was indeed important for determining the magnitude of change in growth optima observed herein (**Fig. 2-2**), with half of shifts toward faster growth also happening toward smaller sizes (**Appendix A**: Extended Data Fig. 4). However, the Eocene shifts in growth rates occurred in lineages that span a wide range of body sizes (e.g. the goby *Eviota sigillata* has a maximum body length of 1.9 cm compared to the bream *Scolopsis margaritifera* with a maximum body length of 28 cm). Therefore, it seems likely that temperature had as strong influence as (or perhaps even stronger than) body size in the temporal accumulation of growth regime shifts in reef fishes. Indeed, the Eocene was the hottest Epoch of the Cenozoic (Westerhold et al. 2020), with a Climatic Optimum that largely coincides with the highest density of positive growth and negative size shifts detected by our models (**Fig. 2-1**; **Appendix A**: Extended Data Fig. 4). This suggests that the high temperatures of the Eocene might have provided the foundation for the evolution of faster life history strategies in reef fishes, which agrees with recent findings that fish develop smaller body sizes and faster growth in response to warming temperatures (Lindmark et al. 2022).

It is important to note that the frequency of shifts toward faster growth rates and smaller sizes was decoupled from the frequency of branching events in the reef fish phylogeny. We expected to find

more shifts in growth trajectories happening in the Oligocene–Miocene, when most reef fish lineage diversification occurred (Cowman and Bellwood 2011; Bellwood et al. 2014; Siqueira et al. 2020); but this was not the case. This temporal decoupling strengthens the idea that there were specific abiotic and biotic conditions of the Eocene that underpinned the shifts in evolutionary regimes. It appears that high global temperatures may have driven the origins of fast-paced life histories in the Eocene, but it was not until the development of new coral reef habitat configurations in the Oligocene–Miocene (Bellwood et al. 2017) that conditions favoured the expansion of reef fish lineages towards the fast end of life history strategies. In essence, the potential for fast life histories seems to have evolved well before the realized expansion of fast-growing and small-bodied reef fish lineages.

Conversely, the Eocene shifts in reef fish growth and size might have been the product of ecological release in the aftermath of the K/Pg mass-extinction. For instance, evidence from the fossil record suggest that niche expansion was facilitated by ecological opportunity in some fish lineages in the early Cenozoic (e.g. Friedman 2010; Sibert and Norris 2015). Therefore, the rise of new life history strategies might represent a similar case. This scenario, however, is less likely for two main reasons. First, evolutionary shifts are concentrated at around 20 million years after the K/Pg boundary and after the origin of most reef fish families, which is a substantial temporal latency for ecological novelty to arise; thus, fast life histories did not arise with the origin of most families, but several million years after. Second, under this latency scenario, one would expect shifts to be equally likely toward both ends of the life history spectrum, but our results show that post-K/Pg regime shifts only occurred into faster growth optima. While asymmetric shifts are not *per se* evidence against this latency hypothesis, they cannot be explained by it, thus requiring a third explanatory factor. Hence, these asymmetric shifts lower the parsimony of the latency hypothesis, further supporting the temperature hypothesis explained above. It appears that there were far fewer constraints into shifting towards accelerated life histories in the evolution of reef fishes than there were towards the slower end of the spectrum.

2.4.2 A new energetic regime on coral reefs

One of the most striking characteristics of present-day coral reefs is the diversity and numerical abundance of small-bodied fish species, particularly in the families Gobiidae, Blenniidae, Pomacentridae, and Apogonidae (Bellwood et al. 2017). Interestingly, all these families belong to clades that have extreme values of growth evolutionary optima (**Fig. 2-2**), even when accounting for their average small body sizes (**Fig. 2-3**). There seems to be, however, a disconnect between the timing of when these clades first shifted toward higher growth rate optima and when they became numerically abundant and diverse. In Gobiaria, for example, the regime shift in growth was estimated to occur in the Cretaceous (**Fig. 2-2**), at the origin of this clade; but only their molecular sequences can be traced this far back in time and there is little evidence in the fossil record to suggest that small-bodied gobiiform lineages were alive prior to the K/Pg boundary (Patterson 1993; Marramà et al. 2016). Despite the uncertainty associated with the paleontological record, fossils from the Early Cenozoic suggest that their abundance and diversity were not as high as they are in modern coral reefs (Marramà et al. 2016; Bellwood et al. 2017). Thus, it appears that habitat shifts in the Miocene underpinned the success of an ancient fast-paced life history strategy that became increasingly advantageous with the formation of modern coral reef configurations.

Some species within the small-bodied, fast-growing fish families have strong associations with branching scleractinian corals in modern reefs (Coker et al. 2014). Could branching scleractinian corals, thus, provide a clue to the Miocene diversification of fast life histories? Interestingly, the initial diversification of these coral growth forms coincides with the timing of expansion of small, fast-growing fish lineages. Modern scleractinian coral groups started to diversify in the Miocene (Mihaljević et al. 2014; Santodomingo et al. 2015), although the dominance of fast-growing branching forms, particularly in the family Acroporidae, is a product of a very recent expansion in the Pliocene–Pleistocene (Renema et al. 2016; Siqueira et al. 2022). Diversification patterns in fishes seem to be more associated with the Miocene expansion of coral growth forms than with the latter Pliocene–Pleistocene event. Thus, small-bodied, fast-growing fish lineages could have benefitted from the refuges provided by the structures of these early scleractinian corals. Indeed, to sustain increasingly fast growth, animals need to increase food intake, with frequent trade-offs between predation risk and

foraging effort (Dmitriew 2011). As a consequence, life in the fast lane can only be evolutionarily advantageous if lineages can somehow overcome the dangers of predation, while maintaining increased foraging rates as small-bodied organisms. Corals likely provided the necessary predation relief in the Miocene for many small-bodied, fast-growing fish lineages that originated earlier in the warm temperatures of the Eocene.

Today, some of the fastest-growing fish lineages appear to have taken a fundamental role in sustaining the productivity of coral reef fishes. Despite contributing relatively little to the process of biomass accumulation, cryptobenthic fishes are among the most important energetic currencies within modern coral reefs (Depczynski et al. 2007; Brandl et al. 2019c). Through extraordinary rates of mortality, very fast growth, and likely enhanced larval retention, cryptobenthic reef fishes contribute between 20 and 70% of all consumed fish biomass on typical coral reefs around the world (Brandl et al. 2019a). The high-productivity-high-mortality life history of cryptobenthic fishes are likely the end-product of a long evolutionary history, potentially shaped by thermally induced origins in the Eocene but sustained by subsequent key Miocene habitat changes and the expansion of modern reefs. The initial shifts in life history evolutionary regimes reported herein, and their subsequent expansion, thus represent the foundations of the fast-turnover energetic dynamics that characterise the highly productive present-day coral reefs.

2.4.3 Conclusions

Here we show that the evolution of crucial life history traits, growth and size, were highly skewed towards faster growth and smaller sizes in reef fishes. We posit that the high global temperatures of the Eocene may have favoured frequent and intense evolutionary shifts in reef fish life histories, while subsequent habitat changes in the Miocene may have provided the essential substrate for the survival and expansion of many small-bodied, fast-growing lineages. To our knowledge, this is the first documentation of large-scale, macroevolutionary patterns in growth rates for an entire vertebrate assemblage. As recently noted (Choat 2021), understanding size-related variation in life history traits during fish evolution is essential. Our work represents a critical contribution in that direction,

providing a roadmap for future studies to analyse macroevolutionary patterns in the life histories of other taxa.

But it is good that we do not have to try to kill the sun or the moon or the stars. It is enough to live on the sea and kill our true brothers.

Ernest Hemingway
The Old Man and the Sea, 1952

Chapter 3: Over a century of global decline in growth performance of commercially valuable fishes

Yan, H.F., Watkins, H.V., Siqueira, A.C., Bellwood, D.R. (In revision). Over a century of global decline in growth performance of commercially valuable fishes. Nature Communications.

Abstract

Anthropogenic pressures are driving large-scale changes in the ecologies and life histories of fishes. Growth performance is a composite life-history trait that captures the trade-off between two fundamental traits: growth and body size. Here, we assessed the global impacts of fishing and climate change on the growth performance of marine teleost fishes over the last century. Using 7,684 growth curves encompassing 1,479 species, we found a global pattern of decline in growth performance from 1908 onwards, with the greatest declines in commercially valuable fishes. Indeed, managed fisheries experienced a 9% decline in growth performance over the last century, which equates to an average decline of 28% in body size. Despite relatively consistent increases in ocean temperatures globally, we only detected a decline in the growth performance of fishes in temperate regions, which is probably indicative of an overrepresentation of commercially valuable fishes at higher latitudes. The declines in growth performance likely reflect legacy effects, shaped by overfishing, on changes in the underlying size structure and demographic processes of fished stocks. Therefore, the potential impacts of climate change on growth performance may be overwhelmingly masked by the impacts of overfishing.

Keywords: body size; climate change; life-history traits; overfishing; state-space models

3.1 Introduction

We are currently in an era of global change. The oceans of the Anthropocene are becoming increasingly impacted by destructive, human-driven activities, threatening critical ecosystem functions and services. Undoubtedly, the two greatest threats to ocean biodiversity are overexploitation and biophysical changes due to climate change (Dulvy et al. 2003; Brander 2007; Halpern et al. 2015). The extinction risk of many of the world's most iconic and culturally valuable fishes is increasingly elevated by overfishing (McCauley et al. 2015; Ripple et al. 2019; Dulvy et al. 2021; Yan et al. 2021). Although fisheries management regimes can improve the status of fished stocks when implementation is strong (Hilborn et al. 2020; Juan-Jordá et al. 2022; Pacoureau et al. 2023), many of the world's managed fisheries are still overfished (Worm et al. 2009; Costello et al. 2016; but see Hilborn et al. 2020). This paradigm is likely an artifact of the temporal mismatch between overfishing and management: strong management is typically triggered once stocks have been seriously depleted (Hilborn and Walters 1992; Sadovy and Cheung 2003; Webb and Mindel 2015). Consequently, large declines in stock abundances have not only led to declines in fisheries production but have also led to demographic changes in the life histories of many commercially valuable species (Trippel 1995; Rochet 1998; Jennings et al. 1999; Swain et al. 2007; Anderson et al. 2008).

Changes in fishes' life histories may be further exacerbated by changes in environmental conditions due to climate change. The impacts of climate change are manifesting throughout the world's oceans, with increasing temperatures and decreasing dissolved oxygen levels (Frölicher et al. 2009) driving changes in relatively plastic critical life-history traits. There is substantial evidence that the expression of life histories differs between conspecifics found across different temperature regimes, with faster life-history traits (e.g. faster growth rates, earlier ages at maturity, smaller body sizes) typically coinciding with warmer temperatures (Brander 1995; Yamahira and Conover 2002; Crozier and Hutchings 2014). Climate change can thus push the physiological limits of fishes towards decreases in body size (Cheung et al. 2013) or range expansions into deeper waters and/or higher latitudes (Perry et al. 2005; Cheung et al. 2013; Rubenstein et al. 2023). The potentially compounding synergism between fishing and climate change may disproportionally impact the population dynamics

of the world's fishes, driving changes in their ecologies and life histories (Brander 2007). The impacts of climate change and overfishing have now extended to all reaches of the ocean (Halpern et al. 2015), yet we are lacking a global evaluation of their respective impacts on the life histories of fishes.

Here, we collated data on 7,683 growth curves encompassing 1,479 species over 113 years of marine teleost fishes and implemented a suite of Bayesian autoregressive state-space models, revealing global declines in growth performance over the last century (**Fig. 3-1a**; from 1908 to 2021). Growth performance (ϕ; sensu Munro and Pauly, 1983) is a composite life-history trait (Wong et al. 2021) that captures the trade-offs between asymptotic body size and early growth rate, two dominant and fundamentally linked life-history traits (Brown et al. 2004; Siqueira et al. 2023; **Appendix B**: Fig. B1). Specifically, growth performance standardises estimates of instantaneous growth rates against a single unit of body size (Munro and Pauly 1983). By separating the underlying population state from observation deviances in a state-space framework (Dennis et al. 2006), we can determine if changes in growth performance coincide largely with increasing temperatures and/or different fisheries management regimes. First, we assessed the global growth performance of fishes from 1908 to 2021. We then adapted a management classification scheme (Costello et al. 2012) to disaggregate these patterns by managed fisheries, unmanaged fisheries, and unfished species. Managed fisheries represented families for which formal stock assessments were available, whereas unmanaged fisheries encompassed families that have global catch landings reported or reconstructed but lacked formal stock assessments; the remaining families were classified as "unfished". Finally, we assessed the spatial patterns in growth performance by separating the time series into temperate, subtropical, and tropical locations, to account for potentially different geographic patterns.

3.2 Methods

3.2.1 Data collation and growth performance

To calculate growth performance, we used the von Bertalanffy growth parameters L_∞ (cm), which is the expected asymptotic size for an individual in a given population, and K (year^{-1}), which is the instantaneous rate at which an individual approaches its asymptotic size (Von Bertalanffy 1949). We

first generated a list of growth studies from FishBase (Froese and Pauly 2021) and manually corrected all detected errors by individually assessing each reference; observations were removed when growth parameters could not be found. We then conducted a systematic literature search using the ISI Web of Science database to find all published articles using von Bertalanffy growth parameters for marine fishes and cross-checked the list with that from FishBase to remove any duplicates (conducted 21 May 2022). We excluded all freshwater species and euryhaline species collected in freshwater habitats. For each study, we recorded the growth parameters L_∞ and K, the length measurement type (i.e. total length, standard length, or fork length), the method used for aging (i.e. mark recapture, otolith rings, other growth rings (e.g. scale rings, vertebrae rings), length frequency, or unknown), the year for which individuals were surveyed, and the geographic location for which individuals were collected. Following Morais and Bellwood (2018), we only included studies where the discrete geographic locations were provided. For example, studies conducted in Chesapeake Bay were included, but those conducted across the entire Atlantic were excluded. To make studies comparable, we used published length-length conversion coefficients from FishBase to convert all estimates of L_∞ to total length in cm. In total, we collected data on 7,683 growth curves encompassing 1,479 species over 113 years (from 1908 to 2021).

Using estimates of L_∞ and K, we are able to calculate growth performance as defined by Munro and Pauly (1983). Growth performance (ϕ) is a composite life history trait (i.e. a life history trait calculated from other life history traits; Wong et al. 2021) and encompasses the trade-off between growth rate and body size (Munro and Pauly 1983). Specifically, it standardises for body size and allows the comparison of growth rates across species and/or populations (Munro and Pauly 1983; Morais and Bellwood 2018). For example, species that have higher growth performance values tend to exhibit higher resting metabolic rates for a given body size (Wong et al. 2021). Growth parameters were converted to estimates of growth performance using the equation:

$$\phi = log_{10}\mathrm{K} + S_L \times log_{10}L_\infty$$

Here, K and L_∞ are the growth parameters and S_L is the slope between $\log_{10} L_\infty$ and $\log_{10} K$ for the population. The parameter S_L can also be defined as

$$S_L = -m \times b$$

Where *m* is the anabolic term exponent from the growth model and *b* is the length-weight regression exponent. We used the metabolic scaling exponent in place of the anabolic exponent *m* (Savage et al. 2004; Morais and Bellwood 2018). The anabolic term was found to be, on average, 0.761 for fishes (Savage et al. 2004), which we applied to our calculation of ϕ.

To evaluate changes in species composition through time, we used the Jaccard index based on presence/absences with species identities as columns and survey years as rows. We used a Principal Coordinate Analysis to visualise the results by separating years into 5 different time slices: prior to 1940, 1941-1960, 1961-1980, 1981-2000, and after 2000. Because there was significant dispersion between groups, we visually compared the overlap of 90% confidence ellipses. We ran multivariate analyses using the `vegan` package 2.6-10 (Oksanen et al. 2020).

3.2.2 Spatial and management regimes

Using the geographic locations of each growth curve, we were able to (1) separate the locations into different regions and (2) extract estimates of sea surface temperature. We used the latitude of each location to delineate locations into different regions (i.e. temperate, subtropical, and tropical). Tropical locations were chosen between -23º and 23º, subtropical were from 23º and 34º in the northern hemisphere and -23º and -34º in the southern hemisphere, and the remaining locations were classified as temperate and included polar regions. Using the geographic location, we also created a 2º buffer around each point and calculated mean sea surface temperature per location per sampling year. Sea surface temperature estimates were calculated as annual means at a 1º x 1º resolution from https://psl.noaa.gov/data/gridded/data.cobe.html.

To reflect different fishing pressures across our samples, we adapted the method by Costello et al. (2012) and separated families into managed fisheries, unmanaged fisheries, and unfished species. Similarly to Costello et al. (2012), all families for which a formal stock assessment existed from the RAM Legacy Database (Ricard et al. 2012) was considered a "managed fishery" (Melnychuk et al.

2017); conversely, families that had reported or reconstructed catches on the Sea Around Us database (Pauly et al. 2020), but no formal stock assessment, were then considered "unmanaged fisheries". All remaining populations were considered unfished species. Because we made separations at the family level, we acknowledge the potential biases that not all species belonging to a family will be formally managed; however, this is likely to make our results more conservative because species belonging to the same families typically exhibit similar ecologies and are likely equally vulnerable to fisheries.

3.2.3 Analyses

We developed separate Bayesian autoregressive state-space models to assess the growth performance of fishes from 1908 to 2021 globally, under different management regimes (i.e. managed, unmanaged, and unfished), and different regions (i.e. temperate, subtropics, and tropics), after accounting for environmental temperature. To assess the changes in growth performance through time, we used a state-space modelling approach treating each growth performance value as an individual observation (taken from a population/stock's calculated growth parameters). Each model jointly estimated trends for the observed data as a product of an underlying population state (Dennis et al. 2006). Due to the inherent biases associated with different aging methods (i.e. mark recapture, otolith rings, other rings (e.g. scales, vertebrae), length frequency analyses, and unknown; Morais and Bellwood 2018), each method was modeled with its own respective observation deviance. We then generated models where all methods shared one underlying population state.

For each aging method, the growth performance of fishes (y_i; where *i* corresponds to a single population/stock) in year *t* was modelled according to a gamma error distribution by specifying the gamma shape (ϕ) and rate parameters ($\lambda_{i,t}$).

$$Gamma(y_{i,t} \mid \phi, \lambda_{i,t})$$

$$\lambda_{i,t} = \frac{\phi}{\mu_{i,t}}$$

$$\log(\mu_{i,t}) = \alpha_t + \alpha_{fam} + \beta X_i$$

Here, the term α_{fam} is the varying effect of family on the growth performance of fishes. The term β is a vector of estimated population-level effects and X is a matrix of covariates impacting growth performance, in this case the extracted temperature for each specified location for each growth performance value y_i. We set the following weakly informative priors on ϕ the gamma shape parameter and the estimated population-level effects (β):

$$\lambda \sim \text{Gamma}(0.01, 0.01)$$

$$\beta \sim \text{Normal}(0, 2)$$

The term α_t (t = 1908, …2021) is the expected mean growth performance for each year for each aging method. Each annual growth performance estimate is considered the observed estimate of an underlying, unobserved population state x_t. The underlying population state x_t changes from year-to-year following a first-order autoregressive process, where

$$x_t = x_{t-1} + u + w_t \qquad w_t \sim \text{Normal}(0, \sigma_q)$$

$$\alpha_t = x_t + v_t \qquad v_t \sim \text{Normal}(0, \sigma_r)$$

Here, w_t represents the random annual deviations (i.e. process deviance) in growth performance resulting from demographic processes of the population and is drawn from a normal distribution with a mean of zero and a process standard deviation of σ_q (note that standard deviations are used to parameterise normal distributions in Stan). The drift term u allows the model to estimate if there is a consistent trend upwards or downwards over time. The "observed" growth performance of a given year represents the underlying state x_t plus some observation error v_t (i.e. observation deviance), which is drawn from a normal distribution with a mean of zero and its respective measurement standard deviation σ_r. This formulation of v_t is identical to drawing v_t from a multivariate normal distribution with a mean of zero and a variance matrix comprising σ_r on the diagonals and zeros across the non-diagonals (Holmes et al. 2021). To estimate the state at $x_{t=1908}$, we estimated the initial state x_0 following the same equation as above.

$$x_{t=1} = x_0 + u + w_{t=1}$$

The initial state x_0 and the drift term u used the following weakly informative priors:

$$x_0 \sim \text{Normal}(0, 5)$$

$$u \sim \text{Normal}(0, 5)$$

Annual estimates of expected growth performance of the same underlying population state x_t may have constant differences between different aging methods (i.e. consistent biases or errors arising from each method). Therefore, we added scalar terms for four of the aging methods (i.e. mark recapture (c_{MR}), other rings (c_{OR}), length frequency (c_{LF}), and unknown (c_{UN})) to scale estimates towards a baseline method (i.e. otoliths). All scalar terms were specified with weakly informative normal priors:

$$c_{MR}, c_{OR}, c_{LF}, c_{UN} \sim \text{Normal}(0, 5)$$

Each aging method also included its own respective measurement error in its estimate of the same underlying population state x_t (i.e. v_{OT}, v_{MR}, v_{OR}, v_{LF}, v_{UN}; OT = otolith rings, MR = mark recapture, OR = other rings, LF = length frequency, and UN = unknown).

$$\begin{bmatrix} \alpha_{OT} \\ \alpha_{MR} \\ \alpha_{OR} \\ \alpha_{LF} \\ \alpha_{UN} \end{bmatrix}_t = x_t + \begin{bmatrix} 0 \\ c_{MR} \\ c_{OR} \\ c_{LF} \\ c_{UN} \end{bmatrix} + \begin{bmatrix} v_{OT} \\ v_{MR} \\ v_{OR} \\ v_{LF} \\ v_{UN} \end{bmatrix}_t$$

$$\begin{gathered} v_{OT,t} \sim \text{Normal}(0, \sigma_{r,OT}) \\ v_{MR,t} \sim \text{Normal}(0, \sigma_{r,MR}) \\ v_{OR,t} \sim \text{Normal}(0, \sigma_{r,OR}) \\ v_{LF,t} \sim \text{Normal}(0, \sigma_{r,LF}) \\ v_{UN,t} \sim \text{Normal}(0, \sigma_{r,UN}) \end{gathered}$$

$$\sigma_r \sim \text{Half-normal}(0, 1)$$

Each model was run with four Markov chain Monte Carlo chains for 6,000 iterations with an initial warmup phase of 3,000 iterations. We visually inspected traceplots and ensured the chains were consistent with convergence for all estimated coefficients by checking that the potential scale reduction factor Rhat < 1.01 and the effective sample size ESS > 1500 (**Appendix B**: Table B1).

Models were run in *Stan* (Carpenter et al. 2017) using the `rstan` v 2.21.8 package (Stan Development Team 2017) in R v 4.2.0 (R Core Team 2024).

3.3 Results and Discussion

3.3.1 Global decline of growth performance

Globally, we found that the average growth performance across 1,479 focal species had declined from 1908 to 2021 by 7.9% (90% credible interval: 4.4% to 11.4%; **Fig. 3-1b**). The median predicted growth performance in 1908 was 3.3, which, based on empirically measured values, is indicative of a fish growing to a mean size of 42.1 cm at an instantaneous rate of 0.35 $year^{-1}$. Given that the median growth performance in 2021 was 3.0 (i.e. fish growing to 33.7 cm at a rate of 0.32 $year^{-1}$; ~20% and ~9% decline, respectively), this global decline is most likely indicative of two co-occurring mechanisms: fishes are growing to relatively smaller sizes (intraspecific) and compositional shifts in the species sampled (interspecific; **Appendix B**: Fig. B2). Given the spatial disparities in fishing pressure and ocean warming around the world, we can further disaggregate these global patterns across different management regimes.

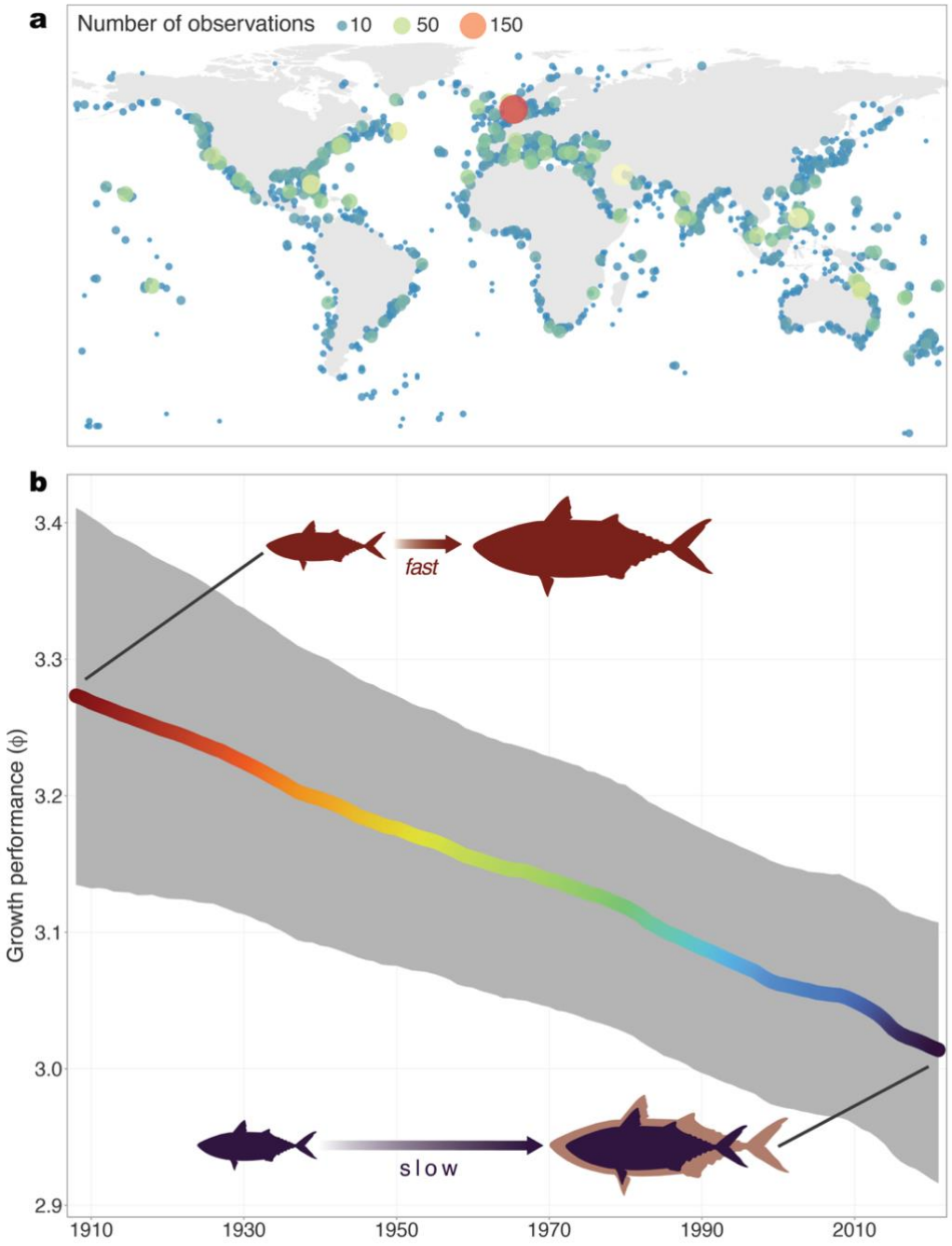

Figure 3-1. Distribution of 7,683 growth curves indicate a global decline in fish growth performance. a *The distribution of all collated growth curves. Points indicate individual observations and are coloured and sized (area) based on the number of observations per location.* ***b*** *The global growth performance (ϕ) of marine fishes from 1908 to 2021. The grey ribbon denotes the 90% credible interval and the thick line is the median modelled estimate, coloured by the growth performance value. Growth performance values around 1908 represent species that grow relatively quickly to larger body sizes (red), whereas lower growth performance values denote species that grow relatively slower to smaller body sizes (blue).*

3.3.2 Overfishing is driving global declines

When we delineated the global time series by management regime, we found that fishes from managed fisheries exhibited the greatest declines in growth performance over the last century. We found a steady decline in growth performance of managed fishes from 1908 onwards, declining by 9.1% (5.0% to 13.2%; **Fig. 3-2a**). This resulted in a decline of a median fitted growth performance of 3.5 in 1908 to 3.2 in 2021, corresponding to an average body size decline of -28% and a 22% increase in growth rate over the last century (when assessing empirically measured body size and growth rates). Unmanaged and unfished species exhibited no change in their respective growth performances through time (**Fig. 3-2bc**). We found that the growth performance of unmanaged fishes, although lower than most managed fishes at a mean of 3.0, exhibited no net change across the time series (-11.0% to 21.6%; **Fig. 3-2b**). Similarly, the growth performance of unfished species remained relatively stable as well (-20.7% to 44.6%; **Fig. 3-2c**).

The declines in growth performance in managed fisheries is not indicative of the role of management *per se*; it is likely a reflection of the legacy of historically intense fishing mortality experienced by commercially valuable fishes. Indeed, declines in the fished biomass of commercially valuable fisheries were similarly matched with increases in fishing effort until the mid-1990's (Hilborn et al. 2020), which is an indication of overfishing. Similarly, the total reported and reconstructed catches of managed fisheries had increased steadily until the mid-1980's before plateauing (Pauly et al. 2020), whereas the number of stock assessments only started to increase after the 1990s (Ricard et al. 2012). Although the catches of unmanaged fishes followed a similar pattern to managed fishes, the magnitude of catch is well below those of managed fisheries (Pauly et al. 2020; **Appendix B**: Fig. B3). Consequently, many commercially valuable fishes had been heavily exploited well before management began, indicating that in some instances, management is likely to be a reaction to decline as opposed to a preventative measure (Sumaila et al. 2011). Additionally, the presence of management alone is not an indication of effective management; some of the most heavily regulated fisheries in the world still resulted in significant overfishing and population collapse (e.g. Hutchings and Myers 1994; Myers et al. 1997). Although effective fisheries management practices can

improve stocks that are in decline (Hilborn et al. 2020; Juan-Jordá et al. 2022; Pacoureau et al. 2023), it may take longer to achieve similar levels of recovery in the life histories of historically exploited fishes.

The declining growth performance of commercially valuable fishes is likely to be a legacy effect of size-based targeting via fisheries. Fishers are incredibly effective hunters and tend to target the largest (and typically oldest) individuals of a stock (Darimont et al. 2015). Unsurprisingly, intense fishing pressures have truncated populations towards smaller average sizes and younger ages (Hutchings and Reynolds 2004; Anderson et al. 2008). The resulting populations characterised by younger individuals (i.e. population juvenescence) not only expresses faster life histories, such as smaller body sizes and/or faster growth rates, but also exhibit less stability through time (Anderson et al. 2008). The dynamic instability of juvenescent populations is likely driven by changes in demographic compensatory mechanisms, such as increased somatic growth or fecundity (Anderson et al. 2008), or potentially through the loss of social learning (Wilson and Giske 2023). The declines in growth performance of commercially valuable fishes could represent the interplay between two synergistic processes: an unfished, residual stock left with smaller, younger individuals from size-selective fishing, which is then further reinforced and amplified by fisheries-induced selection against larger body sizes (Law and Grey 1989; Olsen et al. 2004; Jørgensen et al. 2007; Kuparinen and Merilä 2007). An opposing but equally likely mechanism for the observed declines in growth performance could be due to the "Rosa Lee" phenomenon (Lee 1912). In short, larger, faster-growing individuals are targeted first by size-selective fisheries, allowing the smaller, slower-growing individuals of a population to survive (Kraak et al. 2019). Consequently, for a given age, the remaining individuals are smaller and exhibit slower growth rates than would be expected in the absence of size-selective fishing (Kraak et al. 2019), potentially resulting in declines in growth performance.

Declines in growth performance can be indicative of both intraspecific changes (e.g. Rosa Lee phenomenon) or interspecific compositional changes. Despite considerable overlap in the species that were sampled through time, which suggests relative homogeneity in the species that were sampled through time, there were relatively distinct compositional shifts between specific time periods

(**Appendix B**: Fig. B2). While it is plausible that declines in growth performance could be due to potential sampling biases (i.e. shifting from species with higher growth performance values towards those with lower growth performance through time), it is unlikely that this is the primary mechanism of the observed declines. If declines in growth performance were due to sampling biases alone, we would expect the maximum body size of species to be considerably larger at the beginning of our time series (due to the relatively positive association between body size and growth performance; **Appendix B**: Fig. B1). We found, however, that the species-level maximum body size was relatively larger in more recent years (**Appendix B**: Fig. B2), which should counter our results by producing increasing levels of growth performance if sampling biases were a dominant factor. Therefore, it is unlikely that the observed declined in growth performance are solely due to changes in the species sampled through time. Whether the compositional shift in species that are targeted for growth studies is due to increases in the occurrence of "blue sky" science (i.e. application-independent research) or human-driven changes in the species available to study (e.g. local extinctions from overfishing) is unclear. Regardless of the underlying mechanism, given the inherent temporal lag between management implementation and stock recovery (Costello et al. 2016), the legacy of size-based fishing could manifest throughout populations as declines in growth performance, even when abundances are stable or increasing. Regardless of whether overfishing is the proximate or distal cause for the decline in fish growth performance, changes in the life histories of fishes are likely to be slow to reverse (or potentially irreversible) and can have repercussions on the biomass and productivity of capture fisheries (Law and Grey 1989; Jørgensen et al. 2007).

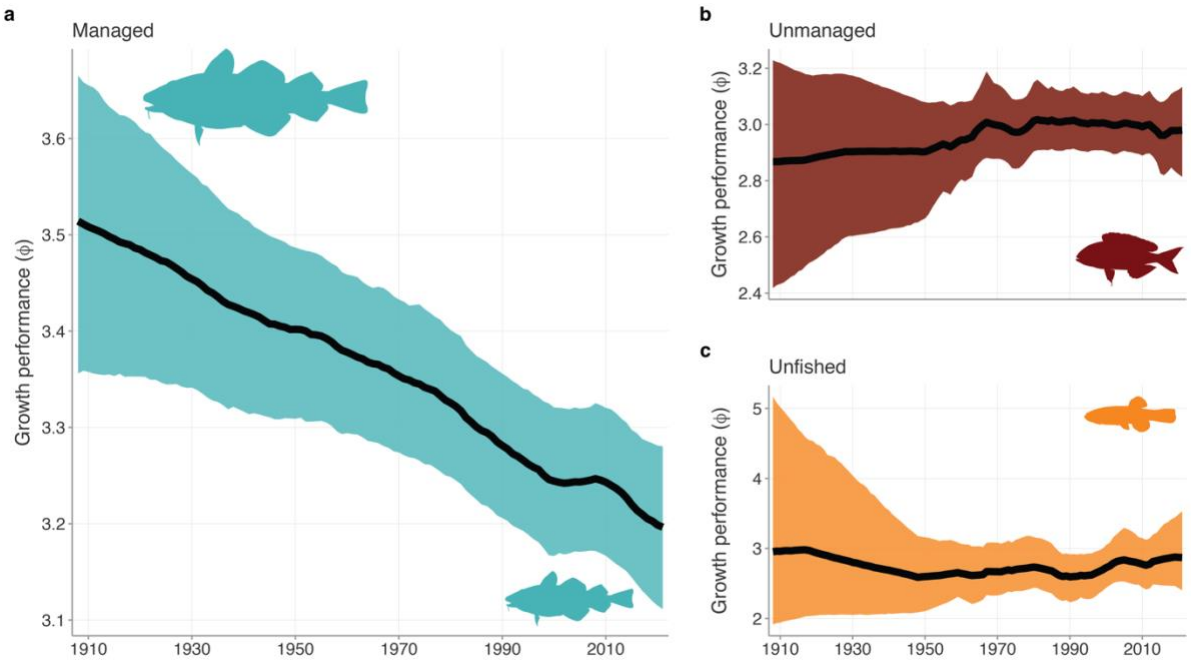

Figure 3-2. Changes in growth performance through time by management status. *Changes in growth performance (ϕ) of fishes in* ***a*** *managed fisheries (n=996 species),* ***b*** *unmanaged fisheries (n=419), and* ***c*** *unfished species (n=64) from 1908 to 2021. The thick ribbons denote the 90% credible intervals, and the thick black lines are the median fitted trends.*

3.3.3 Geographic patterns reflect overfishing

Disaggregating the time series by geographic location largely reflected patterns in fisheries management. Growth performance in temperate locations declined by 8.7% (90% credible interval: -13.2% to -4.2%; **Fig. 3-3a**). Although the decline in growth performance does coincide with an increase in average ocean temperature of 0.7ºC over the same time period (from 4.7ºC in 1908 to 5.4ºC in 2021), we found generally no change in growth performance in subtropical regions (-17.5% to 4.9%), which experienced similar levels of warming (from 21.5ºC in 1908 to 22.5ºC in 2021; **Fig. 3-3b**). Similarly, despite relatively stronger temperature oscillations in the tropics, we also found no change in the growth performance of tropical fishes (-10.3% to 20.8%; **Fig. 3-3c**). The decline in growth performance of fishes in the temperate region is likely a manifestation of the dominance of fisheries management occurring in higher latitudes (Hilborn et al. 2020) in the northern hemisphere (**Fig. 3-4**). Indeed, nearly 90% of the studies in the temperate region comprises managed fisheries (**Appendix B**: Fig. B4) and the strongest evidence of decline was found when separate analyses were run for managed fisheries in temperate regions (**Appendix B**: Fig. B5). The dominance of commercially valuable, and thus managed, fisheries is likely the primary factor driving the decline in the growth performance of fishes in the temperate region.

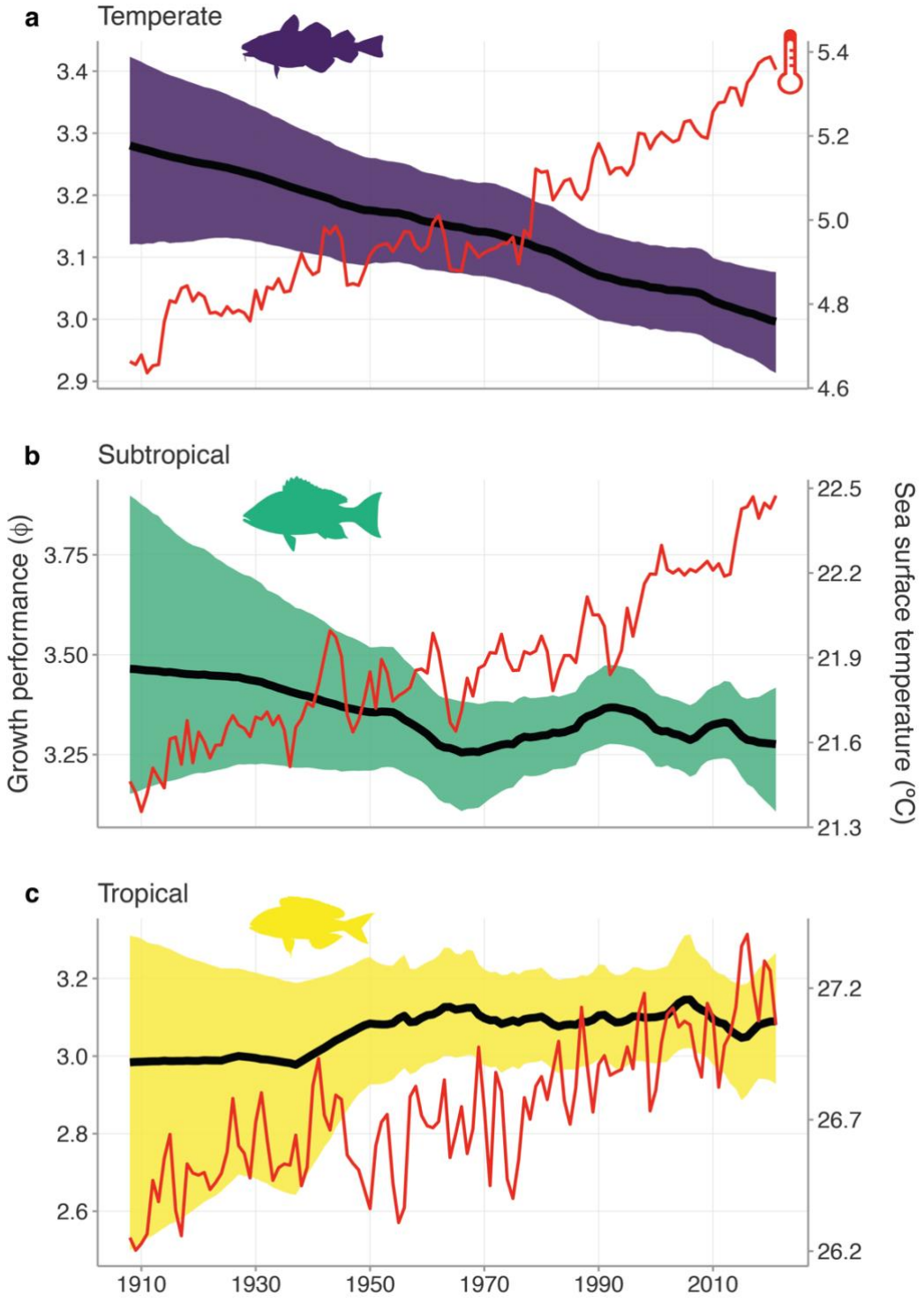

Figure 3-3. Changes in growth performance and increasing ocean temperatures. *Changes in growth performance (ϕ) of fishes in* ***a*** *temperate (top; purple),* ***b*** *subtropical (middle; green), and* ***c*** *tropical regions (bottom; yellow) from 1908 to 2021 (left y axis). The thick ribbons denote the 90% credible intervals of the time series and the thick black lines are the median estimates. The red line in each panel corresponds to the mean sea surface temperature (°C) in each respective region for the same time period (right y axis).*

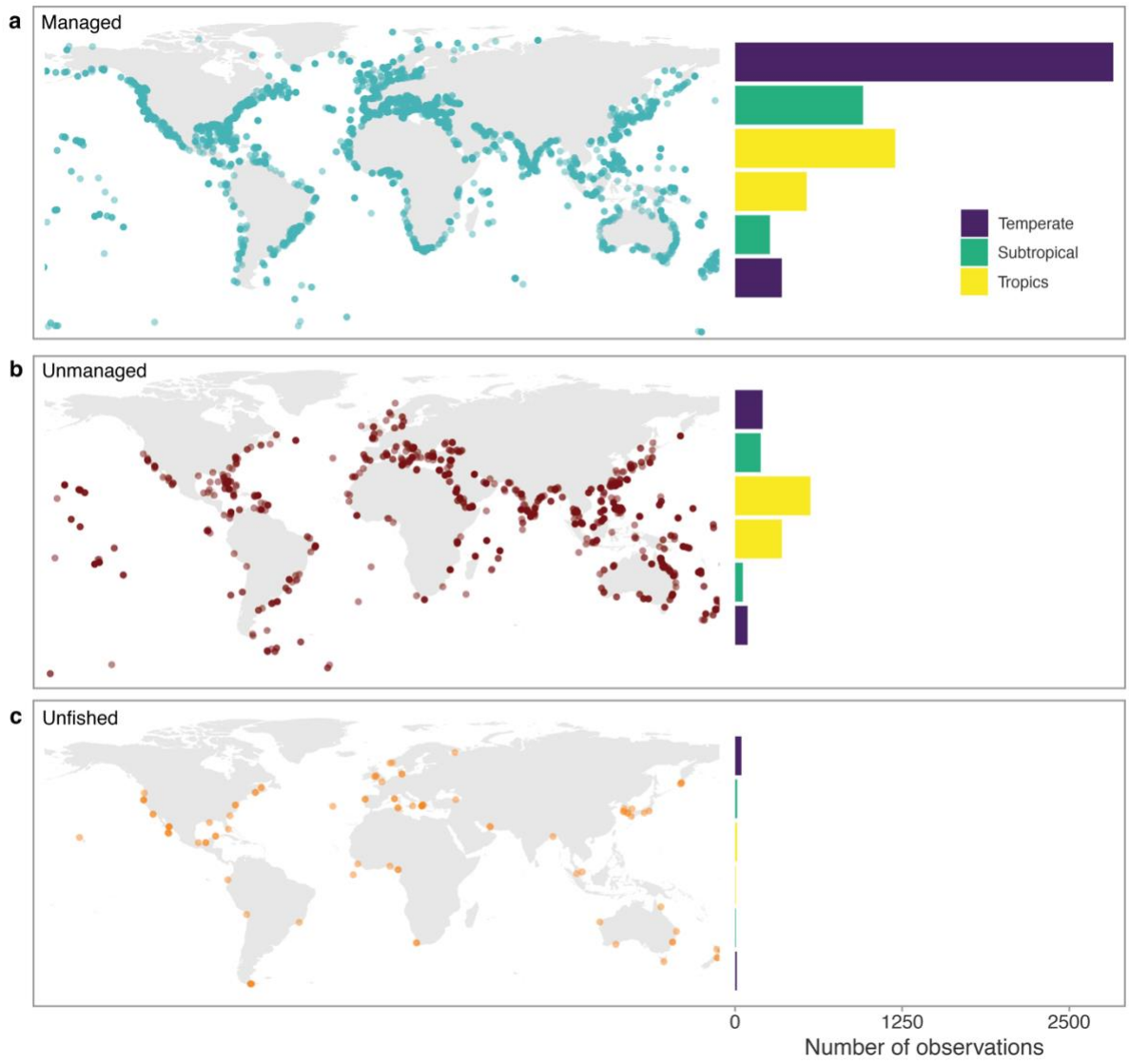

Figure 3-4. Global distribution of fisheries management. *The spatial distribution (left) and total number of growth performance studies (right) from* ***a*** *managed fisheries (top; green),* ***b*** *unmanaged fisheries (middle; red), and* ***c*** *unfished species (bottom; orange). Total number of observations per region are separated by the northern and southern hemisphere.*

The impacts of commercial size-based fishing are likely confounding and masking the potential physiological impacts of climate change on the growth performance of fishes. Across all three regions (i.e. temperate, subtropics, and tropics), the temperature has increased steadily by roughly 1ºC across the entire time series. Increases in ocean temperatures, paired with declines in dissolved oxygen (Frölicher et al. 2009), can push the physiological limits of ectotherms, such as fishes, towards faster metabolic rates (Sheridan and Bickford 2011; Cheung et al. 2013; Deutsch et al. 2015). Given the inherent correlation between metabolic rates and growth (Wong et al. 2021; White et al. 2022), models of energy assimilation predict that under future warming scenarios, the maximum body sizes of fishes are projected to decrease by 14-24% globally in the next 30 years under a high-emissions climate scenario (Cheung et al. 2013). Empirically, while not directly comparable, species' average body sizes have been shown to decrease and increase with warming temperatures (Audzijonyte et al. 2020), indicating that changes in body size can occur relatively quickly (over only a few decades), but in potentially polarising directions. Nevertheless, fishing and climate change may act synergistically to drive further changes in fishes' body size. Declines in body size across commercially valuable fishes would not only have demographic consequences but would also impact fisheries yields and global protein supplies (Sumaila et al. 2011; Cheung et al. 2013).

3.3.4 Conclusion

We uncovered global patterns of decline in the growth performance of marine fishes over the last century. Given the steady increase in temperatures across all three regions, the decline in growth performance of temperate fishes is most likely the by-product of an overrepresentation of commercially valuable, managed fishes in this region. Consequently, the global pattern of declining growth performance in marine fishes is likely the result of commercial size-based fishing practices, particularly in the northern hemisphere, and less likely driven by increasing temperatures due to climate change. The pervasiveness of size-selective fisheries can both change the demographic dynamics of fish populations (Anderson et al. 2008) and trigger relatively strong selection pressures towards smaller body sizes (Law and Grey 1989; Olsen et al. 2004; Jørgensen et al. 2007; Kuparinen

and Merilä 2007), both of which could manifest as declines in growth performance across ocean basins. Improved fisheries management could potentially offset the negative impacts of climate change but would require specialised adaptive reform and immediate action (Gaines et al. 2018). Managing for overfishing and climate change simultaneously can seem like a Herculean task; however, implementing effective fisheries management could increase the resilience of fish stocks (Sumaila and Tai 2020) and potentially prevent further declines in fishes' life histories.

[Eviota afelei] would have probably tasted better without the guts.

Simon Brandl

Chapter 4: Multi-decadal stability of fish productivity despite increasing coral reef degradation

Published as: Yan, H.F., Bellwood, D.R. (2023). Multi-decadal stability of fish productivity despite increasing coral reef degradation. Functional Ecology, 37 (5), 1245-1255.

Abstract

Under current trajectories, it is unlikely that the coral reefs of the future will resemble those of the past. As multiple stressors, such as climate change and coastal development, continue to impact coral reefs, understanding the changes in ecosystem functioning is imperative to protect key ecosystem services. We used a 26-year dataset of benthic reef fishes (including cryptobenthic fishes) to identify multi-decadal trends in fish biomass production on a degraded coral reef. We converted fish abundances into estimates of community productivity to track the long-term trend of fish biomass production through time. Following the first mass coral bleaching event in 1998, the abundance, standing biomass, and productivity of fish communities remained remarkably constant through time, despite the occurrence of multiple stressors, including extreme sedimentation, cyclones, and mass coral bleaching events. Species richness declined following the 1998 bleaching event, but rebounded to pre-bleaching levels and also remained relatively stable. Although the species composition of the communities changed over time, these new community configurations still maintain a steady level of fish biomass production. While these highly dynamic and increasingly degraded systems can still provide some critical ecosystem functions, it is unclear whether these patterns will remain stable over future decades.

Keywords: bleaching, cyclones, cryptobenthic fishes, productivity, resilience, rfishprod, stability

4.1 Introduction

Anthropogenic pressures, such as climate change and overexploitation, are reshaping biological systems across various scales (Johnson et al. 2017). The effects of these stressors can occur in isolation or act synergistically with other co-occurring stressors (Côté et al. 2016); therefore, the impacts of multiple stressors may manifest differently across different levels of community organization (Darling and Côté 2008). Although high diversity systems may be able to resist some of these impacts (Shurin et al. 2007; Craven et al. 2018), it is unclear whether biodiversity can bolster the functioning of degraded systems (e.g. Yan et al. 2022). Given the magnitude at which we are transforming ecosystem structures (Sala et al. 2000; Halpern et al. 2008), understanding the flow-on effects of changes in habitat configurations on critical ecosystem functions and services should be at the forefront of modern-day conservation and management actions.

Of all ecosystems, Anthropocene coral reefs are among the most threatened, with many in a state of transition (Hughes et al. 2017a; Bellwood et al. 2019a). Various benthic components, such as macroalgae (Graham et al. 2006, 2015), sessile epifauna (Norström et al. 2009; Tebbett et al. 2019), and especially algal turfs (Smith et al. 2016; Tebbett et al. 2021, 2023a), are increasing in prevalence as coral cover declines globally. Although climate change is undoubtedly one of the largest drivers of coral mortality, coral reefs are also experiencing a multitude of other, localised stressors (Nyström et al. 2000; Bruno et al. 2018; Bellwood et al. 2019a). For example, increased coastal development and agricultural activity has increased sedimentation and eutrophication on coastal reefs (Fabricius 2005; Kroon et al. 2016), while intensive fishing practices have depleted herbivorous fish stocks and changed ecosystem trophodynamics (Jackson et al. 2001; Hughes et al. 2007). Area-based protection measures (i.e. marine protected areas, MPAs) currently dominate the coral reef management discourse; however, there is a mismatch between the scale of protection and the scale of the stressors (Bruno et al. 2018; Bellwood et al. 2019a). Mainly, local coral reef management strategies (e.g. MPA establishment) are unable to fully mitigate stressors that occur at regional or global levels (Côté and Darling 2010). To circumvent this mismatch in scale, future coral reef management regimes could

instead target their actions towards both understanding and protecting the critical ecosystem functions and services provided by coral reefs transitioning to altered states (Hughes et al. 2018).

Although most previous work has focused on traits or derived parameters as proxies for function (e.g. standing stock biomass, total abundance, diversity), advances in the quantification of critical coral reef ecosystem functions have enabled scientists to approximate energy fluxes on transitioning reefs (Morais and Bellwood 2020; Schiettekatte et al. 2022). While our abilities to evaluate these impacts are increasing rapidly, the magnitude and direction of these energy fluxes in response to various stressors is uncertain, especially when they are assessed at different ecological scales. Specific fish groups tend to react negatively to the loss of corals; for example, increases in the sediment load on reefs coincided with a decrease in herbivorous fish biomass production (Tebbett et al. 2021) and a loss of brightly coloured fishes (Hemingson et al. 2022). Conversely, when the entire communities are sampled across several years, fish biomass production can increase following both mass coral cover decline (Morais et al. 2020) and coral cover recovery (Hamilton et al. 2022). This discrepancy in functional responses raises the question: how will the energy fluxes of entire communities be affected over longer time scales?

Here, we use a long-term dataset, spanning nearly 30 years, to examine changes in a key ecosystem function (i.e. consumer biomass production) of benthic reef fish assemblages through time. The assemblage incorporates a wide range of small, epibenthic fishes, including damselfishes (family Pomacentridae), wrasses (Labridae), butterflyfishes (Chaetodontidae), and various species of cryptobenthic reef fishes, which are small, bottom-dwelling fishes that are behaviourally and morphologically cryptic (Depczynski and Bellwood 2003; Brandl et al. 2018). The physiological constraints associated with small body sizes (e.g. limited respiratory surface area, high mass-specific metabolic rates; Nilsson et al. 2009), paired with the high habitat or microhabitat specialisation (Depczynski and Bellwood 2004; Brandl et al. 2018), are likely to make cryptobenthic reef fishes more susceptible to extreme environmental conditions than larger reef fishes (Brandl et al. 2020). By using a novel approach to calculate fish biomass production at the community level, we quantify the

changes in benthic reef fish productivity through multiple stressor events, including mass coral bleaching and extreme sedimentation.

4.2 Methods

All sampling was conducted in Pioneer Bay on the leeward side of Orpheus Island on Australia's Great Barrier Reef (GBR; 18º35'S, 146º28'E). Although protected from fishing, over the last three decades, Orpheus Island has been exposed to a wide range of environmental stressors, including multiple coral bleaching events, extreme sedimentation, and cyclones (Torda et al. 2018; Bellwood et al. 2019a; Tebbett et al. 2021). Orpheus Island was particularly impacted by the 1998 and 2016-2017 bleaching events on the GBR, and the inorganic sediment load in Pioneer Bay has increased by over 2000% in the last 15 years (Bellwood et al. 2006, 2012; Tebbett et al. 2021). Consequently, Orpheus Island presents an ideal model system to investigate the potential for multiple stressor events to impact the energy fluxes in benthic reef fish communities.

We investigated two different approaches to calculating the changes in energy fluxes of benthic fish communities: (i) a process-based quantification of the biomass production and (ii) the static use of abundance and standing stock biomass as proxies for biomass production. The former estimates productivity as a rate of biomass accumulation in the system by combining somatic growth and probabilities of mortality to estimate the productivity of the community per unit time per unit area (Morais and Bellwood 2020). The latter is easily measured in the field and, although has been correlated with various human processes like fishing (e.g. Cinner et al. 2020), is not necessarily indicative of the true underlying energy fluxes of the system, which is mainly driven by nonlinear scaling relationships between energetic fluxes and biomass (Barneche et al. 2014). Consequently, we included both process-based (i.e. productivity) and static proxies (i.e. abundance and standing stock biomass) of biomass production in our analyses.

4.2.1 Sampling protocol

We sampled benthic reef fishes annually from 1993-2021 (excluding 2014, 2017, and 2020) at approximately 3-5 m depth. Sampling always occurred during the Austral winter to avoid sampling during the peak summer recruitment (Bellwood et al. 2006, 2012). Each year, 2-4 coral outcrops (hereon referred to as stations) of roughly equal sizes were sampled (approximately 2 m^3; Bellwood et al., 2012, 2006). We chose stations that were isolated from continuous reef structures, could be entirely contained within the netting (see below), and had some form of structural complexity; stations were not chosen based on the status of the coral colonies present (i.e. both healthy and dead coral structures were included). Due to the extremely fast turnover and short lifespan of cryptobenthic fishes, which is typically shorter than one year (Brandl et al. 2018), mortality due to sampling likely had no impact on the productivity or community structure of the subsequent year. Because cryptobenthic reef fishes cannot be surveyed adequately using visual surveys, we used enclosed ichthyocide stations to sample the entire small benthic fish communities (e.g. Ackerman and Bellwood 2000; Brandl et al. 2019c; Morais and Bellwood 2019). Each station was enclosed in a 2 mm-mesh mosquito net (double bed), weighed along the perimeter by a 2.3 m long steel chain. The net was sown over the chain to avoid coral abrasion. The net was then enclosed in a 2-man tent, again weighed down by a chain. All fishes within the net were euthanized with rotenone or (after 2000) anesthetized with clove oil (cf. Ackerman and Bellwood, 2000); both rotenone and clove oil equally sample benthic fishes (Ackerman and Bellwood 2002). After five minutes, the divers slowly removed the tent and net, searching for anesthetized fishes. All fishes were collected in plastic bags and placed on ice. In the lab, the fishes were identified to species, where possible, and counted. All collections were done in compliance with approved permits (Great Barrier Reef Marine Park Authority G23/46994.1) and ethics (James Cook University A2752).

4.2.2 Productivity calculations

To calculate productivity, we followed Morais and Bellwood (2020) using the corresponding R package `rfishprod`, which incorporates somatic growth and mortality into estimates of biomass production. Using 1,000 bootstrapped boosted regression tree iterations from the *predKmax* function,

we were able to calculate the standardized growth parameter K_{max} for all species. In short, K_{max} is a standardisation of the Von Bertalanffy growth parameter K (Von Bertalanffy 1949) and can be interpreted as the rate at which fishes would reach their asymptotic size if they grew to the species' maximum recorded size (cf. Morais and Bellwood 2018). For each surveyed species, we recorded the maximum body size ever recorded for each species, dietary preference (i.e. herbivore/detritivore, herbivore/macroalgivore, planktivore, omnivore, mobile invertivore, sessile invertivore, and fish and cephalopod predator), and position in the water column (i.e. benthic, benthopelagic, pelagic) from the literature or from FishBase (Froese and Pauly 2021). Following the framework set forth by Morais and Bellwood (2018, 2020), we then combined these ecological traits with annual estimates of sea surface temperature using boosted regression trees, bootstrapped for 1,000 iterations, to generate estimates of K_{max} (Morais and Bellwood 2018, 2020). We collated annual mean estimates of sea surface temperature from weekly means for the same coordinate (18º35'35.412"S, 146º28'59.934"E) in Pioneer Bay for each year that was sampled from the National Ocean and Atmospheric Administration's Optimum Interpolation Sea Surface Temperature V2 (https://psl.noaa.gov/data/gridded/data.noaa.oisst.v2.html). The mean sea surface temperature over the entire survey period was 26.4ºC: the temperature was lowest in 1994, 1997, 2000, and 2011 (25.9ºC) and highest in 1998 (27.3ºC; **Appendix C**: Table C1). For each species, we recorded the median and the 95% confidence interval of the predicted K_{max} values.

At the community or population level, mortality can be expressed as a rate and is largely dependent on the age and size of each fish (Brown et al. 2004; Gislason et al. 2010; Morais and Bellwood 2020). To calculate the natural mortality rates (i.e. where fishing mortality is zero), we used a subsample of preserved individuals to generate size frequencies of all sampled benthic fish species. Specifically, we recorded the identity and measured the total length of all individuals collected in 2006 and 2011-2013 (**Appendix C**: Table C2). Using these measurements, we were able to generate local size distributions for all surveyed species. When there was not an adequate sample available to generate a size distribution at the species level, we used the distribution at the genus or family level. For each observation, we drew a total of 1,000 random samples from a truncated normal distribution

with a lower limit of zero, centred and shaped based on the corresponding species' mean and standard deviation, respectively. We then used the *predM* function with a Gislason mortality equation (Gislason et al. 2010) to calculate the instantaneous mortality rate of each bootstrapped body size estimate for each observation.

We followed Morais and Bellwood (2020, 2018) to incorporate growth and mortality rates with benthic fish surveys to calculate the productivity of each species. We used the Bayesian length-weight regression coefficients (Froese et al. 2014) to convert all bootstrapped estimates of body size into standing stock biomass (g). We then used the *applyMstoch* function to apply a probability of mortality for each individual by using a Bernoulli distribution based on the instantaneous mortality rate predicted from the *predM* function (see above) to determine the fate of each individual. The *somaGain* function was then used to calculate the somatic growth expected for each surviving individual, which was determined by the instantaneous mortality rate, over the course of one day. To calculate somatic growth, we drew values of K_{max} from a truncated normal distribution bound by the 95% confidence interval of predicted K_{max} values from the above-mentioned *predKmax* function. The total productivity (g day^{-1}) was then calculated as the sum of the somatic growth after one day of all surviving individuals over 1,000 bootstrapped iterations (Morais and Bellwood 2020).

4.2.3 Analysis

We used Bayesian generalised additive models (GAMs) to model the non-linear changes in abundance, standing biomass, species richness, and productivity of the benthic fish communities through time. We specified a negative binomial distribution with a log link to independently model the changes in abundances and richness, and a gamma distribution with a log link to independently model the changes in productivity and standing stock biomass through time. We generated individual GAMs to assess the changes of the entire fish communities. We also fit additional GAM models, fitting individual splines separately for cryptobenthic fishes and non-cryptic families. Because damselfishes (family Pomacentridae) can form relatively large schools around individual coral colonies, which can have disproportionally large impacts on biomass estimates, we further separated non-cryptic families

into Pomacentridae and all other fishes. Distributions were chosen based on the residual error structure of the response variable and by using leave-one-out information criterion (*looic*; see **Appendix C**). All models used 10,000 iterations with an initial burn-in phase of 2,000 iterations and a thinning rate of five. We used the default, weakly-informative priors and the thin plate regression splines as part of the `brms` package (Bürkner 2017). To validate the models, we ran posterior predictive checks, visually inspected simulated residuals from the `DHARMa` package (Hartig 2022), and used leave-one-out cross-validation to ensure that all Pareto-k diagnostic values were less than 0.7. We did not detect any temporal autocorrelation among any of the simulated residuals and achieved chain convergence on all estimated parameters for all models (rhat = 1.00).

To determine whether temporal changes in the abundance, richness, standing stock biomass, and productivity of benthic fishes coincided with disturbance years, we also tested for ecological thresholds in each non-linear time series. Here, ecological thresholds are defined as relatively large changes in the ecosystem state (i.e. abundance, standing biomass, species richness, or productivity) as a response to environmental stressors (Samhouri et al. 2017), such as mass bleaching events or tropical storms. Following Samhouri et al. (2017) and Fewster et al. (2000), we quantified ecological thresholds by calculating the curvature of each time series using its respective second order derivative of each fitted GAM. Positive second order derivatives indicate U-shaped valleys in the time series, whereas negative second order derivatives indicate peaks in the time series; second order derivatives around zero indicate relatively linear patterns (Fewster et al. 2000). We calculated the second order derivatives of each posterior draw for the smoothing term *s(year)* for the whole-community model and *s(year, by = crypto)* for the cryptobenthic model, and determined the strength of the threshold by assessing the median and the 95% credible interval across all posterior draws.

Finally, for all identified ecological thresholds, we assessed the changes in community composition before and after the threshold year. We performed a non-metric multidimensional scaling ordination (NMDS) using a Bray-Curtis dissimilarity matrix based on species' abundances or standing biomass (see Results). We used a fourth root and a Wisconsin double transformation on the abundance/biomass data before using a PERMANOVA to assess the difference in communities before

and after the threshold. We also conducted similarity percentage (SIMPER) analyses to assess the contribution of each species to the separation of each community. All multivariate analyses were conducted using the `vegan` package (Oksanen et al. 2020); all models and figures were generated in R v 4.1.0 (R Core Team 2024).

4.3 Results

Approximately half of all fishes were cryptobenthic fishes (sensu Brandl et al., 2018), mainly gobies; the remainder were mainly planktivorous damselfishes and a range of small-bodied species belonging to large-bodied families (e.g. *Pteragogus cryptus* of the family Labridae; see Brandl et al., 2018). The mean number of cryptobenthic fishes sampled per year ranged from 1.52 in 1997 to 5.89 in 2015, whereas the mean number of fishes from the family Pomacentridae ranged from 3.64 in 1998 to 24.1 in 2000. Only one individual was recorded from non-cryptic fishes (excluding Pomacentridae) in 1993, 1994, 1996, and 1997; in 2001, mean abundance was 3.1. We recorded the fewest number of individuals per station in 1998 (n = 38) and the highest in 2009 (n = 404).

4.3.1 Changes in productivity and proxies

We found a distinct shift in the energetic dynamics between the pre- and post-1998 bleaching benthic fish communities. Despite multiple disturbances, we found an overwhelming pattern of stasis in the productivity of the post-bleaching fish assemblage (i.e. 2001 onwards), with no evidence of any change between 2001 and 2021, despite multiple stressor events (median percent change [95% credible interval]: -24% [-59% to 21%]; **Fig. 4-1a**). These patterns of stasis were similarly mirrored in cryptobenthic fishes (-17.3% [-67.1% to 61.5%; **Fig. 4-1b**), pomacentrids (-39.6% [-70.6% to 5.95%]), and non-cryptic fishes (19.0% [-42.2% to 100.0%]; **Fig. 4-1c**). The pre-bleaching assemblage, however, exhibited a strong increase in the productivity of the entire benthic reef fish communities between 1993 and 2001 by 110% [3% to 284%]. This increase was not likely driven by any particular group, as there was no evidence of an increase across cryptobenthic fishes (130% [-

14.4% to 401%]), pomacentrids (111% [-20.8% to 297%]), nor non-cryptic fishes (58.3% [-21.4% to 268%]).

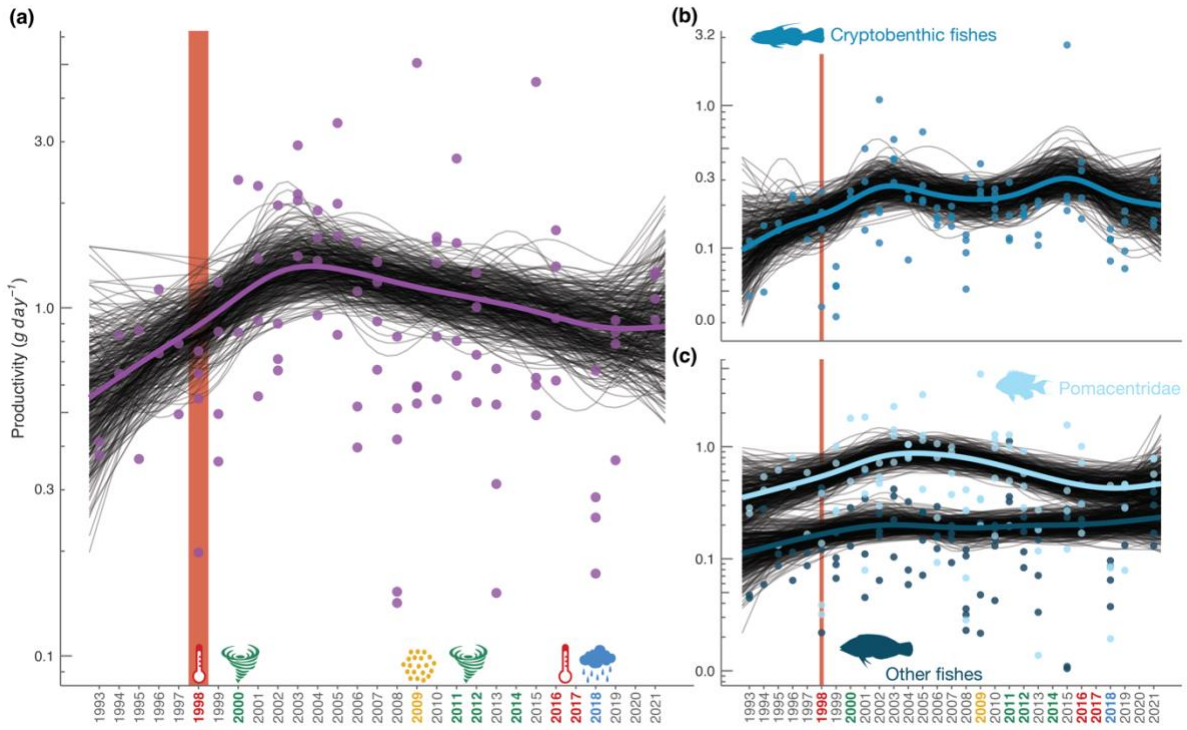

Figure 4-1. Patterns of benthic reef fish productivity. *Patterns of benthic reef fish productivity (g day-1) through time of* ***a*** *the entire fish community,* ***b*** *cryptobenthic fishes, and* ***c*** *non-cryptic fishes. The thin black lines are 400 randomly sampled draws from the posterior distribution and the thick coloured lines show the median trends. The coloured points denote the raw data points. Note the y-axes are different and on the* log_{10} *scale. The red bars indicate the 1998 mass coral bleaching event. The coloured axis labels along the bottom illustrate the major stressors that have impacted Orpheus Island along the timeline, including coral bleaching events (red), cyclones (green), sedimentation (yellow), and floods (blue).*

We found slightly different patterns in the proxies of productivity between the entire community responses compared to the responses of individual fish groups (i.e. cryptobenthic fishes, pomacentrids, and non-cryptic fishes). The abundance of the community followed a similar pattern to the productivity of the community and increased 100% [23% to 198%] from 1993 to 2001, and then stabilised from 2001 to 2021 (-17% [-45% to 19%]; **Fig. 4-2a**). From 1993 to 2001, there was no change in the abundance of pomacentrids (79.9% [-10.5% to 202%]) nor non-cryptic fishes (54.2% [-30.3% to 211%]; **Fig. 4-2b**); however, the abundance of cryptobenthic fishes increased 109% [11% to 237%]. The abundance of cryptobenthic and non-cryptic fishes had remained stable from 2001 to 2021 (6.82% [-39.9% to 64.5%] and 38.6% [-23.1% to 125%], respectively; **Fig. 4-2b**). During this time, however, the abundance of pomacentrids had declined by 44% [-69.8% to -11.2%].

The standing stock biomass of the entire fish community had remained relatively stable between 1993 and 2001 (-73.2% [-11.9% to 189.0%]) and between 2001 and 2021 (-33.4% [-62.9% to 6.1%]; **Fig. 4-2c**). We found no evidence for changes in the standing stock biomass between 1993 and 2001 for cryptobenthic fishes (193% [-33.4% to 587%]), pomacentrids (59.3% [-30.9% to 214%]), nor non-cryptic fishes (40.4% [-26.5% to 223%]; **Fig. 4-2d**). Similarly, between 2001 and 2021, we detected no changes in the biomass of pomacentrids (-42.9% [-73.7% to 2.99%]) nor non-cryptic fishes (-4.9% [-55.2% to 62.5%]; **Fig. 4-2d**). Conversely, the biomass of cryptobenthic fishes had declined by 54.3% [-83.5% to -0.63%].

We found a strong change in the species richness of the community surrounding the 1998 mass bleaching event. Prior to 1999, species richness had strongly declined by -27% [-48 to -3%], then shifted and increased 35% [10% to 63%] over the following four years to near pre-bleaching levels (**Fig. 4-2e**). Species richness then fluctuated but remained relatively stable from 2003 onwards, only changing -9% [-30.3% to 13%]. We found no change in the richness of cryptobenthic fishes (-9.0% [-33.8% to 23.7%]), pomacentrids (-23.2% [-61.0% to 14.9%]), nor non-cryptic fishes from 1993 to 2001 (3.5% [-36.2% to 40.0%]; **Fig. 4-2f**), nor from 2001 to 2021 (cryptobenthic fishes: 3.4% [-23.4% to 34.1%]; pomacentrids: -6.5% [-41.4% to 43%]; non-cryptic fishes: 23.3% [-15.7% to 77.2%]; **Fig. 4-2f**).

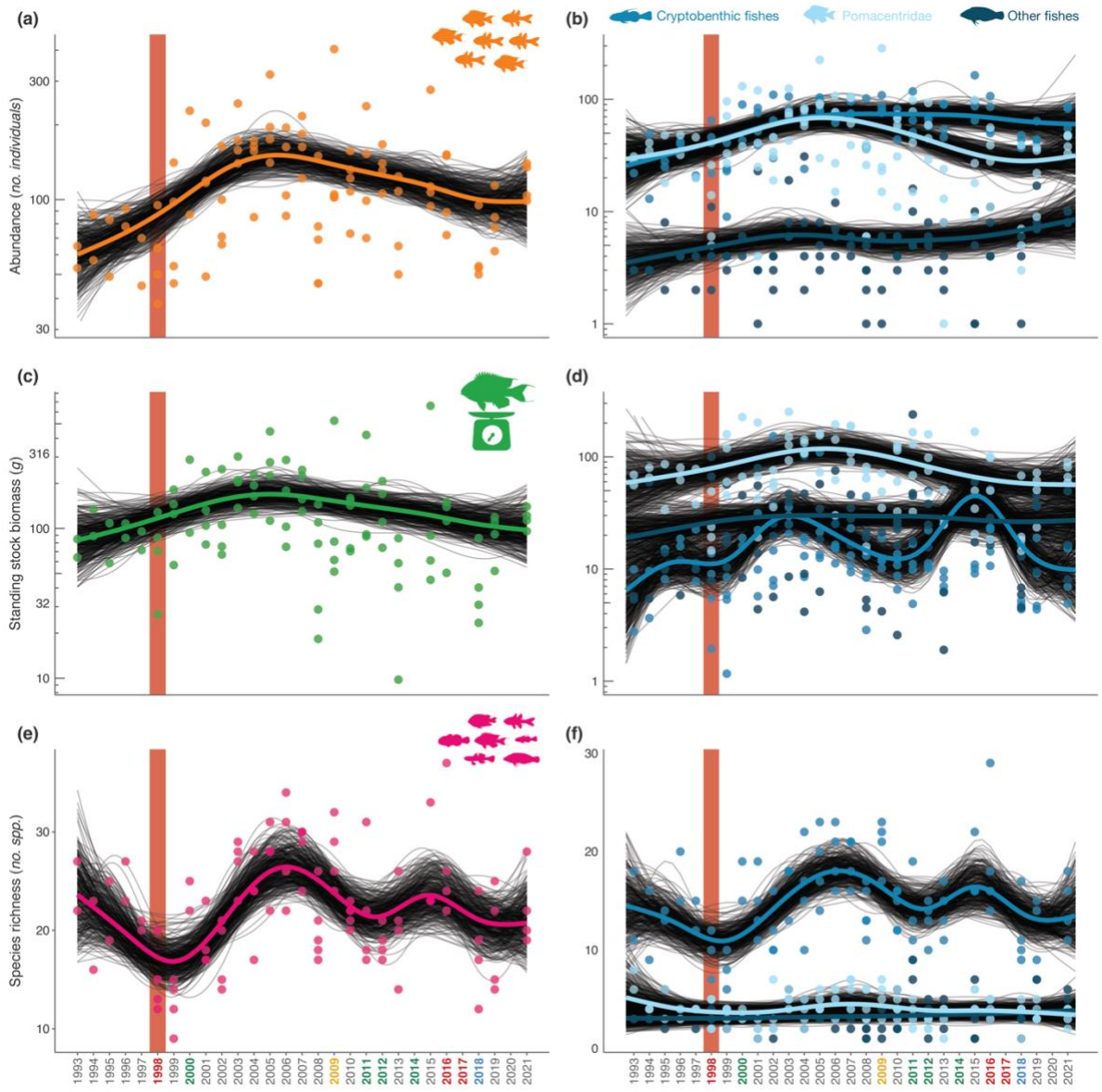

Figure 4-2. Patterns of abundance, standing biomass, and species richness. *Patterns of* ***a-b*** *log_{10} abundance,* ***c-d*** *log_{10} standing stock biomass, and* ***e-f*** *species richness of entire benthic reef fish communities (****a****,* ***c****,* ***e****) through time. Panels (****b****,* ***d****,* ***f****) show the respective patterns, separated by cryptobenthic fishes (medium blue), damselfishes (family Pomacentridae; light blue), and other non-cryptic fishes (dark blue). The thin black lines show 400 random draws sampled from the posterior distribution, while the thick coloured lines denote the median trends. The red bars indicate the 1998 mass coral bleaching event and the coloured points are showing the raw data points. The axis text colours along the bottom denote the stressors as shown in* ***Figure 4-1****.*

4.3.2 Ecological thresholds

By assessing the second order derivatives at the community level, we found no evidence for ecological thresholds in the productivity, abundance, nor the standing biomass of benthic fishes through time (**Fig. 4-3a-c**). We found a single ecological threshold in species richness in 1999, only one year after the 1998 mass bleaching (median second order derivative [95% credible interval]: 0.051 [0.0026 to 0.11]; **Fig. 4-3d**). This ecological threshold surrounding the 1998 mass bleaching event resulted in a distinct shift in community composition. The PERMANOVA explained 80.9% of the variation in species' abundances and used 999 permutations (**Fig. 4-4a**). The centroids of the pre-bleaching and post-bleaching benthic fish assemblages were significantly different from one another (*d.f.* = 1, F = 5.3, $p < 0.01$), as illustrated by completely separate community clusters (**Fig. 4-4a**). The 10 most influential species show a distinct shift in coral feeding fishes and carnivores loading towards the pre-bleaching assemblage (**Fig. 4-4b**).

We found a single, negative ecological threshold in the time series assessing the standing stock biomass of cryptobenthic fishes in 2015 (-3.29 [-5.89 to -0.933]; **Appendix C**: Fig. C1). Using 999 permutations, the PERMANOVA on the biomass of cryptobenthic fishes explained 81.7% of the variation and showed a significant deviation from the centroid between the two communities (*d.f.* = 1, F = 2.1, p = 0.03; **Appendix C**: Fig. C2). Although there is overlap between the two community convex hulls, we also found significant dispersion between the two communities, whereby the community of cryptobenthic fishes became less variable after 2015 (*d.f.* = 1, F = 6.0, p = 0.02; **Appendix C**: Fig. C2).

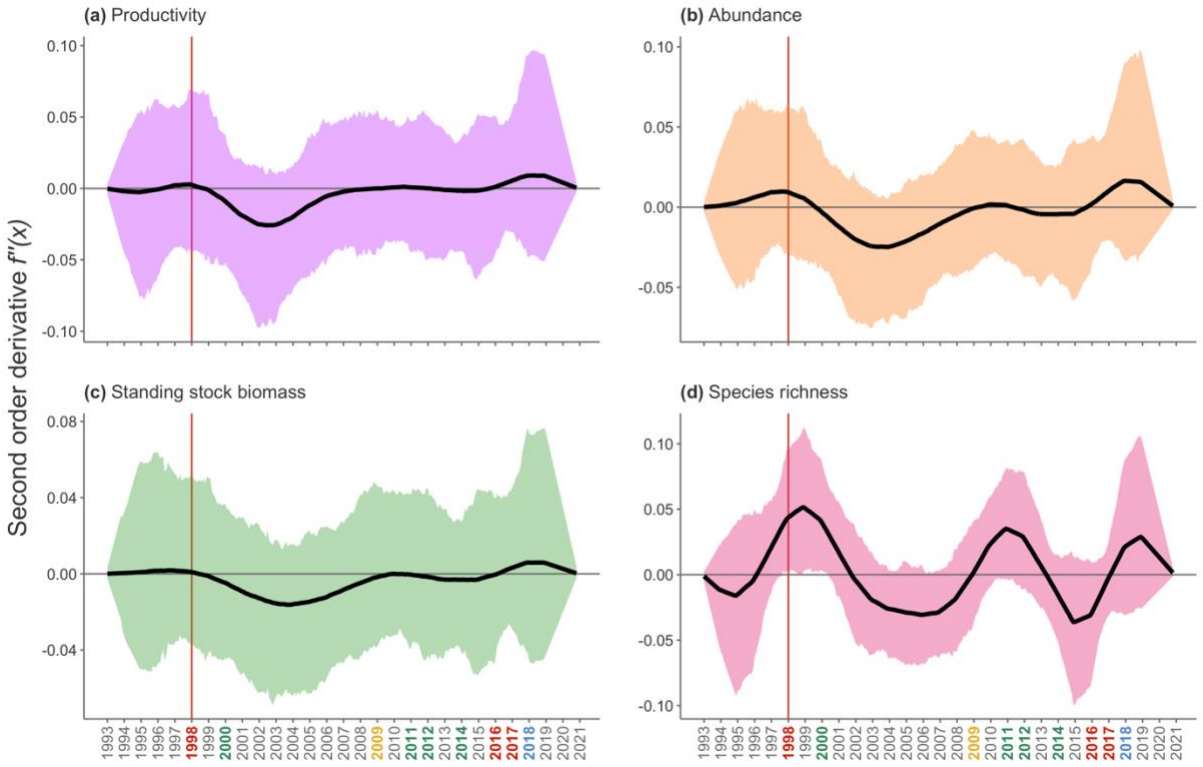

Figure 4-3. The detection of ecological thresholds. *Second order derivatives calculated for* ***a*** *productivity,* ***b*** *abundance,* ***c*** *standing stock biomass, and* ***d*** *species richness of the entire benthic fish assemblage. The coloured ribbons denote the 95% credible intervals and the thick black lines denote the median trend lines. Ribbons crossing zero indicate relatively linear patterns; positive values indicate U-shaped valleys and negative values indicate peaks in the time series. The red line indicates the 1998 mass coral bleaching events and the coloured axis text along the bottom denotes the stressors as shown in* ***Figures 4-1*** *and* ***4-2****.*

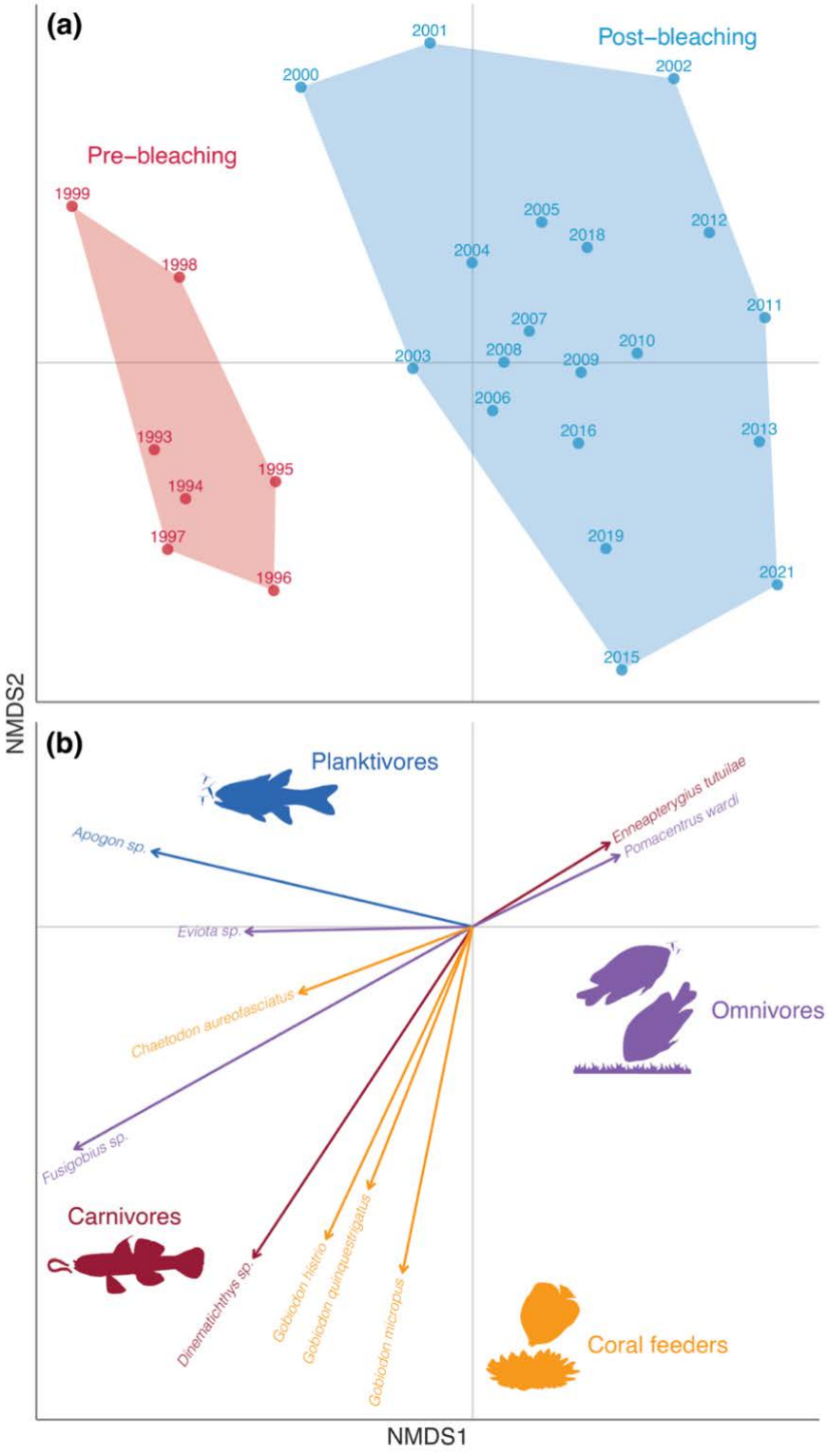

Figure 4-4. The effect of the 1998 bleaching event on community composition. a *Non-metric multidimensional scaling (NMDS) ordination of benthic fish communities before (i.e., pre-bleaching; red) and after (i.e., post-bleaching; blue) the 1998 mass coral bleaching event on the Great Barrier Reef. Sample years are labelled above their respective points and polygons encapsulate all points for a given sample period (i.e. before or after bleaching).* ***b*** *The relative contribution of the ten most important species contributing to the separation of the pre- and post-bleaching assemblages, coloured by dietary preferences.*

4.4 Discussion

By applying a novel assessment of fish biomass production to a long-term monitoring dataset of high spatial and temporal resolution, we were able to assess the changes in benthic fish productivity through time. Despite the magnitude of coral loss and disturbance over the last three decades at Orpheus Island, we only detected a discernable shift in the productivity, total abundance, and richness of benthic reef fish assemblages after the first mass coral bleaching event in 1998, where roughly 65% of the corals near Pioneer Bay were affected by bleaching and between 5-10% died (Marshall and Baird 2000). Before 2001, we found increases in both the productivity and abundance of benthic fishes coinciding with a decrease in species richness, which was mirrored by an increase in the abundance of cryptobenthic fishes. However, the productivity and abundance of benthic reef fishes began stabilising around 2001, with species richness returning to pre-bleaching levels in 2003 and fluctuating only slightly during the remainder of the time series. From 2001 onwards, we found a decline in the abundance of pomacentrids and a decline in the standing stock biomass of cryptobenthic fishes. Despite changes in productivity, abundance, and species richness, we found no discernable change in standing stock biomass over the entire sampling period. Overall, although there has been a considerable reshuffling of the benthic fishes following the first mass coral bleaching event in 1998, the key ecosystem function of fish biomass production was maintained by this altered system, despite major ongoing stressors.

The 1998 mass coral bleaching event experienced on the GBR has undeniably reshaped the community composition of benthic reef fishes at Orpheus Island (Bellwood et al. 2006, 2012; Hemingson et al. 2022); consequently, specific species or families have exhibited a range of responses in productivity through time. Such variation in productivity has been reported in specific groups of fishes across various reef systems, including studies on the GBR (e.g. Morais et al. 2020; Tebbett et al. 2021) and the Seychelles (Hamilton et al. 2022). Interestingly, despite this relatively high species turnover, the functioning of the benthic fish communities after the first mass bleaching event has remained remarkably stable, which was consistent in both process-based and static proxies of productivity. This is likely driven by the specific life history traits and mortality rates expressed by

small benthic reef fishes, including cryptobenthics, which are epitomised by their high-turnover-high-productivity lifestyles. Their small body sizes and subsequent extremely high mortality rates drive shorter lifespans in cryptobenthic fishes, while high abundances and constant reproduction result in a steady supply of nearshore cryptobenthic reef fish larvae (Brandl et al. 2018, 2019c). Consequently, the loss of corals and coral-associated fishes creates new niches that can be quickly colonized by the nearby larvae of cryptobenthic fishes that prefer degraded reef configurations (e.g. detritivores; Bellwood et al., 2012).

The extent and intensity of the first mass bleaching event on the GBR marked a clear shift in the energetic dynamics of small benthic fishes. Indeed, this shift from coral-associated fishes towards species that are less dependent on corals is well documented by Bellwood et al., (2012, 2006). Similarly, brightly coloured benthic fishes, which are associated with high coral cover, declined drastically immediately after the 1998 bleaching event and shifted towards communities comprising duller colours, a characteristic of degraded reef habitats (Hemingson et al. 2022). We found similar shifts in the benthic fish communities: species richness declined before the bleaching event, which coincided with an increase in total abundance and productivity (see **Figs. 4-1** and **4-2**). Additionally, the community composition immediately following the bleaching event was significantly different from the pre-bleaching assemblage (see **Fig. 4-4**). 87% of inshore reefs, such as those found near Orpheus Island, experienced bleaching during the 1998 mass bleaching event on the GBR (Berkelmans and Oliver 1999). The subsequent coral mortality, which was roughly 5% near Pioneer Bay (Baird and Marshall 2002, 2002), may have shifted the community composition from comprising slower-growing, coral-associated fishes, including a loss of coral-associated damselfishes, to highly productive detritivores and planktivores. Indeed, despite the decline in standing stock biomass of cryptobenthic fishes (and a peak-shaped threshold around 2015), their stable productivity likely represents a shift from larger-bodied, coral-associated gobies (e.g. *Gobiodon* spp.) to smaller-bodied, detritivorous gobies (e.g. *Eviota* spp.).

While environmental stressors are shifting the composition of fish communities, they may also be generating communities that can withstand subsequent disturbance events. Although species

richness may not buffer communities against large-scale habitat changes *per se* (Yan et al. 2022), communities comprising species with diverse habitat/diet preferences may contribute to the stability in ecosystem functioning via the "portfolio effect" (Schindler et al. 2010, 2015). For example, the loss of corals has been associated with a shift in fisheries catch composition (Robinson et al. 2019) and trophic-specific community size structuring (Rogers et al. 2018a), yet the total biomass yield in both instances has remained relatively stable (or increasing). These altered communities, which are capitalising on newly available resources, may be positively co-tolerant to subsequent stressor events (i.e. more functionally resilient) and can sustain consistent levels of biomass production and abundance.

This constancy of small benthic reef fish productivity may provide a glimpse into the future functioning of coral reefs impacted by multiple stressors. Although specific families and the functions they supply likely declined following the first mass bleaching event in 1998, the altered, post-bleaching community as a whole may be able to maintain functioning at a consistent level. Cryptobenthic reef fishes contribute disproportionally more to the consumed biomass on coral reefs (Brandl et al. 2019c); therefore, their ability to maintain high levels of productivity indicates that these bottom-up processes on degraded reefs may be resilient to large-scale perturbations, regardless of the species composition of the community. Consequently, the productivity of benthic reef fishes may provide a strong foundation to fuel the productivity of higher trophic levels on transitioning coral reefs. Given that millions of people globally are reliant on the productivity of coral reef fishes for food and financial security through fisheries (Wilkinson 2004; Teh et al. 2013), understanding the resilience of the key ecosystem functions and services of degraded coral reefs will be pivotal to the effective conservation of reefs in the Anthropocene.

Progress in basic natural science is a matter of constantly rebuilding from the very foundations. Significant progress is generally a matter, not of adding further facts, but of changing the framework itself…Science in the main develops not by way of cumulation but by way of substitution and replacement.

Nicholas Rescher
The Limits of Science

Chapter 5: Species abundances surpass richness effects in global biodiversity-ecosystem function relationships

Published as: Yan, H.F., Morais, R.A., Bellwood, D.R. (Accepted). Species abundances surpass richness effects in the biodiversity-ecosystem function relationship across marine fishes. Nature Communications.

Abstract

High biological diversity (or biodiversity), scaling from genomes to entire ecoregions, has been thought to bolster communities against disturbances, leading to disproportionally higher levels of ecosystem functioning (i.e. the movement or storage of energy/matter). While the biodiversity-ecosystem function relationship, or BEF, has been particularly evident in studies equating diversity to species richness, it is still unclear which ecological mechanisms can produce different observational BEF effects. We used 7,686 individual growth curves across 1,480 species to generate a process-based estimate of a key function, biomass production, to assess the BEF across marine reef fishes. We found that Hill diversity emphasising abundances outpaced the effects of species richness and community evenness. In high-latitude temperate regions, species abundances and richness had indistinguishable effects on reef fish productivity. In the tropics, however, species abundances vastly surpassed species richness effects on functioning, indicating that species richness had only a limited impact on functions in the tropics. These geographic disparities were driven by trade-offs in the relationship between abundance and per-capita productivity: low-diversity communities were characterised by lower abundances but higher per-capita productivity; high-diversity communities the opposite. Because whole-community productivity remained relatively stable across diversity gradients, these trade-offs were presumably driven by metabolic constraints on growth and body size imposed by warmer temperatures. It appears that biodiversity can only bolster ecosystem functioning to a limited extent; environmental stressors will likely limit the function delivery of marine fishes globally.

Keywords: diversity-stability; growth; Hill diversity; productivity; Reef Life Survey; Von Bertalanffy

5.1 Introduction

With increasing anthropogenic threats to biodiversity (Ceballos et al. 2015; Mace et al. 2018), a pervasive question that has arisen is whether natural communities possess internal regulatory mechanisms that can bolster critical ecosystem functions. Grounded in ecological theory, the biodiversity-ecosystem function relationship, or BEF, has been posited as a positive causal link between biodiversity and ecosystem functioning through complementary resource use via coexistence and niche partitioning (i.e. functional complementarity; Naeem et al. 1994; Loreau 2000; McCann 2000; Loreau and Hector 2001; Blüthgen and Klein 2011; Thibaut et al. 2012; Tilman et al. 2014). While there is a general consensus that biodiversity has a positive, albeit saturating, relationship with ecosystem functioning (e.g. Cardinale et al. 2012), these effects appear to be sensitive to the choice of function (e.g. Lefcheck et al. 2015), the choice of diversity metric [e.g. Simpson Index, Shannon Entropy, or richness (Roswell et al. 2021) vs. taxonomic, functional, or evolutionary (e.g. Barber et al. 2017)], or the choice of analytical method (e.g. generalised models or causal inferences; Dee et al. 2023). Indeed, scientists have scrutinised nearly every axis of the BEF, yet there is one critical factor that influences community assembly that has been widely overlooked: species abundances (Barneche et al. 2016, but see Winfree et al. 2015; Woodcock et al. 2019). In an attempt to isolate the role of biodiversity on ecosystem functioning in experimental studies, scientists have artificially controlled for the role of abundance (Schmid et al. 2002), which typically do not reflect naturally occurring abundances in the field. Across observational BEF studies, abundances have been typically consolidated within the "function" component (Pillai and Gouhier 2019), such as the calculation of standing stock biomass (e.g. Duffy et al. 2016), or standardised against during analyses (e.g. Mora et al. 2011). Dominance, which indirectly considers species relative abundances, has been used in observational BEF studies, however, it can have variable effects across both functions (e.g. Schiettekatte et al. 2022) and ecosystems (e.g. Dangles and Malmqvist 2004; Hodapp et al. 2015; Maureaud et al. 2020). While commonly used biodiversity metrics (e.g. species richness) and indices (e.g. Shannon, Simpson), and using coverage-based sampling can mitigate differences in rarity and detection biases (Chao and Jost 2012; Chao et al. 2014), they are unable to eliminate the effects arising from species relative abundances (Roswell et al. 2021). Indeed, experimental studies have highlighted

that relative abundances can sway the direction of BEF studies (Polley et al. 2007; Dee et al. 2023; Roswell et al. 2023) with higher abundances typically translating into higher function delivery (e.g. Mason et al. 2008; Wittebolle et al. 2009; Stuart-Smith et al. 2013; Woodcock et al. 2019; Morais et al. 2021; Munger et al. 2023). Consequently, the role of species' abundances may provide a valuable mechanistic link between biodiversity and function delivery.

Here, we used one of the world's largest standardised global survey programs on marine fishes, the Reef Life Survey program (Edgar and Stuart-Smith 2014; Edgar et al. 2020), to assess whether species' abundances would influence the BEF globally. Marine fishes exhibit extraordinary patterns of taxonomic and life history trait diversity (Stuart-Smith et al. 2013; Siqueira et al. 2023), while contributing to a range of ecosystem functions (Morais and Bellwood 2020; Schiettekatte et al. 2022) and providing valuable ecosystem services via fisheries. In particular, fish biomass production is one of the few key processed-based ecosystem functions (Bellwood et al. 2019b; Brandl et al. 2019b; Morais and Bellwood 2020), that can be readily estimated by using mechanistic relationships (i.e. somatic growth models) with direct ramifications for fisheries (Robinson et al. 2019; Morais et al. 2023). Here, productivity is defined as the biomass accumulated via ontogenetic growth of all individuals (without mortality) over the survey area over the course of one day (Morais and Bellwood 2020). By building predictive models from 7,686 growth curves across 1,480 species, we were able to estimate the local per-capita productivity of marine fishes from 2,957 sites comprising coral and rocky reefs, spanning tropical to polar locations (**Appendix D**: Fig. D1). In doing so, we were able to (1) disentangle the role of species' abundances on the total community biomass production of marine fishes and (2) assess the role of biodiversity both globally and across geographic regions.

5.2 Methods

We defined ecosystem functions as the movement or storage of energy or materials through an ecosystem (Bellwood et al. 2019b; Brandl et al. 2019b). We therefore adapted and applied a relatively novel approach for calculating biomass production (Morais and Bellwood 2020), which is quantified as the rate of biomass produced via ontogenetic growth of all surveyed individuals over 500 m^2 over

the course of one day, instead of using a proxy for functioning [e.g. standing stock biomass as seen in Duffy et al. (2016)]. We first conducted a systematic literature review on all published Von Bertalanffy growth models on marine teleost fishes from around the world to build a machine learning model to predict growth coefficients for fishes without empirically measured growth curves [as in Siqueira et al. (2023)]. Predictive models used a combination of ecological and environmental trait data, while also accounting for the aging method used (see below). We then used predicted growth coefficients to calculate the biomass production of reef fishes censused from one of the largest standardized global survey programs in the world: the Reef Life Survey program (Edgar and Stuart-Smith 2014; Edgar et al. 2020). Although the Reef Life Survey program specifically censuses relatively shallow reef habitats, some of the species recorded have lower depth limits beyond 1000 m, hence we included all fishes in our systematic literature review. We then used Hill numbers to holistically capture multiple axes of biodiversity and assessed the BEF from the best-fitting Hill diversity metric. All models accounted for potential sources of environmental variation (i.e. water visibility, survey depth, temperature) and spatial heterogeneity (i.e. realm- and site-level effects).

5.2.1 Data collation

We expanded on the framework developed by Morais and Bellwood (2018) to generate standardised species-level estimates of somatic growth across marine teleost fishes. In short, we used a derivation of the Von Bertalanffy Growth Model (Von Bertalanffy 1949) known as K_{max}, which can be interpreted as the rate at which an individual along a specific growth trajectory would reach its asymptotic size if it grew to the species' maximum recorded size (Morais and Bellwood 2018). Please see Morais and Bellwood (2018) for a detailed description of the quantification of K_{max} and its associated equations. Because Morais and Bellwood (2018) only considered coral reef fishes, we expanded on this by (1) first conducting a systematic literature review of all published Von Bertalanffy growth curves for all marine fishes, including reef and non-reef habitats; and (2) generating new predictive models to predict K_{max} across all marine teleost fishes. Although we are estimating growth rates for fishes surveyed in relatively shallow coastal, hard substratum-associated

habitats, fishes found in pelagic systems or from deeper waters have been recorded on Reef Life Survey transects. To ensure accurate growth estimates for all available fishes, we included observations from all non-reef habitats in our predictive models.

We collated a list of growth studies from FishBase (Froese and Pauly 2021; accessed May 2022; *n = 5,770*), which we supplemented with a systematic literature review (completed September 2022; *n = 1,816*; as used in Chapter 3). We used the ISI Web of Science database using the search string *fish * AND (growth OR von Bertalanffy)*, which resulted in 141,649 articles. We filtered articles based on their titles and abstracts, removed all duplicates between the two sources, and corrected any recorded any typological/rounding errors recorded from FishBase. We only included studies where species were collected from marine habitats (we omitted all freshwater species that were recorded in euryhaline habitats) and those where the discrete geographic locations were provided (see Morais and Bellwood (2018) for a detailed explanation). This yielded 7,686 growth curves encompassing 1,480 species. From each study, we extracted the Von Bertalanffy growth parameters L_∞ and K, the length measurement type (i.e. total length, standard length, or fork length), the method used for aging (i.e. mark recapture, growth rings (e.g. otolith, scale, or vertebrae), length frequency, or unknown), and the geographic location. We then used the length-length conversion factors from FishBase to transform all estimates of L_∞ to total length in cm.

With the mined growth values from the literature, we generated predictive Extreme Gradient Boosting models to use a series of traits and environmental variables to (1) explain variation in K_{max} across fishes with empirically measured growth values and (2) predict K_{max} for fishes lacking data [as in Siqueira et al. (2023)]. Specifically, we predicted growth trajectories for all the fishes recorded using a standardised global underwater visual census program, the Reef Life Survey program (accessed 16 December 2021). In short, reef fish communities were censused along 50 m-long transects along coral and rocky reefs around the world. Trained divers recorded the identity, size class, and abundance of all fishes across one-to-two 250 m^2-area blocks along a transect along relatively shallow depth ranges (< 20 m). Detailed explanations of the survey methods can be found online (www.reeflifesurvey.com). We removed all surveys that were only composed of a single block from

analyses (n = 171). For each species, including those from the mined literature and those recorded from the Reef Life Survey, we recorded the following trait data: maximum body size (total length, cm), trophic level (continuous), maximum depth (m), and position in the water column (categorical). Most of the trait data came from FishBase or the primary literature; when data were not available at the species level, we used estimates at the genus or family level. We used a 2º buffer around their respective locations and the years that they were sampled to generate an estimate of sea surface temperature (ºC) using raster data from the National Oceanic and Atmospheric Administration (https://psl.noaa.gov/data/gridded/data.noaa.oisst.v2.html).

5.2.2 Predicting growth

We combined the trait data (i.e. maximum body size, maximum depth, trophic level, and position in the water column) with estimates of sea surface temperature and the aging method (i.e. mark recapture, otolith rings, scale rings, other rings, length frequency, and unknown) in an Extreme Gradient Boosting framework (Chen and Guestrin 2016; Chen et al. 2018) to explain the variation and predict the growth trajectories (K_{max}) of all the fishes recorded on Reef Life Survey (i.e. all surveyed fishes were given a predicted growth trajectory). Extreme Gradient Boosting models are a form of machine learning algorithm that combine multiple decision trees with a boosting algorithm, exhibit relatively high predictive accuracy, and are able to handle non-linearities and complex interactions (Elith et al. 2008). We modelled K_{max} using a Gamma loss function and selected hyperparameters using the two-step tuning method from Morais and Bellwood (2018) and Siqueira et al. (2023), which involved varying the learning rate (eta; 0.1-0.9), regularising parameter (gamma; 0.1-0.9), maximum tree depth (max_depth; 5, 10, or 15), and the subsample rate (0.1-0.9). The final hyperparameters reduced the negative log likelihood from 2.88 to 1.70 using the following hyperparameters: eta = 0.098, gamma = 0.89, max_depth = 10, subsample = 0.096.

We used a cross-validation procedure to model and predict K_{max}. The model was built and trained on 80% of the data and assessed against the remaining 20% test set. We assessed the model's bias by subtracting the predicted K_{max} value from the test set against the observed value; a well-fitted

model should have a bias close to zero. The model performance was also assessed by extracting the R^2 (i.e. the goodness of fit) value from fitting a linear model between log(predicted) against log(observed) values from the test set. Finally, we predicted K_{max} values for all the species recorded from the Reef Life Survey program. Due to the stochastic model-building procedure of Extreme Gradient Boosting models, we bootstrapped the entire process for 1,000 iterations, using the `XGBoost` package v.1.4.1.1 (Chen and Guestrin 2016; Chen et al. 2018) in R v.4.1.0 (R Core Team 2024). We chose to predict growth using the aforementioned method because our XGBoost models achieved a low median prediction bias of -0.005 (minimum, maximum: -0.01, 0.0008) and a high median precision R^2 of 0.72 (0.65, 0.76; **Appendix D**: Fig. D2), whereas phylogenetic predictive models (e.g. Thorson et al. 2023) can produce predictions with an accuracy as low as 51%. As in Morais and Bellwood (2018) and Siqueira et al. (2023), maximum body size was the best predictor of K_{max} (median variable importance: 43.1%), followed by sea surface temperature (21.1%), maximum depth (14.6%), trophic level (12.1%), aging method (5.3%), and position in the water column (3.7%; **Appendix D**: Fig. D3; Table D1).

5.2.3 Calculating productivity

We calculated productivity following the methods set forth by Morais and Bellwood (2020) using our newly estimated values of K_{max}. In short, productivity is measured as the amount of biomass acquired via somatic growth of all individuals in a community over the course of one day.

$$Productivity = standing\ biomass + somatic\ growth$$

Here, the expected biomass is the standing biomass plus the expected biomass arising via somatic growth, the observed biomass is the community standing biomass, and *t* is the day. This generates a functional, process-based quantification of biomass production (Bellwood et al. 2019b; Brandl et al. 2019b; Streit and Bellwood 2022), which captures the underlying energetic and elemental fluxes experienced by the community compared to static proxies, such as standing stock biomass (Morais and Bellwood 2020; Schiettekatte et al. 2022). To place each individual within their growth trajectories, we randomly drew K_{max} values from a truncated normal distribution from their 90% predicted quantile

range. We then simulated the growth that would be expressed by each individual over the course of one day and used the difference between the two biomass estimates as the estimate of productivity. The total productivity was therefore calculated as the sum of the somatic growth of all individuals over the course of one day over 1,000 bootstrapped simulations (Morais and Bellwood 2020).

5.2.4 Quantifying biodiversity

To capture multiple axes of biodiversity, namely abundance and richness, we used Hill numbers with different scaling parameters. Common indices used to quantify biodiversity (e.g. species richness) can be sensitive to rare species occurring in low abundances, whereas Hill numbers provide a continuous framework to estimate the effective number of species present (Hill 1973; Jost 2006). Following Roswell et al. (2021, 2023), we calculated Hill diversity (*D*) as:

$$D = \left(\sum_{i=1}^{S} p_i \left(\frac{1}{p_i} \right)^{\ell} \right)^{1/\ell}$$

Here, p_1, p_2, …, p_S are species relative abundances for species richness *S*. This formulation of D allows for the differentiation between weights via abundance and rarity by controlling values of the scaling parameter ℓ (Roswell et al. 2021, 2023). Specifically, setting ℓ to different values (or calculating the limit as ℓ approaches zero) generates different diversity indices and can drastically influence BEF relationships (Roswell et al. 2023). We explicitly tested the inverse Simpson Index (ℓ = -1), exponentiated Shannon entropy (ℓ = 0), species richness (ℓ = 1), and the maximum abundance emphasis value tested by Roswell et al. (2023; ℓ = 10). Increasing emphasis on rarity will mathematically emphasise abundances: because the lowest possible count for a species is one individual (i.e. a singleton), increasing rarity can only be achieved by increasing the total abundance of all other species in the community (Roswell et al. 2023). Therefore, Hill numbers that emphasise rarity more than species richness place de facto emphasis on communities with high total abundances (Roswell et al. 2023). We ran individual BEF analyses with each metric of biodiversity (i.e. Simpson

Index, exponentiated Shannon entropy, species richness, and abundance index) and compared models by assessing relative effect sizes and using leave-one-out information criterion (*looic*).

5.2.5 Analyses

We first conducted a principal component analysis (PCA) to assess the correlation of all Hill diversity metrics, which were log-transformed prior to all analyses to reduce the leverage of transects with disproportionally high diversity values. We presented figures with non-logged values, however, to highlight our hypotheses that each additional species would have the greatest impact in low-diversity systems, with the effect of each additional species having a saturating effect. To assess the biodiversity-ecosystem function relationships, we used Bayesian generalised linear mixed-effects models (GLMMs) using productivity as the response variable. We individually modelled a global BEF model with productivity as a function of each Hill diversity metric (i.e. Simpson index, exponentiated Shannon entropy, species richness, and abundance index). We chose the top model as that which produced the smallest *looic* value. All models included an interaction term between Hill diversity and latitudinal position; latitudinal position was separated into temperate and tropical locations based on their respective geographic realms. We specified a gamma error distribution for all models by specifying gamma shape (ϕ) and rate (λ_i) parameters.

$$Gamma(y_i \mid \phi, \lambda_i)$$

$$\lambda_i = \frac{\phi}{\mu_i}$$

$$\log(\mu_i) = \beta_0 + \beta_D \log(x_D) + \beta_{trop} x_{trop} + \beta_{D*trop} \log(x_D)\, x_{trop} + \beta_{sst,vis,depth} \boldsymbol{X}_i + \alpha_{site}$$

$$\alpha_{site} \sim \alpha_{realm} + \varepsilon_{site}$$

$$\varepsilon_{site} \sim Normal(0, \sigma_{site})$$

$$\beta_0 \sim Normal(0, 5)$$

$$\beta_{D,trop,D*trop,sst,vis,depth} \sim Normal(0, 1)$$

Here, y_i is the observed community productivity for transect *i*, β_0 is the overall intercept, β_{D*trop} is the interaction term between diversity and the tropics, $\beta_{D,trop,sst,vis,depth}$ are the estimated effects for Hill diversity (*D*), tropics (*trop*), sea surface temperate (*sst*), visibility (*vis*), and depth, respectively. We ran an additional model following the top model structure, but used the Boltzmann-Arrhenius relationship to convert temperature to inverse temperature (1/temperature x Boltzmann's constant) with temperature in Kelvin (Gillooly et al. 2001). The term $\boldsymbol{X}_i$ is the design matrix of covariates. Site- and realm-level grouping factors are denoted as α_{site} and α_{realm}, respectively, following a nested structure of site within realm. We specified weakly informative priors on all estimated effects. We modelled per-capita productivity following the same model structure as total community productivity, but we added log-transformed abundance as an offset in the model. Adding an offset in the model allows us to measure productivity on a per-capita basis, while still following the same underlying gamma error distribution.

We followed a similar model structure when modelling changes in abundance (y_i) with diversity between temperate and tropical regions, but we specified a negative binomial distribution using the inverse shape parameter (ϕ) for overdispersion.

$$Negative\ Binomial(y_i \mid \mu_i, \phi)$$

$$\log(\mu_i) = \beta_0 + \beta_D \log(x_D) + \beta_{trop} x_{trop} + \beta_{D*trop} \log(x_D)\, x_{trop} + \beta_{sst,vis,depth} \boldsymbol{X}_i + \alpha_{site}$$

$$Var(y_i) = \mu_i + \frac{\mu_i^2}{\phi}$$

$$\alpha_{site} \sim \alpha_{realm} + \varepsilon_{site}$$

$$\varepsilon_{site} \sim Normal(0, \sigma_{site})$$

$$\beta_0 \sim Normal(0, 5)$$

$$\beta_{D,trop,sst,vis,depth} \sim Normal(0, 1)$$

For all models, we scaled and centred all continuous fixed effects by subtracting the mean and dividing by the standard deviation prior to analysis. All models used four Markov-Chain Monte Carlo

chains for 4,000 iterations after an initial warmup phase of 2,000 iterations using the `brms` package v.2.16.4 (Bürkner 2017). We assessed model fit using posterior predictive checks and simulated residuals from the `DHARMa` package v.0.4.5 (Hartig 2022) and achieved chain convergence for all estimate parameters (scale reduction factor Rhat < 1.01) and effective sample sizes were all greater than 1,800 (**Appendix D**: Table D2). Using Moran's I, we detected no spatial autocorrelation in the simulated residuals of any of the models. All modelled coefficients from GLMMs can be found in **Appendix D**: Table D2.

5.3 Results and Discussion

5.3.1 Abundances skew global BEF

Biodiversity encapsulates multiple intrinsic characteristics of biological communities, including species richness and abundance (Purvis and Hector 2000). Here, we used Hill diversity as a means to quantify biodiversity and evaluate different diversity indices in explaining variation in biomass production. In short, Hill diversity is a general measure of species diversity, which can be scaled to calculate common diversity indices (e.g. Simpson Index, Shannon Entropy), but allows all measured to be expressed using the same units (i.e. units of species; Roswell et al. 2021). Unliked other diversity metrics, changes in Hill diversity values intuitively reflect changes in the community; for example, the loss of species in a community would proportionally scale with a decrease in Hill diversity. Because Hill diversity is a generalised equation, we can produce commonly used diversity indices within a single equation by varying the scaling parameter ℓ within a single equation (see Methods; Roswell et al. 2021, 2023). By changing the scaling parameter ℓ, we can specifically emphasise common species (e.g. Simpson Index, Shannon entropy) or rare species (e.g. abundance effects) more than richness, thereby placing communities along an evenness-rarity continuum (Roswell et al. 2021, 2023).

We explicitly tested four diversity indices by varying ℓ to generate the inverse Simpson index (which emphasises relative abundances and, thus, common species; ℓ = -1), the exponentiated Shannon entropy (ℓ = 0), richness effects (which emphasises rare species by considering all species equally; ℓ = 1), and abundance effects (ℓ = 10, the maximum value used Roswell et al. (2023); see

Methods). All models were similarly structured, but with different specifications of ℓ used to quantify biodiversity. While all four diversity indices were relatively correlated and loaded positively on the first axis of a principal component analysis (PC1), which explained 68.4% of the total variation of the data (i.e. a matrix of productivity by sites [rows] and diversity metrics [columns], **Fig. 5-1a**; **Appendix D**: Table D3), increasing ℓ from -1 to 10 resulted in a shift in strength and magnitude of the BEF relationship [mirroring those found by Roswell et al. (2023)]. BEF relationships varied from negative when using the inverted Simpson index (ℓ = -1; median coefficient [90% credible interval]: -0.11 [-0.13 to -0.09]) and the exponentiated Shannon entropy (ℓ = 0; -0.11 [-0.13 to -0.08]), to positive with richness effects (ℓ = 1; 1.05 [1.01 to 1.08]) and abundance effects (ℓ = 10; 1.10 [1.09 to 1.12]; **Fig. 5-1b**). The abundance index was the least correlated with all other Hill diversity metrics and PC1 (**Appendix D**: Fig. D4) and, based on leave-one-out information criterion (i.e. information criterion using a cross-validation procedure; *looic*), generated the best-fitting BEF relationship (**Appendix D**: Table D2). We therefore used Hill diversity emphasising abundance effects as the measure of biodiversity in all subsequent analyses unless otherwise stated (hereon referred to as "diversity").

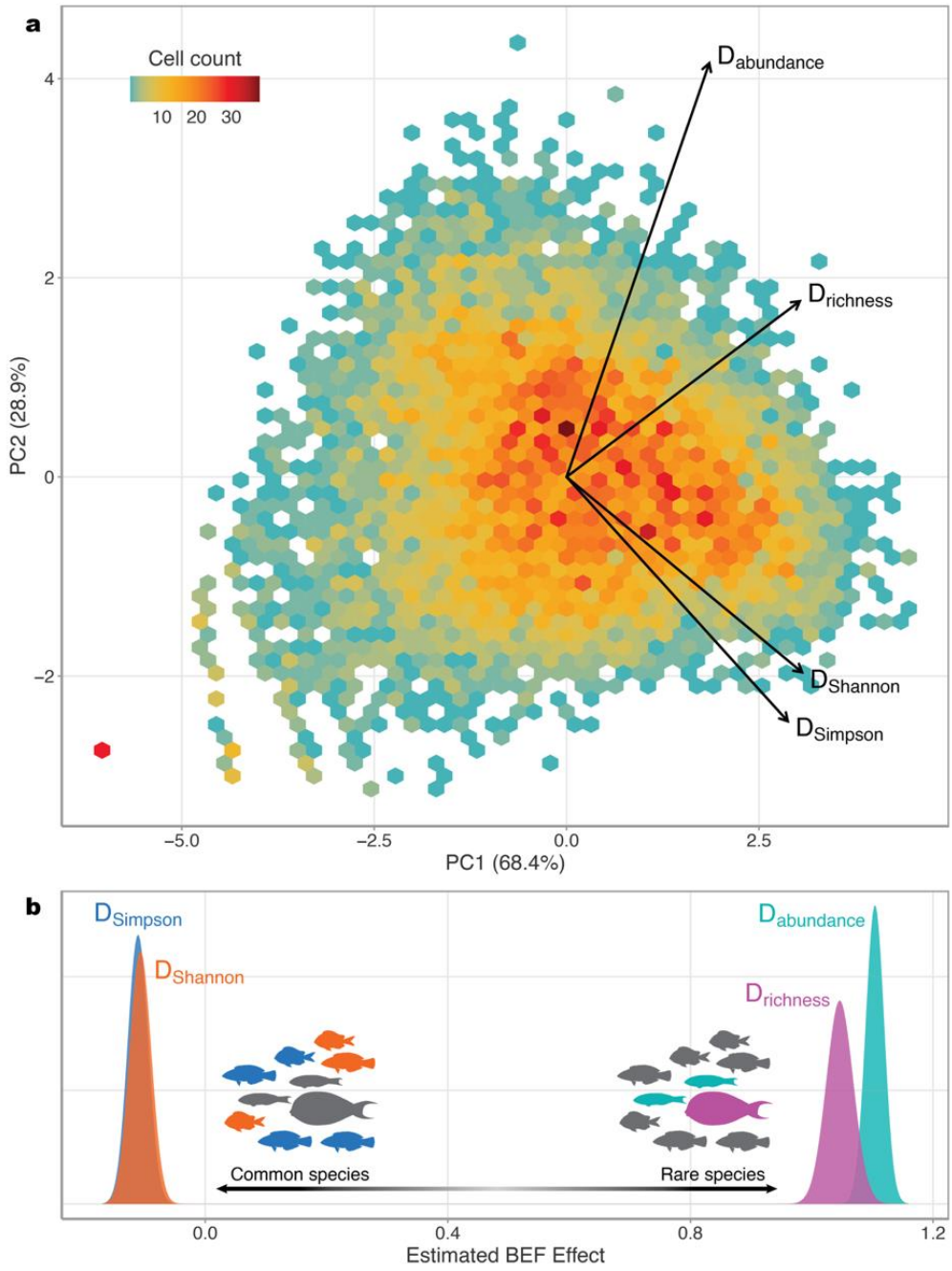

Figure 5-1. Variation in Hill diversity metrics on ecosystem function. a *Principal component analysis (PCA) ordination displaying Hill diversity values (D) representing Simpson Index ($D_{Simpson}$), Shannon Index ($D_{Shannon}$), richness effects ($D_{richness}$), and abundance effects ($D_{abundance}$). Principal component axes 1 and 2 (PC1 and PC2, respectively) explain 68.4% and 28.9% of the variation of the data, respectively. Size of the arrows denote the magnitude and the direction denote the sign of each eigenvector. Hexagons are coloured based on the number of observations in a given bin. Note, the outlying red point towards negative PC1 and PC2 values is depicting the surveys that recorded a single species.* ***b*** *Posterior distributions of estimated biodiversity-ecosystem function (BEF) effects on biomass production (g $500m^{-2}$ day^{-1}) using Simpson Index (blue), Shannon Index (orange), richness effects (purple), and abundance effects (teal) as quantifications of biodiversity. Both Simpson and Shannon indices emphasise common species, whereas richness and abundance effects emphasise rare species. All diversity indices were logged prior to analysis.*

We found a decelerating relationship between diversity and community-level biomass production (**Fig. 5-2**). Despite generally positive global BEF effects, the magnitude of effects across geographic regions (i.e. tropical vs temperate regions) differed. Indeed, the BEF was strongest in the tropics (1.16 [1.12 to 1.19]) and relatively flatter in temperate regions (1.08 [1.06 to 1.11]; **Fig. 5-2**), indicating that species abundances had a greater impact on community biomass production in warm-water environments compared to cooler, high-latitude locations. While the BEF emphasising abundance effects was the best-fitting model based on *looic*, we also compared the magnitude of abundance- versus richness-emphasised BEF effects because species richness is still a dominant component of biodiversity (Hill 1973; Jost 2006) and produced the second-best-fitting model (**Appendix D**: Table D2).

The impacts of richness and abundance BEF effects varied across tropical and temperate regions. Regardless of the index used, BEF effects in temperate regions produced nearly identical results (abundance index: 1.08 [1.06 to 1.11]; richness index: 1.08 [1.04 to 1.12]; **Fig. 5-2**), which suggests that species richness and abundances may have indistinguishable impacts on community biomass production in temperate regions. The impact of species abundances and richness on fish biomass production in tropical regions, however, differed. While both BEF effects were positive, richness effects were substantially weaker than abundance effects (0.96 [0.91 to 1.02] and 1.16 [1.12 to 1.19], respectively; **Fig. 5-2**). Namely, increases in abundance-emphasised diversity correlated with greater increases in productivity than increases in species richness-emphasised diversity, which suggests that species abundances, not richness, may be the primary community-level feature giving rise to/or the consequence of highly productive tropical fish communities. Indeed, many of the richest tropical communities are characterised by small-bodied fishes occurring in higher abundances (Barneche et al. 2019), while the disproportionately high abundances of planktivorous fishes, which capitalise on external pelagic subsidies, correlated with higher community productivity than planktivore richness (Morais et al. 2021). Although we cannot discount the role of species richness as a correlate of productivity, it appears that the iconic productivity of high-diversity systems in the tropics are predominantly driven by species abundances. The saturating effect of diversity on

community productivity would therefore suggest that the mechanisms by which fish communities are producing biomass differs between temperate and tropical regions.

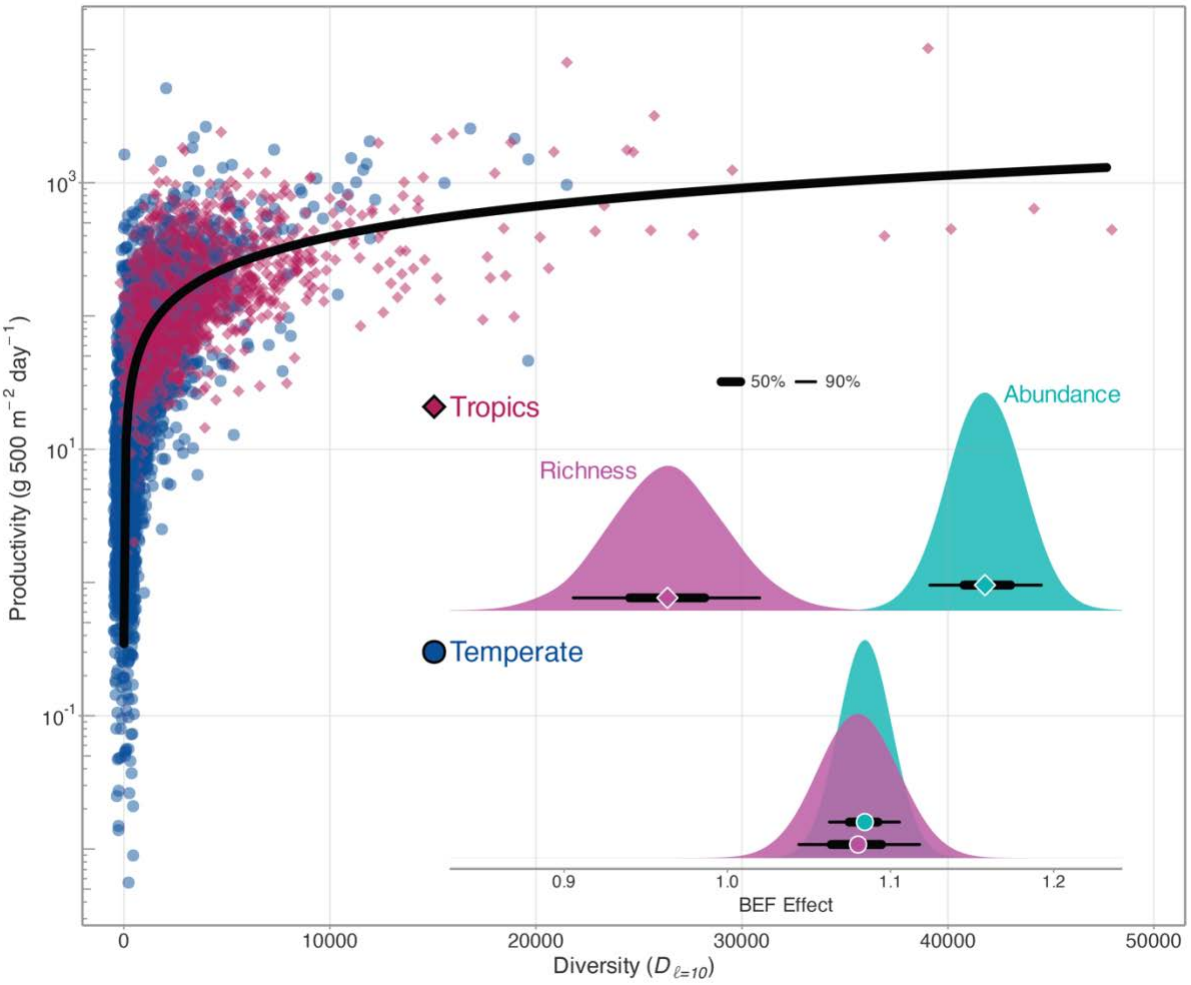

Figure 5-2. Global biodiversity-ecosystem function relationship (BEF) across marine fishes. *Global BEF relationship across temperate (blue; circles) and tropical regions (red; diamonds). Each point is one survey and the thick black line is the median fitted trend from 400 randomly sampled draws. Note the y axis is on the log_{10} scale and the points have been jittered (i.e. a very small random number has been added) to improve clarity and interpretability of the figure. Inset: posterior distributions of modelled BEF relationships in tropical (top row) and temperate regions (bottom row) using Hill diversity emphasising abundance effects (teal) and richness effects (purple). The points denote the median coefficient estimates, while the thick and thin bars denote the 50% and 90% credible intervals, respectively. Coefficients estimates can be found in* ***Appendix D****: Table D2.*

5.3.2 Mechanistic patterns of community productivity

The decomposition of community-level biomass production may provide insight into the geographic discrepancies in BEF effects. Specifically, community productivity is the product of species total abundances and per-capita biomass production (Roswell et al. 2023), which can be independently evaluated against abundance-emphasised diversity. While in temperate regions, increasing diversity positively correlated with increasing abundance (1.42 [1.41 to 1.43; **Fig. 5-3a**), this increase was much steeper in tropical regions (1.56 [1.55 to 1.58]; **Fig. 5-3b**). Likewise, the observed decrease in per-capita productivity with diversity was much steeper in the tropics (-0.41 [-0.44 to -0.38]; **Fig. 5-3d**) than in temperate regions (-0.33 [-0.35 to -0.31]; **Fig. 5-3c**). Therefore, the shift in configuration of the relationship between abundance and per-capita productivity (i.e. high per-capita productivity and low abundances towards low per-capita productivity and high absolute abundances) is strongest in the tropics, which suggests that the ecological mechanisms underpinning the BEF across marine fish communities (i.e. changes in per-capita biomass production versus abundance) are likely physiologically constrained in warm-water environments (Barneche et al. 2016; Pauly 2021).

While all Hill diversity indices were higher in the tropics (**Appendix D**: Fig. D5), the largest concentration of high-diversity communities was above ~23ºC (Fig. 4-4). In warm, high-diversity systems, species are likely metabolically limited in their capacities to attain larger sizes (Brown et al. 2004). Scaling temperature using the Boltzmann's-Arrhenius relationship, a procedure accounting for non-linearities in how metabolic rates vary with temperature (Gillooly et al. 2001), changed the units, but not the shape of the relationship (see Methods; **Appendix D**: Table D2). Indeed, conspecifics found across temperature gradients tend to grow faster to smaller body sizes in warmer waters (Atkinson 1994; Berrigan and Charnov 1994; Barneche et al. 2021). Similarly, species abundances scale negatively with body size (Damuth 1981; Brown et al. 2004; Martins et al. 2023), whereby conspecifics occurring in higher densities tend to exhibit smaller body sizes (Barneche et al. 2016). Taken together, these two relationships imply challenges with producing biomass in warm, high-abundance communities, possibly owing to trade-offs occurring between the increased costs of growth (Barneche and Allen 2018) and extrinsic environmental and ecological factors (Van Denderen et al.

2020), such as competition in resource-limiting contexts. Although energetic constraints on total community fluxes (Barneche et al. 2014) can also be modified by external energy subsidies, such as via pelagic pathways (Morais et al. 2021), shifts towards higher abundances and lower per-capita productivity would also allow communities to circumvent physiological constraints due to warmer temperatures. Populations of conspecifics in warmer conditions may compensate for the enhanced difficulty in producing biomass via somatic growth by increasing their relative abundances compared to their conspecifics in cold conditions through trade-offs between size-based growth and mortality (as suggested by the "energetic-equivalence rule"; Damuth 1987). Thus, increased community productivity could emerge from such shifts. Indeed, declines in fishes' body sizes over time were similarly matched by increases in intraspecific abundances, leading to relatively stable levels of community standing biomass (Martins et al. 2023). While species interactions, such as intraspecific competition, can contribute to the trade-off between abundance and per-capita productivity (e.g. via self-thinning in resource-limited populations; Smith et al. 2013), there appears to be an upper energetic limit of community function delivery (i.e. productivity), which is imposed by environmental conditions working beyond resource availability.

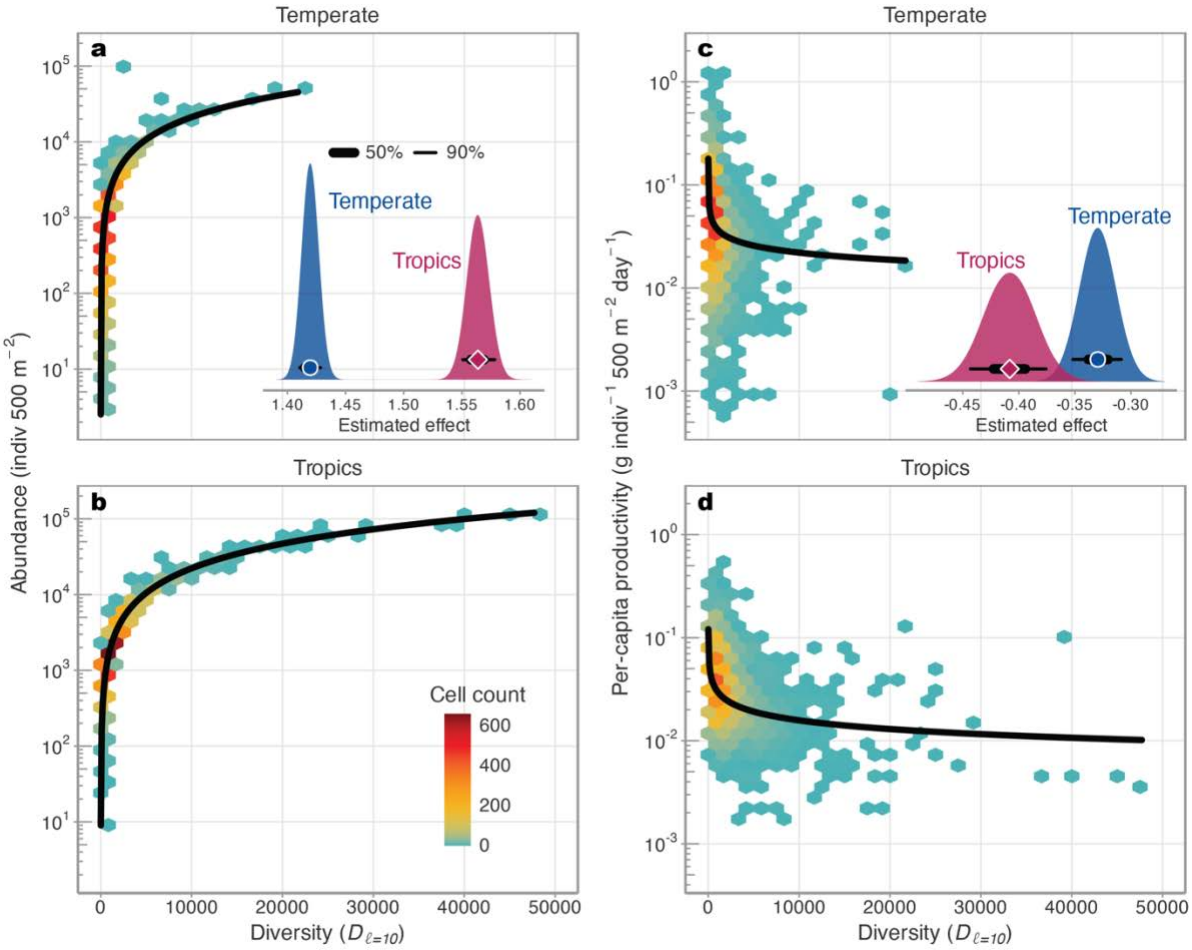

Figure 5-3. Deconstructing the BEF across geographic regions. a-b *The effects of Hill diversity emphasising abundance effects (i.e. diversity $D_{\ell=10}$) on total community abundance across* ***a*** *temperate and* ***b*** *tropical regions.* ***c-d*** *The effects of Hill diversity on per-capita biomass production (g indiv^{-1} 500m^{-2} day^{-1}) across c temperate and d tropical regions. Hexagons denote the density of the raw data and are coloured by the number of observations per bin. The thick black lines are the median fits from 400 randomly sampled draws. The insets in* ***a*** *and* ***c*** *show the posterior distributions of the estimated slope coefficients for tropical and temperate regions in red and blue, respectively. The points denote the median estimates and the thick and thin bars represent the 50% and 90% credible intervals, respectively. Note the 50% credible intervals in panel* ***b*** *are nearly too narrow to be shown. Coefficient estimates for all models can be found in* ***Appendix D****: Table D2. Note all y axes are on the log_{10} scale.*

The effects of diversity on abundance and per-capita productivity were dampened, but still distinguishable, across temperate regions, indicating that the energetic constraints placed on tropical communities may impact temperate communities as well, especially given that reef fishes tend to be larger towards higher latitudes (Barneche et al. 2019; Coghlan et al. 2024). However, given that species richness exhibited nearly an identical BEF effect on total community productivity as species abundances, these constraints are unlikely to be due to temperature alone and could be shaped by species interactions surrounding resource limitations. Temperate reef fish communities typically exhibit less community compositional change (Yan et al. 2022) and higher evenness across latitudes (Stuart-Smith et al. 2013), which could contribute to the relatively higher biomass production in these regions compared to the tropics. Increasing species richness in temperate regions had a greater impact on total community biomass production than tropical communities (**Fig. 5-2**), which mainly conforms to the traditional BEF paradigm: increasing richness correlates with increasing function delivery. In species-depauperate systems, such as those most often found in temperate areas, each additional species in a community would expand into relatively unoccupied ecological niches (Blüthgen and Klein 2011; Stuart-Smith et al. 2013). Consequently, with relatively low interspecific competition, each additional species could theoretically attain larger population sizes and, thus, deliver higher levels of functions, such as biomass production. Indeed, while evenness was not a strong predictor of functioning across geographic regions (see **Fig. 5-1b**), the dominance of high-performing species assessed within temperate regions has been shown as a mechanistic driver of functioning in local marine communities (e.g. Dangles and Malmqvist 2004; Hodapp et al. 2015; Maureaud et al. 2019). It is therefore possible that the strong, positive richness-emphasised BEF expressed in temperate regions across marine reef-associated fishes may reflect greater generalisations found throughout the BEF narrative. If the inherent biases derived from experimental BEF studies in high-latitude locations (Clarke et al. 2017) are matched with the possibility that BEF effects can be stronger in temperate regions, then these biases could have been responsible for the disproportional emphasis on the dominant role of species richness, not abundances, on ecosystem functioning across observational BEF studies.

Given our empirical finding that high-diversity tropical communities are characterised by high abundances and low per-capita productivity, it appears that function delivery in hyperdiverse systems, such as coral reefs, is primarily mediated by species' abundances, a factor which has largely been overlooked in previous BEF field studies. Indeed, high-diversity communities would require disproportionally higher abundances to maintain steady increases in community-level biomass production as low-to-moderately high-diversity communities. In other words, increases in both species' abundances and biodiversity would need to be maintained to support continuously increasing levels of ecosystem functioning in high-diversity systems. Although the communities that are delivering the highest rates of function (in this case, biomass production) are necessarily the communities with the highest biodiversity, the difference in their average capacity to provide this function relative to some communities with much lower biodiversity may be small, often with negligible biological impacts. Regardless of the relationship between diversity and biomass production, all tropical communities appear to be physiologically limited by temperature (see **Fig. 5-4**, **Appendix D**: Fig. D6; Barneche et al. 2014). Under future warming scenarios, it is likely that increased ocean warming will further constrain the magnitude of function delivery expressed by communities that appear to be at their physiological limits (such as those in the tropics), regardless of their species composition. The thermal tolerance-induced geographic ranges of cold-water fishes is continuously constrained by ocean warming, indicating that cool-water species are likely to be more vulnerable than their tropical counterparts (Sunday et al. 2011). Therefore, BEF effects in temperate regions may shift towards tropical strategies, with increased emphases on abundances instead of species richness. We can therefore expect that with warming oceans, the temperature-related metabolic constraints on per-capita biomass production and the changes in ecological dynamics (e.g. species interactions) will reshape the productivity of fishes differently across geographic regions.

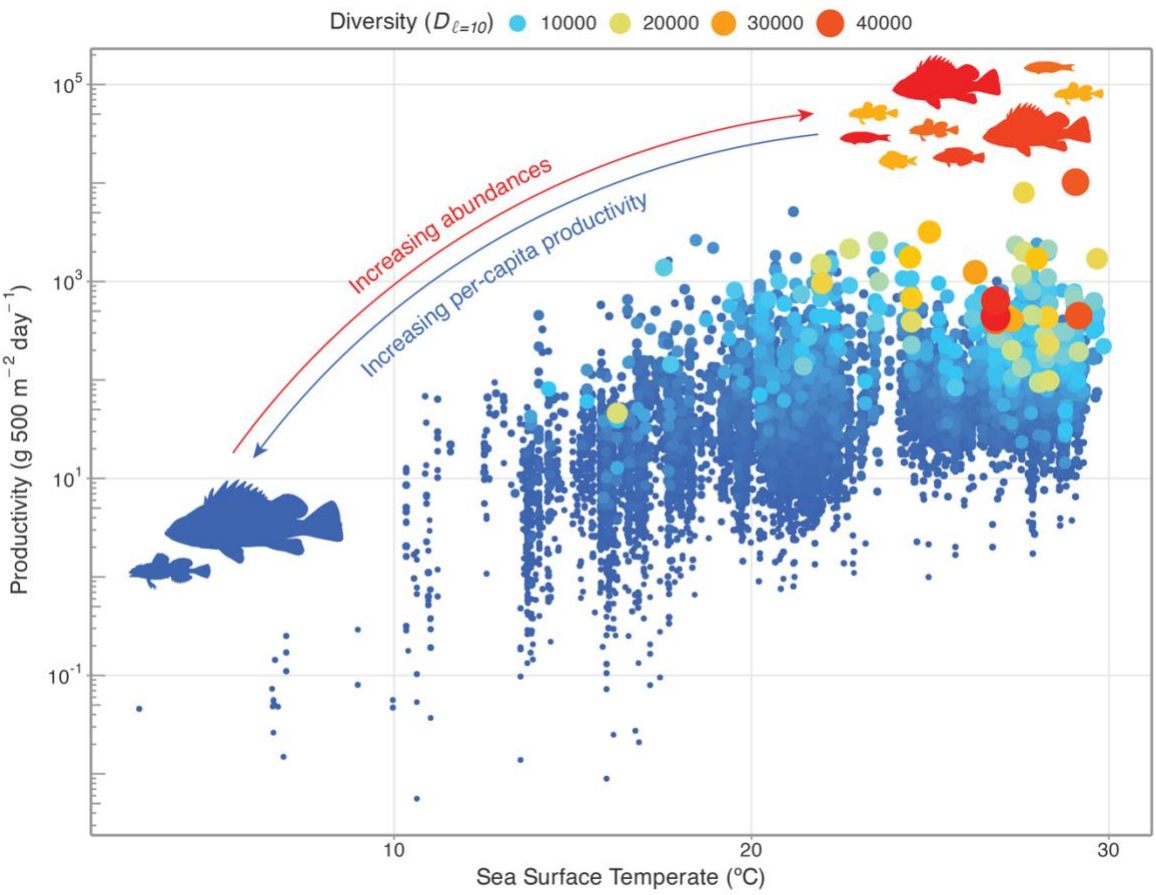

Figure 5-4. Temperature limits the BEF. *Patterns in fish productivity (g 500m^{-2} day^{-1}) across sea surface temperature (°C) gradients. Points are sized and coloured based on their respective Hill diversity values emphasising abundance effects. Note the y axis is on the log_{10} scale.*

What escapes the eye, however, is a much more insidious kind of extinction: the extinction of ecological interactions.

Daniel H. Janzen
The deflowering in central America, Natural History, 1974

Chapter 6: Humans outpace sharks as dominant predators on coral reefs

Abstract

Overexploitation has reshaped the structure and functioning of the world's coral reefs. With more than half of the world's reef sharks threatened, an urgent question has arisen: what are the ecological consequences of shark depletions on coral reef fishes? Here, we combined two of the largest reef survey programs in the world to assess the impacts of human gravity and shark abundances on the trophic structuring of coral reef fish communities. Across 622 coral reef sites around the world, we found overwhelming evidence of strong negative impacts of human gravity on reef fish communities: high anthropogenic pressures led to low fish biomass and abundances, driven by the removal of large-bodied individuals. By contrast, we found no evidence of a predator-induced ecological impact of sharks on reef fishes. Reef communities with higher shark abundances were characterised by inverted trophic structures (i.e. disproportionally higher biomasses in larger size classes), pointing to energetically subsidising effects from external resources. Fisheries-induced declines in the abundance of sharks and fishes over the last half century indicate that the magnitude of fish biomass removal from shark predators is negligible compared to human harvesting rates; humans far exceed sharks as the dominant predators across the world's coral reefs.

Keywords: BRUVS, ecosystem function, FinPrint, INLA, Reef Life Survey, size spectra

6.1 Introduction

Overfishing is one of the greatest threats to marine biodiversity (Dulvy et al. 2003; Ripple et al. 2019; Miranda et al. 2022). The size-discriminate nature of fisheries (i.e. targeting the largest individuals of a given stock; Darimont et al. 2015) has sequentially depleted high-trophic level fishes across ecosystems (Pauly et al. 1998). Consequently, fisheries-induced extinction risks are becoming increasingly elevated for the largest predatory fishes around the world (Dulvy et al. 2021; Juan-Jordá et al. 2022). More than one-third of the world's chondrichthyans (i.e. sharks, rays, and chimaeras) are threatened with an elevated risk of extinction from overfishing (Dulvy et al. 2021), making them one of the most threatened groups across the entire vertebrate tree of life (Gumbs et al. 2024). While the impacts of overfishing have extended to all reaches of the ocean (Halpern et al. 2015; Kroodsma et al. 2018; Finucci et al. 2024), the threat of fisheries-induced extinction is disproportionally concentrated across warmer latitudes: 59% of the world's coral reef-associated sharks and rays are threatened (Sherman et al. 2023) and up to 73% of reef shark species have exhibited population declines (Simpfendorfer et al. 2023). Indeed, the drastic declines in abundance around the world suggests that reef sharks are no longer capable of delivering ecosystem functions at biologically relevant levels across coral reefs (MacNeil et al. 2020; Simpfendorfer et al. 2023; Dedman et al. 2024). Because sharks theoretically occupy the peaks of marine trophic pyramids as apex/mesopredators (Heupel et al. 2014; Roff et al. 2016; Dedman et al. 2024), the globally pervasive decline of reef shark abundances begs the question: has overfishing surpassed sharks as the dominant predators on coral reefs?

Ecosystem functions – defined as the movement or storage of energy and materials through a system (Bellwood et al. 2019b; Brandl et al. 2019b) – are strongly influenced by species' abundances (e.g. Mason et al. 2008; Morais et al. 2021; Munger et al. 2023); therefore, large-scale declines in shark abundances may have cascading consequences through marine food webs via reduced piscivory rates (Roff et al. 2016). Specifically, the loss of sharks is theorized to trigger trophic cascades by releasing mesopredators from predation (Ritchie and Johnson 2009; Roff et al. 2016) and fear effects (e.g. Rasher et al. 2017; but see Tebbett et al. 2024c), leading to subsequent declines in herbivores. Although there is some evidence of shark-related trophic cascades across low-diversity ecosystems

with relatively short trophic links (e.g. Myers et al. 2007; Duffy et al. 2015), the evidence reported from high-diversity coral reefs has been equivocal (Roff et al. 2016; Dedman et al. 2024). While it is possible that the complexity of high-diversity food webs can mask or buffer against potential cascading effects, anthropogenic pressures that are simultaneously targeting multiple trophic levels may also hinder our abilities to detect trophic cascades across coral reefs (Dedman et al. 2024). Notably, selective fishing practices of reef fishes can significantly alter the detection of shark-driven trophic cascades (Bascompte et al. 2005), with evidence for cascades appearing when fishing of reef fishes is ignored (e.g. Ruppert et al. 2013), and disappearing when fishing is included (e.g. Casey et al. 2017; Desbiens et al. 2021). We are therefore lacking a global evaluation of the role of fishing and shark abundances on the trophic structure of reef fishes.

Here, we combined two of the largest reef survey programs in the world – the Global FinPrint project (https://globalfinprint.org) and the Reef Life Survey project (https://reeflifesurvey.com; Edgar and Stuart-Smith 2014; Edgar et al. 2020) – to comprehensively assess the trophic consequences of fishing and the loss of sharks on coral reef fishes across 1,852 surveys around the world (**Appendix E**: Fig. E1). Shark abundances were estimated using baited remote underwater video stations (BRUVS) and relative abundances were calculated as the maximum number of individual sharks recorded within a single frame of each 60-min deployment, averaged across deployments per reef and standardised by the number of cameras dropped (MaxN; see MacNeil et al. 2020; Simpfendorfer et al. 2023). We included the variables that best represented fishing effort and management capacity from MacNeil et al. (2020): human gravity and the presence of shark sanctuaries, respectively. Human gravity reflects the intensity of human impacts on surrounding ecosystems by combining human population sizes with the accessibility to neighbouring reefs (Cinner et al. 2018). Shark sanctuaries, however, are a country-level management indicator and are defined as countries with zero targeted catch and trade of shark products (MacNeil et al. 2020). While there is a plethora of socioeconomic variables that can be used to infer fishing pressure and management capacity (e.g. Yan et al. 2021; Sherman et al. 2023), both human gravity and shark sanctuaries have effectively captured the abundance and conservation of reef sharks from BRUVS data (MacNeil et al. 2020; Goetze et al. 2024). Due to the inherent non-

independence arising from clusters of sites, we used separate spatially explicit Bayesian hierarchical models to evaluate the effects of human gravity (a proxy for fishing pressure), shark abundance, presence of shark sanctuaries, and the abiotic variables sea surface temperature, survey depth, and visibility on reef fish standing biomass, abundance, and size structure. To evaluate the trophic cascade narrative, we individually modelled the biomass and abundance of all reef fishes, big reef fishes (i.e. upper 20% size quantile; see methods), and nominally herbivorous fishes [as defined by Siqueira et al. (2023) and Tebbett et al. (2024b)].

6.2 Methods

6.2.1 Data collation

We combined two of the world's largest reef survey programs: the Global FinPrint project (https://globalfinprint.org/) and the Reef Life Survey program. In short, Global FinPrint is a dedicated global survey that used baited remote underwater video systems (BRUVS) to quantify the abundance and diversity of reef sharks between 2015 and 2018. Following MacNeil et al. (2020) and Simpfendorfer et al. (2023), we quantified shark abundances as the maximum number of individuals detected within a single frame (MaxN), standardised by the number of cameras that have been dropped. MaxN has become a standardised metric to quantify the relative abundances from BRUVS data because it eliminates the possibility of counting the same individual twice and thus overinflating abundance estimates (Willis et al. 2000). Please refer to MacNeil et al. (2020) and Simpfendorfer et al. (2023) for detailed descriptions of BRUVS deployments and video analyses, and additional sensitivity analyses of MaxN from MacNeil et al. (2020). We included human gravity, measured as the size of the human population divided by the squared distance to the surveyed reefs (Cinner et al. 2018; MacNeil et al. 2020), as a proxy for the anthropogenic impacts exhibited at the site level. To account for management effectiveness, we included the presence of shark sanctuaries, which were defined as countries (including territories) with no targeted catch nor trade in sharks or shark products (MacNeil et al. 2020).

We used the Reef Life Survey program (Edgar and Stuart-Smith 2014; Edgar et al. 2020) to quantify the standing biomass, abundance, and size structure of reef fishes (as used in Chapter 5). This program is a standardised fish censusing survey that quantifies the size, abundance, and identity of all fishes over one-to-two 250 m^2 blocks along a 50 m transect within relatively shallow depths (< 20 m). Because not all surveys were composed of two blocks, we standardised all estimates of abundance and biomass to 250 m^2. Detailed survey methods can be found online (https://reeflifesurvey.com/). We used the regression length-weight conversion factors from FishBase (Froese and Pauly 2021) to convert estimates of total length to standing biomass. The fish survey-level abiotic variables included survey depth, the water visibility, and the sea surface temperature, which was extracted for each survey location for each sampling year using raster data from the National Oceanic and Atmospheric Administration (https://psl.noaa.gov/data/gridded/data.noaa.oisst.v2.html).

We created three separate groupings of fishes to assess the trophic cascade narrative: large fishes, nominally herbivorous fishes, and all fishes. The classic trophic cascade discourse involving sharks and fishes typically describe sharks as apex predators feeding on mesopredatory fish families, such as those belonging to the families Lutjanidae, Serranidae, and Lethrinidae (e.g. Casey et al. 2017). Although larger shark species may fulfill the role as apex predators in their adult size classes (e.g. *Galeocerdo cuvier* or *Carcharhinus leucas*), the majority of common reef shark species behave more like mesopredators (e.g. *C. melanopterus* or *Triaenodon obesus*; Heupel et al. 2014; Roff et al. 2016; Barley et al. 2020). Using taxonomic delineations to define mesopredators would likely introduce biases because the majority of piscivores on coral reefs are relatively small fishes (roughly 3.5 cm in total length; Mihalitsis et al. 2022) and piscivores are morphologically limited based on their respective size when selecting prey (Mihalitsis and Bellwood 2017). This means that prey type/size changes throughout ontogeny and scales differently for teleosts compared to sharks (Barley et al. 2020). We therefore used a size-based cut-off to delineate upper-trophic level fishes. Specifically, we defined large fishes as those in the upper 20% size classes (i.e. ranging from 20-400 cm in total length), which has previously been used as a size threshold to calculate fishable biomass (Cinner et al.

2020). We followed (Morais and Bellwood 2018; Siqueira et al. 2023) and included detritivores and macroalgivores as herbivores.

We spatially matched shark abundances from the Global FinPrint project with reef fish surveys conducted as part of the Reef Life Survey program. We first reprojected all points using the Eckert IV projection, which is a pseudocylindrical equal-area projection that minimises the distortion when calculating both area and shapes. Buffers around each survey location were then intersected to create sites of overlap. We used two different buffer radii, 10 km and 50 km, as these distances represent the relative movement distances of most reef shark species (Espinoza et al. 2015) and is predicated on the rationale that sharks that are present within a certain radius of BRUVS will likely be present on a reef within that area. Both buffer sizes resulted in representative shark abundances compared to the full dataset (**Appendix E**: Fig E2); the 50 km buffer overlapped with 622 fish sites and the 10 km buffer with 390 fish sites. Although we have run the biomass and abundance analyses using both buffer sizes, we present the results using the 50 km buffer in the main text because it produced better-fitting models based on Watanabe-Akaiki information criterion (Watanabe 2010). The results were nearly identical when using the 10 km buffer (**Appendix E**: Fig. E3).

6.2.2 Spatially explicit models

Due to the inherent spatial clustering of sites, we used Bayesian geostatistical generalised linear mixed-effects models with spatially correlated random effects using integrated nested Laplace approximation (INLA). INLA is a powerful technique that can approximate the Bayesian posterior distribution (Rue et al. 2009; Martins and Rue 2014), while allowing the incorporation of Stochastic Partial Differential Equations (SPDE) as approximations to Gaussian random fields (Lindgren et al. 2011; Lindgren and Rue 2015). We first reprojected all site-level coordinates using an equidistant cylindrical projection to retain linear distances before generating a mesh with a cut-off set to 3 km to generate solutions to the SPDE (**Appendix E**: Fig. E4). To account for repeated sampling occurring at certain sites, we also included site and basin (i.e. Indo-Pacific or Western Atlantic) as grouping factors by specifying random intercepts. All biomass and body size (B) models were specified as:

$$Gamma(B_{total,i}|\phi, \lambda_i)$$

$$\lambda_i = \frac{\phi}{\omega_i}$$

$$Tweedie\left(B_{large,herb,i}|\mu_i, \theta, \rho\right)$$

$$\log(\omega_i) \; or \; \log(\mu_i) = \beta_0 + \boldsymbol{\beta X}_i + \alpha_{site} + \alpha_{basin} + g(site)$$

Here, B_{total}, B_{large}, and B_{herb} are the observed values for transect *i* for total community, large fishes, and herbivore standing biomass or body size, respectively. Parameters ϕ and λ_i are the gamma shape and rate parameters, respectively; θ is the dispersion parameter and ρ is the Tweedie power parameter. Both ω and μ are the respective means of the Gamma and Tweedie distributions. In each model, β_0 is the overall intercept, $\boldsymbol{\beta}$ is a vector of estimated main effects for human gravity, shark abundance, shark sanctuary (dummy coded), depth, sea surface temperature, and visibility; and $\boldsymbol{X}$ is a design matrix of covariates. We log-transformed human gravity and shark abundance for all modelling procedures to reduce the leverage of extreme sites. Site- and basin-level random effects are denoted as α_{site} and α_{basin}, respectively. Finally, *g(site)* is the estimated spatial random field at each site. The biomass and body size of large fishes and herbivores were modelled specifying a Tweedie error distribution to account for locations with zero individuals. Biomass models for large and herbivorous fishes were converted to 100 x kg prior to analysis to improve the Tweedie model-fitting procedure but converted back to kg for all figures. We modelled community-level abundances (*A*) following a similar model structure:

$$Negative\ Binomial(A_i|\ \mu_i, \phi)$$

$$Var(A_i) = \mu_i + \frac{\mu_i^2}{\phi}$$

$$\log(\mu_i) = \beta_0 + \boldsymbol{\beta X}_i + \alpha_{site} + \alpha_{basin} + g(site)$$

For all abundance models (i.e. total fish abundance, large fishes, and herbivores), we specified a negative binomial distribution using the inverse shape parameter (ϕ) for overdispersion. For the whole

community standing biomass and abundance models, the plotted fitted versus observed values can be found in **Appendix E**: Fig. E5.

We used size spectrum analyses to assess the biomass distribution across fishes' size classes. Here, we used the normalised biomass size spectrum, which produces more-accurate estimates compared to other size spectra techniques because it corrects for unequal size bin widths (Blanchard et al. 2005; Edwards et al. 2017). In short, we parsed all individuals into equal $\log_2$ biomass bins and calculated the sum of the total standing biomass in each bin. We then normalised the biomass in each bin by dividing it by its respective bin width (Edwards et al. 2017). A traditional size spectrum analysis then plots the normalised biomass (B_N) against the bin midpoint on a double $\log_{10}$-$\log_{10}$ scale. We specified all size spectrum models as:

$$Normal(B_{N,i}, \sigma^2)$$

$$log_{10}(B_{N,i}) = \beta_0 + \boldsymbol{\beta X}_i + \beta_{int} log_{10}(x_{bin}) x_{gravity,shark} + \alpha_{site} + \alpha_{basin} + g(site)$$

Here, σ^2 is the variance of the distribution. We ran two size spectra models, each with an interaction (β_{int}) between the $\log_{10}$ bin width (x_{bin}) with either gravity ($x_{gravity}$) or shark abundance (x_{shark}); both models still included the non-interacting effect of shark abundance and gravity, respectively. For all modelling procedures, we centred and scaled all continuous variables by subtracting their respective means and diving by their respective standard deviations. We validated models by visually inspecting residual plots. To calculate posterior probabilities for each effect, we randomly drew 1000 samples from their respective marginal distributions. All models used the default non-informative priors as part of the `INLA` package and were conducted in R v 4.4.0 (R Core Team 2024) using `INLA` 24.05.10 (Rue et al. 2009).

6.2.3 Catch per unit effort

We extracted the total reconstructed catch (mt) and fishing effort (kW) data from the publicly available Sea Around Us Project (Pauly et al. 2020; accessed on 25 March 2023). We only retained catch and effort data for the Exclusive Economic Zones (EEZs) for which we had paired shark and

reef fish survey data (using the 50km buffer), resulting in the inclusion of 52 EEZs. For shark catches, we included all sharks and rays to capture the landings (and likely misreporting) of shark-like rays (e.g. of the family Pristidae); reef fishes were categorised as all "reef-associated" fishes. For each year, we calculated catch per unit effort (CPUE; mt kW^{-1}) by taking the sum of all shark or reef fish catches across all three fishing sectors (i.e. Industrial, Artisanal, and Subsistence) across EEZs and dividing it by the summed fishing effort across all fishing entities. Although catch data is available until 2019, effort data is only available until 2010. We therefore chose to model time series trends using empirical data (i.e. without predicting the trajectory of effort from 2011-2019).

We developed separate Bayesian univariate autoregressive state-space models to evaluate the changes in CPUE for sharks and reef fishes from 1950 to 2010. For time series analyses, state-space models assume that the underlying true CPUE changes according to a first-order autoregressive process arising from demographic processes (Dennis et al. 2006). Here, we modelled CPUE (y_i; where i corresponds to the CPUE of a given EEZ) in year t according to a gamma error distribution by specifying the gamma shape (ϕ) and rate parameters ($\lambda_{i,t}$).

$$Gamma(y_{i,t}|\phi, \lambda_i)$$

$$\lambda_i = \frac{\phi}{\omega_i}$$

$$\log(\omega_i) = \alpha_t$$

$$\lambda \sim \text{Gamma}(0.01, 0.01)$$

The term α_t (t = 1950, …2010) is the expected CPUE for each year and is considered the observed estimate of the underlying, unobserved population state x_t plus some observation error v_t. The underlying population state x_t changes from year-to-year following a first-order autoregressive process, which includes a drift term u and random annual deviations (i.e. process deviance; w_t) arising from demographic processes in the population. Both w_t and v_t are drawn from normal distributions with process and observation standard deviations σ_q and σ_r, respectively. Here, the drift term u allows the model to estimate whether there is a consistent directional trend over time.

$$x_t = x_{t-1} + u + w_t \qquad w_t \sim \text{Normal}(0, \sigma_q)$$

$$\alpha_t = x_t + v_t \qquad v_t \sim \text{Normal}(0, \sigma_r)$$

The state at $x_{t=1950}$ was fitted by estimating an initial state x_0 following the same first-order autoregressive process.

$$x_{t=1} = x_0 + u + w_{t=1}$$

We specified the following weakly informative priors:

$$u \sim \text{Normal}(0, 1)$$

$$x_0 \sim \text{Normal}(0, 1)$$

$$\sigma_q \sim \text{Half-normal}(0, 1)$$

$$\sigma_r \sim \text{Half-normal}(0, 1)$$

All state-space models were run with four Markov chain Monte Carlo chains for 4,000 iterations with an initial warmup phase of 2,000 iterations. To validate models, we inspected simulated residuals from the `DHARMa` package (Hartig 2022); we visually inspected traceplots and ensured all potential scale reduction factors Rhat < 1.01 to assess chain convergence. The effective sample size was > 7000 for all models. We ran all state-space models in *Stan* (Carpenter et al. 2017) using `rstan` v 2.21.8 package (Stan Development Team 2017).

6.3 Results and Discussion

6.3.1 Human gravity outweighs shark abundances

Human gravity, which reflects human impacts via fishing intensity, vastly outweighed the effects of shark abundances. After accounting for spatial covariance, we found overwhelming evidence of a strong negative effect of human gravity on the standing biomass of all fishes (posterior probability $p(\beta) < 0 = 99.8\%$), which was similarly reflected across both big fishes ($p(\beta) < 0 = 100\%$) and herbivores ($p(\beta) < 0 = 98.3\%$; **Fig. 6-1a**). The strong negative effects of human gravity on reef fish

abundances mirrored those of standing biomass: increasing human gravity was related to lower abundances across all fishes ($p(\beta) < 0 = 98.4\%$), big fishes ($p(\beta) < 0 = 99.9\%$), and herbivores ($p(\beta) < 0 = 88.5\%$; **Fig. 6-1b**). While human impacts were uniformly impacting the biomass and abundance of reef fishes, the management effects provided by shark sanctuaries varied. There was weak evidence of a positive effect of the presence of shark sanctuaries on the standing biomass of all fishes ($p(\beta) > 0 = 79.0\%$) and big fishes ($p(\beta) > 0 = 76.8\%$), and stronger evidence of a positive effect on the biomass of herbivores ($p(\beta) > 0 = 87.7\%$; **Appendix E**: Table E1). Conversely, there appeared to be no difference in the abundance of all fishes found within and outside shark sanctuaries ($p(\beta) > 0 = 36.2\%$); however, the abundance of big fishes and herbivores within sanctuary nations were considerably higher than those outside sanctuary borders ($p(\beta) > 0 = 90.4\%$ and $p(\beta) > 0 = 99.8\%$, respectively; **Appendix E**: Table E1).

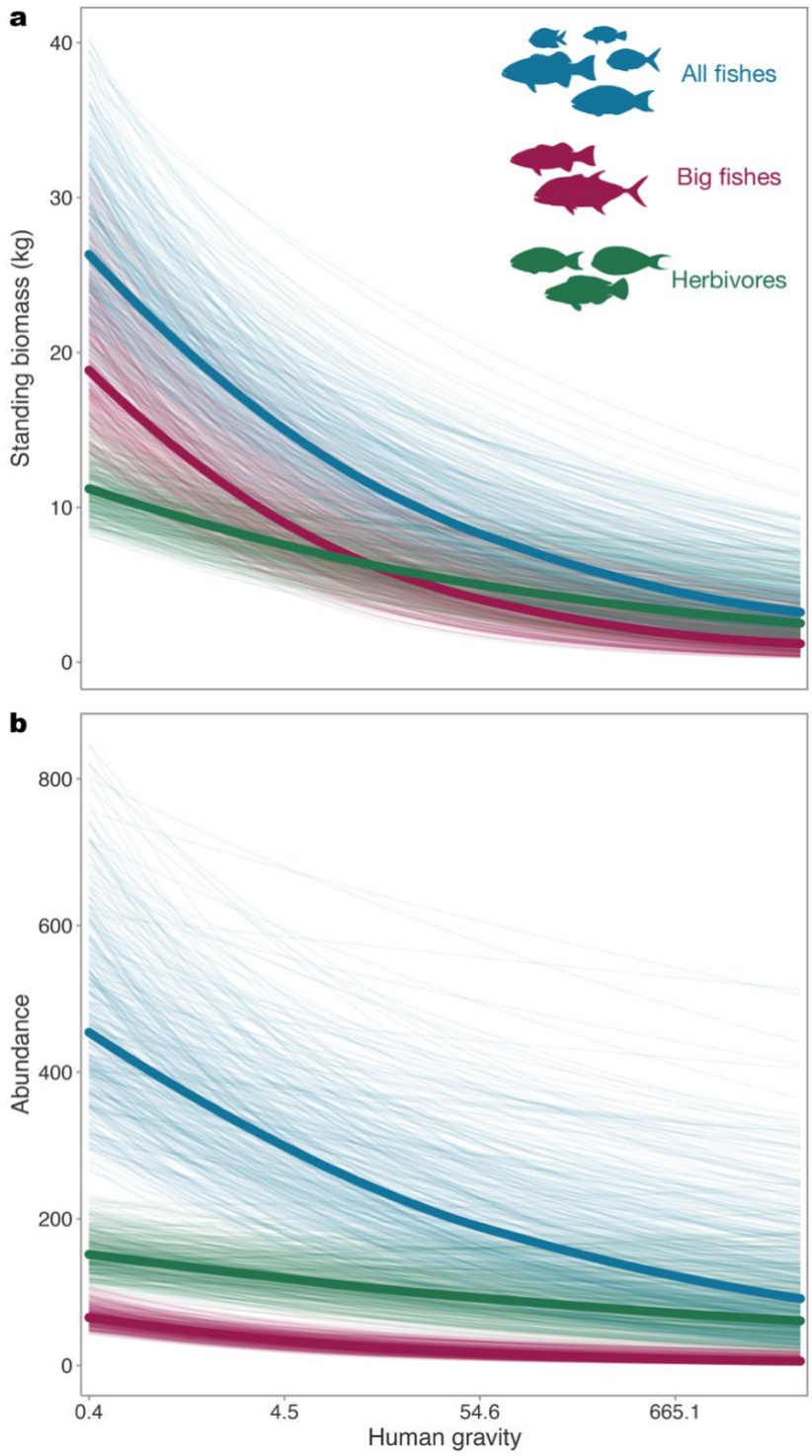

Figure 6-1. Anthropogenic impacts on reef fishes. *Conditional effects of* ***a-b*** *human gravity on the biomass (**a**) and abundance (**b**) of all reef fishes (blue), big fishes (red), and herbivores (green). The thin lines denote randomly sampled draws within the 90% credible interval from the marginal distributions and the thick lines denote the median fitted value from spatially explicit models (see methods). Note that human gravity is on the natural log scale. All estimated coefficients can be found in* ***Appendix E****: Table E1.*

While human impacts were relatively well detected across our models, we found little evidence of an effect of sharks across reef fishes. There was no evidence of an effect of shark abundances on the biomass of all reef fishes ($p(\beta) > 0 = 62.3\%$) nor big fishes ($p(\beta) > 0 = 66.7\%$). We did, however, find some evidence of a positive effect of shark abundances on the biomass of herbivorous fishes ($p(\beta) > 0 = 85.2\%$; **Fig. 6-2a**). Although we found weak evidence of an effect of shark abundances on the abundance of herbivorous and big fishes ($p(\beta) > 0 = 73.5\%$ and 40.3%, respectively), we found a strong negative correlation between shark abundances and total fish abundance ($p(\beta) < 0 = 98.4\%$; **Fig. 6-2a**), which mirrors the effects of human gravity on total fish abundance (**Fig. 6-1b**). While similarities between human gravity and shark abundances on reef fishes would suggest similar top-down pressures, the two appear to be manifestations of entirely different underlying mechanisms.

The inherent role of high-trophic level predators is to target subordinate body sizes (Trebilco et al. 2013); therefore, under this paradigm, humans and sharks should be expected to exert similar pressures on the trophic/size structuring of fish communities. Using size spectrum analyses, which are a taxonomy-independent approach to assess the biomass distribution across size classes throughout an entire community (Trebilco et al. 2013; see Methods), we found that the size structuring of fish communities responded entirely differently to increasing human gravity compared to increasing shark abundance. The negative size spectrum slope of reef fish biomass across size classes became drastically more negative with increasing human gravity ($p(\beta) < 0 = 100\%$; **Fig. 6-2b**). While these patterns can arise from increases in the abundance of smaller size classes, this is unlikely given the uniformly strong negative effect of human gravity across all reef fish abundances (**Fig. 6-1b**). Similarly, increasing human gravity was strongly related to decreasing mean fish body sizes across all fishes and large fishes ($p(\beta) < 0 = 89.1\%$ and 90.2%, respectively), with no evidence of an effect on herbivores ($p(\beta) < 0 = 43.8\%$; **Fig. 6-2c**). Consequently, the changes in the size structuring of reef fishes is likely driven by the removal of the largest size classes, which is indicative of strong top-down fishing pressures (Dulvy et al. 2004a; Blanchard et al. 2005).

Although the slope of the reef fish community size spectrum steepened with increasing human gravity, we found that the slope became considerably less negative with increasing shark abundances ($p(\beta) > 0 = 100\%$; **Fig. 6-2b**). Higher shark abundances were weakly related to larger mean body sizes of all fishes and big fishes ($p(\beta) > 0 = 79.3\%$ and 73.8%, respectively), with stronger evidence for larger herbivorous fishes ($p(\beta) > 0 = 88.9\%$; **Fig. 6-2c**). Positive size spectrum slopes typically arise from a surplus of biomass in larger size classes, pointing towards inverted trophic pyramid structures (Trebilco et al. 2013). While energetically paradoxical, inverted trophic structures can arise with the addition of external nutrient subsidies (Trebilco et al. 2013), such as the addition of spawning Pacific salmon carcasses to soil insect communities (Hocking et al. 2013) and pelagic resources to coral reefs (Morais and Bellwood 2019). Indeed, pulse energetic contributions by spawning fishes across relatively pristine coral reefs can support disproportionally higher reef shark abundances, resulting in exceptionally inverted biomass structures (Mourier et al. 2016). Conversely, pelagically subsidised systems can result in higher abundances of all mesopredator/predator species (including sharks), which could lead to stronger top-down predation pressures resulting in lower abundances of small-bodied individuals (as denoted by the decline across smaller size classes with increasing shark abundances; **Fig. 6-2b**). It is therefore likely that the negative relationship found between shark and total fish abundances (**Fig. 6-2a**) is the manifestation of more large-bodied fishes (but occurring in lower relative abundances compared to the small-bodied fishes) in sites influenced by higher pelagic subsidies (e.g. Lord Howe Island in Australia, **Appendix E**: Fig. E1).

Ecosystem function delivery at the community level is highly dependent on species abundances (e.g. Mason et al. 2008; Munger et al. 2023); therefore, the functional role of sharks is likely only energetically relevant in pristine ecosystems with minimal human impacts, such as unfished atolls (Williams et al. 2018). Although we found some evidence for a positive association between shark abundances and herbivore biomass and body size, this is unlikely a result of direct predation of sharks on mesopredators. Matching the findings from smaller-scale studies (e.g. Casey et al. 2017; Desbiens et al. 2021), we found no effect of sharks on the abundance nor biomass of larger fishes (**Fig. 6-2a**), which should be negative under a classic trophic cascade narrative (Roff et al.

2016). Stomach content analyses of reef sharks have revealed that sharks frequently consume herbivorous fishes and are less likely to feed on predatory species (Frisch et al. 2016); therefore, shark-mediated predation should actually drive declines in herbivore biomass. On the other hand, the distribution and abundance of herbivorous fishes can be strongly influenced by the quality of their algal food sources. For example, higher sediment loads in algal turfs, a dominant benthic component of Anthropocene coral reefs (Tebbett et al. 2023b), can drive declines in the abundance and productivity of herbivores (Tebbett et al. 2021, 2024a). Given that higher hydrodynamic energy is correlated with lower benthic sediment loads (Tebbett et al. 2023c), the oceanographic conditions giving rise to large influxes of pelagic subsidies, which support higher shark abundances (Mourier et al. 2016; Simpfendorfer and Heupel 2016), may simultaneously produce favourable benthic conditions for herbivores (Desbiens et al. 2021). Indeed, the reef zones exposed to pelagic resources that mainly benefit planktivores also support higher herbivore biomass levels (Morais and Bellwood 2019; Desbiens et al. 2021), while herbivore productivity is highest in ecoregions characterised by stronger oceanographic conditions (Tebbett et al. 2024d). The positive relationships between sharks and herbivores are therefore likely indicative of bottom-up processes shaped by oceanographic currents. Taken together, reefs that harbour higher shark abundances are likely representative of relatively pristine and energetically subsidised trophic structures (e.g. Mourier et al. 2016), whereas reefs that are strongly affected by human influences (i.e. high human gravity) are exposed to strong fishing pressures. The dichotomies in abundance, biomass, and size structuring of reef fishes have therefore revealed that humans, not reef sharks, are the dominant predators across the world's coral reefs.

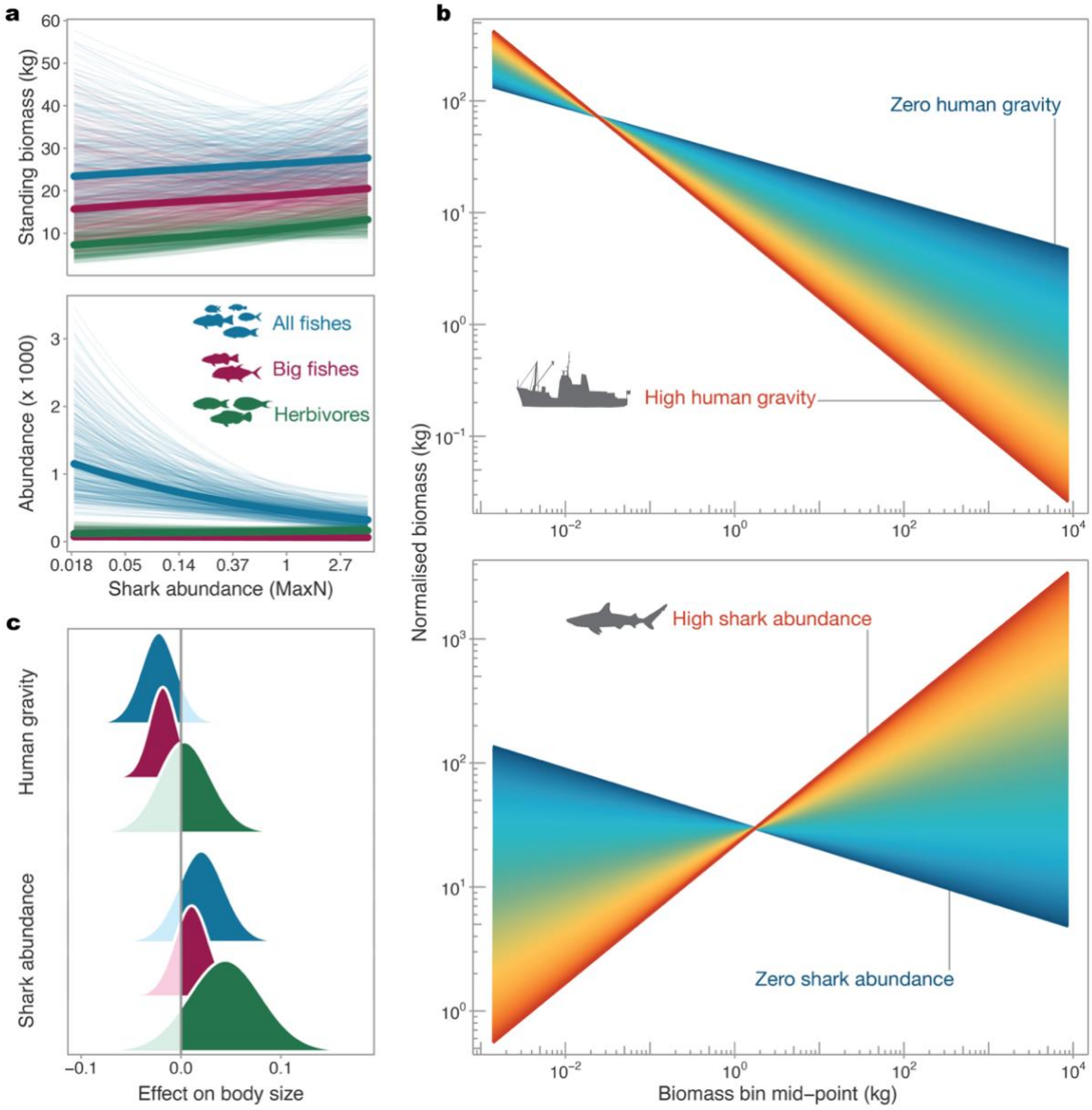

Figure 6-2. The dichotomy between sharks and human gravity on reef fishes. a *The modelled effects of shark abundance (MaxN; see methods) on standing reef fish biomass (top) and abundance (bottom) across all fishes (blue), large fishes (red), and herbivores (green). Thin lines represent randomly sampled draws within the 90% credible interval from the marginal distributions and the thick lines denote the median fitted values. Note the x axes are on the natural log scale.* ***b*** *Size spectrum analyses showing the interacting effects of increasing human gravity (top) and increasing shark abundances (bottom) on the normalised biomass size spectrum of reef fishes. Increasing values (i.e. human gravity and shark abundances) are denoted by warmer colours. Note both axes are on the* log_{10} *scale.* ***c*** *Posterior probabilities based on 1,000 simulated draws on the effects of human gravity (top) and shark abundance (bottom) on the mean body size of all fishes (blue), large fishes (red), and herbivores (green). The majority of the posterior distribution is shown in the darker colours.*

6.3.2 Overfishing through coral reefs

The overwhelming negative effects of human gravity across all groups of fishes (**Fig. 6-1ab**), paired with overexploitation-induced depletion of reef sharks (MacNeil et al. 2020; Sherman et al. 2023; Simpfendorfer et al. 2023), indicates that fisheries have reshaped the trophic structuring of coral reef communities. To capture the scale at which fisheries are affecting sharks and reef fishes, we extracted the reconstructed catch and effort data (Pauly and Zeller 2016) for all sharks, rays, and chimaeras (hereon referred to as 'sharks'; see Methods); and all reef fishes for the countries and territories assessed herein (n = 52). We found drastic declines in the catch per unit effort (CPUE), an indication of relative abundances, across both sharks and reef fishes from 1950 to 2010. Indeed, by 1969, the CPUE for reef sharks had declined by 86.1% (90% credible interval: 81.3-90.6%) and by 60.0% for reef fishes (50.4-69.3%). By 2010, the CPUE for sharks had declined by 94.3% (92.2-96.4%; **Fig. 6-3a**) and for reef fishes by 91.6% (89.3-93.9%; **Fig. 6-3b**). The late 1960's marks the rapid growth in reef fish catches, while shark catches remained relatively stagnant (**Fig. 6-3c**). Given the large decline in shark CPUE during this time, this expansion could be indicative of fishers switching targets (e.g. fishing down the food web; Pauly et al. 1998), supplementing catches with lower trophic level fishes (e.g. fishing through the food web; Essington et al. 2006), or a combination of the two. While catches appear to remain relatively high, increasing fishing effort resulted in shark and reef fish CPUE declining at a rate of 4.8% (2.1-7.5%) and 4.1% (2.6-5.5%) per year, respectively (**Fig. 6-3d**).

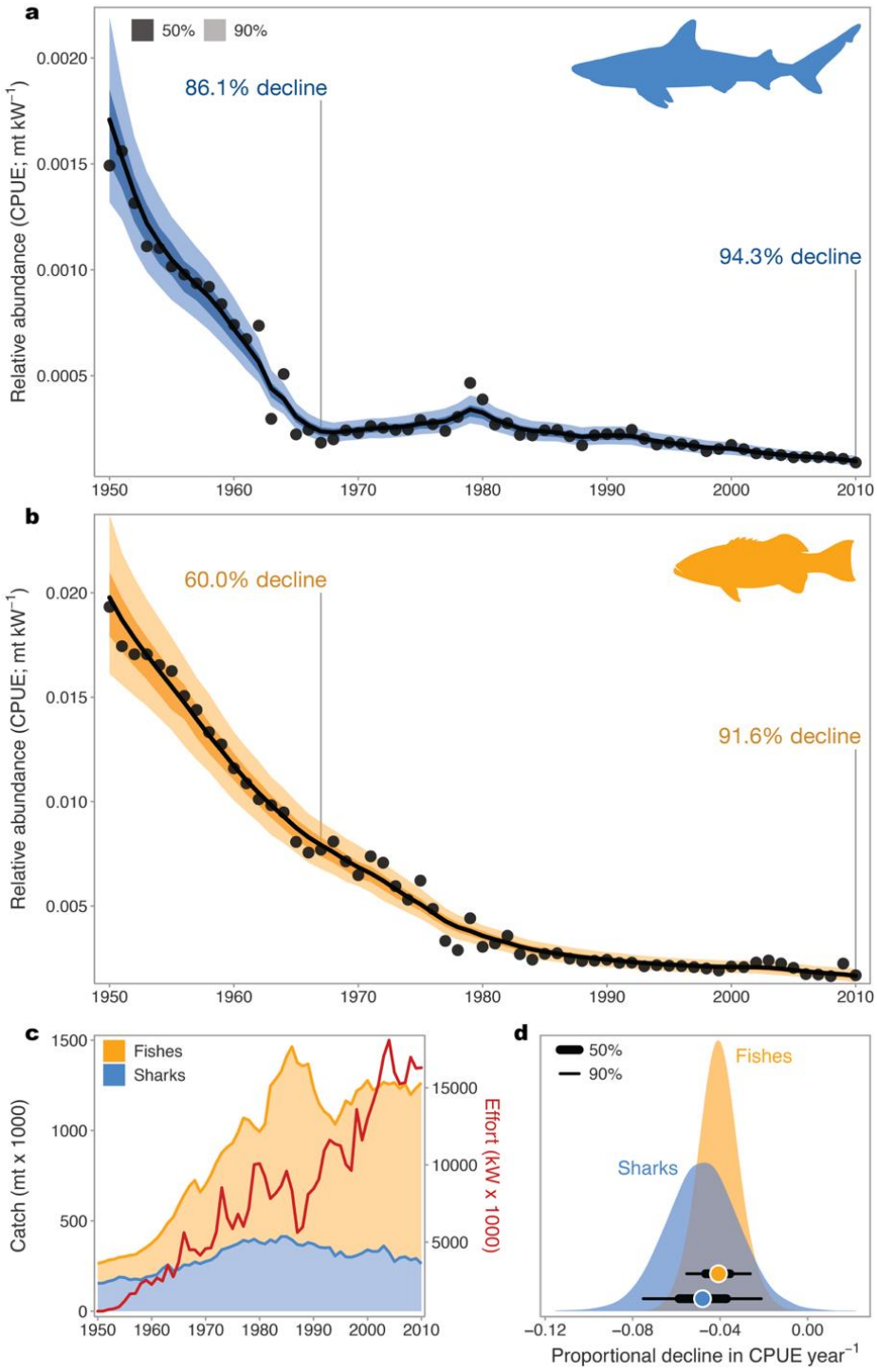

Figure 6-3. Fishing down coral reef communities. *Half-century of changes in catch per unit effort (CPUE; mt kW^{-1}), an index for relative abundances, across* ***a*** *sharks and* ***b*** *reef fishes from 1950 to 2010. Points indicate the mean values across 52 Exclusive Economic Zones. The thick black lines represent the median fitted trend of the underlying state, and the dark and light ribbons denote the 50% and 90% credible intervals, respectively. Calculations of catch per unit effort were calculated from* ***c*** *time series of reconstructed catches of sharks (blue) and reef fishes (orange; mt x 1000; left y axis) with estimates of fishing effort (red line; kW x 1000; right y axis).* ***d*** *Proportional decline in CPUE for sharks (blue) and reef fishes (orange); the dots represent the median fitted values and the thick and thin bars denote the 50% and 90% credible intervals, respectively.*

The simultaneous depletion of sharks and fishes across coral reefs points to a nuanced interpretation of the functioning of coral reef trophodynamics: the contribution of reef sharks to fish biomass removal via piscivory is negligible compared to human harvesting rates. With large-scale technological advances and increased government incentives that encourage unsustainable harvesting practices (Kroodsma et al. 2018; Sumaila et al. 2019), fisheries target the highest prey diversity (Darimont et al. 2023) and can remove biomass at ecologically incompatible rates compared to natural predators (Darimont et al. 2015). Overfishing poses the greatest threat to marine fishes (Ripple et al. 2019; Miranda et al. 2022) whereby some fisheries can extirpate individuals at rates more than 14 times higher than those of natural predators (Darimont et al. 2015). Consequently, more than half of the world's coral reefs are considered overfished (Zamborain-Mason et al. 2023). Here, we showed that the relative abundances of sharks and reef fishes have declined by over 90% over the last half century across 52 Exclusive Economic Zones. While these declines are relatively on par with global CPUE estimates for sharks (Dedman et al. 2024), our findings exceed the global estimate for reef fishes by more than 100% (Eddy et al. 2021). The relatively positive effects of shark sanctuaries on reef fishes (**Fig. 6-1cd**) suggests that countries that harbour a portfolio of effective fisheries management practices (Dulvy and Yan 2020; MacNeil et al. 2020) can benefit lower-trophic level fishes as well as sharks. Therefore, calls to protect the abundance and functioning of reef sharks (Dedman et al. 2024) need to be matched with multispecies fisheries management practices if protecting coral reef ecosystem functions in the Anthropocene is the ultimate goal.

There are no baselines – natural baselines disappeared long ago.

Jeremy Jackson

Chapter 7: General discussion

The overarching goal of my thesis was to evaluate the various factors impacting the growth and productivity of the world's marine fishes. Spanning millions of years of evolution (**Chapter 2**) and various socioeconomic (**Chapters 3** and **6**) and environmental disturbances or gradients (**Chapters 4** and **5**, respectively), the collection of work in my thesis has revealed that human impacts can vastly outweigh the ecological and evolutionary expression of life histories and functioning. I hope that this thesis has shed light on the extent that we, as humans, have altered marine environments, with repercussions reverberating throughout entire ecosystems.

7.1 Growth in an era of relentless change

From various spatial and temporal scales, there appears to be opposing forces that are simultaneously affecting the growth of marine fishes: changes in environmental conditions and direct human exploitation. The differential expression of life histories across fishes, while rooted in the co-evolution and optimisation of traits (Dmitriew 2011), is shaped by species' metabolic ecology (Wong et al. 2021; Gravel et al. 2024). Indeed, the Metabolic Theory of Ecology scales metabolic rates upwards to explain patterns observed at larger ecosystem scales by emphasising the dependence of metabolism on two key components: body size and temperature (Gillooly et al. 2002; Brown et al. 2004). Given the tight physiological links that exists between metabolism and life histories (Wong et al. 2021; Gravel et al. 2024), we can reasonably deduce that stressors impacting either the body size of or the ambient temperature experienced by fishes will affect their respective metabolic rates and/or life histories, which can then manifest as changes in the delivery of functions.

While studies assessing multiple stressors describe effects as being potentially synergistic, antagonistic, or additive (Côté et al. 2016), disentangling the interactions of large stressors, such as climate change or overexploitation, in observational field studies presents immense methodological and ethical challenges. Indeed, **Chapters 2** and **3** illustrate some of these challenges relatively clearly; not all stressors can be measured across the same ecological scales. Across evolutionary time,

Chapter 2 showed that the warmer temperatures of the Eocene (Westerhold et al. 2020), paired with the habitat reconfigurations occurring shortly after (Bellwood et al. 2017), likely contributed to the evolution of faster growth rates across coral reef fishes. Indeed, with fishes spanning many orders of magnitude in body size, it is plausible that temperature was the dominant driver in the accumulation of faster growth rates across reef fishes. Although the findings from this chapter are the product of evaluating growth across millions of years of evolutionary time, they are also predicated on the absence of human pressures.

The role of humans in shaping the growth of fishes is addressed in **Chapter 3**. Although only on the scale of 113 years, this chapter combined both anthropogenic impacts, via fisheries, and changes in environmental temperature. In this chapter, I showed that the historical exploitation of commercially valuable fishes correlated with declines in the growth performance of marine fishes, which were concentrated in temperate regions. These declines were likely driven by the legacy of size-based harvesting as opposed to the physiological consequences of warmer temperatures. The lessons learned from the first two data chapters, therefore, highlight that temperature has the power to shape evolutionary patterns in growth, but it is dwarfed by the impacts of commercial fisheries in the Anthropocene.

While my thesis was aimed at assessing changes in the growth *and* productivity of fishes, an obvious question that we must ask is: will changes in growth actually affect productivity? Like all other well-trained ecologists, I will have to answer generically with: it *might*. The reason for this uncertainty is that biological systems are inherently complex – which, as an aside, is the primary reason why parsimony was never used as a model selection tool in this thesis – meaning that changes in one life-history trait can have repercussions across all other life-history traits. Evolutionary and ecological processes shape and select for the co-evolution of optimised life histories (Charnov and Berrigan 1991; Dmitriew 2011; Healy et al. 2019), so declines in growth rates could be matched with increases in fecundity (as suggested by the slow-fast continuum of life histories; Bielby et al. 2007; Beukhof et al. 2019; Gravel et al. 2024), leading to higher abundances and thus productivity. Indeed, fisheries scientists have long been attempting to model this phenomenon using various surplus

production frameworks, recognizing the differential biomass output of relatively juvenescent populations compared to a stock comprising older individuals (Hilborn and Walters 1992). Similarly, disparities in the expression of life histories can dictate whether species are more likely to move between habitats due to changes in environmental conditions (Perry et al. 2005). In many cases, as long as numerical abundances have not been severely depleted, compensatory mechanisms (e.g. changes in fecundity, emigration/immigration) can still result in relatively productive fish communities. It is therefore unclear whether changes in growth will lead to changes in community productivity, providing an incredibly rich research avenue for the future. The covariation and differential expression of critical life-history traits could buffer communities against large-scale stressors and remain productive; the species that are present, however, could be fundamentally different.

7.2 Biodiversity and productivity: two sides of two different coins?

For many decades, biodiversity has been thought of as a causal mechanism leading to higher levels of ecosystem functioning (Loreau 2000; McCann 2000; Loreau and Hector 2001; Blüthgen and Klein 2011). The biodiversity-ecosystem function relationship, or BEF for short, drew attention to the looming reality that if we lose species to extinction, we may simultaneously lose ecosystem functions (Naeem et al. 1994; Naeem 2002; Cardinale et al. 2012), thus instilling a functional value to biodiversity. Despite the relatively strong evidence for the BEF theory in experimental studies (Tilman et al. 2014), the evidence from observational field studies has been equivocal (Hagan et al. 2021). There are multiple schools of thought addressing why there is a dichotomy between experimental and observational studies, many of which are centred around differences with scale (e.g. regional versus local species pools; Thompson et al. 2018) and the difficulties in detecting species interactions (e.g. the filtering of species that occurs during community assembly; Hagan et al. 2021). It is also unclear if diversity is a causal factor for functioning, or if the two arose simultaneously. Indeed, it is possible that the underlying biogeographical history of the oceans led to the formation of both richness *and* functional gradients.

In coral reef fishes, species richness is concentrated in the Indo-Australian Archipelago (Tittensor et al. 2010), which arose from multiple co-occurring processes (i.e. accumulation, survival, origination, and export; Cowman and Bellwood 2013). On modern-day coral reefs, planktivorous fishes contribute disproportionally to (i) the productivity of fish communities (Morais et al. 2021) and (ii) the formation of the richness patterns (Siqueira et al. 2021). Access to highly nutritious planktonic resources (Gahan et al. 2024) likely contributes to their productive success, while highly stable historical oceanographic conditions, paired with the abundance of planktonic resources, allowed for the partitioning of niches (Siqueira et al. 2021). Therefore, it is possible that the abundance of plankton among other environmental conditions supported both the productivity and richness of planktivores. An added layer of complexity, which I highlight in **Chapter 5**, is that we can also produce fundamentally different BEF effects depending on how we choose to define biodiversity. Indeed, when we disentangle the various elements of biodiversity, we can start to understand the mechanisms that may underpin community productivity. In **Chapter 5**, I showed that abundance-emphasised diversity better explained patterns of productivity than species richness across the world's tropics. Similarly, in **Chapter 4**, I found a notable shift in species composition and a decline in species richness following the 1998 mass coral bleaching event, but community abundance and productivity remained stable. In both chapters, I highlight the capacity of communities to remain productive independent of the number of species present.

Under ecological theory, higher species richness supports the recovery of functioning via mechanisms such as the portfolio effect or functional redundancy (Loreau 2004; Schindler et al. 2010, 2015). In short, a richer species pool equates to a higher probability of functionally similar species, which can replace those that are lost due to disturbances (Yachi and Loreau 1999). This pattern arose in **Chapter 4**, where the pre-bleaching fish assemblage was dominated by coral-associated fishes and the post-bleaching assemblage was composed of detritivorous fishes. While the response diversity of a community can increase its resilience against disturbances (Elmqvist et al. 2003; Laliberté et al. 2010), and has been used to rationalise the conservation of biodiversity, it appears that we have created a disconnect between the delivery of functions and the *actors* delivering the functions (Bellwood et al.

2024). When I first published this chapter, I had never received so much press attention for a publication before, despite having published in higher impact journals. It appears that people were given a glimmer of hope with regards to the state of the Great Barrier Reef: the productivity of fishes could be sustained despite multiple environmental disturbances. While this headline clearly attracted the attention of a lot of people, reaching 149 different media outlets, it also garnered the attention of some high-profile critics. Notable scientists responded with public criticisms, one stating that my work was promoting coral reefs "overrun by cockroaches".

We see similar disconnects between ecosystem functions and the species present in other examples. The coral reef crown-of-thorns starfish, a naturally occurring coral-feeding echinoderm, is actively being culled in an effort to protect corals (Hall et al. 2017), which are ultimately threatened by climate change, not corallivory. Similarly, in Yellowstone National Park, wolves were also being culled in an attempt to protect herbivorous elk populations, which control low-lying shrubs across the park (Ripple et al. 2001). In all three examples, ecosystem functions are effectively being ignored (i.e. productivity, corallivory, and predation) and replaced by species identities (i.e. coral-associated fishes, corals, and elk, respectively). So, it appears that we have underprioritised the conservation value of ecosystem functioning while increasing the value of species.

Does this mean that species richness does not matter in terms of ecosystem functioning? Well, it ultimately depends on our attribution of value to what *matters*. For some functions, simply having fishes present means that some level of functioning is occurring. This is well represented by **Figure 5-2** from **Chapter 5**, which illustrates that there are numerous fish communities that have relatively low diversity but high productivity. Similarly, in **Chapter 4**, fluctuations in species richness were not mirrored by changes in productivity; productivity remained stable. Indeed, across the world's coral reefs, species richness has variable effects on a range of ecosystem functions, including polarising effects on piscivory and herbivory (Schiettekatte et al. 2022). As long as there are fishes present assimilating resources to maintain metabolic processes, then ecosystem functioning is occurring to some extent (Brandl et al. 2022). There are instances, however, where species identities cannot be ignored. Across the world's fisheries, many species are specifically targeted by commercial harvesters,

with some single-species fisheries dominating country-level catches (e.g. anchovy in Peru; Pauly et al. 2020). Indeed, even across multispecies coral reef fisheries, specific species are targeted over others due to factors such as body size (e.g. Bellwood et al. 2003; Dulvy et al. 2004b), commercial value (e.g. Khasanah et al. 2020), or disease prevalence (e.g. ciguatera; Schoelinck et al. 2014). Across many coastal communities, there are deep-seated cultural values associated with notable species that are present. For example, each species of Pacific salmon (genus *Oncorhynchus*) found along the coast of the northeastern Pacific Ocean is deeply engrained in the historical and local cultural practices of the indigenous nations in those regions (Alfred 2010; Reid et al. 2022). While the functional value of biodiversity can be contentious, its intrinsic value is indisputable. We have therefore reached a potential philosophical dichotomy, where regardless of whether we want to protect biodiversity or functioning, we must face the reality that we might have to sacrifice one to prioritise the other.

7.3 More data, more problems

Nearly the entirety of my thesis was reliant on data that was collected by others, which was necessary to answer questions across space (i.e. across all the oceans) and time (i.e. dating back millions of years). While it is exciting making inferences across macroecological scales, as many have previously noted, big data is full of big disappointments. In other words, we are sacrificing our abilities to disentangle fine-scale mechanisms when we are looking at the 'big picture'. For example, some studies reported sex-specific von Bertalanffy growth curves, indicating that there are different growth trajectories between the males and females of certain species. While these differences can have important ecological consequences, the inconsistencies in sexing individuals across studies means that growth could only be assessed at a broader species level (i.e. combining males and females). Indeed, many of the ecological variables that could not be measured or generalised to the species level were effectively omitted from my analyses.

The inclusion of socioeconomic variables fall victim to similar shortfalls. For example, the separation of fisheries management schemes in **Chapter 3** are reliant on the presence of stock assessments, which do not capture locally managed fisheries. In the case of coral reef fisheries, local

management practices can be incredibly effective and are misrepresented in national census measures, such as national development indices or fisheries landings data (Basurto et al. 2025). Consequently, some species that are otherwise considered as "unmanaged" or "unfished" many be of high fisheries importance at small scales (e.g. for individual villages), but less so at larger, global scales. Similarly, global landings data for non-commercial species (such as those used in **Chapter 6**), are limited to the taxonomic resolution reported by each nation to the Food and Agriculture Organisation of the United Nations. Therefore, a holistic use of "reef-associated species" provides an inclusive, but taxonomically vague description of catches. Therefore, while there is tremendous value in identifying generalised patterns that transcend political borders, we must acknowledge the fine-scale details that we are forfeiting with every step back we take.

My thesis work and really, all macroecological studies, stands on the shoulders of organismal/integrative/field biologists. Although high-impact journals are currently favouring the publication of "big data" papers, the only way in which our macroecological inferences can improve is with the continued production of smaller field studies to further our understanding of the underlying ecological and socioeconomic mechanisms regulating our ecosystems. In turn, we can better validate our assumptions while adding more data to improve our macroecological inferences. We are currently on the frontier of understanding how energy and matter is moving through marine systems. With increased resolution in our estimates of various function-related parameters via increased field sampling, such as demographic growth models, we can generate improved macroecological inferences.

7.4 The ghost of functions past: shifts without a baseline

At this point, you might be wondering: why was **Chapter 6** added to this thesis if it did not technically measure growth nor productivity? Did I simply add it here to boost the page count of my thesis? While a completely valid question, I have chosen to include it for two reasons that are *marginally* less self-serving. The first reason is that, based on the findings from **Chapter 5**, the functioning of fishes is ultimately driven by species abundances; therefore, we can reasonably deduce that species are

effectively functionally extinct at the community level when numerical abundances are severely depleted (e.g. Galetti et al. 2013; MacNeil et al. 2020). Indeed, using the same dataset of shark abundances, MacNeil et al. (2020) found that across more than 350 coral reefs around the world, they did not observe a single shark across roughly 20% of the surveyed reefs. Therefore, across many of the world's coral reefs, the rates at which sharks are declining means that, for now, we will have to infer functioning at macroecological scales from proxies, such as abundances. Although proxies are not always indicative of ecosystem function delivery, as Dr Jillian Dunic wrote with regards to the declines in seagrass meadows: "Waiting for more data is not a prudent strategy for [species] at high risk of loss/destruction" (Dunic 2023).

While the perilous status of the world's sharks therefore suggests that their contribution to the consumed biomass on coral reefs is much smaller than theorised, there are still some reefs that harbour very high abundances of reef sharks. Species interactions in high-diversity communities, such as coral reefs, are inherently complex, which can dampen the roles of individual species and/or groups (Pace et al. 1999). Despite their large body sizes, it is possible that the top-down predatory pressures exerted by sharks are not ubiquitous across different reefs. For example, Rasher et al. (2017) reported fear effects on herbivore feeding rates in Fiji, while Tebbett et al. (2024c) found no effects on herbivorous fishes on the Great Barrier Reef. These discrepancies are further emphasised when the effects of fishing are considered (e.g. Casey et al. 2017; Desbiens et al. 2021). Additionally, the biomass consumption across coral reefs is also relatively bottom heavy. The smallest benthic fishes, which are not targeted by sharks, contribute disproportionally to the total consumed reef fish biomass (Brandl et al. 2019c). Indeed, the average size of a fish predator on coral reefs is less than 4 cm in total length (Mihalitsis et al. 2022). The inconsistencies in the influence of sharks as predators, paired with the bottom-heavy trophodynamics of reef fish communities, suggests that external factors may shape communities more than natural predators. As illustrated by **Figure 6-2** in **Chapter 6**, the biogeography and/or external energetic process, such as pelagic subsidies, may have a larger influence on the biomass distribution of reef fish communities, even when shark abundances are relatively high.

The second reason why I chose to include **Chapter 6** in my thesis is that it contextualises what it means to study ecosystem functions across today's seascapes. **Figure 6-3** from **Chapter 6** shows the changes in catch per unit effort (CPUE) of sharks and reef fishes across 52 Exclusive Economic Zones since 1950, with marked declines across both groups. Declines in CPUE can be indicative of declines in the relative abundances of those groups, namely sharks and reef fishes that are targeted by fishers. By the time that I officially started my thesis work in 2021, the abundances of sharks and some reef fishes had already declined by more than 90% compared to 1950 (as suggested by their respective declines in CPUE). Even by 1950, many tropical species in the Caribbean had been driven to local extinction with notable fishing-induced changes in reef fish communities (Jackson 1997). These shifted baselines are not unique to tropical systems. For example, before their extirpation as "destructive pests" to fishing boats, basking sharks (*Cetorhinus maximus*) were once so abundant in a single bay in the northeast Pacific that "*one could cross the entire bay by simply walking across their backs*". Pachena Bay, situated on the traditional territory of the Huu-ay-aht First Nations, could historically support a tremendous fish biomass, pointing to an incredible energetic regime. Now, because of the post-extermination rarity of basking sharks in this region, I would probably vastly underestimate the energetic capacity of Pachena Bay. It is therefore very likely that the world's marine ecosystems are already functioning in fundamentally different ways than they did historically.

We tend to think of shifting baselines with regards to declines in abundance or changes in maximum body size. Daniel Pauly first coined the term when describing the severe depletion of fish stocks with the onset of industrialised fisheries (Pauly 1995). The impacts of these shifted baselines were relatively easy to describe; poetic descriptions of walking across the backs of sharks or black-and-white pictures of monstrous trophy fishes allowed us to imagine what once was. While we can describe the magnitude of these shifts with (some) empirical evidence, without using proxies like abundance, it's unlikely we'll ever fully understand how much the function delivery of fishes has shifted. Without an adequate baseline to make useful comparisons, studying ecosystem functions in the Anthropocene is pigeonholed to current ecological and socioeconomic conditions. This reality ties into one of the main lessons drawn from **Chapter 6**, which highlights the rather Sisyphean attempt of

trying to understand ecological functions that were once shaped by natural selection but are now at the mercy of relentless anthropogenic change.

7.5 The growth of a failed fish

At the start of Professor Bellwood's Evolution and Ecology of Reef Fishes class at JCU, he highlights that we're all failed fish. Our ancestors couldn't handle the cut-throat conditions of the oceans and had to adapt to a terrestrial lifestyle, whereas fishes in the wet thrived. While we, as humans, arose as the evolutionary by-product of harsh marine environments, we have ironically made the conditions in the oceans even harsher. Throughout this thesis, I showed that human avarice could shape the life histories and functioning of fishes more than environmental stressors, but none of this really came as a shock to me. I knew we were capable of changing the world. I came into this PhD with the goal of understanding how fishes would react to this changing world because I thought this work was important. I had convinced myself that managers and practitioners needed to know how ecosystems were functioning, emphasising that we need to understand the underlying energetic fluxes of these transitioning communities to know how fishes will respond in the future. Now, sitting at the end of my doctoral journey, I'm forced to reflect and ask myself: does any of this actually matter?

Last year, my friend and echinoderm enthusiast, Dr Hannah Watkins, was grappling with writing this portion of her thesis. She was trying to answer the question that plagues nearly all scientists: does any of this matter? As Hannah eloquently described in the conclusions of her thesis, we can essentially apply any philosophical school of thought as to why our work matters, none of which could be objectively disputed (Watkins 2024). While frustratingly inconclusive, she's absolutely right. At this point, we're all relatively well equipped with the tools to convince funders and/or editors to support our work, that our findings will fundamentally reshape how we view/use/manage/understand/study/protect/etc. various marine ecosystems. But, at the end of the day, conservation and management policies can both succeed and fail without understanding ecosystem functions. Managers, scientists, and the general public can all value nature differently, so while *I* believe that studying functions is valuable, others may disagree.

So, after a global pandemic and 3.5 years of thesis work, what value do I, a failed fish, place on my work? For the sake of understanding the natural world around us, I think studying ecosystem functions is an incredibly fruitful venture. Instead of studying the who, what, and where, we get to understand the how and why ecosystems operate the way they do. Selfishly, I garner a great deal of satisfaction in understanding how the natural world around us works. I would be disingenuous if I didn't think that my work could still have *some* application, but I'm more aware that this may be the penultimate reason why I pursued a PhD. While I think our priorities are currently centred around preventing extinctions, I do think it's only a matter of time until we need to think about managing functions as well. Finally, despite my generally interrogative tone throughout this chapter, I do care about biodiversity. I firmly believe that we have a moral obligation to prevent extinctions and to be transparent that our ethical views on nature alone can justify our actions; we do not need to invoke functions. In other words, there is value to conserving biodiversity regardless of the functioning of the communities.

References

Abrams PA, Leimar O, Nylin S, Wiklund C (1996) The effect of flexible growth rates on optimal sizes and development times in a seasonal environment. The American Naturalist 147:381–395

Ackerman J, Bellwood D (2000) Reef fish assemblages: a re-evaluation using enclosed rotenone stations. Marine Ecology Progress Series 206:227–237

Ackerman JL, Bellwood DR (2002) Comparative efficiency of clove oil and rotenone for sampling tropical reef fish assemblages. Journal of Fish Biology 60:893–901

Alfred G (2010) Development and evaluation of "salmon – the lifeline to our culture." University of Victoria

Anderson CNK, Hsieh C, Sandin SA, Hewitt R, Hollowed A, Beddington J, May RM, Sugihara G (2008) Why fishing magnifies fluctuations in fish abundance. Nature 452:835–839

Arendt JD (1997) Adaptive intrinsic growth rates: an integration across taxa. The Quarterly Review of Biology 72:149–177

Atkinson D (1994) Temperature and organism size - a biological law for ectotherms? Advances in Ecological Research 25:1–58

Audzijonyte A, Richards SA, Stuart-Smith RD, Pecl G, Edgar GJ, Barrett NS, Payne N, Blanchard JL (2020) Fish body sizes change with temperature but not all species shrink with warming. Nature Ecology & Evolution 4:809-814

Baird A, Marshall P (2002) Mortality, growth and reproduction in scleractinian corals following bleaching on the Great Barrier Reef. Marine Ecology Progress Series 237:133–141

Bannikov AF (2008) Revision of some Eocene fishes from Bolca, Northern Italy, previously classified with the Apogonidae and Enoplosidae (Perciformes). Studi e Ricerche sui giacimenti Terziari di Bolca, XII Miscellanea Paleontologica 9:65–76

Barber NA, Jones HP, Duvall MR, Wysocki WP, Hansen MJ, Gibson DJ (2017) Phylogenetic diversity is maintained despite richness losses over time in restored tallgrass prairie plant communities. Journal of Applied Ecology 54:137–144

Bardach JE (1959) The Summer Standing Crop of Fish on a Shallow Bermuda Reef. Limnology and Oceanography 4:77–85

Barley SC, Clark TD, Meeuwig JJ (2020) Ecological redundancy between coral reef sharks and predatory teleosts. Reviews in Fish Biology and Fisheries 30:153–172

Barneche DR, Allen AP (2018) The energetics of fish growth and how it constrains food-web trophic structure. Ecology Letters 21:836–844

Barneche DR, Hulatt CJ, Dossena M, Padfield D, Woodward G, Trimmer M, Yvon-Durocher G (2021) Warming impairs trophic transfer efficiency in a long-term field experiment. Nature 592:76–79

Barneche DR, Kulbicki M, Floeter SR, Friedlander AM, Allen AP (2016) Energetic and ecological constraints on population density of reef fishes. Proceedings of the Royal Society B: Biological Sciences 283:20152186

Barneche DR, Kulbicki M, Floeter SR, Friedlander AM, Maina J, Allen AP (2014) Scaling metabolism from individuals to reef-fish communities at broad spatial scales. Ecology Letters 17:1067–1076

Barneche DR, Rezende EL, Parravicini V, Maire E, Edgar GJ, Stuart-Smith RD, Arias-González JE, Ferreira CEL, Friedlander AM, Green AL, Luiz OJ, Rodríguez-Zaragoza FA, Vigliola L, Kulbicki M, Floeter SR (2019) Body size, reef area and temperature predict global reef-fish species richness across spatial scales. Global Ecology and Biogeography 28:315–327

Bascompte J, Melián CJ, Sala E (2005) Interaction strength combinations and the overfishing of a marine food web. Proceedings of the National Academy of Sciences 102:5443–5447

Basurto X, Gutierrez NL, Franz N, Mancha-Cisneros MDM, Gorelli G, Aguión A, Funge-Smith S, Harper S, Mills DJ, Nico G, Tilley A, Vannuccini S, Virdin J, Westlund L, Allison EH, Anderson CM, Baio A, Cinner J, Fabinyi M, Hicks CC, Kolding J, Melnychuk MC, Ovando D, Parma AM, Robinson JPW, H. Thilsted S (2025) Illuminating the multidimensional contributions of small-scale fisheries. Nature 637:875-884

Bellwood DR, Baird AH, Depczynski M, González-Cabello A, Hoey AS, Lefèvre CD, Tanner JK (2012) Coral recovery may not herald the return of fishes on damaged coral reefs. Oecologia 170:567–573

Bellwood DR, Brandl SJ, McWilliam M, Streit RP, Yan HF, Tebbett SB (2024) Studying functions on coral reefs: past perspectives, current conundrums, and future potential. Coral Reefs 43:281–297

Bellwood DR, Goatley CHR, Bellwood O (2017) The evolution of fishes and corals on reefs: form, function and interdependence. Biological Reviews 92:878–901

Bellwood DR, Goatley CHR, Cowman PF, Bellwood O (2015) The evolution of fishes on coral reefs: fossils, phylogenies, and functions. In: Mora C. (eds) Ecology of Fishes on Coral Reefs. Cambridge University Press, Cambridge, pp 55–63

Bellwood DR, Hoey AS, Ackerman JL, Depczynski M (2006) Coral bleaching, reef fish community phase shifts and the resilience of coral reefs. Global Change Biology 12:1587–1594

Bellwood DR, Hoey AS, Bellwood O, Goatley CHR (2014) Evolution of long-toothed fishes and the changing nature of fish–benthos interactions on coral reefs. Nature Communications 5:3144

Bellwood DR, Hoey AS, Choat JH (2003) Limited functional redundancy in high diversity systems: resilience and ecosystem function on coral reefs. Ecology Letters 6:281–285

Bellwood DR, Pratchett MS, Morrison TH, Gurney GG, Hughes TP, Álvarez-Romero JG, Day JC, Grantham R, Grech A, Hoey AS, Jones GP, Pandolfi JM, Tebbett SB, Techera E, Weeks R, Cumming GS (2019a) Coral reef conservation in the Anthropocene: Confronting spatial mismatches and prioritizing functions. Biological Conservation 236:614–615

Bellwood DR, Streit RP, Brandl SJ, Tebbett SB (2019b) The meaning of the term 'function' in ecology: a coral reef perspective. Functional Ecology 33:948–961

Bellwood DR, Wainwright PC (2002) The history and biogeography of fishes on coral reefs. Sale PF (ed) Coral reef fishes: dynamics and diversity in a complex ecosystem. Academic Press, San Diego, pp 5–32

Berkelmans R, Oliver JK (1999) Large-scale bleaching of corals on the Great Barrier Reef. Coral Reefs 18:55–60

Berrigan D, Charnov EL (1994) Reaction norms for age and size at maturity in response to temperature: a puzzle for life historians. Oikos 70:474

Beukhof E, Frelat R, Pecuchet L, Maureaud A, Dencker TS, Sólmundsson J, Punzón A, Primicerio R, Hidalgo M, Möllmann C, Lindegren M (2019) Marine fish traits follow fast-slow continuum across oceans. Scientific Reports 9:17878

Beverton RJH, Holt SJ (1957) On the dynamics of exploited fish populations. Springer, Dordrecht, the Netherlands

Bielby J, Mace GM, Bininda-Emonds ORP, Cardillo M, Gittleman JL, Jones KE, Orme CDL, Purvis A (2007) The fast-slow continuum in mammalian life history: an empirical reevaluation. The American Naturalist 169:10

Blanchard JL, Dulvy NK, Jennings S, Ellis JR, Pinnegar JK, Tidd A, Kell LT (2005) Do climate and fishing influence size-based indicators of Celtic Sea fish community structure? ICES Journal of Marine Science 62:405–411

Blüthgen N, Klein A-M (2011) Functional complementarity and specialisation: the role of biodiversity in plant–pollinator interactions. Basic and Applied Ecology 12:282–291

Brander K (1995) The effect of temperature on growth of Atlantic cod (*Gadus morhua* L.). ICES Journal of Marine Science 52:1–10

Brander KM (2007) Global fish production and climate change. Proceedings of the National Academy of Sciences 104:19709–19714

Brandl SJ, Goatley CHR, Bellwood DR, Tornabene L (2018) The hidden half: ecology and evolution of cryptobenthic fishes on coral reefs: cryptobenthic reef fishes. Biological Reviews 93:1846–1873

Brandl SJ, Johansen JL, Casey JM, Tornabene L, Morais RA, Burt JA (2020) Extreme environmental conditions reduce coral reef fish biodiversity and productivity. Nature Communications 11:3832

Brandl SJ, Lefcheck JS, Bates AE, Rasher DB, Norin T (2022) Can metabolic traits explain animal community assembly and functioning? Biological Reviews 98:1-18

Brandl SJ, Morais RA, Casey JM, Parravicini V, Tornabene L, Goatley CHR, Côté IM, Baldwin CC, Schiettekatte NMD, Bellwood DR (2019a) Response to Comment on "Demographic dynamics of the smallest marine vertebrates fuel coral reef ecosystem functioning." Science 366:eaaz1301

Brandl SJ, Rasher DB, Côté IM, Casey JM, Darling ES, Lefcheck JS, Duffy JE (2019b) Coral reef ecosystem functioning: eight core processes and the role of biodiversity. Frontiers in Ecology and the Environment 17:445–454

Brandl SJ, Tornabene L, Goatley CHR, Casey JM, Morais RA, Côté IM, Baldwin CC, Parravicini V, Schiettekatte NMD, Bellwood DR (2019c) Demographic dynamics of the smallest marine vertebrates fuel coral reef ecosystem functioning. Science 364:1189–1192

Brown JH, Gillooly JF, Allen AP, Savage VM, West GB (2004) Toward a metabolic theory of ecology. Ecology 85:1771–1789

Bruno JF, Côté IM, Toth LT (2018) Climate change, coral loss, and the curious case of the parrotfish paradigm: why don't marine protected areas improve reef resilience? Annual Review of Marine Science 11:307–334

Bürkner P-C (2017) *brms*: An R package for Bayesian multilevel models using Stan. Journal of Statistical Software 80:1–28

Caley MJ, Schwarzkopf L (2004) Complex growth rate evolution in a latitudinally widespread species. Evolution 58:862–869

Cantalice KM, Alvarado-Ortega J, Bellwood DR, Siqueira AC (2022) Rising from the ashes: the biogeographic origins of modern coral reef fishes. BioScience 72:769–777

Cardinale BJ, Duffy JE, Gonzalez A, Hooper DU, Perrings C, Venail P, Narwani A, Mace GM, Tilman D, Wardle DA, Kinzig AP, Daily GC, Loreau M, Grace JB, Larigauderie A, Srivastava DS, Naeem S (2012) Biodiversity loss and its impact on humanity. Nature 486:59–67

Carlson P, Davis K, Warner R, Caselle J (2017) Fine-scale spatial patterns of parrotfish herbivory are shaped by resource availability. Marine Ecology Progress Series 577:165–176

Carpenter B, Gelman A, Hoffman MD, Lee D, Goodrich B, Betancourt M, Brubaker M, Guo J, Li P, Riddell A (2017) Stan: a probabilistic programming language. Journal of Statistical Software 76:1–32

Casey JM, Baird AH, Brandl SJ, Hoogenboom MO, Rizzari JR, Frisch AJ, Mirbach CE, Connolly SR (2017) A test of trophic cascade theory: fish and benthic assemblages across a predator density gradient on coral reefs. Oecologia 183:161–175

Ceballos G, Ehrlich PR, Barnosky AD, García A, Pringle RM, Palmer TM (2015) Accelerated modern human–induced species losses: entering the sixth mass extinction. Science Advances 1:e1400253

Chao A, Gotelli NJ, Hsieh TC, Sander EL, Ma KH, Colwell RK, Ellison AM (2014) Rarefaction and extrapolation with Hill numbers: a framework for sampling and estimation in species diversity studies. Ecological Monographs 84:45–67

Chao A, Jost L (2012) Coverage-based rarefaction and extrapolation: standardizing samples by completeness rather than size. Ecology 93:2533–2547

Charnov EL, Berrigan D (1991) Evolution of life history parameters in animals with indeterminate growth, particularly fish. Evolutionary Ecology 5:63–68

Chen T, Guestrin C (2016) XGBoost: A Scalable Tree Boosting System. KDD '16: The 22nd ACM SIGKDD International Conference on Knowledge Discovery and Data Mining 785–794

Chen T, He T, Benesty M, Khotilovich V, Tang Y (2018) *xgboost*: Extreme gradient boosting.

Cheung WWL, Sarmiento JL, Dunne J, Frölicher TL, Lam VWY, Deng Palomares ML, Watson R, Pauly D (2013) Shrinking of fishes exacerbates impacts of global ocean changes on marine ecosystems. Nature Climate Change 3:254–258

Choat JH (2021) Marine biology: Ageing a 'living fossil.' Current Biology 31:R998–R1000

Cinner JE, Maire E, Huchery C, MacNeil MA, Graham NAJ, Mora C, McClanahan TR, Barnes ML, Kittinger JN, Hicks CC, D'Agata S, Hoey AS, Gurney GG, Feary DA, Williams ID, Kulbicki M, Vigliola L, Wantiez L, Edgar GJ, Stuart-Smith RD, Sandin SA, Green A, Hardt MJ, Beger M, Friedlander AM, Wilson SK, Brokovich E, Brooks AJ, Cruz-Motta JJ, Booth DJ, Chabanet P, Gough C, Tupper M, Ferse SCA, Sumaila UR, Pardede S, Mouillot D (2018) Gravity of human impacts mediates coral reef conservation gains. Proceedings of the National Academy of Sciences 115:E6116–E6125

Cinner JE, Zamborain-Mason J, Gurney GG, Graham NAJ, MacNeil MA, Hoey AS, Mora C, Villéger S, Maire E, McClanahan TR, Maina JM, Kittinger JN, Hicks CC, D'agata S, Huchery C, Barnes ML, Feary DA, Williams ID, Kulbicki M, Vigliola L, Wantiez L, Edgar GJ, Stuart-Smith RD, Sandin SA, Green AL, Beger M, Friedlander AM, Wilson SK, Brokovich E, Brooks AJ, Cruz-Motta JJ, Booth DJ, Chabanet P, Tupper M, Ferse SCA, Sumaila UR, Hardt MJ, Mouillot D (2020) Meeting fisheries, ecosystem function, and biodiversity goals in a human-dominated world. Science 368:307–311

Clarke DA, York PH, Rasheed MA, Northfield TD (2017) Does biodiversity–ecosystem function literature neglect tropical ecosystems? Trends in Ecology & Evolution 32:320–323

Clavel J, Escarguel G, Merceron G (2015) *mvmorph*: an R package for fitting multivariate evolutionary models to morphometric data. Methods in Ecology and Evolution 6:1311–1319

Coghlan AR, Blanchard JL, Wotherspoon S, Stuart-Smith RD, Edgar GJ, Barrett N, Audzijonyte A (2024) Mean reef fish body size decreases towards warmer waters. Ecology Letters 27:e14375

Coker DJ, Wilson SK, Pratchett MS (2014) Importance of live coral habitat for reef fishes. Reviews in Fish Biology and Fisheries 24:89–126

Constance J, Ebert DA, Fahmi, Finucci B, Simeon B, Kyne PM (2023) *Urolophus javanicus*. The IUCN Red List of Threatened Species e.T60095A229337053

Costello C, Ovando D, Clavelle T, Strauss CK, Hilborn R, Melnychuk MC, Branch TA, Gaines SD, Szuwalski CS, Cabral RB, Rader DN, Leland A (2016) Global fishery prospects under contrasting management regimes. Proceedings of the National Academy of Sciences 113:5125–5129

Costello C, Ovando D, Hilborn R, Gaines SD, Deschenes O, Lester SE (2012) Status and solutions for the world's unassessed fisheries. Science 338:517–520

Côté IM, Darling ES (2010) Rethinking ecosystem resilience in the face of climate change. PLOS Biology 8:e1000438

Côté IM, Darling ES, Brown CJ (2016) Interactions among ecosystem stressors and their importance in conservation. Proceedings of the Royal Society B: Biological Sciences 283:20152592

Cowman PF, Bellwood DR (2011) Coral reefs as drivers of cladogenesis: expanding coral reefs, cryptic extinction events, and the development of biodiversity hotspots. Journal of Evolutionary Biology 24:2543–2562

Cowman PF, Bellwood DR (2013) The historical biogeography of coral reef fishes: global patterns of origination and dispersal. Journal of Biogeography 40:209–224

Cowman PF, Bellwood DR, van Herwerden L (2009) Dating the evolutionary origins of wrasse lineages (Labridae) and the rise of trophic novelty on coral reefs. Molecular Phylogenetics and Evolution 52:621–631

Craven D, Eisenhauer N, Pearse WD, Hautier Y, Isbell F, Roscher C, Bahn M, Beierkuhnlein C, Bönisch G, Buchmann N, Byun C, Catford JA, Cerabolini BEL, Cornelissen JHC, Craine JM, De Luca E, Ebeling A, Griffin JN, Hector A, Hines J, Jentsch A, Kattge J, Kreyling J, Lanta V, Lemoine N, Meyer ST, Minden V, Onipchenko V, Polley HW, Reich PB, van Ruijven J, Schamp B, Smith MD, Soudzilovskaia NA, Tilman D, Weigelt A, Wilsey B, Manning P (2018) Multiple facets of biodiversity drive the diversity–stability relationship. Nature Ecology & Evolution 2:1579–1587

Crozier LG, Hutchings JA (2014) Plastic and evolutionary responses to climate change in fish. Evolutionary Applications 7:68–87

Damuth J (1981) Population density and body size in mammals. Nature 290:699–700

Damuth J (1987) Interspecific allometry of population density in mammals and other animals: the independence of body mass and population energy-use. Biological Journal of the Linnean Society 31:193–246

Dangles O, Malmqvist B (2004) Species richness–decomposition relationships depend on species dominance. Ecology Letters 7:395–402

Darimont CT, Cooke R, Bourbonnais ML, Bryan HM, Carlson SM, Estes JA, Galetti M, Levi T, MacLean JL, McKechnie I, Paquet PC, Worm B (2023) Humanity's diverse predatory niche and its ecological consequences. Communications Biology 6:609

Darimont CT, Fox CH, Bryan HM, Reimchen TE (2015) The unique ecology of human predators. Science 349:858–860

Darling ES, Côté IM (2008) Quantifying the evidence for ecological synergies. Ecology Letters 11:1278–1286

Dawson MN (2012) Species richness, habitable volume, and species densities in freshwater, the sea, and on land. Frontiers of Biogeography 4:105–116

Dedman S, Moxley JH, Papastamatiou YP, Braccini M, Caselle JE, Chapman DD, Cinner JE, Dillon EM, Dulvy NK, Dunn RE, Espinoza M, Harborne AR, Harvey ES, Heupel MR, Huveneers C, Graham NAJ, Ketchum JT, Klinard NV, Kock AA, Lowe CG, MacNeil MA, Madin EMP, McCauley DJ, Meekan MG, Meier AC, Simpfendorfer CA, Tinker MT, Winton M, Wirsing AJ, Heithaus MR (2024) Ecological roles and importance of sharks in the Anthropocene Ocean. Science 385:1–13

Dee LE, Ferraro PJ, Severen CN, Kimmel KA, Borer ET, Byrnes JEK, Clark AT, Hautier Y, Hector A, Raynaud X, Reich PB, Wright AJ, Arnillas CA, Davies KF, MacDougall A, Mori AS, Smith MD, Adler PB, Bakker JD, Brauman KA, Cowles J, Komatsu K, Knops JMH, McCulley RL, Moore JL, Morgan JW, Ohlert T, Power SA, Sullivan LL, Stevens C, Loreau M (2023) Clarifying the effect of biodiversity on productivity in natural ecosystems with longitudinal data and methods for causal inference. Nature Communications 14:2607

Defriez EJ, Sheppard LW, Reid PC, Reuman DC (2016) Climate change-related regime shifts have altered spatial synchrony of plankton dynamics in the North Sea. Global Change Biology 22:2069–2080

Denney NH, Jennings S, Reynolds JD (2002) Life–history correlates of maximum population growth rates in marine fishes. Proceedings of the Royal Society of London Series B: Biological Sciences 269:2229–2237

Dennis B, Ponciano JM, Lele SR, Taper ML, Staples DF (2006) Estimating density dependence, process noise, and observation error. Ecological Monographs 76:323–341

Depczynski M, Bellwood D (2003) The role of cryptobenthic reef fishes in coral reef trophodynamics. Marine Ecology Progress Series 256:183–191

Depczynski M, Bellwood DR (2004) Microhabitat utilisation patterns in cryptobenthic coral reef fish communities. Marine Biology 145:455–463

Depczynski M, Bellwood DR (2006) Extremes, plasticity, and invariance in vertebrate life history traits: Insights from coral reef fishes. Ecology 87:3119–3127

Depczynski M, Fulton CJ, Marnane MJ, Bellwood DR (2007) Life history patterns shape energy allocation among fishes on coral reefs. Oecologia 153:111–120

Desbiens AA, Roff G, Robbins WD, Taylor BM, Castro-Sanguino C, Dempsey A, Mumby PJ (2021) Revisiting the paradigm of shark-driven trophic cascades in coral reef ecosystems. Ecology 102:e03303

Deutsch C, Ferrel A, Seibel B, Pörtner H-O, Huey RB (2015) Climate change tightens a metabolic constraint on marine habitats. Science 348:1132–1135

Dirzo R, Young HS, Galetti M, Ceballos G, Isaac NJB, Collen B (2014) Defaunation in the Anthropocene. Science 345:401–406

Dmitriew CM (2011) The evolution of growth trajectories: what limits growth rate? Biological Reviews 86:97–116

Duffy JE, Lefcheck JS, Stuart-Smith RD, Navarrete SA, Edgar GJ (2016) Biodiversity enhances reef fish biomass and resistance to climate change. Proceedings of the National Academy of Sciences 113:6230–6235

Duffy JE, Reynolds PL, Boström C, Coyer JA, Cusson M, Donadi S, Douglass JG, Eklöf JS, Engelen AH, Eriksson BK, Fredriksen S, Gamfeldt L, Gustafsson C, Hoarau G, Hori M, Hovel K, Iken K, Lefcheck JS, Moksnes P-O, Nakaoka M, O'Connor MI, Olsen JL, Richardson JP, Ruesink JL, Sotka EE, Thormar J, Whalen MA, Stachowicz JJ (2015) Biodiversity mediates top–down control in eelgrass ecosystems: a global comparative-experimental approach. Ecology Letters 18:696–705

Dulvy NK, Freckleton RP, Polunin NVC (2004a) Coral reef cascades and the indirect effects of predator removal by exploitation. Ecology Letters 7:410–416

Dulvy NK, Pacoureau N, Rigby CL, Pollom RA, Jabado RW, Ebert DA, Finucci B, Pollock CM, Cheok J, Derrick DH, Herman KB, Sherman CS, VanderWright WJ, Lawson JM, Walls RHL, Carlson JK, Charvet P, Bineesh KK, Fernando D, Ralph GM, Matsushiba JH, Hilton-Taylor C, Fordham SV, Simpfendorfer CA (2021) Overfishing drives over one-third of all sharks and rays toward a global extinction crisis. Current Biology 31:4773-4787

Dulvy NK, Polunin NV, Mill AC, Graham NA (2004b) Size structural change in lightly exploited coral reef fish communities: evidence for weak indirect effects. Canadian Journal of Fisheries and Aquatic Sciences 61:466–475

Dulvy NK, Sadovy Y, Reynolds JD (2003) Extinction vulnerability in marine populations. Fish and Fisheries 4:25–64

Dulvy NK, Yan HF (2020) Conservation: Goldilocks nations for restoring reef sharks. Current Biology 30:R1415–R1418

Dunic JC (2023) Understanding the effect of multiple stressors using seagrass as a model system. Simon Fraser University

Eastman JM, Harmon LJ, Tank DC (2013) Congruification: support for time scaling large phylogenetic trees. Methods in Ecology and Evolution 4:688–691

Eddy TD, Lam VWY, Reygondeau G, Cisneros-Montemayor AM, Greer K, Palomares MLD, Bruno JF, Ota Y, Cheung WWL (2021) Global decline in capacity of coral reefs to provide ecosystem services. One Earth 4:1278–1285

Edgar GJ, Cooper A, Baker SC, Barker W, Barrett NS, Becerro MA, Bates AE, Brock D, Ceccarelli DM, Clausius E, Davey M, Davis TR, Day PB, Green A, Griffiths SR, Hicks J, Hinojosa IA, Jones BK, Kininmonth S, Larkin MF, Lazzari N, Lefcheck JS, Ling SD, Mooney P, Oh E, Pérez-Matus A, Pocklington JB, Riera R, Sanabria-Fernandez JA, Seroussi Y, Shaw I, Shields D, Shields J, Smith M, Soler GA, Stuart-Smith J, Turnbull J, Stuart-Smith RD (2020) Establishing the ecological basis for conservation of shallow marine life using Reef Life Survey. Biological Conservation 252:108855

Edgar GJ, Stuart-Smith RD (2014) Systematic global assessment of reef fish communities by the Reef Life Survey program. Scientific Data 1:140007

Edwards AM, Robinson JPW, Plank MJ, Baum JK, Blanchard JL (2017) Testing and recommending methods for fitting size spectra to data. Methods in Ecology and Evolution 8:57–67

Elith J, Leathwick JR, Hastie T (2008) A working guide to boosted regression trees. Journal of Animal Ecology 77:802–813

Elmqvist T, Folke C, Nyström M, Peterson G, Bengtsson J, Walker B, Norberg J (2003) Response diversity, ecosystem change, and resilience. Frontiers in Ecology and the Environment 1:488–494

Espinoza M, Lédée EJI, Simpfendorfer CA, Tobin AJ, Heupel MR (2015) Contrasting movements and connectivity of reef-associated sharks using acoustic telemetry: implications for management. Ecological Applications 25:2101–2118

Essington TE, Beaudreau AH, Wiedenmann J (2006) Fishing through marine food webs. Proceedings of the National Academy of Sciences 103:3171–3175

Fabricius KE (2005) Effects of terrestrial runoff on the ecology of corals and coral reefs: review and synthesis. Marine Pollution Bulletin 50:125–146

Fewster RM, Buckland ST, Siriwardena GM, Baillie SR, Wilson JD (2000) Analysis of population trends for farmland birds using generalized additive models. Ecology 81:1970–1984

Finucci B, Pacoureau N, Rigby CL, Matsushiba JH, Faure-Beaulieu N, Sherman CS, VanderWright WJ, Jabado RW, Charvet P, Mejía-Falla PA, Navia AF, Derrick DH, Kyne PM, Pollom RA, Walls RHL, Herman KB, Kinattumkara B, Cotton CF, Cuevas J-M, Daley RK, Ebert DA, Fernando D, Fernando SMC, Francis MP, Huveneers C, Ishihara H, Kulka DW, Leslie RW, Neat F, Orlov AM, Rincon G, Sant GJ, Volvenko IV, Walker TI, Simpfendorfer CA, Dulvy NK (2024) Fishing for oil and meat drives irreversible defaunation of deepwater sharks and rays. Science 383:1135–1141

Fox R, Bellwood D (2007) Quantifying herbivory across a coral reef depth gradient. Marine Ecology Progress Series 339:49–59

Francis FT, Côté IM (2018) Fish movement drives spatial and temporal patterns of nutrient provisioning on coral reef patches. Ecosphere 9:e02225

Friedman M (2010) Explosive morphological diversification of spiny-finned teleost fishes in the aftermath of the end-Cretaceous extinction. Proceedings of the Royal Society B: Biological Sciences 277:1675–1683

Frisch AJ, Ireland M, Rizzari JR, Lönnstedt OM, Magnenat KA, Mirbach CE, Hobbs J-PA (2016) Reassessing the trophic role of reef sharks as apex predators on coral reefs. Coral Reefs 35:459–472

Froese R, Pauly D (2021) FishBase.

Froese R, Thorson JT, Reyes RB (2014) A Bayesian approach for estimating length-weight relationships in fishes. Journal of Applied Ichthyology 30:78–85

Frölicher TL, Joos F, Plattner G-K, Steinacher M, Doney SC (2009) Natural variability and anthropogenic trends in oceanic oxygen in a coupled carbon cycle-climate model ensemble. Global Biogeochemical Cycles 23:GB1003

Frýdlová P, Mrzílková J, Šeremeta M, Křemen J, Dudák J, Žemlička J, Minnich B, Kverková K, Němec P, Zach P, Frynta D (2020) Determinate growth is predominant and likely ancestral in squamate reptiles. Proceedings of the Royal Society B: Biological Sciences 287:20202737

Gahan J, Bellwood DR, Bellwood O, Schlaefer J (2024) Gelatinous versus non-gelatinous zooplankton: their value as food for planktivorous coral reef fishes. Coral Reefs 43:243–252

Gaines SD, Costello C, Owashi B, Mangin T, Bone J, Molinos JG, Burden M, Dennis H, Halpern BS, Kappel CV, Kleisner KM, Ovando D (2018) Improved fisheries management could offset many negative effects of climate change. Science Advances 4:eaao1378

Galetti M, Guevara R, Côrtes MC, Fadini R, Von Matter S, Leite AB, Labecca F, Ribeiro T, Carvalho CS, Collevatti RG, Pires MM, Guimarães PR, Brancalion PH, Ribeiro MC, Jordano P (2013) Functional extinction of birds drives rapid evolutionary changes in seed size. Science 340:1086–1090

Ghezelayagh A, Harrington RC, Burress ED, Campbell MA, Buckner JC, Chakrabarty P, Glass JR, McCraney WT, Unmack PJ, Thacker CE, Alfaro ME, Friedman ST, Ludt WB, Cowman PF, Friedman M, Price SA, Dornburg A, Faircloth BC, Wainwright PC, Near TJ (2022) Prolonged morphological expansion of spiny-rayed fishes following the end-Cretaceous. Nature Ecology & Evolution 6:1211–1220

Gillooly JamesF, Charnov EL, West GB, Savage VM, Brown JH (2002) Effects of size and temperature on developmental time. Nature 417:70–73

Gillooly JF, Brown JH, West GB, Savage VM, Charnov EL (2001) Effects of size and temperature on metabolic rate. Science 293:2248–2251

Gislason H, Daan N, Rice JC, Pope JG (2010) Size, growth, temperature and the natural mortality of marine fish: Natural mortality and size. Fish and Fisheries 11:149–158

Goatley CHR, Bellwood DR (2016) Body size and mortality rates in coral reef fishes: a three-phase relationship. Proceedings of the Royal Society B: Biological Sciences 283:20161858

Goetze JS, Heithaus MR, MacNeil MA, Harvey E, Simpfendorfer CA, Heupel MR, Meekan M, Wilson S, Bond ME, Speed CW, Currey-Randall LM, Fisher R, Sherman CS, Kiszka JJ, Rees MJ, Udyawer V, Flowers KI, Clementi GM, Asher J, Beaufort O, Bernard ATF, Berumen ML, Bierwagen SL, Boslogo T, Brooks EJ, Brown JJ, Buddo D, Cáceres C, Casareto S, Charloo V, Cinner JE, Clua EEG, Cochran JEM, Cook N, D'Alberto BM, De Graaf M, Dornhege-Lazaroff MC, Fanovich L, Farabaugh NF, Fernando D, Ferreira CEL, Fields CYA, Flam AL, Floros C, Fourqurean V, Barcia LG, Garla R, Gastrich K, George L, Graham R, Hagan V, Hardenstine RS, Heck SM, Heithaus P, Henderson AC, Hertler H, Hueter RE, Johnson M, Jupiter SD, Kaimuddin M, Kasana D, Kelley M, Kessel ST, Kiilu B, Kyne F, Langlois T, Lawe J, Lédée EJI, Lindfield S, Maggs JQ, Manjaji-Matsumoto BM, Marshall A, Matich P, McCombs E, McLean D, Meggs L, Moore S, Mukherji S, Murray R, Newman SJ, O'Shea OR, Osuka KE, Papastamatiou YP, Perera N, Peterson BJ, Pina-Amargós F, Ponzo A, Prasetyo A, Quamar LMS, Quinlan JR, Razafindrakoto CF, Rolim FA, Ruiz-Abierno A, Ruiz H, Samoilys MA, Sala E, Sample WR, Schärer-Umpierre M, Schoen SN, Schlaff AM, Smith ANH, Sparks L, Stoffers T, Tanna A, Torres R, Travers MJ, Valentin-Albanese J, Warren JD, Watts AM, Wen CK, Whitman ER, Wirsing AJ, Zarza-González E, Chapman DD (2024) Directed conservation of the world's reef sharks and rays. Nature Ecology & Evolution 8:1118–1128

Graham NAJ, Jennings S, MacNeil MA, Mouillot D, Wilson SK (2015) Predicting climate-driven regime shifts versus rebound potential in coral reefs. Nature 518:94–97

Graham NAJ, Wilson SK, Jennings S, Polunin NVC, Bijoux JP, Robinson J (2006) Dynamic fragility of oceanic coral reef ecosystems. Proceedings of the National Academy of Sciences 103:8425–8429

Gravel S, Bigman JS, Pardo SA, Wong S, Dulvy NK (2024) Metabolism, population growth, and the fast-slow life history continuum of marine fishes. Fish and Fisheries 25:349–361

Gumbs R, Scott O, Bates R, Böhm M, Forest F, Gray C, Hoffmann M, Kane D, Low C, Pearse W, Pipins S, Tapley B, Turvey S, Jetz W, Owen N, Rosindell J (2024) Global conservation status of the jawed vertebrate Tree of Life. Nature Communications 15:1101

Hagan JG, Vanschoenwinkel B, Gamfeldt L (2021) We should not necessarily expect positive relationships between biodiversity and ecosystem functioning in observational field data. Ecology Letters 24:2537–2548

Hall MR, Kocot KM, Baughman KW, Fernandez-Valverde SL, Gauthier MEA, Hatleberg WL, Krishnan A, McDougall C, Motti CA, Shoguchi E, Wang T, Xiang X, Zhao M, Bose U, Shinzato C, Hisata K, Fujie M, Kanda M, Cummins SF, Satoh N, Degnan SM, Degnan BM (2017) The crown-of-thorns starfish genome as a guide for biocontrol of this coral reef pest. Nature 544:231–234

Halpern BS, Frazier M, Potapenko J, Casey KS, Koenig K, Longo C, Lowndes JS, Rockwood RC, Selig ER, Selkoe KA, Walbridge S (2015) Spatial and temporal changes in cumulative human impacts on the world's ocean. Nature Communications 6:7615

Halpern BS, Walbridge S, Selkoe KA, Kappel CV, Micheli F, D'Agrosa C, Bruno JF, Casey KS, Ebert C, Fox HE, Fujita R, Heinemann D, Lenihan HS, Madin EMP, Perry MT, Selig ER, Spalding M, Steneck R, Watson R (2008) A global map of human impact on marine ecosystems. Science 319:948–952

Hamilton M, Robinson JPW, Benkwitt CE, Wilson SK, MacNeil MA, Ebrahim A, Graham NAJ (2022) Climate impacts alter fisheries productivity and turnover on coral reefs. Coral Reefs 41:921–935

Harmon LJ, Weir JT, Brock CD, Glor RE, Challenger W (2008) GEIGER: investigating evolutionary radiations. Bioinformatics 24:129–131

Hartig F (2022) *DHARMa*: Residual diagnostics for hierarchical (multi-Level/mixed) regression models.

Healy K, Ezard THG, Jones OR, Salguero-Gómez R, Buckley YM (2019) Animal life history is shaped by the pace of life and the distribution of age-specific mortality and reproduction. Nature Ecology & Evolution 3:1217–1224

Heino, Kaitala (1999) Evolution of resource allocation between growth and reproduction in animals with indeterminate growth. Journal of Evolutionary Biology 12:423–429

Hemingson CR, Mihalitsis M, Bellwood DR (2022) Are fish communities on coral reefs becoming less colourful? Global Change Biology 28:3321–3332

Heupel M, Knip D, Simpfendorfer C, Dulvy N (2014) Sizing up the ecological role of sharks as predators. Marine Ecology Progress Series 495:291–298

Hilborn R, Amoroso RO, Anderson CM, Baum JK, Branch TA, Costello C, de Moor CL, Faraj A, Hively D, Jensen OP, Kurota H, Little LR, Mace P, McClanahan T, Melnychuk MC, Minto C, Osio GC, Parma AM, Pons M, Segurado S, Szuwalski CS, Wilson JR, Ye Y (2020) Effective fisheries management instrumental in improving fish stock status. Proceedings of the National Academy of Sciences 117:2218–2224

Hilborn R, Walters CJ (1992) Quantitative fisheries stock assessment: choice, dynamics and uncertainty. Kluwer Academic Publishers, Massachusetts, USA

Hill MO (1973) Diversity and evenness: a unifying notation and its consequences. Ecology 54:427–432

Hocking MD, Dulvy NK, Reynolds JD, Ring RA, Reimchen TE (2013) Salmon subsidize an escape from a size spectrum. Proceedings of the Royal Society B: Biological Sciences 280:20122433

Hodapp D, Meier S, Muijsers F, Badewien TH, Hillebrand H (2015) Structural equation modeling approach to the diversity-productivity relationship of Wadden Sea phytoplankton. Marine Ecology Progress Series 523:31–40

Holmes EE, Scheuerell MD, Ward EJ (2021) Applied time series analysis for fisheries and environmental data. NOAA Fisheries, Northwest Fisheries Science Center, Seattle WA

Hughes T, Bellwood D, Folke C, Mccook L, Pandolfi J (2007) No-take areas, herbivory and coral reef resilience. Trends in Ecology & Evolution 22:1–3

Hughes TP, Anderson KD, Connolly SR, Heron SF, Kerry JT, Lough JM, Baird AH, Baum JK, Berumen ML, Bridge TC, Claar DC, Eakin CM, Gilmour JP, Graham NAJ, Harrison H, Hobbs J-PA, Hoey AS, Hoogenboom MO, Lowe RJ, McCulloch MT, Pandolfi JM, Pratchett MS, Schoepf V, Torda G, Wilson SK (2018) Spatial and temporal patterns of mass bleaching of corals in the Anthropocene. Science 359:80–83

Hughes TP, Barnes ML, Bellwood DR, Cinner JE, Cumming GS, Jackson JBC, Kleypas J, van de Leemput IA, Lough JM, Morrison TH, Palumbi SR, van Nes EH, Scheffer M (2017a) Coral reefs in the Anthropocene. Nature 546:82–90

Hughes TP, Kerry JT, Álvarez-Noriega M, Álvarez-Romero JG, Anderson KD, Baird AH, Babcock RC, Beger M, Bellwood DR, Berkelmans R, Bridge TC, Butler IR, Byrne M, Cantin NE, Comeau S, Connolly SR, Cumming GS, Dalton SJ, Diaz-Pulido G, Eakin CM, Figueira WF, Gilmour JP, Harrison HB, Heron SF, Hoey AS, Hobbs J-PA, Hoogenboom MO, Kennedy EV, Kuo C, Lough JM, Lowe RJ, Liu G, McCulloch MT, Malcolm HA, McWilliam MJ, Pandolfi JM, Pears RJ, Pratchett MS, Schoepf V, Simpson T, Skirving WJ, Sommer B, Torda G, Wachenfeld DR, Willis BL, Wilson SK (2017b) Global warming and recurrent mass bleaching of corals. Nature 543:373–377

Hutchings JA, Myers RA (1994) What can be learned from the collapse of a renewable resource? Atlantic Cod, *Gadus morhua*, of Newfoundland and Labrador. Canadian Journal of Fisheries and Aquatic Sciences 51:2126–2146

Hutchings JA, Reynolds JD (2004) Marine fish population collapses: consequences for recovery and extinction risk. BioScience 54:297–309

Jackson JBC (1997) Reefs since Columbus. Coral Reefs 16:S23–S32

Jackson JBC, Kirby MX, Berger WH, Bjorndal KA, Botsford LW, Bourque BJ, Bradbury RH, Cooke R, Erlandson J, Estes JA, Hughes TP, Kidwell S, Lange CB, Lenihan HS, Pandolfi JM, Peterson CH, Steneck RS, Tegner MJ, Warner RR (2001) Historical overfishing and the recent collapse of coastal ecosystems. Science 293:629–637

Jennings S, Greenstreet SimonPR, Reynolds JohnD (1999) Structural change in an exploited fish community: a consequence of differential fishing effects on species with contrasting life histories. Journal of Animal Ecology 68:617–627

Johnson CN, Balmford A, Brook BW, Buettel JC, Galetti M, Guangchun L, Wilmshurst JM (2017) Biodiversity losses and conservation responses in the Anthropocene. Science 356:270–275

Jørgensen C, Enberg K, Dunlop ES, Arlinghaus R, Boukal DS, Brander K, Ernande B, Gårdmark AG, Johnston F, Matsumura S, Pardoe H, Raab K, Silva A, Vainikka A, Dieckmann U, Heino M, Rijnsdorp AD (2007) Ecology: managing evolving fish stocks. Science 318:1247–1248

Jost L (2006) Entropy and diversity. Oikos 113:363–375

Juan-Jordá MJ, Murua H, Arrizabalaga H, Merino G, Pacoureau N, Dulvy NK (2022) Seventy years of tunas, billfishes, and sharks as sentinels of global ocean health. Science 378:eabj0211

Khasanah M, Nurdin N, Sadovy de Mitcheson Y, Jompa J (2020) Management of the grouper export trade in Indonesia. Reviews in Fisheries Science & Aquaculture 28:1–15

Kraak SBM, Haase S, Minto C, Santos J (2019) The Rosa Lee phenomenon and its consequences for fisheries advice on changes in fishing mortality or gear selectivity. ICES Journal of Marine Science 76:2179–2192

Kroodsma DA, Mayorga J, Hochberg T, Miller NA, Boerder K, Ferretti F, Wilson A, Bergman B, White TD, Block BA, Woods P, Sullivan B, Costello C, Worm B (2018) Tracking the global footprint of fisheries. Science 359:904–908

Kroon FJ, Thorburn P, Schaffelke B, Whitten S (2016) Towards protecting the Great Barrier Reef from land-based pollution. Global Change Biology 22:1985–2002

Kuparinen A, Merilä J (2007) Detecting and managing fisheries-induced evolution. Trends in Ecology & Evolution 22:652–659

Laliberté E, Wells JA, DeClerck F, Metcalfe DJ, Catterall CP, Queiroz C, Aubin I, Bonser SP, Ding Y, Fraterrigo JM, McNamara S, Morgan JW, Merlos DS, Vesk PA, Mayfield MM (2010) Land-use intensification reduces functional redundancy and response diversity in plant communities. Ecology Letters 13:76–86

Law R, Grey DR (1989) Evolution of yields from populations with age-specific cropping. Evolutionary Ecology 3:343–359

Lee RM (1912) An investigation into the methods of growth determination in fishes by means of scales. Journal du Conseil s1:3–34

Lefcheck JS, Byrnes JEK, Isbell F, Gamfeldt L, Griffin JN, Eisenhauer N, Hensel MJS, Hector A, Cardinale BJ, Duffy JE (2015) Biodiversity enhances ecosystem multifunctionality across trophic levels and habitats. Nature Communications 6:6936

Lewis SL, Maslin MA (2015) Defining the Anthropocene. Nature 519:171–180

Lindgren B, Laurila A (2005) Proximate causes of adaptive growth rates: growth efficiency variation among latitudinal populations of *Rana temporaria*. Journal of Evolutionary Biology 18:820–828

Lindgren F, Rue H (2015) Bayesian spatial modelling with *R-INLA*. Journal of Statistical Software 63:1–25

Lindgren F, Rue H, Lindström J (2011) An explicit link between Gaussian Fields and Gaussian Markov Random Fields: the stochastic partial differential equation approach. Journal of the Royal Statistical Society Series B: Statistical Methodology 73:423–498

Lindmark M, Audzijonyte A, Blanchard JL, Gårdmark A (2022) Temperature impacts on fish physiology and resource abundance lead to faster growth but smaller fish sizes and yields under warming. Global Change Biology 28:6239–6253

Loreau M (2000) Biodiversity and ecosystem functioning: recent theoretical advances. Oikos 91:3–17

Loreau M (2004) Does functional redundancy exist? Oikos 104:606–611

Loreau M, Hector A (2001) Partitioning selection and complementarity in biodiversity experiments. Nature 412:72–76

Mace GM, Barrett M, Burgess ND, Cornell SE, Freeman R, Grooten M, Purvis A (2018) Aiming higher to bend the curve of biodiversity loss. Nature Sustainability 1:448–451

MacNeil MA, Chapman DD, Heupel M, Simpfendorfer CA, Heithaus M, Meekan M, Harvey E, Goetze J, Kiszka J, Bond ME, Currey-Randall LM, Speed CW, Sherman CS, Rees MJ, Udyawer V, Flowers KI, Clementi G, Valentin-Albanese J, Gorham T, Adam MS, Ali K, Pina-Amargós F, Angulo-Valdés JA, Asher J, Barcia LG, Beaufort O, Benjamin C, Bernard ATF, Berumen ML, Bierwagen S, Bonnema E, Bown RMK, Bradley D, Brooks E, Brown JJ, Buddo D, Burke P, Cáceres C, Cardeñosa D, Carrier JC, Caselle JE, Charloo V, Claverie T, Clua E, Cochran JEM, Cook N, Cramp J, D'Alberto B, de Graaf M, Dornhege M, Estep A, Fanovich L, Farabough NF, Fernando D, Flam AL, Floros C, Fourqurean V, Garla R, Gastrich K, George L, Graham R, Guttridge T, Hardenstine RS, Heck S, Henderson AC, Hertler H, Hueter R, Johnson M, Jupiter S, Kasana D, Kessel ST, Kiilu B, Kirata T, Kuguru B, Kyne F, Langlois T, Lédée EJI, Lindfield S, Luna-Acosta A, Maggs J, Manjaji-Matsumoto BM, Marshall A, Matich P, McCombs E, McLean D, Meggs L, Moore S, Mukherji S, Murray R, Kaimuddin M, Newman SJ, Nogués J, Obota C, O'Shea O, Osuka K, Papastamatiou YP, Perera N, Peterson B, Ponzo A, Prasetyo A, Quamar LMS, Quinlan J, Ruiz-Abierno A, Sala E, Samoilys M, Schärer-Umpierre M, Schlaff A, Simpson N, Smith ANH, Sparks L, Tanna A, Torres R, Travers MJ, van Zinnicq Bergmann M, Vigliola L, Ward J, Watts AM, Wen C, Whitman E, Wirsing AJ, Wothke A, Zarza-Gonzâlez E, Cinner JE (2020) Global status and conservation potential of reef sharks. Nature 583:801–806

Marramà G, Garbelli C, Carnevale G (2016) A clade-level morphospace for the Eocene fishes of Bolca: Patterns and relationships with modern tropical shallow marine assemblages. Bollettino della Società Paleontologica Italiana 139–156

Marshall PA, Baird AH (2000) Bleaching of corals on the Great Barrier Reef: differential susceptibilities among taxa. Coral Reefs 19:155–163

Martins IS, Schrodt F, Blowes SA, Bates AE, Bjorkman AD, Brambilla V, Carvajal-Quintero J, Chow CFY, Daskalova GN, Edwards K, Eisenhauer N, Field R, Fontrodona-Eslava

A, Henn JJ, van Klink R, Madin JS, Magurran AE, McWilliam M, Moyes F, Pugh B, Sagouis A, Trindade-Santos I, McGill BJ, Chase JM, Dornelas M (2023) Widespread shifts in body size within populations and assemblages. Science 381:1067–1071

Martins TG, Rue H (2014) Extending integrated nested Laplace approximation to a class of near-Gaussian latent models. Scandinavian Journal of Statistics 41:893–912

Mason NWH, Lanoiselée C, Mouillot D, Wilson JB, Argillier C (2008) Does niche overlap control relative abundance in French lacustrine fish communities? A new method incorporating functional traits. Journal of Animal Ecology 77:661–669

Maureaud A, Andersen KH, Zhang L, Lindegren M (2020) Trait-based food web model reveals the underlying mechanisms of biodiversity–ecosystem functioning relationships. Journal of Animal Ecology 89:1497–1510

Maureaud A, Hodapp D, van Denderen PD, Hillebrand H, Gislason H, Spaanheden Dencker T, Beukhof E, Lindegren M (2019) Biodiversity–ecosystem functioning relationships in fish communities: biomass is related to evenness and the environment, not to species richness. Proceedings of the Royal Society B: Biological Sciences 286:20191189

McCann KS (2000) The diversity-stability debate. Nature 405:228–233

McCauley DJ, Pinsky ML, Palumbi SR, Estes JA, Joyce FH, Warner RR (2015) Marine defaunation: Animal loss in the global ocean. Science 347:1255641–1255641

Medley PA, Gaudian G, Wells S (1993) Coral reef fisheries stock assessment. Reviews in Fish Biology and Fisheries 3:242–285

Melnychuk MC, Peterson E, Elliott M, Hilborn R (2017) Fisheries management impacts on target species status. Proceedings of the National Academy of Sciences 114:178–183

Mihalitsis M, Bellwood DR (2017) A morphological and functional basis for maximum prey size in piscivorous fishes. PLOS ONE 12:1–19

Mihalitsis M, Morais RA, Bellwood DR (2022) Small predators dominate fish predation in coral reef communities. PLOS Biology 20:e3001898

Mihaljević M, Renema W, Welsh K, Pandolfi JM (2014) Eocene–Miocene shallow-water carbonate platforms and increased habitat diversity in Sarawak, Malaysia. PALAIOS 29:378–391

Miranda R, Miqueleiz I, Darwall W, Sayer C, Dulvy NK, Carpenter KE, Polidoro B, Dewhurst-Richman N, Pollock C, Hilton-Taylor C, Freeman R, Collen B, Böhm M (2022) Monitoring extinction risk and threats of the world's fishes based on the Sampled Red List Index. Reviews in Fish Biology and Fisheries 32:975–991

Mitchell R, Frank E (2017) Accelerating the XGBoost algorithm using GPU computing. PeerJ Computer Science 3:e127

Mitov V, Bartoszek K, Asimomitis G, Stadler T (2020) Fast likelihood calculation for multivariate Gaussian phylogenetic models with shifts. Theoretical Population Biology 131:66–78

Mitov V, Bartoszek K, Stadler T (2019) Automatic generation of evolutionary hypotheses using mixed Gaussian phylogenetic models. Proceedings of the National Academy of Sciences 116:16921–16926

Mora C, Aburto-Oropeza O, Ayala Bocos A, Ayotte PM, Banks S, Bauman AG, Beger M, Bessudo S, Booth DJ, Brokovich E, Brooks A, Chabanet P, Cinner JE, Cortés J, Cruz-Motta JJ, Cupul Magaña A, DeMartini EE, Edgar GJ, Feary DA, Ferse SCA, Friedlander AM, Gaston KJ, Gough C, Graham NAJ, Green A, Guzman H, Hardt M, Kulbicki M, Letourneur Y, López Pérez A, Loreau M, Loya Y, Martinez C, Mascareñas-Osorio I, Morove T, Nadon M-O, Nakamura Y, Paredes G, Polunin NVC, Pratchett MS, Reyes Bonilla H, Rivera F, Sala E, Sandin SA, Soler G, Stuart-Smith R, Tessier E, Tittensor DP, Tupper M, Usseglio P, Vigliola L, Wantiez L, Williams I, Wilson SK, Zapata FA (2011) Global human footprint on the linkage between biodiversity and ecosystem functioning in reef fishes. PLOS Biology 9:e1000606

Morais RA, Bellwood DR (2018) Global drivers of reef fish growth. Fish and Fisheries 19:874–889

Morais RA, Bellwood DR (2019) Pelagic subsidies underpin fish productivity on a degraded coral reef. Current Biology 29:1521-1527.e6

Morais RA, Bellwood DR (2020) Principles for estimating fish productivity on coral reefs. Coral Reefs 39:1221–1231

Morais RA, Depczynski M, Fulton C, Marnane M, Narvaez P, Huertas V, Brandl SJ, Bellwood DR (2020) Severe coral loss shifts energetic dynamics on a coral reef. Functional Ecology 34:1507–1518

Morais RA, Siqueira AC, Smallhorn-West PF, Bellwood DR (2021) Spatial subsidies drive sweet spots of tropical marine biomass production. PLOS Biology 19:e3001435

Morais RA, Smallhorn-West P, Connolly SR, Ngaluafe PF, Malimali S, Halafihi T, Bellwood DR (2023) Sustained productivity and the persistence of coral reef fisheries. Nature Sustainability 6:1199-1209

Mourier J, Maynard J, Parravicini V, Ballesta L, Clua E, Domeier ML, Planes S (2016) Extreme inverted trophic pyramid of reef sharks supported by spawning groupers. Current Biology 26:2011–2016

Munger R, Watkins HV, Dunic JC, Côté IM (2023) Abundance modulates the ecosystem functional contributions of two sympatric Caribbean sea cucumbers. PeerJ 11:e14823

Munro JL, Pauly D (1983) A simple method for comparing the growth of fishes and invertebrates. Fishbyte 1:5–6

Myers RA, Baum JK, Shepherd TD, Powers SP, Peterson CH (2007) Cascading effects of the loss of apex predatory sharks from a coastal ocean. Science 315:1846–1850

Myers RA, Hutchings JA, Barrowman NJ (1997) Why do fish stocks collapse? The example of cod in Atlantic Canada. Ecological Applications 7:91–106

Naeem S (2002) Ecosystem consequences of biodiversity loss: The evolution of a paradigm. Ecology 83:1537–1552

Naeem S, Thompson LJ, Lawler SP, Lawton JH, Woodfin RM (1994) Declining biodiversity can alter the performance of ecosystems. Nature 368:734–737

Nilsson GE, Crawley N, Lunde IG, Munday PL (2009) Elevated temperature reduces the respiratory scope of coral reef fishes. Global Change Biology 15:1405–1412

Norström A, Nyström M, Lokrantz J, Folke C (2009) Alternative states on coral reefs: beyond coral–macroalgal phase shifts. Marine Ecology Progress Series 376:295–306

Nyström M, Folke C, Moberg F (2000) Coral reef disturbance and resilience in a human-dominated environment. Trends in Ecology & Evolution 15:413–417

Oksanen J, Blanchet FG, Friendly M, Kindt R, Legendre P, McGlinn D, Minchin PR, O'Hara RB, Simpson GL, Solymos P, Stevens HH, Szoecs E, Wagner H (2020) *vegan*: Community Ecology Package.

Olsen EM, Heino M, Lilly GR, Morgan MJ, Brattey J, Ernande B, Dieckmann U (2004) Maturation trends indicative of rapid evolution preceded the collapse of northern cod. Nature 428:932–935

Pace ML, Cole JJ, Carpenter SR, Kitchell JF (1999) Trophic cascades revealed in diverse ecosystems. Trends in Ecology & Evolution 14:483–488

Pacoureau N, Carlson JK, Kindsvater HK, Rigby CL, Winker H, Simpfendorfer CA, Charvet P, Pollom RA, Barreto R, Sherman CS, Talwar BS, Skerritt DJ, Sumaila UR, Matsushiba JH, VanderWright WJ, Yan HF, Dulvy NK (2023) Conservation successes and challenges for wide-ranging sharks and rays. Proceedings of the National Academy of Sciences 120:e2216891120

Patterson C (1993) An overview of the early fossil record of Acanthomorphs. Bulletin of Marine Science 52:29–59

Pauly D (1979) Gill size and temperature as governing factors in fish growth: A generalization of von Bertalanffy's growth formula. Berichte aus dem Institut für Meereskunde Kiel 63:1–156

Pauly D (1995) Anecdotes and the shifting baseline syndrome of fisheries. Trends in Ecology & Evolution 10:430

Pauly D (2021) The gill-oxygen limitation theory (GOLT) and its critics. Science Advances 7:eabc6050

Pauly D, Christensen V, Dalsgaard J, Froese R, Torres F (1998) Fishing down marine food webs. Science 279:860–863

Pauly D, Hilborn R, Branch TA (2013) Fisheries: Does catch reflect abundance? Nature 494:303–306

Pauly D, Zeller D (2016) Catch reconstructions reveal that global marine fisheries catches are higher than reported and declining. Nature Communications 7:10244

Pauly D, Zeller D, Palomares MLD (2020) Sea Around Us Concepts, Design and Data. (seaaroundus.org)

Perry AL, Low PJ, Ellis JR, Reynolds JD (2005) Climate change and distribution shifts in marine fishes. Science 308:1912–1915

Pillai P, Gouhier TC (2019) Not even wrong: the spurious measurement of biodiversity's effects on ecosystem functioning. Ecology 100:e02645

Polley HW, Wilsey BJ, Tischler CR (2007) Species abundances influence the net biodiversity effect in mixtures of two plant species. Basic and Applied Ecology 8:209–218

Price NW, Chen K-S, Chen CA, Wen CK-C (2021) Scraping and grazing herbivorous/detritivorous fish display opposite feeding behaviours under different protection regulations. Marine Biology Research 17:876–891

Purvis A, Hector A (2000) Getting the measure of biodiversity. Nature 405:212–219

R Core Team (2024) R: A language and environment for statistical computing.

Rabosky DL, Chang J, Title PO, Cowman PF, Sallan L, Friedman M, Kaschner K, Garilao C, Near TJ, Coll M, Alfaro ME (2018) An inverse latitudinal gradient in speciation rate for marine fishes. Nature 559:392–395

Rasher DB, Hoey AS, Hay ME (2017) Cascading predator effects in a Fijian coral reef ecosystem. Scientific Reports 7:15684

Reid AJ, Young N, Hinch SG, Cooke SJ (2022) Learning from Indigenous knowledge holders on the state and future of wild Pacific salmon. FACETS 7:718–740

Renema W, Pandolfi JM, Kiessling W, Bosellini FR, Klaus JS, Korpanty C, Rosen BR, Santodomingo N, Wallace CC, Webster JM, Johnson KG (2016) Are coral reefs victims of their own past success? Science Advances 2:e1500850

Revell LJ (2012) *Phytools*: an R package for phylogenetic comparative biology (and other things). Methods in Ecology and Evolution 3:217–223

Reynolds JD (2003) Life histories and extinction risk. Macroecology. Blackwell Publishing, Oxford, UK, pp 195–217

Ricard D, Minto C, Jensen OP, Baum JK (2012) Examining the knowledge base and status of commercially exploited marine species with the RAM Legacy Stock Assessment Database: The RAM Legacy Stock Assessment Database. Fish and Fisheries 13:380–398

Ricklefs RE, Wikelski M (2002) The physiology/life-history nexus. Trends in Ecology & Evolution 17:462–468

Ripple WJ, Larsen EJ, Renkin RA, Smith DW (2001) Trophic cascades among wolves, elk and aspen on Yellowstone National Park's northern range. Biological Conservation 102:227–234

Ripple WJ, Wolf C, Newsome TM, Betts MG, Ceballos G, Courchamp F, Hayward MW, Valkenburgh B, Wallach AD, Worm B (2019) Are we eating the world's megafauna to extinction? Conservation Letters e12627

Ritchie EG, Johnson CN (2009) Predator interactions, mesopredator release and biodiversity conservation. Ecology Letters 12:982–998

Robinson JPW, Wilson SK, Robinson J, Gerry C, Lucas J, Assan C, Govinden R, Jennings S, Graham NAJ (2019) Productive instability of coral reef fisheries after climate-driven regime shifts. Nature Ecology & Evolution 3:183–190

Rochet M (1998) Short-term effects of fishing on life history traits of fishes. ICES Journal of Marine Science 55:371–391

Roff G, Doropoulos C, Rogers A, Bozec Y-M, Krueck NC, Aurellado E, Priest M, Birrell C, Mumby PJ (2016) The ecological role of sharks on coral reefs. Trends in Ecology & Evolution 31:395–407

Rogers A, Blanchard JL, Mumby PJ (2018a) Fisheries productivity under progressive coral reef degradation. Journal of Applied Ecology 55:1041–1049

Rogers A, Blanchard JL, Newman SP, Dryden CS, Mumby PJ (2018b) High refuge availability on coral reefs increases the vulnerability of reef-associated predators to overexploitation. Ecology 99:450–463

Roswell M, Dushoff J, Winfree R (2021) A conceptual guide to measuring species diversity. Oikos 130:321–338

Roswell M, Harrison T, Genung MA (2023) Biodiversity–ecosystem function relationships change in sign and magnitude across the Hill diversity spectrum. Proceedings of the Royal Society B: Biological Sciences 378:20220186

Rubenstein MA, Weiskopf SR, Bertrand R, Carter SL, Comte L, Eaton MJ, Johnson CG, Lenoir J, Lynch AJ, Miller BW, Morelli TL, Rodriguez MA, Terando A, Thompson LM (2023) Climate change and the global redistribution of biodiversity: substantial variation in empirical support for expected range shifts. Environmental Evidence 12:7

Rue H, Martino S, Chopin N (2009) Approximate Bayesian inference for latent Gaussian models by using integrated nested Laplace approximations. Journal of the Royal Statistical Society Series B: Statistical Methodology 71:319–392

Ruppert JLW, Travers MJ, Smith LL, Fortin M-J, Meekan MG (2013) Caught in the middle: combined impacts of shark removal and coral loss on the fish communities of coral reefs. PLOS ONE 8:1–9

Sadovy Y, Cheung WL (2003) Near extinction of a highly fecund fish: the one that nearly got away. Fish and Fisheries 4:86–99

Sala OE, Chapin FS, Armesto JJ, Berlow E, Bloomfield J, Dirzo R, Huber-Sanwald E, Huenneke LF, Jackson RB, Kinzig A, Leemans R, Lodge DM, Mooney HA, Oesterheld M, Poff NL, Sykes MT, Walker BH, Walker M, Wall DH (2000) Global Biodiversity Scenarios for the Year 2100. Science 287:1770–1774

Samhouri JF, Andrews KS, Fay G, Harvey CJ, Hazen EL, Hennessey SM, Holsman K, Hunsicker ME, Large SI, Marshall KN, Stier AC, Tam JC, Zador SG (2017) Defining ecosystem thresholds for human activities and environmental pressures in the California Current. Ecosphere 8:e01860

Santodomingo N, Wallace CC, Johnson KG (2015) Fossils reveal a high diversity of the staghorn coral genera Acropora and Isopora (Scleractinia: Acroporidae) in the Neogene of Indonesia. Zoological Journal of the Linnean Society 175:677–763

Savage VM, Gillooly JF, Brown JH, West GB, Charnov EL (2004) Effects of body size and temperature on population growth. The American Naturalist 163:429–441

Schaefer MB (1954) Some aspects of the dynamics of populations important to the management of the commercial marine fisheries. Inter-American Tropical Tuna Commission 1:25–56

Schaefer MB (1957) A study of the dynamics of the fishery for yellowfin tuna in the Eastern Tropical Pacific Ocean. Bulletin, Inter-American Tropical Tuna Commission 2:247–285

Schiettekatte NMD, Barneche DR, Villéger S, Allgeier JE, Burkepile DE, Brandl SJ, Casey JM, Mercière A, Munsterman KS, Morat F, Parravicini V (2020a) Nutrient limitation, bioenergetics and stoichiometry: A new model to predict elemental fluxes mediated by fishes. Functional Ecology 34:1857–1869

Schiettekatte NMD, Brandl SJ, Casey JM (2020b) *fishualize*: color palettes based on fish species.

Schiettekatte NMD, Brandl SJ, Casey JM, Graham NAJ, Barneche DR, Burkepile DE, Allgeier JE, Arias-Gonzaléz JE, Edgar GJ, Ferreira CEL, Floeter SR, Friedlander AM, Green AL, Kulbicki M, Letourneur Y, Luiz OJ, Mercière A, Morat F, Munsterman KS, Rezende EL, Rodríguez-Zaragoza FA, Stuart-Smith RD, Vigliola L, Villéger S, Parravicini V (2022) Biological trade-offs underpin coral reef ecosystem functioning. Nature Ecology & Evolution 6:701-708

Schindler DE, Armstrong JB, Reed TE (2015) The portfolio concept in ecology and evolution. Frontiers in Ecology and the Environment 13:257–263

Schindler DE, Hilborn R, Chasco B, Boatright CP, Quinn TP, Rogers LA, Webster MS (2010) Population diversity and the portfolio effect in an exploited species. Nature 465:609–612

Schmid B, Hector A, Huston MA, Inchausti P, Nijs I, Leadley PW, Tilman D (2002) The design and analysis of biodiversity experiments. Loreau, M., Naeem, S. & Inchausti,

P. (Eds.) Biodiversity and Ecosystem Functioning: Synthesis and Perspectives. Oxford University Press, Oxford, pp 61–79

Schoelinck C, Hinsinger DD, Dettaï A, Cruaud C, Justine J-L (2014) A phylogenetic re-analysis of groupers with applications for ciguatera fish poisoning. PLOS ONE 9:e98198

Sebens KP (1987) The ecology of indeterminate growth in animals. Annual Review of Ecology and Systematics 18:371–407

Sheridan JA, Bickford D (2011) Shrinking body size as an ecological response to climate change. Nature Climate Change 1:401–406

Sherman CS, Simpfendorfer CA, Pacoureau N, Matsushiba JH, Yan HF, Walls RHL, Rigby CL, VanderWright WJ, Jabado RW, Pollom RA, Carlson JK, Charvet P, Bin Ali A, Fahmi, Cheok J, Derrick DH, Herman KB, Finucci B, Eddy TD, Palomares MLD, Avalos-Castillo CG, Kinattumkara B, Blanco-Parra M-P, Dharmadi, Espinoza M, Fernando D, Haque AB, Mejía-Falla PA, Navia AF, Pérez-Jiménez JC, Utzurrum J, Yuneni RR, Dulvy NK (2023) Half a century of rising extinction risk of coral reef sharks and rays. Nature Communications 14:15

Shurin JB, Arnott SE, Hillebrand H, Longmuir A, Pinel-Alloul B, Winder M, Yan ND (2007) Diversity-stability relationship varies with latitude in zooplankton. Ecology Letters 10:127–134

Sibert EC, Norris RD (2015) New age of fishes initiated by the Cretaceous−Paleogene mass extinction. Proceedings of the National Academy of Sciences 112:8537–8542

Simpfendorfer CA, Heithaus MR, Heupel MR, MacNeil MA, Meekan M, Harvey E, Sherman CS, Currey-Randall LM, Goetze JS, Kiszka JJ, Rees MJ, Speed CW, Udyawer V, Bond ME, Flowers KI, Clementi GM, Valentin-Albanese J, Adam MS, Ali K, Asher J, Aylagas E, Beaufort O, Benjamin C, Bernard ATF, Berumen ML, Bierwagen S, Birrell C, Bonnema E, Bown RMK, Brooks EJ, Brown JJ, Buddo D, Burke PJ, Cáceres C, Cambra M, Cardeñosa D, Carrier JC, Casareto S, Caselle JE, Charloo V, Cinner JE, Claverie T, Clua EEG, Cochran JEM, Cook N, Cramp JE, Espinoza M, Estep A, Fanovich L, Farabaugh NF, Fernando D, Ferreira CEL, Fields CYA, Flam AL, Floros C, Fourqurean V, Gajdzik L, Barcia LG, Garla R, Gastrich K, George L, Giarrizzo T, Graham R, Guttridge TL, Hagan V, Hardenstine RS, Heck SM, Henderson AC, Heithaus P, Hertler H, Padilla MH, Hueter RE, Jabado RW, Joyeux J-C, Jaiteh V, Johnson M, Jupiter SD, Kaimuddin M, Kasana D, Kelley M, Kessel ST, Kiilu B, Kirata T, Kuguru B, Kyne F, Langlois T, Lara F, Lawe J, Lédée EJI, Lindfield S, Luna-Acosta A, Maggs JQ, Manjaji-Matsumoto BM, Marshall A, Martin L, Mateos-Molina D, Matich P, McCombs E, McIvor A, McLean D, Meggs L, Moore S, Mukherji S, Murray R, Newman SJ, Nogués J, Obota C, Ochavillo D, O'Shea O, Osuka KE, Papastamatiou YP, Perera N, Peterson B, Pimentel CR, Pina-Amargós F, Pinheiro HT, Ponzo A, Prasetyo A, Quamar LMS, Quinlan JR, Reis-Filho JA, Ruiz H, Ruiz-Abierno A, Sala E, Salinas-de-León P, Samoilys MA, Sample WR, Schärer-Umpierre M, Schlaff AM, Schmid K, Schoen SN, Simpson N, Smith ANH, Spaet JLY, Sparks L, Stoffers T, Tanna A, Torres R, Travers MJ, Bergmann M van Z, Vigliola L, Ward J, Warren JD, Watts AM, Wen CK, Whitman ER, Wirsing AJ,

Wothke A, Zarza-González E, Chapman DD (2023) Widespread diversity deficits of coral reef sharks and rays. Science 380:1155–1160

Simpfendorfer CA, Heupel MR (2016) Ecology: The upside-down world of coral reef predators. Current Biology 26:R708–R710

Siqueira AC, Kiessling W, Bellwood DR (2022) Fast-growing species shape the evolution of reef corals. Nature Communications 13:2426

Siqueira AC, Morais RA, Bellwood DR, Cowman PF (2020) Trophic innovations fuel reef fish diversification. Nature Communications 11:2669

Siqueira AC, Morais RA, Bellwood DR, Cowman PF (2021) Planktivores as trophic drivers of global coral reef fish diversity patterns. Proceedings of the National Academy of Sciences 118:e2019404118

Siqueira AC, Yan HF, Morais RA, Bellwood DR (2023) The evolution of fast-growing coral reef fishes. Nature 618:322–327

Smith JA, Baumgartner LJ, Suthers IM, Fielder DS, Taylor MD (2013) Density-dependent energy use contributes to the self-thinning relationship of cohorts. The American Naturalist 181:331–343

Smith JE, Brainard R, Carter A, Grillo S, Edwards C, Harris J, Lewis L, Obura D, Rohwer F, Sala E, Vroom PS, Sandin S (2016) Re-evaluating the health of coral reef communities: baselines and evidence for human impacts across the central Pacific. Proceedings of the Royal Society B: Biological Sciences 283:20151985

Smith SA, O'Meara BC (2012) *treePL*: divergence time estimation using penalized likelihood for large phylogenies. Bioinformatics 28:2689–2690

Stan Development Team (2017) *RStan*: R interface to Stan.

Stearns SC (1989) Trade-offs in life-history evolution. Functional Ecology 3:259

Streit RP, Bellwood DR (2022) To harness traits for ecology, let's abandon 'functionality.' Trends in Ecology & Evolution 38:402–411

Streit RP, Cumming GS, Bellwood DR (2019) Patchy delivery of functions undermines functional redundancy in a high diversity system. Functional Ecology 33:1144–1155

Stuart-Smith RD, Bates AE, Lefcheck JS, Duffy JE, Baker SC, Thomson RJ, Stuart-Smith JF, Hill NA, Kininmonth SJ, Airoldi L, Becerro MA, Campbell SJ, Dawson TP, Navarrete SA, Soler GA, Strain EMA, Willis TJ, Edgar GJ (2013) Integrating abundance and functional traits reveals new global hotspots of fish diversity. Nature 501:539–542

Sully S, Burkepile DE, Donovan MK, Hodgson G, van Woesik R (2019) A global analysis of coral bleaching over the past two decades. Nature Communications 10:1264

Sumaila UR, Cheung WWL, Lam VWY, Pauly D, Herrick S (2011) Climate change impacts on the biophysics and economics of world fisheries. Nature Climate Change 1:449–456

Sumaila UR, Ebrahim N, Schuhbauer A, Skerritt D, Li Y, Kim HS, Mallory TG, Lam VWL, Pauly D (2019) Updated estimates and analysis of global fisheries subsidies. Marine Policy 109:103695

Sumaila UR, Tai TC (2020) End overfishing and increase the resilience of the ocean to climate change. Frontiers in Marine Science 7:523

Sunday JM, Bates AE, Dulvy NK (2011) Global analysis of thermal tolerance and latitude in ectotherms. Proceedings of the Royal Society B: Biological Sciences 278:1823–1830

Swain DP, Sinclair AF, Mark Hanson J (2007) Evolutionary response to size-selective mortality in an exploited fish population. Proceedings of the Royal Society B: Biological Sciences 274:1015–1022

Tebbett SB, Bellwood DR, Bassett T, Cuttler MVW, Moustaka M, Wilson SK, Yan HF, Evans RD (2024a) The limited role of herbivorous fishes and turf-based trophic pathways in the functioning of turbid coral reefs. Reviews in Fish Biology and Fisheries 34:439–460

Tebbett SB, Bennett S, Bellwood DR (2024b) A functional perspective on the meaning of the term 'herbivore': patterns versus processes in coral reef fishes. Coral Reefs 43:219–232

Tebbett SB, Connolly SR, Bellwood DR (2023a) Benthic composition changes on coral reefs at global scales. Nature Ecology & Evolution 7:71–81

Tebbett SB, Crisp SK, Evans RD, Fulton CJ, Pessarrodona A, Wernberg T, Wilson SK, Bellwood DR (2023b) On the challenges of identifying benthic dominance on Anthropocene coral reefs. BioScience 73:220–228

Tebbett SB, Faul SI, Bellwood DR (2024c) Quantum of fear: Herbivore grazing rates not affected by reef shark presence. Marine Environmental Research 196:106442

Tebbett SB, Morais RA, Goatley CHR, Bellwood DR (2021) Collapsing ecosystem functions on an inshore coral reef. Journal of Environmental Management 289:112471

Tebbett SB, Schlaefer JA, Bowden CL, Collins WP, Hemingson CR, Ling SD, Morais J, Morais RA, Siqueira AC, Streit RP, Swan S, Bellwood DR (2023c) Bio-physical determinants of sediment accumulation on an offshore coral reef: A snapshot study. Science of The Total Environment 895:165188

Tebbett SB, Streit RP, Bellwood DR (2019) Expansion of a colonial ascidian following consecutive mass coral bleaching at Lizard Island, Australia. Marine Environmental Research 144:125–129

Tebbett SB, Yan HF, Lutzenkirchen LL, Siqueira AC, Bellwood DR (2024d) Global patterns of herbivorous reef fish productivity: the role of *Prionurus laticlavius* in the Galápagos. Coral Reefs 43:299–305

Teh LSL, Teh LCL, Sumaila UR (2013) A global estimate of the number of coral reef fishers. PLOS ONE 8:10

Thibaut LM, Connolly SR, Sweatman HPA (2012) Diversity and stability of herbivorous fishes on coral reefs. Ecology 93:891–901

Thompson PL, Isbell F, Loreau M, O'Connor MI, Gonzalez A (2018) The strength of the biodiversity–ecosystem function relationship depends on spatial scale. Proceedings of the Royal Society B: Biological Sciences 285:20180038

Thorson JT, Maureaud AA, Frelat R, Mérigot B, Bigman JS, Friedman ST, Palomares MLD, Pinsky ML, Price SA, Wainwright P (2023) Identifying direct and indirect associations among traits by merging phylogenetic comparative methods and structural equation models. Methods in Ecology and Evolution 14:1259-1275

Thygesen UH, Farnsworth KD, Andersen KH, Beyer JE (2005) How optimal life history changes with the community size-spectrum. Proceedings of the Royal Society B: Biological Sciences 272:1323–1331

Tilman D, Isbell F, Cowles JM (2014) Biodiversity and ecosystem functioning. Annual Review of Ecology, Evolution, and Systematics 45:471–493

Tittensor DP, Mora C, Jetz W, Lotze HK, Ricard D, Berghe EV, Worm B (2010) Global patterns and predictors of marine biodiversity across taxa. Nature 466:1098–1101

Torda G, Sambrook K, Cross P, Sato Y, Bourne DG, Lukoschek V, Hill T, Torras Jorda G, Moya A, Willis BL (2018) Decadal erosion of coral assemblages by multiple disturbances in the Palm Islands, central Great Barrier Reef. Scientific Reports 8:11885

Trebilco R, Baum JK, Salomon AK, Dulvy NK (2013) Ecosystem ecology: size-based constraints on the pyramids of life. Trends in Ecology & Evolution 28:423–431

Trippel EA (1995) Age at maturity as a stress indicator in fisheries. BioScience 45:759–771

Uyeda JC, Harmon LJ (2014) A novel Bayesian method for inferring and interpreting the dynamics of adaptive landscapes from phylogenetic comparative data. Systematic Biology 63:902–918

Van Denderen D, Gislason H, Van Den Heuvel J, Andersen KH (2020) Global analysis of fish growth rates shows weaker responses to temperature than metabolic predictions. Global Ecology and Biogeography 29:2203–2213

Von Bertalanffy L (1949) Problems of organic growth. Nature 163:156–158

Watanabe S (2010) Asymptotic equivalence of Bayes cross validation and widely applicable information criterion in singular learning theory. J Mach Learn Res 11:3571–3594

Watkins HV (2024) Echinoderms in decline: modeling trends, assessing consequences, and reversing course. Simon Fraser University

Webb TJ, Mindel BL (2015) Global patterns of extinction risk in marine and non-marine systems. Current Biology 25:506–511

West GB, Brown JH, Enquist BJ (2001) A general model for ontogenetic growth. Nature 413:628–631

Westerhold T, Marwan N, Drury AJ, Liebrand D, Agnini C, Anagnostou E, Barnet JSK, Bohaty SM, De Vleeschouwer D, Florindo F, Frederichs T, Hodell DA, Holbourn AE, Kroon D, Lauretano V, Littler K, Lourens LJ, Lyle M, Pälike H, Röhl U, Tian J, Wilkens RH, Wilson PA, Zachos JC (2020) An astronomically dated record of Earth's climate and its predictability over the last 66 million years. Science 369:1383–1387

White CR, Alton LA, Bywater CL, Lombardi EJ, Marshall DJ (2022) Metabolic scaling is the product of life-history optimization. Science 377:834–839

Wilkinson C (2004) Status of coral reefs of the world: 2004. Australian Institute of Marine Science, Australia

Williams JJ, Papastamatiou YP, Caselle JE, Bradley D, Jacoby DMP (2018) Mobile marine predators: an understudied source of nutrients to coral reefs in an unfished atoll. Proceedings of the Royal Society B: Biological Sciences 285:20172456

Willis TJ, Millar RB, Babcock RC (2000) Detection of spatial variability in relative density of fishes: comparison of visual census, angling, and baited underwater video. Marine Ecology Progress Series 198:249–260

Wilson JA, Giske J (2023) Does fishing dismantle fish culture and ecosystem structure? Questions about the implications of social learning among fish and fishers. Fish and Fisheries 24:889–895

Winfree R, W. Fox J, Williams NM, Reilly JR, Cariveau DP (2015) Abundance of common species, not species richness, drives delivery of a real-world ecosystem service. Ecology Letters 18:626–635

Wittebolle L, Marzorati M, Clement L, Balloi A, Daffonchio D, Heylen K, De Vos P, Verstraete W, Boon N (2009) Initial community evenness favours functionality under selective stress. Nature 458:623–626

Wong S, Bigman JS, Dulvy NK (2021) The metabolic pace of life histories across fishes. Proceedings of the Royal Society B: Biological Sciences 1953:7

Woodcock BA, Garratt MPD, Powney GD, Shaw RF, Osborne JL, Soroka J, Lindström SAM, Stanley D, Ouvrard P, Edwards ME, Jauker F, McCracken ME, Zou Y, Potts SG, Rundlöf M, Noriega JA, Greenop A, Smith HG, Bommarco R, van der Werf W, Stout JC, Steffan-Dewenter I, Morandin L, Bullock JM, Pywell RF (2019) Meta-analysis reveals that pollinator functional diversity and abundance enhance crop pollination and yield. Nature Communications 10:1481

Worm B, Branch TA (2012) The future of fish. Trends in Ecology & Evolution 27:594–599

Worm B, Hilborn R, Baum JK, Branch TA, Collie JS, Costello C, Fogarty MJ, Fulton EA, Hutchings JA, Jennings S, Jensen OP, Lotze HK, Mace PM, McClanahan TR, Minto C, Palumbi SR, Parma AM, Ricard D, Rosenberg AA, Watson R, Zeller D (2009) Rebuilding global fisheries. Science 325:578–585

Yachi S, Loreau M (1999) Biodiversity and ecosystem productivity in a fluctuating environment: The insurance hypothesis. Proceedings of the National Academy of Sciences 96:1463–1468

Yamahira K, Conover DO (2002) Intra- vs. interspecific latitudinal variation in growth: Adaption to temperature or seasonality? Ecology 83:1252–1262

Yan HF, Casey JM, Knowlton N, Duffy JE, Brandl SJ (2022) Examining the diversity, stability and functioning of marine fish communities across a latitudinal gradient. Global Ecology and Biogeography 32:166-177

Yan HF, Kyne PM, Jabado RW, Leeney RH, Davidson LNK, Derrick DH, Finucci B, Freckleton RP, Fordham SV, Dulvy NK (2021) Overfishing and habitat loss drives range contraction of iconic marine fishes to near extinction. Science Advances 7:eabb6026

Zamborain-Mason J, Cinner JE, MacNeil MA, Graham NAJ, Hoey AS, Beger M, Brooks AJ, Booth DJ, Edgar GJ, Feary DA, Ferse SCA, Friedlander AM, Gough CLA, Green AL, Mouillot D, Polunin NVC, Stuart-Smith RD, Wantiez L, Williams ID, Wilson SK, Connolly SR (2023) Sustainable reference points for multispecies coral reef fisheries. Nature Communications 14:5368

Appendix A – Supplementary materials for Chapter 2

Supplementary text

Calculating empirical S_L

We followed the same method outlined by Morais and Bellwood (2018) to contrast the empirically-measured and theoretical slope of a growth curve (S_L). Recall that S_L pertains to the slope between K and L_∞ on a $\log_{10}$-$\log_{10}$ scale for each individual growth curve. The theoretical slope combines the anabolic exponent (or metabolic scaling exponent; m) from Savage et al. (2004) with the average length-weight conversion exponent (b; Froese et al. 2014) in Pauly's equation ($S_L = -m/b$; 1979), resulting in a mean S_L centered on -2.31 (95% confidence interval: -2.75 to -1.91). The addition of data from 2019 to present resulted in the addition of one more species (n = 75) and 27 additional growth curves. We calculated the empirical S_L for species with at least six growth curves by modelling $\log_{10}(K) \sim \log_{10}(L_\infty)$ and weighted each curve by the method used to generate the data. We weighted individually derived parameters more heavily than population-level parameters: mark recapture studies were given the highest weight of 1, followed by otolith rings (0.8), other calcified rings (i.e., scale rings, other rings; 0.7), and all other methods received the lowest weight (i.e., length frequency or unknown; 0.5). For each model, we extracted the slope coefficient (i.e., S_L), the standard error of the coefficient, and the R^2.

To contrast the empirically measured S_L values from the theoretical value (-2.31), we generated a mean empirically measured S_L value using a Bayesian meta-analysis. We weighted each model with the standard error and the goodness of fit (R^2) and used family as a grouping factor to account for the non-independence of related species. This model used 4,000 iterations with an initial burn-in phase of 1,500 iterations and was thinned for every third step of each chain. Finally, we used a strong informative prior centered around the theoretical S_L using a normal distribution with a mean of -2.31 and a standard deviation of 0.149. Using leave-one-out cross validation, all Pareto-k values were below 0.5, indicating that no points were disproportionally impacting the model and we achieved chain convergence (all rhat values = 1.00).

The mean estimate of our empirical S_L was -1.97 [95% credible interval = -2.08 to -1.86], which brackets both the empirical S_L from Morais and Bellwood (2018; -2.18 [-2.31 to -2.06]) and the theoretical value from Pauly (1979; -2.31 [-2.75 to -1.91]; **Appendix A**: Fig. A2a). In both the simulated and data-informed S_L values, positive values were rare and the distributions were centered around -2. Because our empirically-measured S_L values were not different from the values from Morais and Bellwood (2018) nor from Pauly (1979), we used the theoretical S_L for all calculations of K_{max} (**Appendix** A: Fig. A2b). We combined equations (5-6) from Morais and Bellwood (2018) to calculate K_{max}:

$$log_{10}K_{max} = log_{10}K - S_L \cdot log_{10}(L_\infty \cdot L_{\max})$$

Where K and L_∞ are derived from the Von Bertalanffy growth equation, S_L is the theoretical slope from above, and L_{max} is the maximum size recorded for that species.

Comparing reef with non-reef fishes

To compare the growth rates of reef-associated versus non-reef-associated fishes, we collected additional growth curves from the peer-reviewed literature and FishBase. This resulted in an additional 1,170 empirically measured growth curves for 83 non-reef fish families. We then used the temperature preference for each species, as reported on FishBase, to select species that exhibited a minimum preferred temperature within the range of those used in our study. In short, preferred temperatures are derived from modelled range maps and calculated based on the estimated temperatures over the species' distributional range (Bellwood et al. 2017). This process then selects species that are found within the same geographical areas as those used in our study, but are not associated with coral reefs (e.g. the spined anchovy *Stolephorus tri*).

Extended data figures

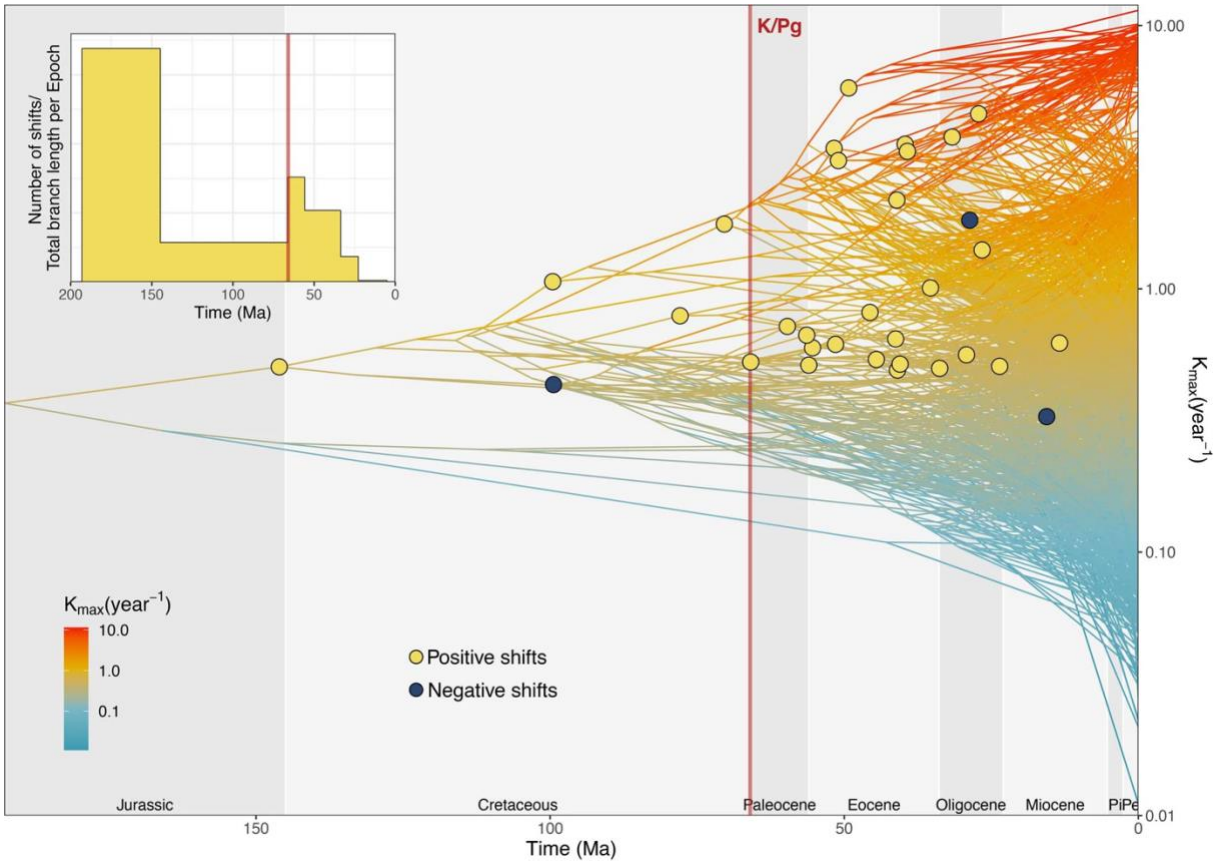

Extended Data Figure 1 Phylogenetic reconstruction of reef fish growth. *Standardised growth coefficient (K_{max}) reconstructed through time across the phylogenetic tree of coral reef-associated fishes. The points represent estimated shifts in the evolutionary regime of growth detected through multi-optima Ornstein–Uhlenbeck models, using 50% as the threshold for posterior probabilities. Light-yellow points represent shifts toward higher values of evolutionary optima (i.e. faster growth rates), while dark-blue points represent the opposite. Please note that the y-axis is on a log_{10} scale. The inset depicts the number of positive shifts divided by the total branch length in the phylogeny per geological epoch (y-axis) through time (x-axis). This metric gives an indication of the probability of shifts controlled by the availability of locations for them to occur, which is biased towards very old shifts. We note that the higher number of shifts/branch length detected for the Jurassic is a product of this bias and should be interpreted with caution given that it is the result of only one shift in that Period. The red line represents the Cretaceous-Paleogene (K/Pg) boundary. Pi: Pliocene; Pe: Pleistocene.*

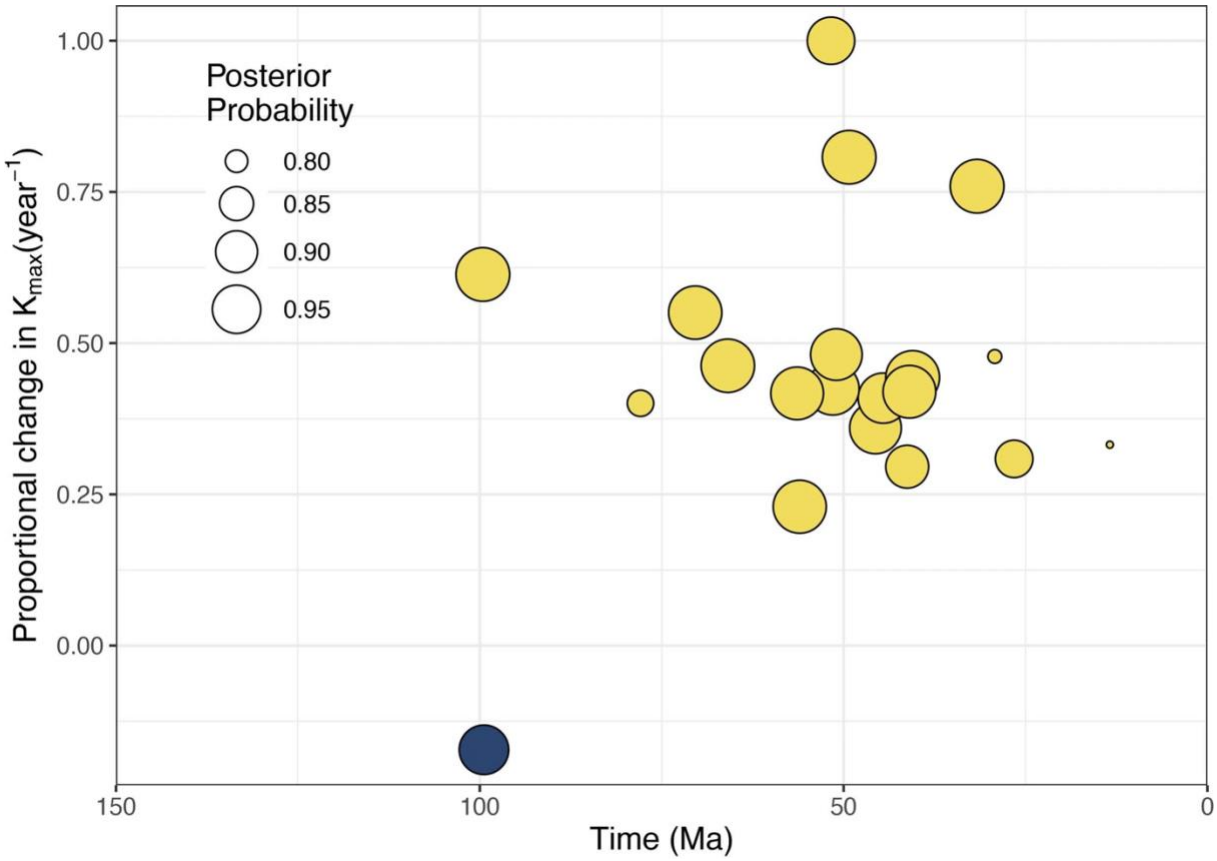

Extended Data Figure 2 Proportional change in reef fish K_{max} evolutionary optima through time. *Light-yellow points represent shifts toward higher values of evolutionary optima (i.e. faster growth rates), while the dark-blue point represents the opposite. The size of points is scaled according to their posterior probability in Ornstein–Uhlenbeck models.*

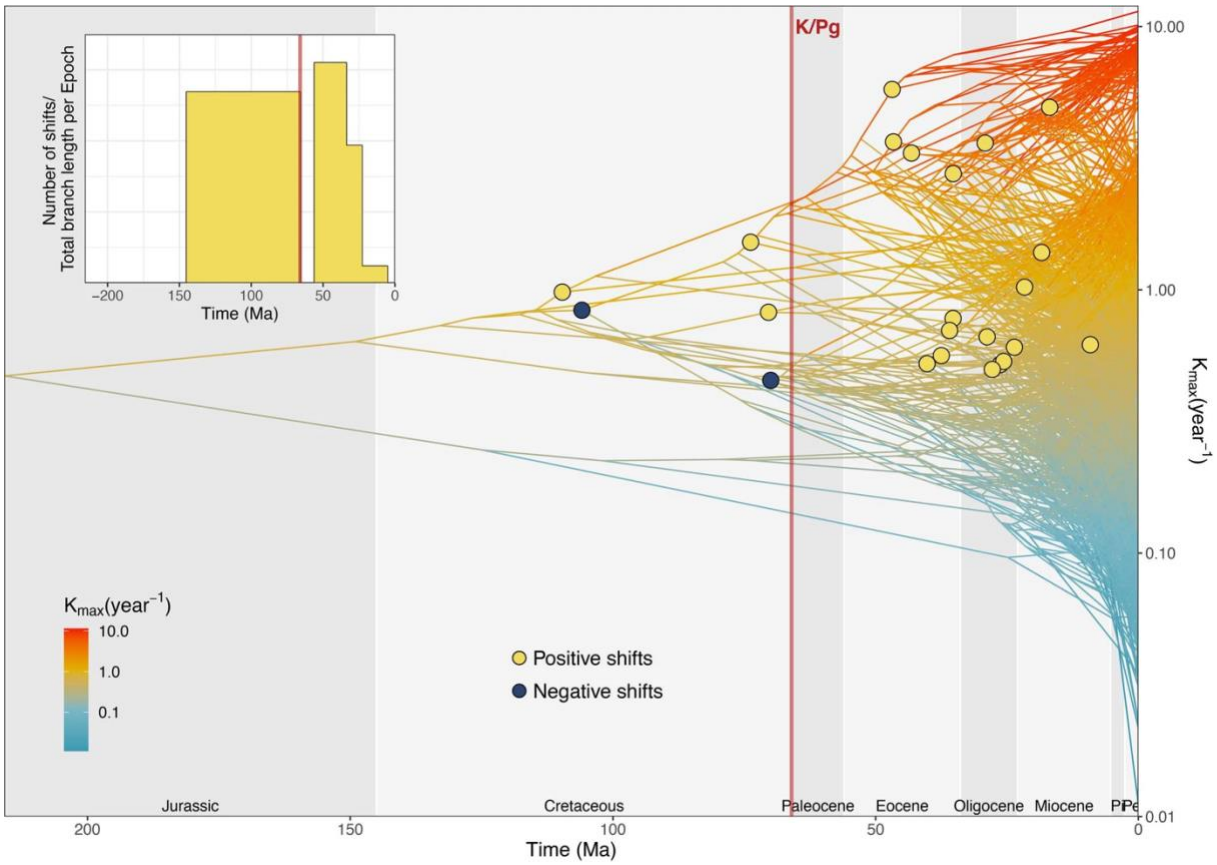

Extended Data Figure 3 Phylogenetic reconstruction of reef fish growth. *Standardised growth coefficient (K_{max}) reconstructed through time across the phylogenetic tree of coral reef-associated fishes, recalibrated based on Ghezelayagh et al. (2022; see Methods). The points represent estimated shifts in the evolutionary regime of growth detected through multi-optima Ornstein–Uhlenbeck models. Light-yellow points represent shifts toward higher values of evolutionary optima (i.e. faster growth rates), while dark-blue points represent the opposite. Please note that the y-axis is on a log_{10} scale. The inset depicts the number of positive shifts divided by the total branch length in the phylogeny per geological epoch (y-axis) through time (x-axis). This metric gives an indication of the probability of shifts controlled by the availability of locations for them to occur. The red line represents the Cretaceous-Paleogene (K/Pg) boundary. Pi: Pliocene; Pe: Pleistocene.*

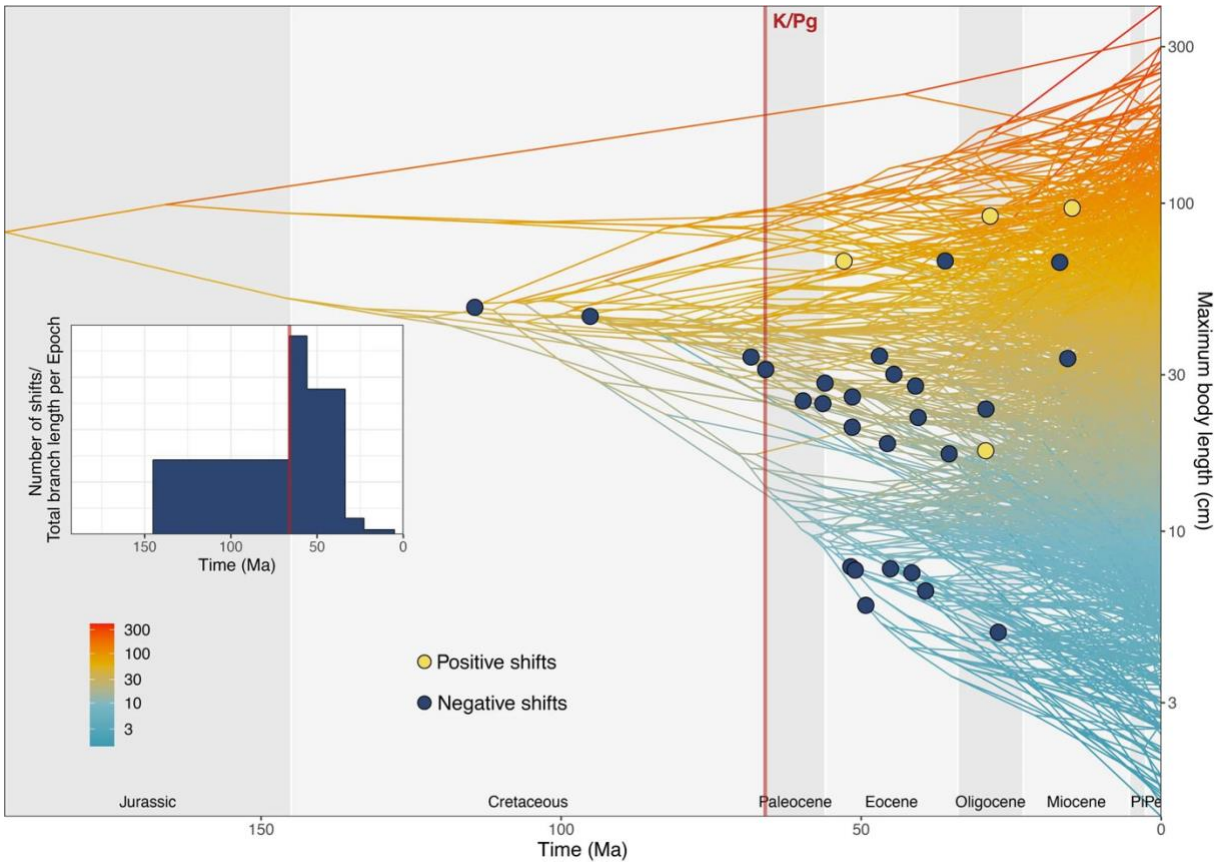

Extended Data Figure 4 Phylogenetic reconstruction of reef fish body size. *Maximum body length reconstructed through time across the phylogenetic tree of coral reef-associated fishes. The points represent estimated shifts in the evolutionary regime of body size detected through multi-optima Ornstein–Uhlenbeck models. Light-yellow points represent shifts toward higher values of evolutionary optima (i.e. larger body sizes), while dark-blue points represent the opposite. Please note that the y-axis is on a* log_{10} *scale. The inset depicts the number of negative shifts (i.e. towards smaller body sizes) divided by the total branch length in the phylogeny per geological epoch (y-axis) through time (x-axis). This metric gives an indication of the probability of shifts controlled by the availability of locations for them to occur. The red line represents the Cretaceous-Paleogene (K/Pg) boundary. Pi: Pliocene; Pe: Pleistocene.*

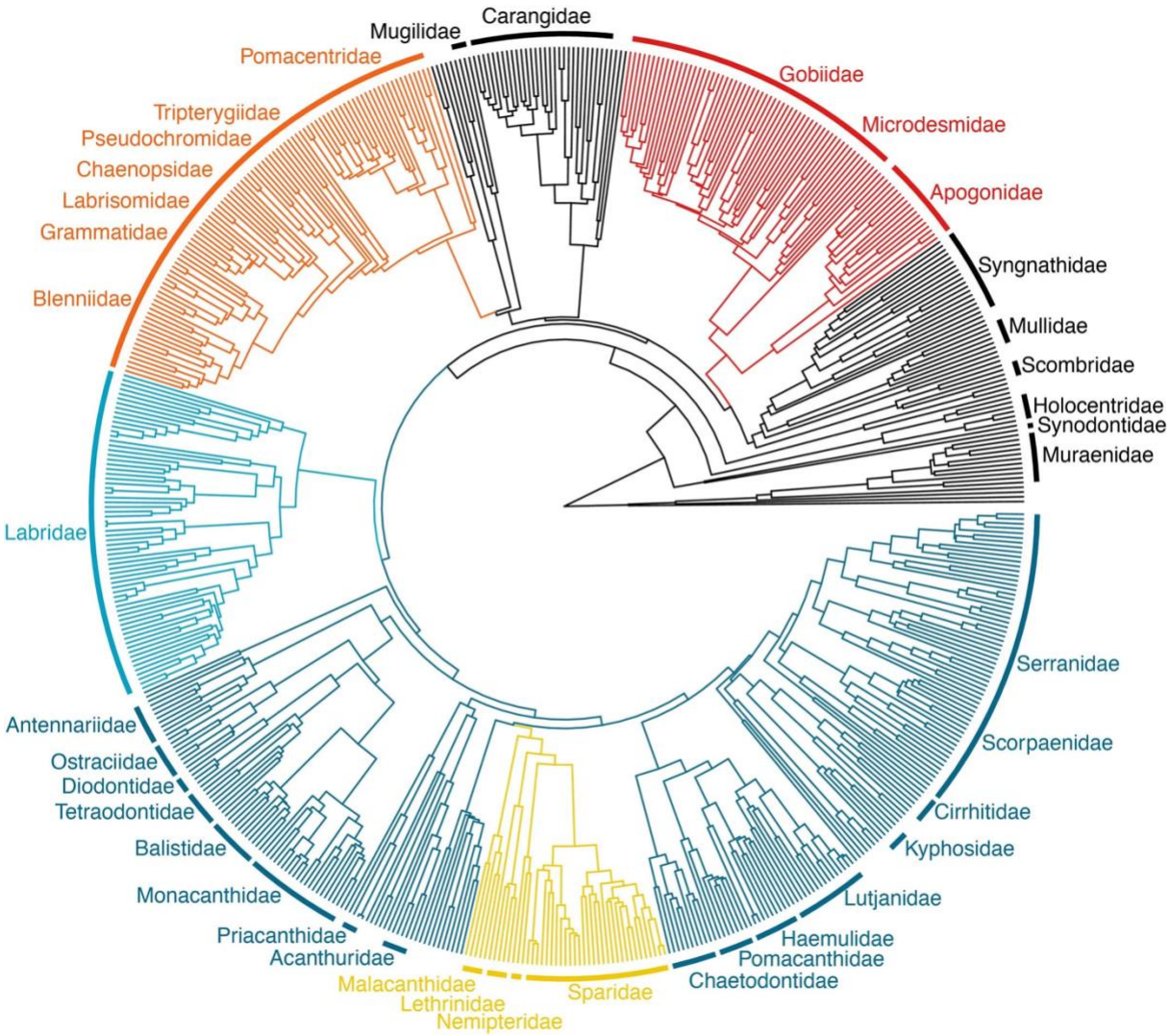

Extended Data Figure 5 Evolutionary regimes in the allometry growth/body size in reef fishes. *Reef fish phylogeny at the genus level with depicted evolutionary regimes for the allometric relationship between the growth coefficient (K_{max}) and maximum body length. The different colours across the branches represent the clades with different evolutionary regimes detected by the mixed Gaussian phylogenetic model (see Methods). The coefficients estimated for each regime are shown in* ***Fig. 2-3****, with the respective colours. External arcs show the extant families represented by each clade, along with respective allometric evolutionary regime.*



Extended Data Figure 6 Empirical K_{max} values for reef vs. non-reef fish species. *Density plots illustrating the distribution of empirical K_{max} values for coral reef-associated species considered in this study (orange) and non-reef-associated species (blue). Details on data collection for non-reef-associated species can be found in the supplementary material. The thick lines indicate the median K_{max} values for each group. Please note that the x-axis is on a log_{10} scale.*

Supplementary figures

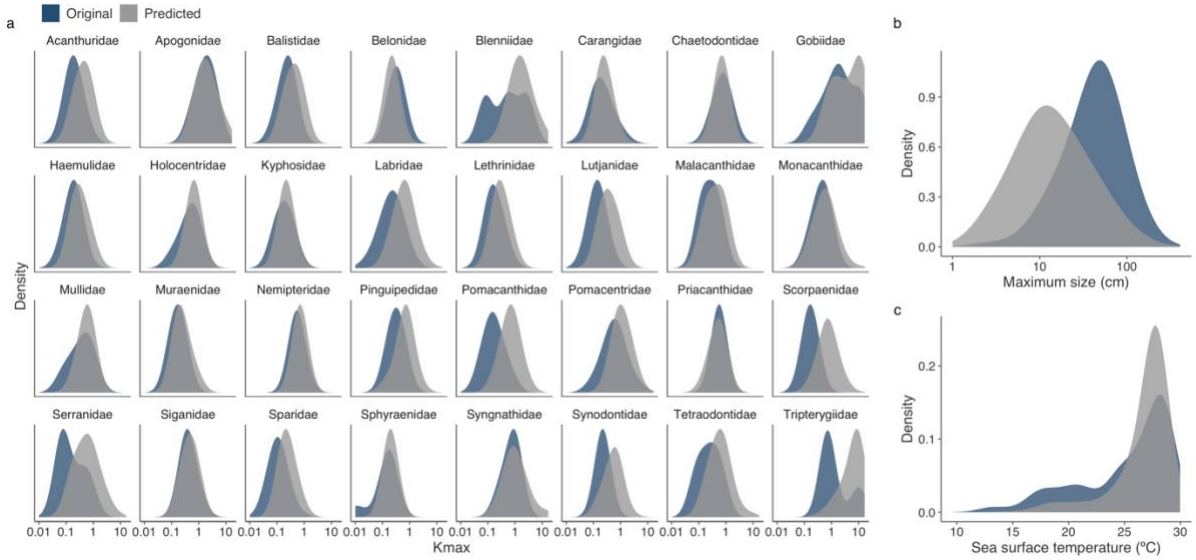

Figure A1. *Density plots illustrating the distributions of empirically measured growth values (blue) and predicted outputs (grey) from our boosted regression tree analyses across (a) families, (b) body sizes, and (c) sea surface temperature. Families were only included when both empirically measured and predicted growth curves were found (i.e. we omitted families for which growth was only empirically measured or predicted). Note that in a-b, the x axes are on the* log_{10} *scale.*

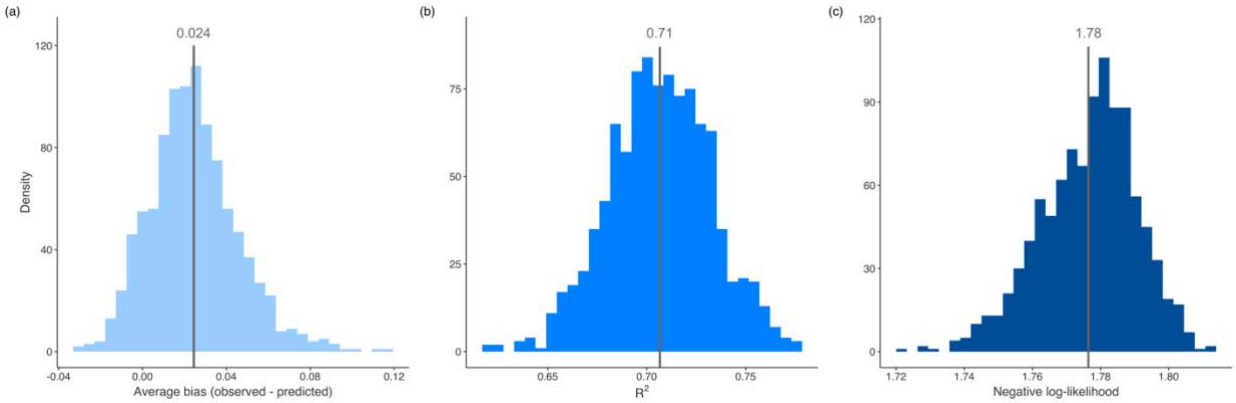

Figure A2. *Boosted regression tree model diagnostics over 1,000 bootstrapped iterations. (a) The average bias in the test set, calculated as the predicted K_{max} value from each model iteration subtracted from the observed value (mean [minimum, maximum]: 0.02 [-6.6, 13.7]). (b) The mean R^2 value from the linear regression model with predicted K_{max} as a function of the observed K_{max} on a log_{10}- log_{10} scale (0.71 [0.62, 0.78]). (c) The mean negative log-likelihood (i.e., the loss function) across 1,000 bootstrapped iterations (1.78 [1.72, 1.81]).*

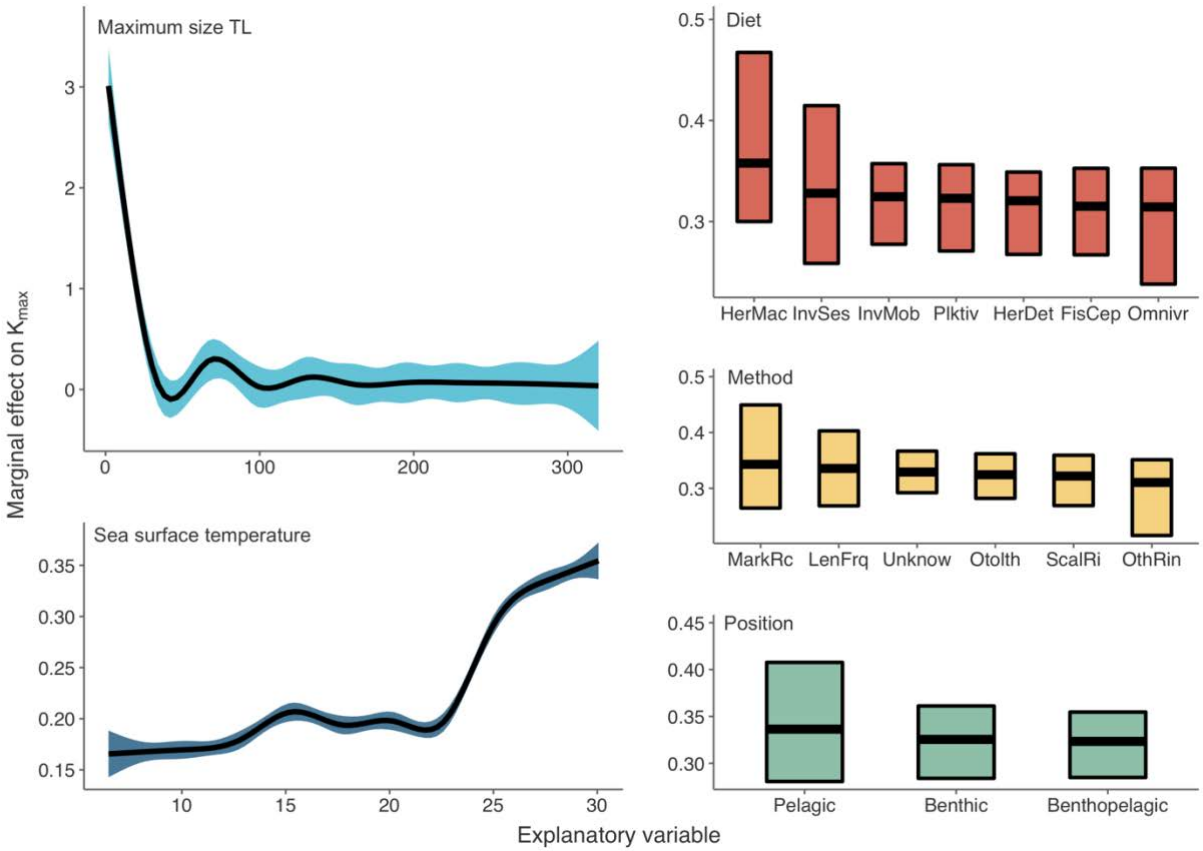

Figure A3. *Partial dependence plots showing the effects of maximum body size, sea surface temperature, diet, method, and position on the water column on empirically measured values of K_{max}. The medians are shown in black and the 99% confidence intervals are shown as coloured ribbons for continuous predictors (i.e., maximum body size and sea surface temperature) and coloured boxes for categorical predictors (i.e., diet, method, and position). The variable with the highest relative importance for predicting K_{max} was maximum body size (mean variable importance [minimum, maximum]: 72% [67.6-75.2%]), followed by sea surface temperature (17.7% [14.7-20.9%], method (4.4% [3.0-5.9%]), diet (3.6% [2.5-5.1%]), and position relative to reef (2.3% [1.3-3.4%]).*

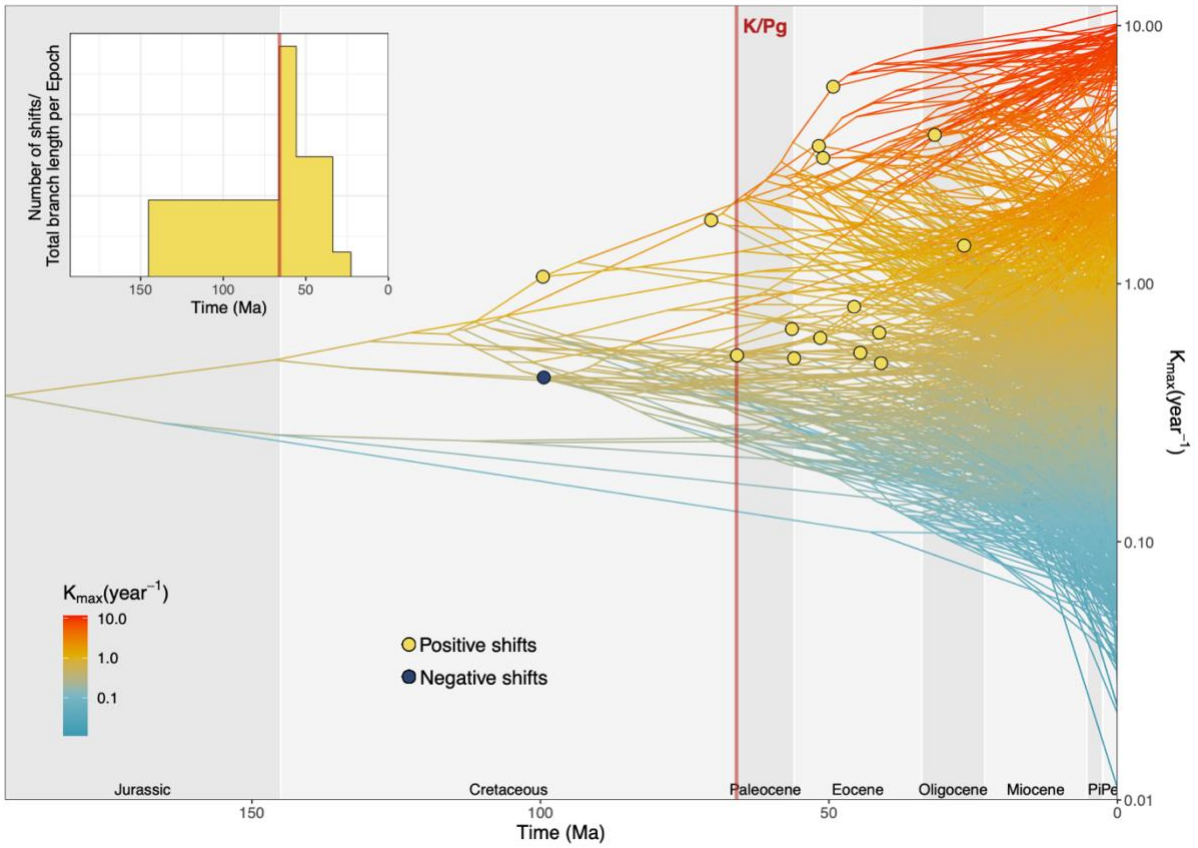

Figure A4. *Standardised growth coefficient (K_{max}) reconstructed through time across the phylogenetic tree of coral reef-associated fishes. The points represent estimated shifts in the evolutionary regime of growth detected through multi-optima Ornstein–Uhlenbeck models, using 90% as the threshold for posterior probabilities. Light-yellow points represent shifts toward higher values of evolutionary optima (i.e. faster growth rates), while the dark-blue point represents the opposite. Please note that the y-axis is on a log_{10} scale. The inset depicts the number of positive shifts divided by the total branch length in the phylogeny per geologic Epoch (y-axis) through time (x-axis). This metric gives an indication of the probability of shifts controlled by the availability of locations for them to occur. The red line represents the Cretaceous-Paleogene (K/Pg) boundary. Pi: Pliocene; Pe: Pleistocene.*

Supplementary tables

Table A1. Comparison between a multi-optima OU model based on shifts in growth optima detected through `bayou` (see Methods), a single evolutionary optimum (single-optimum OU) model, and a Brownian Motion (global BM) model. Model comparison was performed using the maximum likelihood framework of `mvMORPH`. The models are ordered according to *AIC*, showing that the multi-optima OU model had a substantially better fit. *AICw* represents the model weight.

	AIC	**ΔAIC**	**AICw**
Multi-optima OU	1557	0	1
Single-optimum OU	3330	1773	0
Global BM	6989	5432	0

Table A2. Model comparison between a mixed Gaussian (MGPM) and combinations of global BM and OU models of growth and body size evolution in reef fishes. Models are ordered according to lowest *AIC*, where p represents the number of parameters in each model. The global models were specified following Mitov et al.9: BM_A (H = 0, diagonal S): Brownian Motion with uncorrelated traits; BM_B (H = 0, symmetric S): Brownian Motion with correlated traits; OU_C (diagonal H, diagonal S): Ornstein–Uhlenbeck with uncorrelated traits; OU_D (diagonal H, symmetric S): Ornstein–Uhlenbeck with correlated traits, but simple (diagonal) selection strength matrix; OU_E (symmetric H, symmetric S): Ornstein–Uhlenbeck with nondiagonal symmetric H and nondiagonal symmetric S; OU_F (asymmetric H, symmetric S): Ornstein–Uhlenbeck with nondiagonal asymmetric H and nondiagonal symmetric S. On a k-variate OU process, the parameter H is a k x k-dimensional eigendecomposable real matrix that specifies the trajectory of the population mean through time. The parameter S is a k x k-dimensional real positive definite matrix, which defines the magnitude and shape of the momentary fluctuations in the mean vector due to genetic drift. The MGPM is the model in which traits are estimated to evolve according to each of these six default models (A–F) in different parts of the phylogenetic tree.

	p	**logLik**	**AIC**	**ΔAIC**
MGPM	51	244.14275	-364.2855	0
OU_F	11	177.36395	-330.7279	33.55760
OU_D	9	159.24109	-298.4822	65.80332
OU_E	10	143.86399	-265.7280	98.55751
BM_B	5	74.25736	-136.5147	227.7707
OU_C	8	-98.78204	215.5641	579.8495
BM_A	4	-111.51281	233.0256	597.3111

Appendix B – Supplementary materials for Chapter 3

Supplementary figures

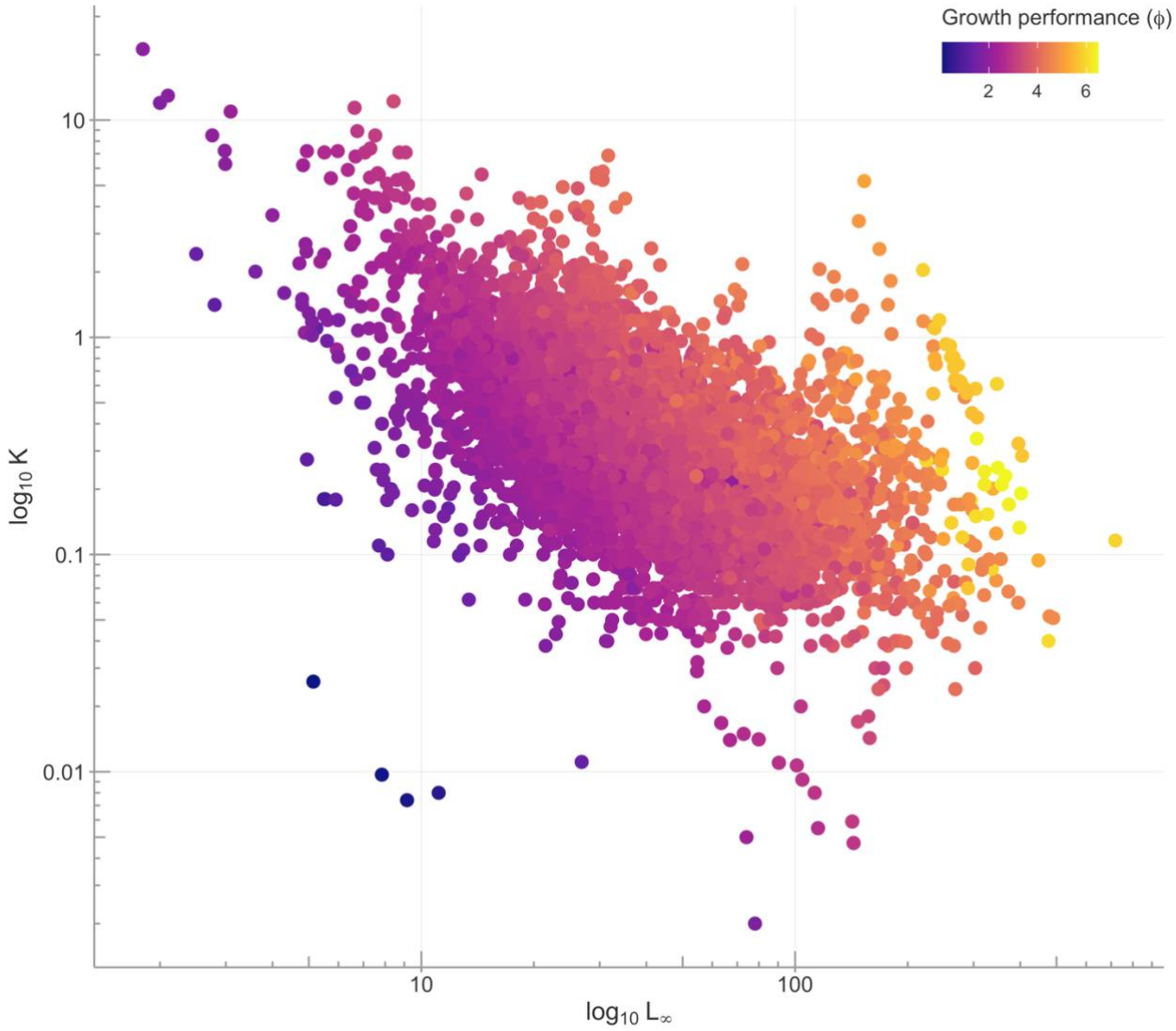

Figure B1. Growth performance of marine fishes. *Each point is representative of a single population/stock and is illustrating the mined growth parameters L_∞ and K, shown on the x and y axes, respectively. Points are coloured based on the calculated growth performance value (ϕ), whereby the lowest values are in purple and the highest are in yellow. Note both x and y axes are on the log_{10} scale.*

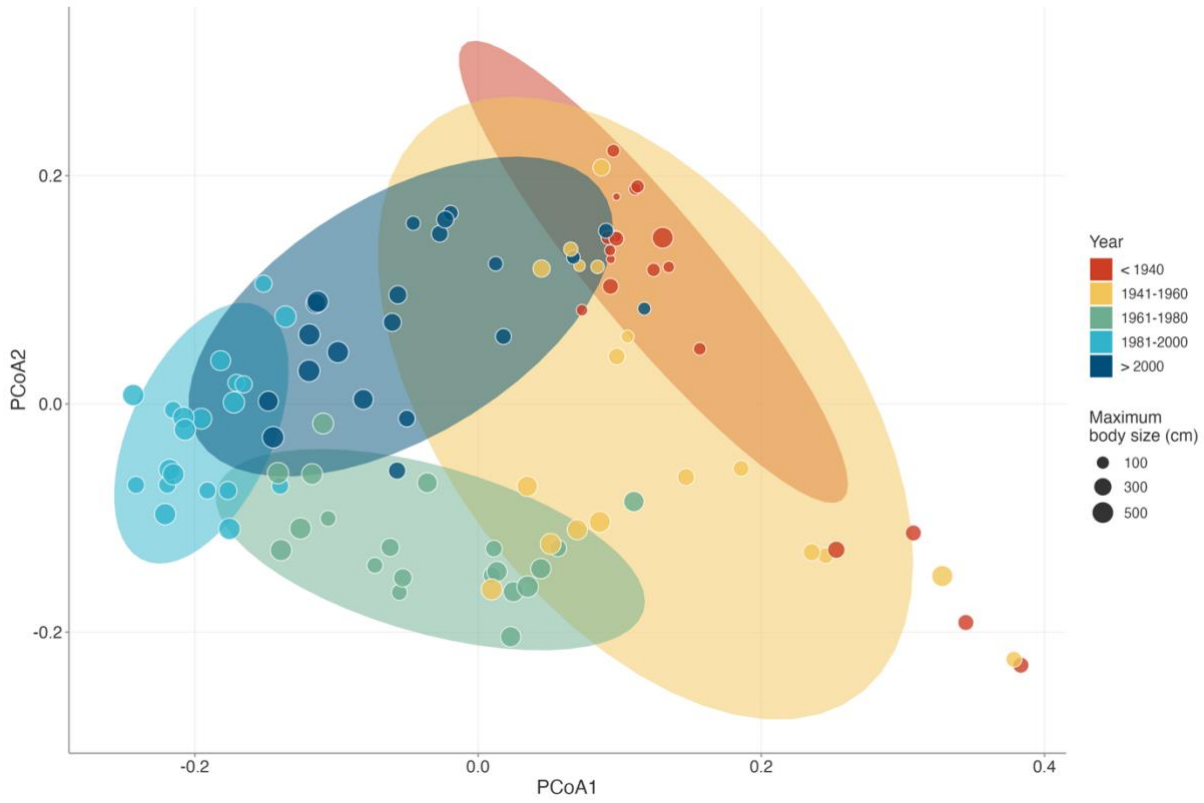

Figure B2. Principal Coordinate Analysis (PCoA) of species compositional changes in growth studies through time. *Each point is representative of the species composition for a given year based on presence/absence and are sized based on the species-level maximum body size per year. Ellipses show the 90% confidence spread in the data. Points and ellipses are coloured based on their respective 20-year time slices: prior to 1940 (red), 1941-1960 (yellow), 1961-1980 (green), 1981-2000 (light blue), and after 2000 (dark blue).*

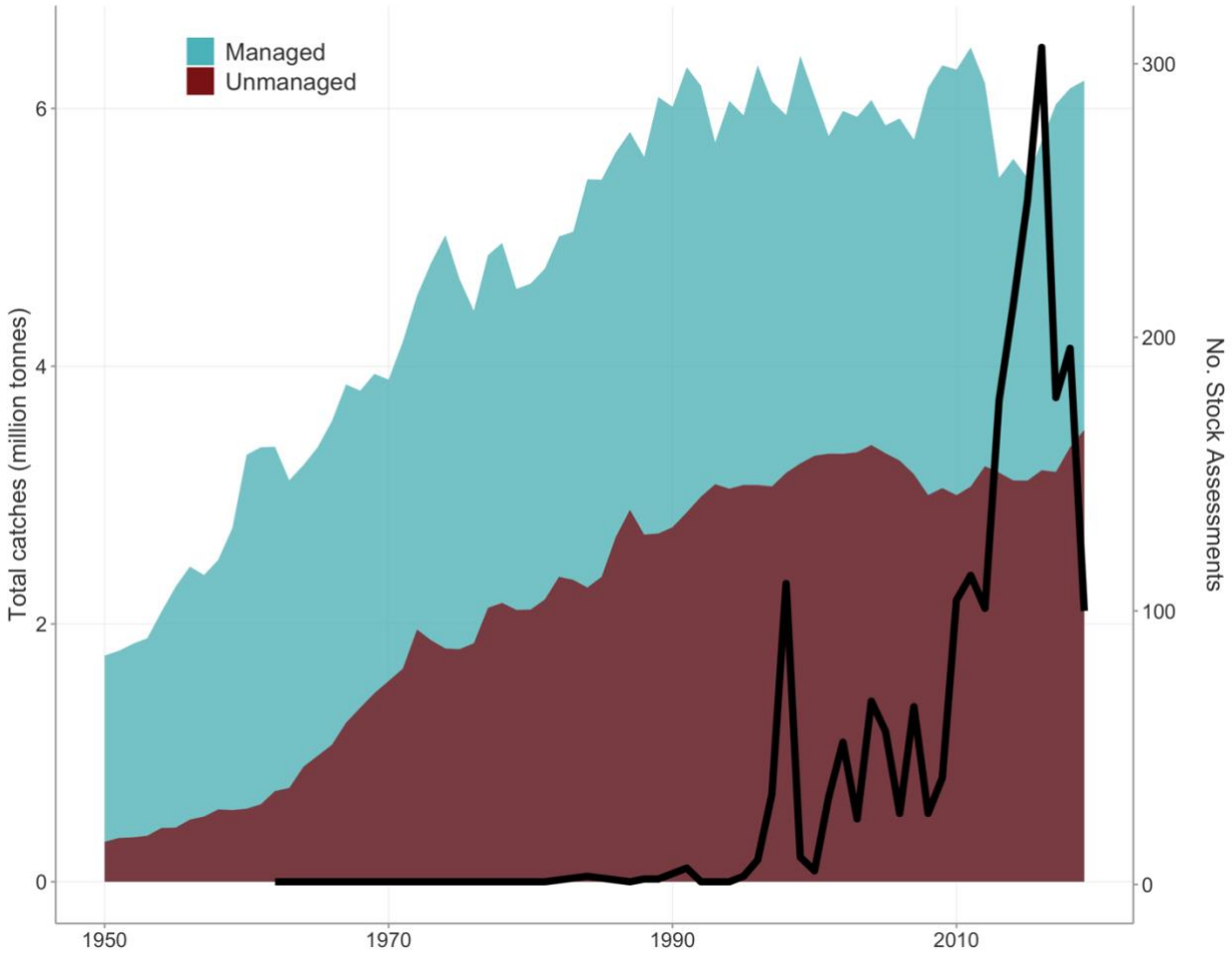

Figure B3. Temporal mismatch between fishing and management. *The total reported and reconstructed landed tonnes of managed fishes (blue) and unmanaged fishes (red) from 1950 to 2021 (left y axis) across all countries. The black line denotes the number of stock assessments in a given year (right y axis) across the time series.*

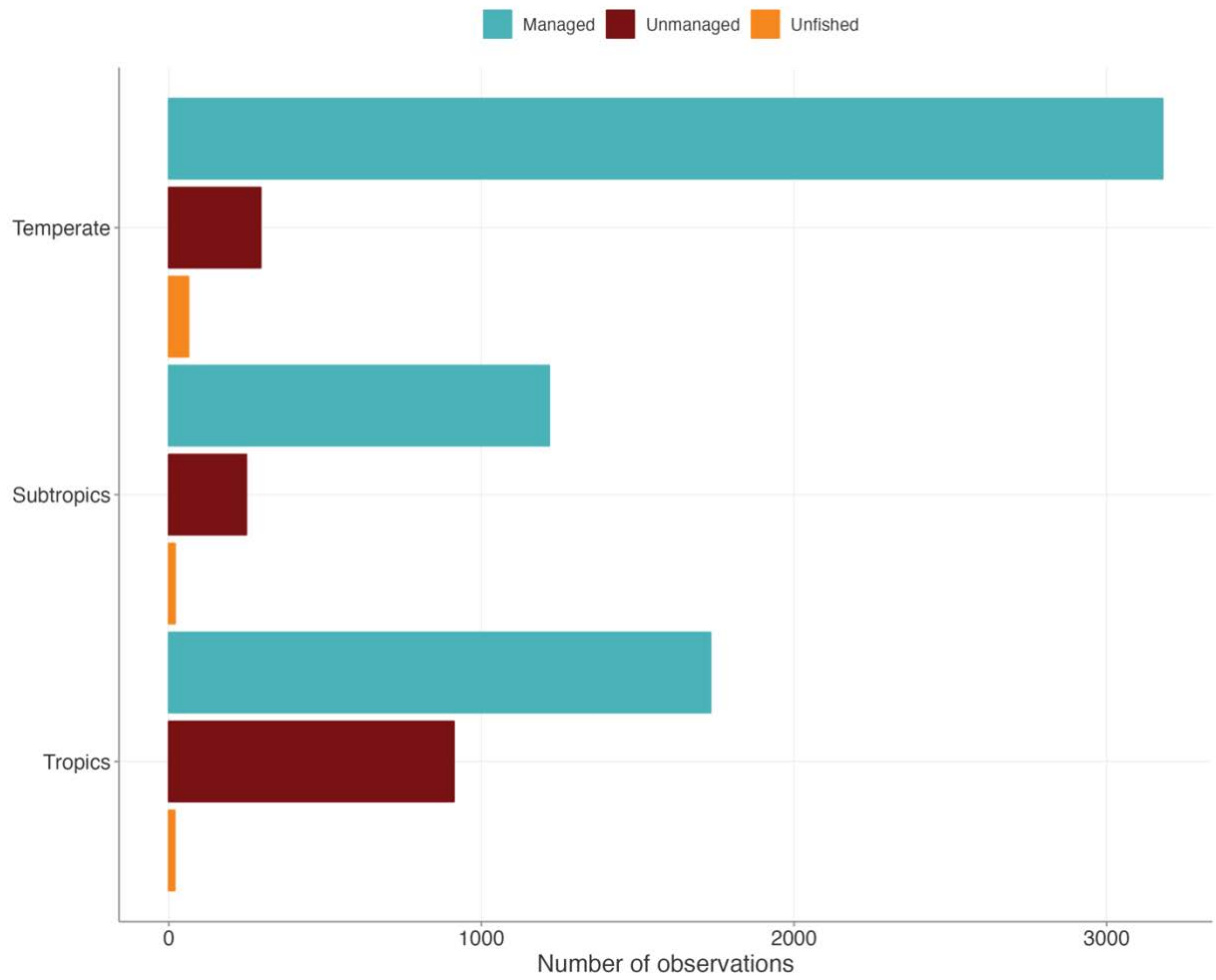

Figure B4. Dominance of managed fisheries in temperate regions. *Total number of observations in the study from managed fisheries (green), unmanaged fisheries (red), and unfished species (orange) in temperate (top), subtropical (middle), and tropical regions (bottom).*

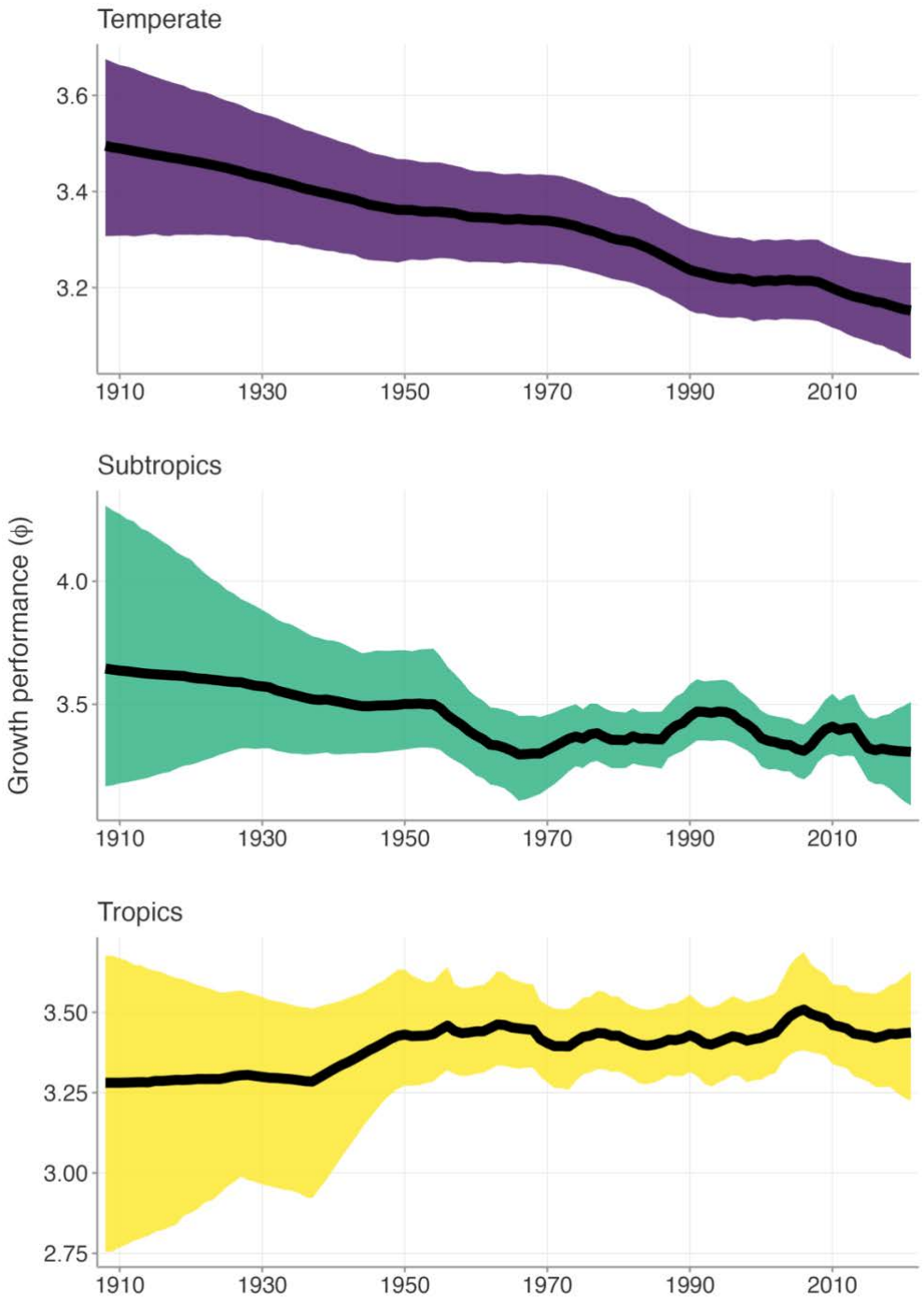

Figure B5. Changes in growth performance of managed fishes across regions. *Changes in growth performance (ϕ) of managed fishes in temperate (top; purple), subtropical (middle; green), and tropical regions (bottom; yellow) from 1908 to 2021. The thick ribbons denote the 90% credible intervals of the time series and the thick black lines are the median estimates.*

Appendix C – Supplementary materials for Chapter 4

Supplementary text

General additive model distributions

To choose the distributions of the generalized additive models (GAMs), we competed models with different distributions and chose the distributions that minimized the leave-one-out information criterion (*looic*). To model productivity, the model with a gamma distribution was a much better fit than a gaussian model (*looic* = 171.3 (± 23.6) and 238.9 (± 34.7), respectively). The abundance model specifying a negative binomial distribution had a lower *looic* value than the gaussian distribution (997.3 (± 19.3) and 1038.9 (± 27.8), respectively). The gamma distribution was a better fir than the gaussian model when modelling the change in standing stock biomass (*looic* = 1082 (± 25.5) and 1148 (± 38), respectively). To model species richness, the negative binomial model was indistinguishable from the gamma model based on *looic* (568.0 (± 11.1) and 569.3 (± 13.0), respectively), so we chose to use the negative binomial model based on its posterior predictive check.

Supplementary figures

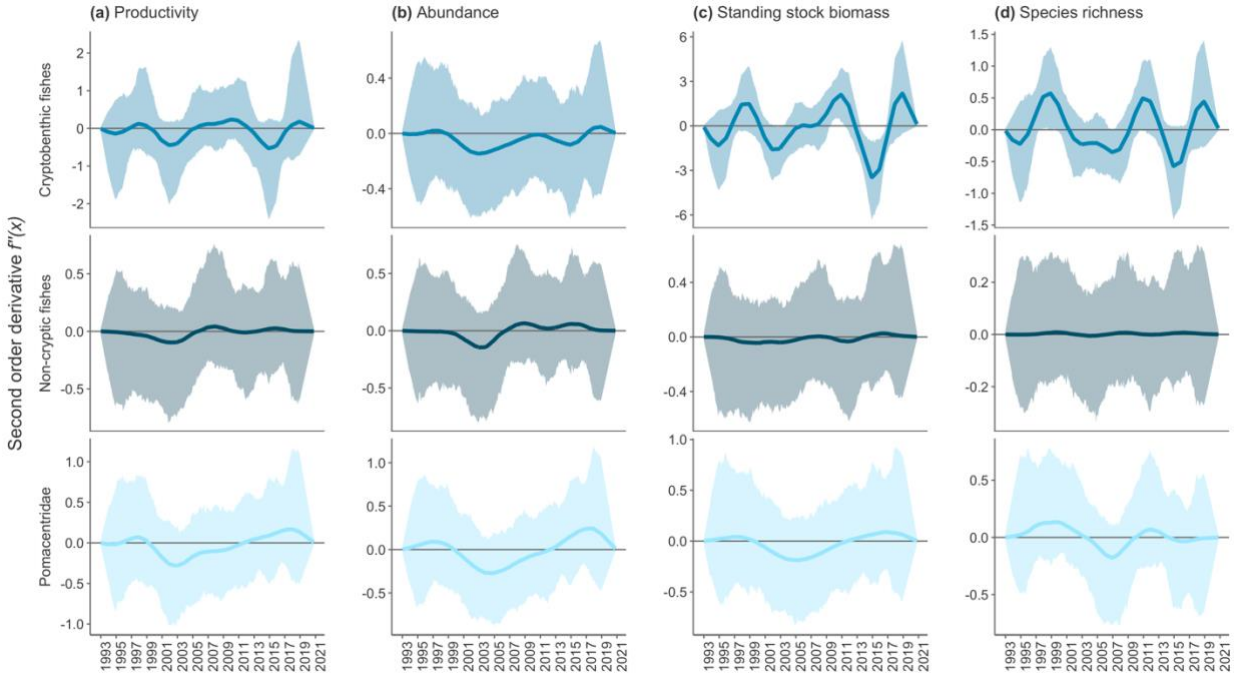

Figure C1. *Second order derivatives from the time series models for (a) productivity, (b) abundance, (c) standing stock biomass, and (d) species richness separated for cryptobenthic fishes (top, medium blue), non-cryptic fishes (middle; dark blue), and pomacentrids (bottom, light blue). The coloured ribbons denote the 95% credible intervals and the thick coloured lines denote the median trend lines.*

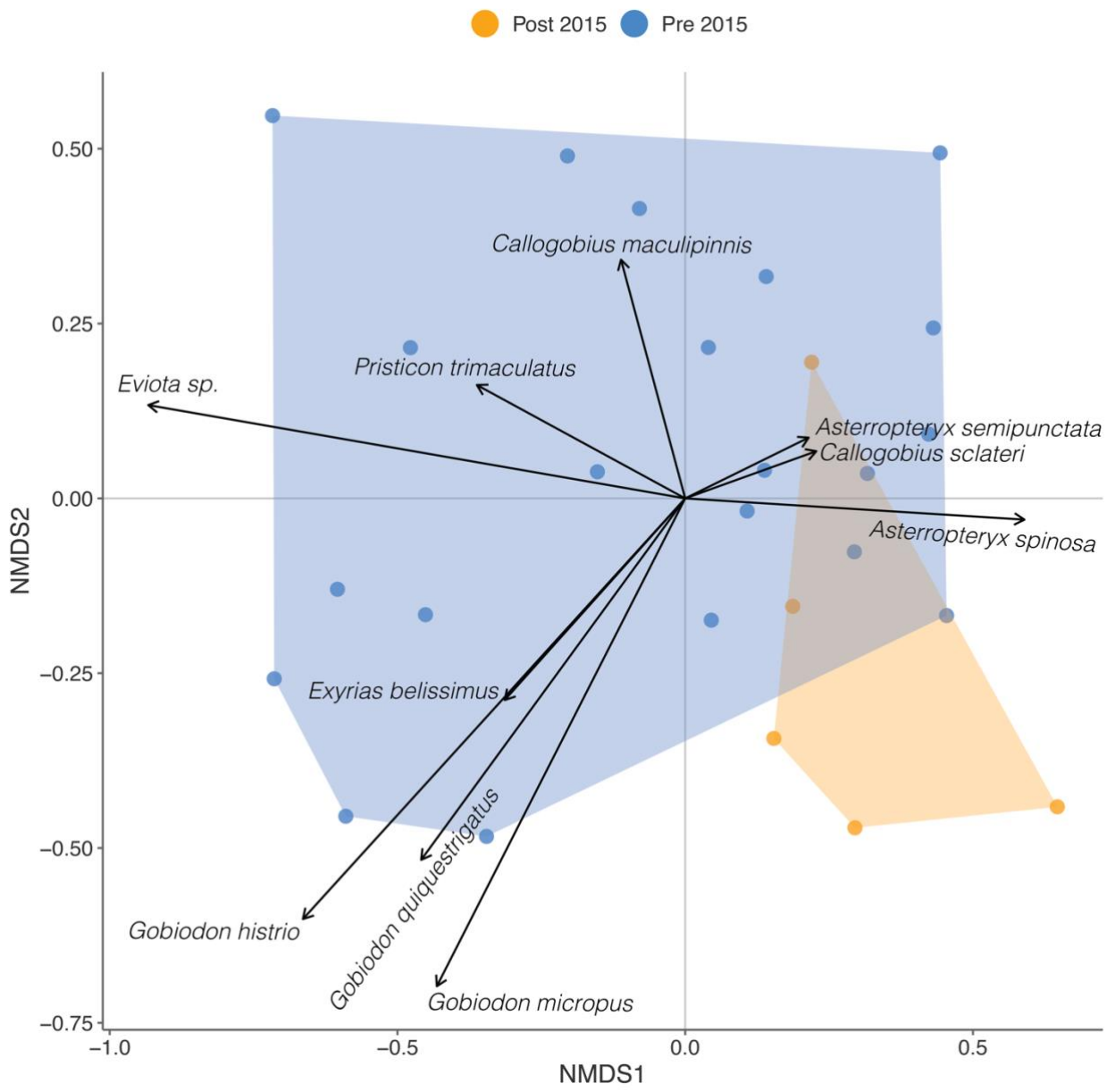

Figure C2. *Non-metric multidimensional scaling (NMDS) ordination of cryptobenthic fishes before (blue) and after (orange) the 2015 ecological threshold. Polygons depict convex hulls, which is the smallest polygon that encapsulates all points for a given sample period. Arrows and labels denote the magnitude and direction of the 10 most influential species from a SIMPER analysis.*

Appendix C

Supplementary tables

Table C1. Annual mean sea surface temperature taken from Pioneer Bay in Orpheus Island (18º35’35.412”S, 146º28’59.934”E) from 1993-2021 (excl. 2014, 2017, and 2020).

Year	Temperature (ºC)
1993	26.1
1994	25.9
1995	26.5
1996	26.7
1997	25.9
1998	27.3
1999	26.1
2000	25.9
2001	26.7
2002	26.6
2003	26.7
2004	26.4
2005	26.5
2006	26
2007	26.1
2008	26.1
2009	26.6
2010	26.8
2011	25.9
2012	26.1
2013	26.4
2015	26.7
2016	27.1
2018	26.3
2019	26
2021	26.9

Table C2. Summary of total length (cm) size distributions for subsampled fishes.

Family	Species	Minimum	Mean	Maximum
Apogonidae	*Apogon sp.*	2.1	3.4	4.8
	Apogon timaculatus	4	6.9	12.6
	Cheilodipterus quinquilineatus	5	5	5
Batrachoididae	*Halophryne diemensis*	7.2	7.4	7.7
Blenniidae	*Cirripectes sp.*	4.5	4.5	4.5
	Ecsenius mandibularis	3.4	4.2	5.1
Caesionidae	*Caesio cunning*	1.4	4.7	6.2
Chaetodontidae	*Chaetodon aureofasciatus*	1.9	5.5	9.1
Gobiidae	*Amblygobious rainfordi*	2.7	3.8	5.1
	Asteropteryx spinosa	2.5	3.1	3.6
	Bathygobious fuscus	2	2.4	2.9
	Callogobius macullipinnis	2.9	5	8.9
	Eviota melasma	1.9	2	2.2
	Eviota monostigma	1.7	1.8	2.1
	Eviota pellucida	2.4	2.4	2.4
	Eviota sp.	1.7	1.7	1.7
	Eviota zebrina	1.3	1.8	2.4
	Exyrias belissimus	6.2	6.8	7.5
	Gobiodon brochus	1.3	1.3	1.3
	Gobiodon micropus	1.9	2.9	3.3
	Gobiodon oculolineatus	2	2.7	3.1
	Gobiodon okinawae	2.2	2.2	2.2
	Gobiodon quinquestrigatus	1.1	2.6	3.5
	Gobiodon rivulatus	1.7	1.7	1.7
	Istigobius sp.	2.1	3	3.7
	Priolepis sp.	0.7	2	2.6
	Trimma capostriatum	1.8	2.3	2.6
	Trimma fangi	2.2	2.6	3.1
	Trimma lantana	2	2	2
	Trimma sp.	1.8	2.5	3.1
Holocentridae	*Myripristis murdjan*	4.4	12.2	17.5
	Sargocentron cornutum	13.8	13.8	13.8
Labridae	*Cheilinus fasciatus*	1.9	3.9	10.6
	Halichoeres melanurus	2.1	2.9	3.8
	Scarus ghobban	6.9	6.9	6.9
	Scarus rivulatus	3.1	3.2	3.2
	Thalassoma lunare	3	3	3
Muraenidae	*Echidna polyzona*	25.1	25.1	25.1
	Gymnothorax sp.	16	16	16
Platycephalidae	*Platycephalidae sp.*	2.8	2.8	2.8
Pomacentridae	*Amblyglyphidodon curacao*	11	11	11
	Chrysiptera rollandi	3.4	4.1	4.7
	Neopomacentrus azysron	3.2	4.8	6.2
	Neopomacentrus bankieri	1.5	3.8	33.3
	Pomacentrus adelus	4.9	5.9	7

	Pomacentrus brachialis	2.5	5.9	8.9
	Pomacentrus moluccensis	2.3	3.8	6
	Pomacentrus wardi	3.9	6.4	8.7
Pseudochromidae	*Psuedochromis wilsoni*	1.6	3.6	4.9
Serranidae	*Cephalopholis boenak*	2.6	6	17.4
Tripterygiidae	*Enneapterygius sp.*	2.4	2.5	2.6
	Heliogramma sp.	4.5	4.5	4.5

Appendix D – Supplementary materials for Chapter 5

Supplementary figures

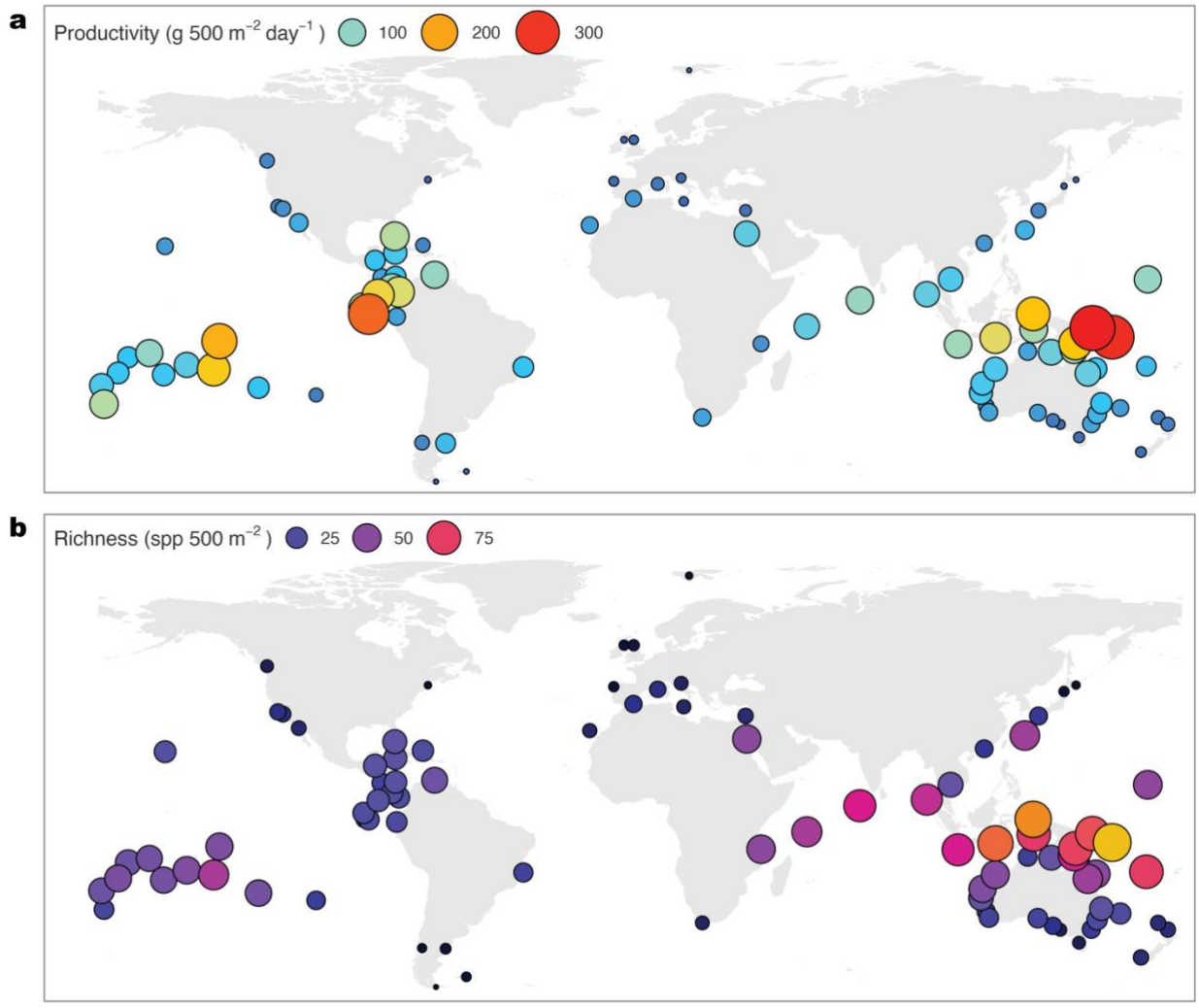

Figure D1. Global patterns of marine fish productivity and richness. a *Fish biomass production (g 500 m^{-2} day^{-1}) of all surveyed marine teleost fishes whereby the size and colour of the points denote the magnitude of productivity.* ***b*** *Global distribution of species richness (number of species per 500 m^{-2}); the points are sized and coloured based on the number of species per survey. Each point is the median value per ecoregion.*

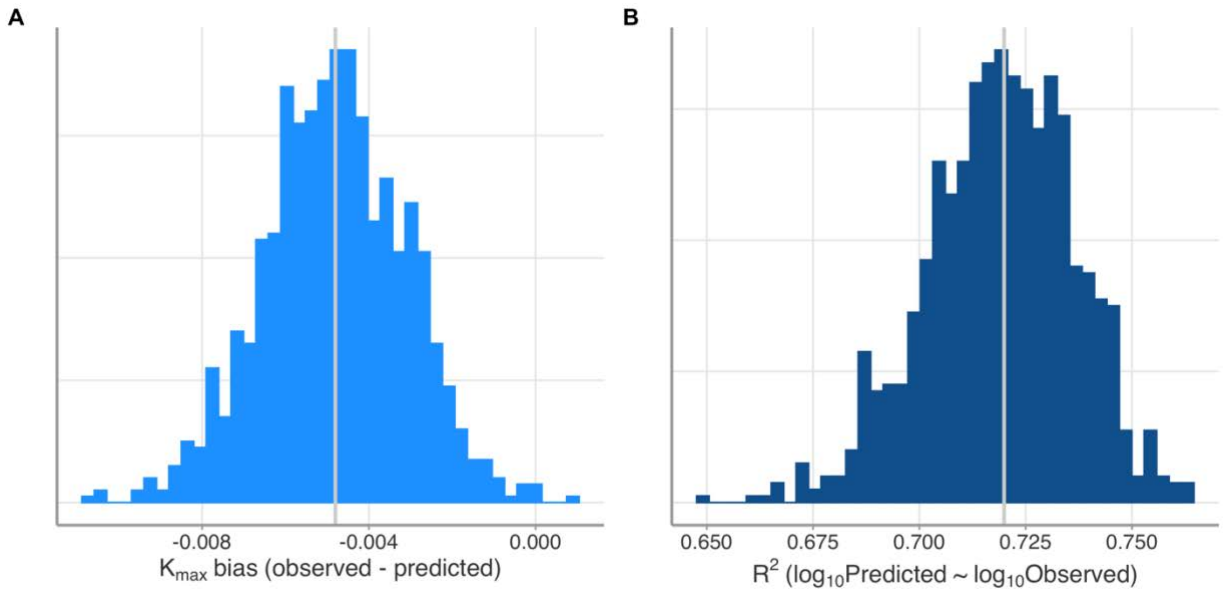

Figure D2. Boosted regression tree diagnostics. A *Prediction biases of K_{max} values across 1,000 bootstrapped iterations. Bias was calculated by subtracting the predicted values from the observed values.* ***B*** *The predicted R^2 value by fitting the log_{10}Predicted values from the log_{10}Observed values.*

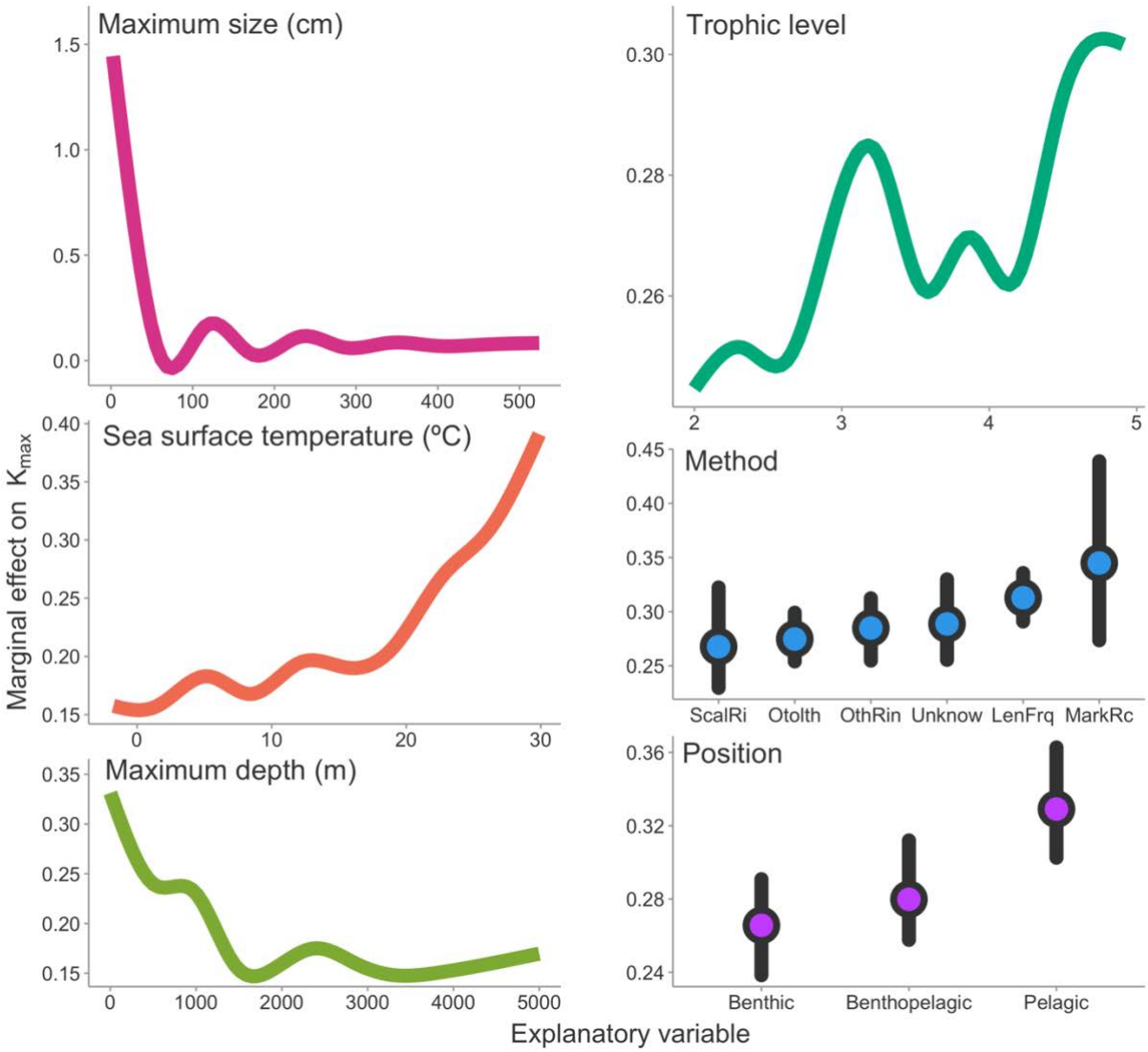

Figure D3. Predictors of fish growth. *Partial dependence plots showing the effects of maximum body size (cm), sea surface temperature (°C), maximum depth (m), trophic level, aging method, and position in the water column on K_{max} from 1,000 bootstrapped boosted regression tree models. ScalRi = scale rings, Otolth = otoliths, OthRin = other rings, Unknow = unknown, LenFrq = length frequency, MarkRc = mark recapture.*

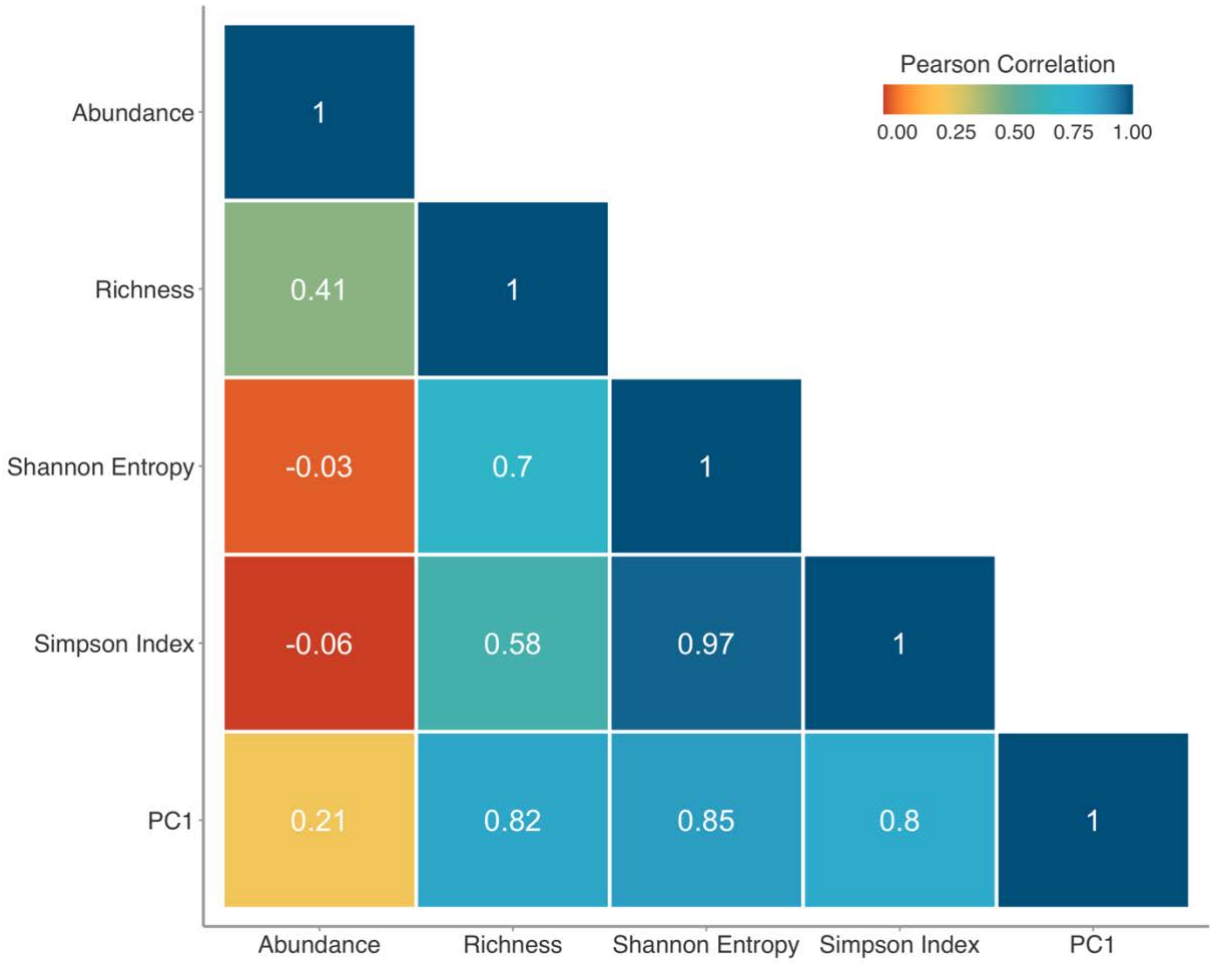

Figure D4. *Correlation heatmap of different Hill diversity metrics with principal component axis 1 (PC1, as seen in* ***Fig. 5-1a****). Tiles in red/orange denote negative correlations, while cooler colours denote positive correlations.*

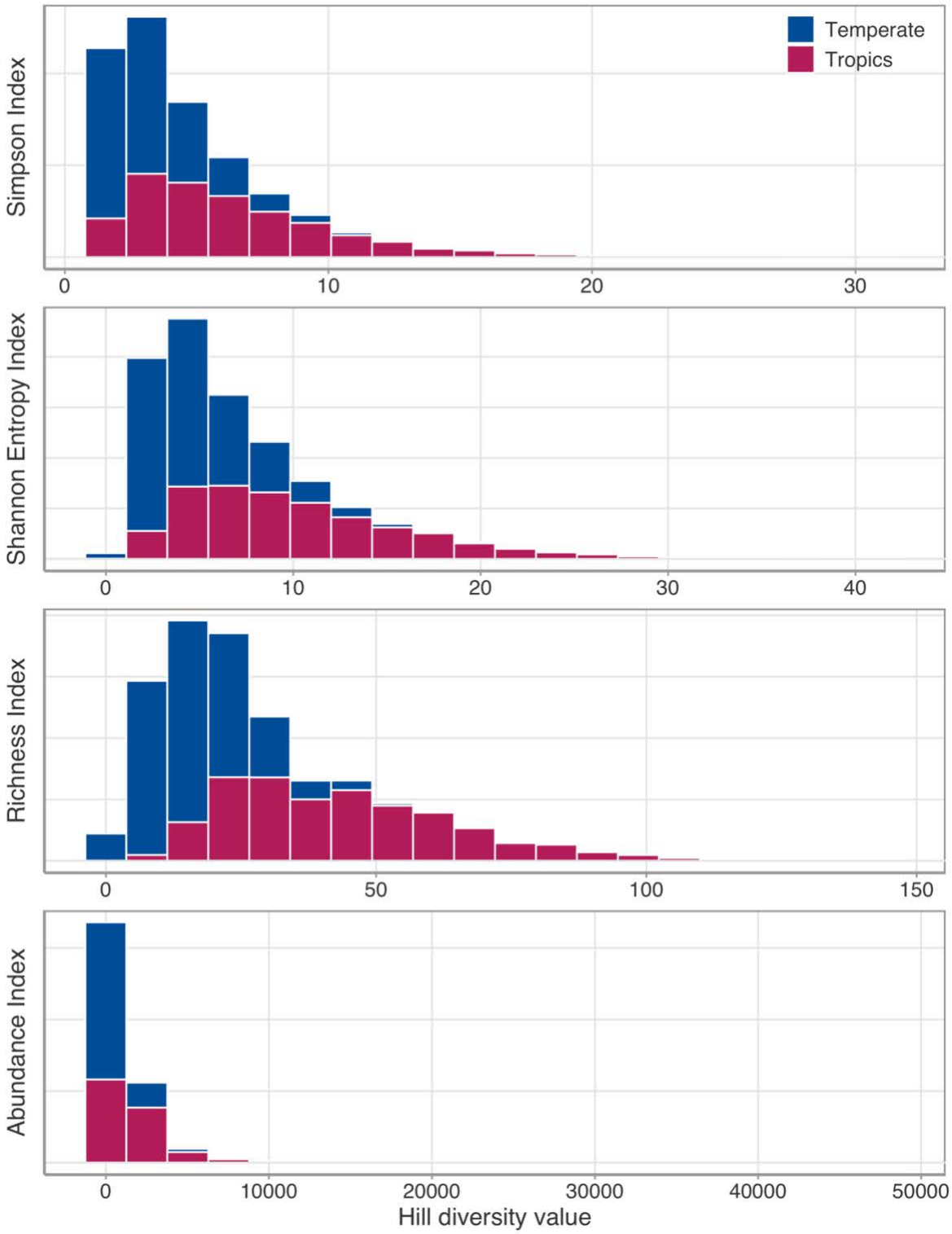

Figure D5. Hill diversity gradients across geographic regions. *Simpson Index (ℓ = -1), Shannon Entropy Index (ℓ = 0), richness index (ℓ = 1), and abundance index (ℓ = 10) gradients across temperate (blue) and tropical (red) locations. All diversity indices were logged prior to model fitting.*

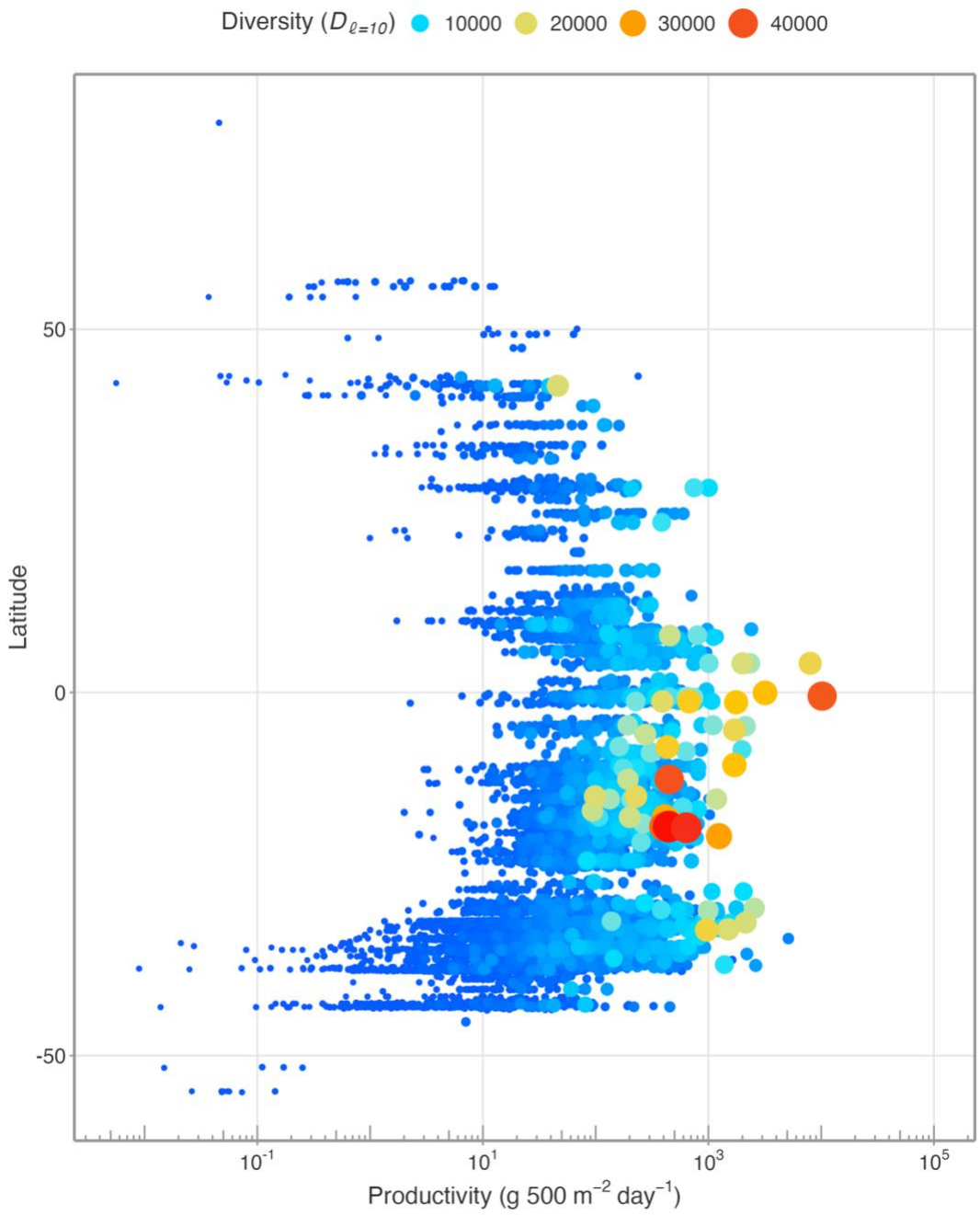

Figure D6. Latitudinal patterns of reef fish productivity. *Patterns of fish productivity (g 500m^{-2} day^{-1}) across latitudinal gradients. Points are sized and coloured based on their respective Hill diversity values emphasising abundance effects. Note the x axis is on the log$_{10}$ scale.*

Appendix D

Supplementary tables

Table D1. Variable importance (%) of explanatory variables used to predict K_{max} across fishes shown as the median, minimum, and maximum across 1,000 bootstrapped models.

Variable	Median	Minimum	Maximum
Maximum body size	43.1	38.8	47.5
Sea surface temperature	21.1	18.5	23.8
Maximum depth	14.6	12.5	17.5
Trophic level	12.1	10.2	13.9
Aging method	5.3	4.1	6.8
Position in the water column	3.7	3.0	4.9

Table D2. Estimated fixed effects from model outputs of the regional BEF testing different Hill diversity metrics (D_ℓ) and per-capita biomass production generalised linear mixed effects model (region = temperate or tropical). Coefficient estimates are shown as the median of the posterior distribution; lower and upper refer to the bounds of the 90% credible intervals (CI). Leave-one-out information criterion (*looic* ± standard error) is shown in parentheses for competing BEF models using different Hill diversity metrics. ESS = bulk effective sample size.

Coefficients	Estimate	Lower CI	Upper CI	ESS
BEF with abundance index (89533.3 ± 351.7)				
Intercept	3.99	3.56	4.39	2295
Log ($D_{\ell = 10}$)	1.08	1.06	1.10	4685
Tropics	-0.43	-0.98	-0.15	2286
Tropics * log ($D_{\ell = 10}$)	0.074	0.033	0.11	4616
Sea surface temperature	0.21	0.17	0.25	2508
Visibility	0.060	0.039	0.080	3881
Depth	0.025	0.0093	0.041	4535
BEF with richness index (93866.9 ± 356.2)				
Intercept	4.46	3.95	4.97	2002
Log ($D_{\ell = 1}$)	1.08	1.04	1.12	4009
Tropics	-0.81	-1.42	-0.13	2268
Tropics * log ($D_{\ell = 1}$)	-0.11	-0.18	-0.045	3193
Sea surface temperature	0.25	0.19	0.30	2176
Visibility	0.042	0.016	0.071	3782
Depth	0.077	0.058	0.098	4406
BEF with exponentiated Shannon entropy (95849.4 ± 328.7)				
Intercept	4.06	3.75	4.37	2442
Log ($D_{\ell = 0}$)	-0.088	-0.12	-0.055	4032
Tropics	-0.66	-1.09	-0.21	2698
Tropics * log ($D_{\ell = 0}$)	-0.040	-0.087	0.0093	3540
Sea surface temperature	1.04	0.99	1.10	1805
Visibility	0.14	0.11	0.17	3318
Depth	0.082	0.058	0.11	3932
BEF with inverse Simpson Index (95852.8 ± 328.9)				
Intercept	4.05	3.73	4.36	2667
Log ($D_{\ell = -1}$)	-0.11	-0.13	-0.075	5114

Tropics	-0.66	-1.08	-0.22	3033
Tropics * log ($D_{\ell = -1}$)	-0.0088	-0.050	0.038	4581
Sea surface temperature	1.04	0.98	1.10	2210
Visibility	0.14	0.11	0.17	4433
Depth	0.084	0.061	0.11	4759
Per-capita model with abundance index				
Intercept	-3.16	-3.47	-2.88	2829
Log ($D_{\ell = 10}$)	-0.33	-0.35	-0.31	4763
Tropics	-0.18	-0.57	0.24	2825
Tropics * log ($D_{\ell = 10}$)	-0.080	-0.12	-0.041	4657
Sea surface temperature	0.23	0.18	0.27	2472
Visibility	0.063	0.042	0.083	4602
Depth	0.022	0.0062	0.037	4954
Abundance model with abundance index				
Intercept	7.15	6.87	7.43	2828
Log ($D_{\ell = 10}$)	1.42	1.41	1.43	5597
Tropics	-0.24	-0.63	0.15	3052
Tropics * log ($D_{\ell = 10}$)	0.14	0.13	0.16	3052
Sea surface temperature	-0.037	-0.055	-0.019	2147
Visibility	-0.0060	-0.015	0.0027	3900
Depth	-0.0018	-0.0083	0.0043	5583
BEF with abundance index and Boltzmann temperature				
Intercept	3.99	3.55	4.41	2501
Log ($D_{\ell = 10}$)	1.08	1.06	1.10	5076
Tropics	-0.44	-0.98	0.17	2381
Tropics * log ($D_{\ell = 10}$)	0.075	0.035	0.12	4546
Boltzmann temperature	-0.22	-0.26	-0.17	2574
Visibility	0.059	0.038	0.081	4538
Depth	0.025	0.0082	0.041	4810

Table D3. Principal Component Analysis (PCA) results showing the loadings of the inverted Simpson Index, exponentiated Shannon entropy, richness effects, and abundance effects on all four principal components. The proportion of variation explained by each axis is denoted in the parentheses.

Dimension	**PC1** (68.4%)	**PC2** (28.9%)	**PC3** (2.5%)	**PC4** (0.3%)
Simpson Index	0.52	-0.45	-0.45	-0.57
Shannon Index	0.56	-0.36	0.05	0.75
Richness	0.55	0.32	0.71	-0.3
Abundance	0.34	0.76	-0.54	0.14

Appendix E – Supplementary materials for Chapter 6

Supplementary figures

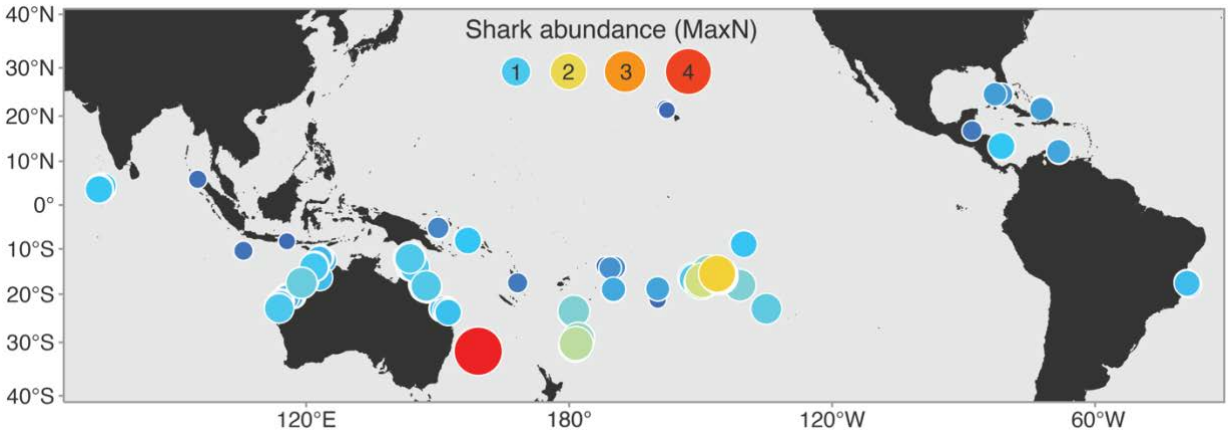

Figure E1. Relative shark abundance across sites. *Shark abundance (MaxN; see methods) across all sites using the 50km buffer size. The colour and the size of the points denote MaxN values.*

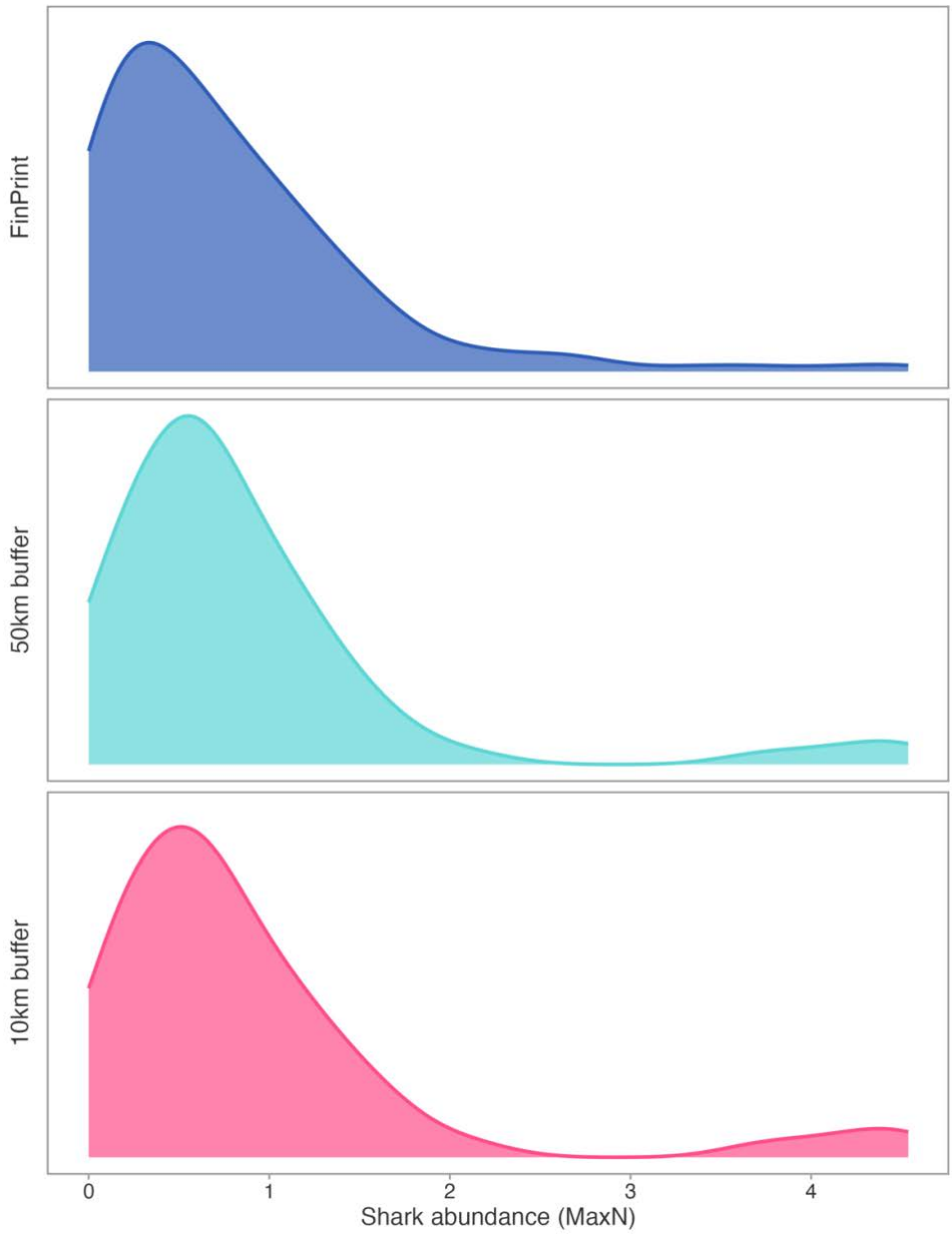

Figure E2. Shark abundances across different buffer sizes. *Shark abundance densities across the entire FinPrint dataset (top, dark blue), using 50km buffers (middle, light blue), and 10km buffers (bottom, pink).*

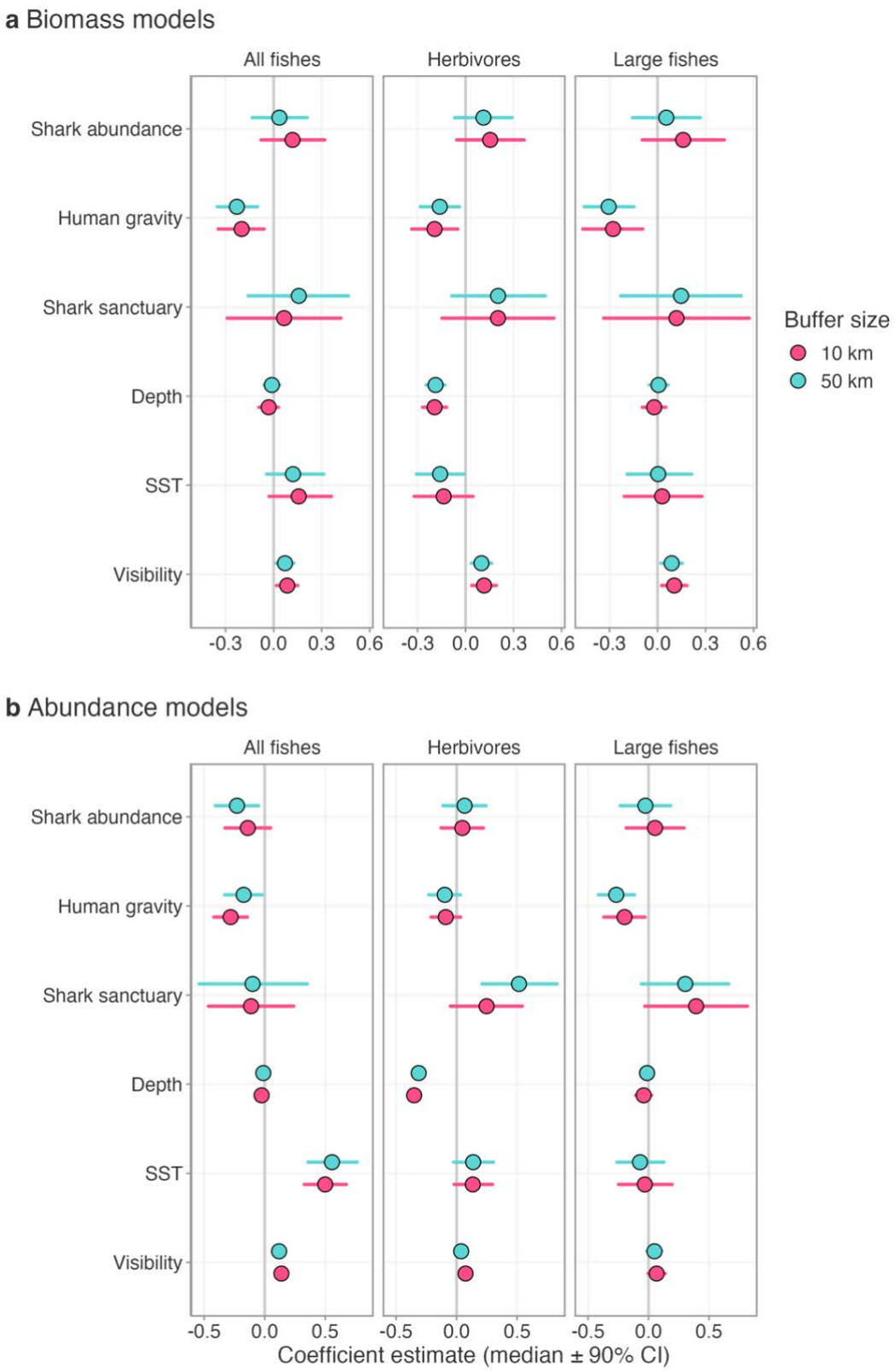

Figure E3. Biomass and abundance models using different buffer sizes. *Modelled coefficients from spatially explicit Bayesian generalised linear mixed-effects models for* ***a*** *standing biomass and* ***b*** *abundance for all fishes (left), herbivores (middle), and large fishes (right). Models using the 10km and 50km buffers are shown in pink and blue, respectively. Points indicate the median and whiskers are the 90% credible intervals. SST = sea surface temperature.*

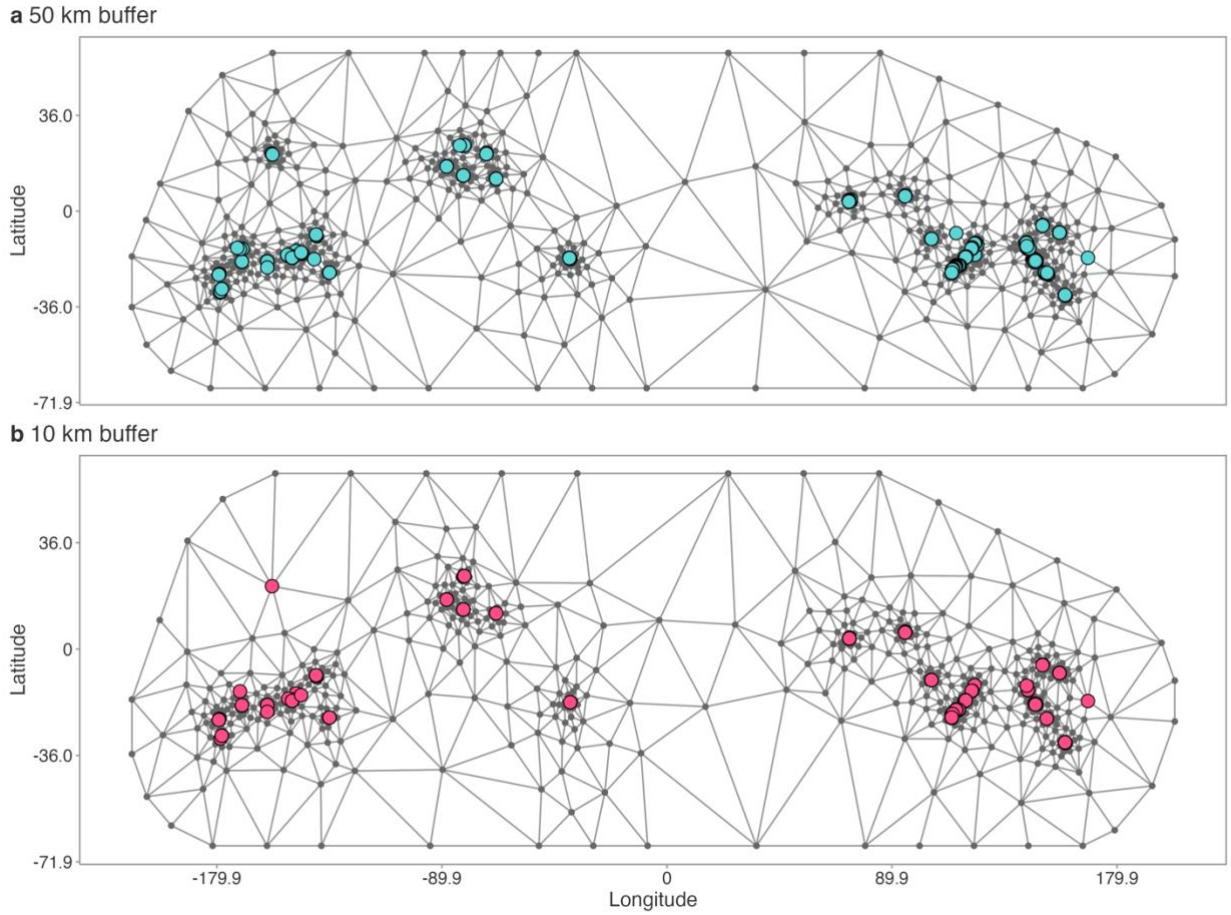

Figure E4. Triangulated meshes used in Bayesian geostatistical generalised linear mixed-effects models. *Meshes used to calculate solutions to the SPDEs for all INLA models using* ***a*** *the 50km buffer and* ***b*** *the 10km buffer. Coloured points in both plots represent the sites.*

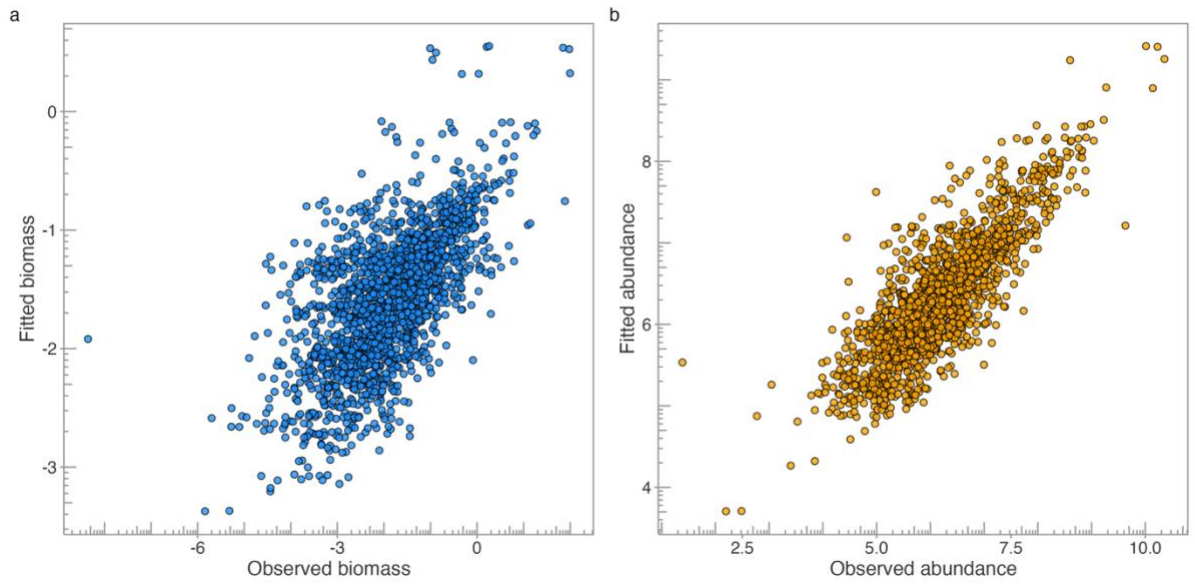

Figure E5. Model performance of standing biomass and abundance. a *Fitted standing biomass against observed biomass and* ***b*** *fitted abundance against observed abundance of the entire community from spatially explicit generalised linear mixed-effects models using the 50 km buffer size. Each point is an observation and note both plots are on the double-log axis.*

Appendix E

Supplementary tables

Table E1. Coefficients and posterior probabilities from INLA models using a 50km buffer. The estimate refers to the median coefficient estimate with its respective lower and upper 90% credible interval (CI). The columns p(β) indicates the posterior probability of a negative (< 0) or positive (> 0) effect (shown as %).

Coefficient	Estimate	Lower CI	Upper CI	p(β) < 0	p(β > 0)
Standing biomass of all fishes					
Intercept	-1.45	-1.66	-1.27	100	0
ln Human gravity	-0.23	-0.35	-0.10	99.8	0.20
ln Shark abundance	0.036	-0.13	0.21	37.7	62.3
Shark sanctuary	0.16	-0.16	0.47	21.0	79.0
Depth	-0.011	-0.062	0.039	65.7	34.3
Sea surface temperature	0.12	-0.045	0.31	11.1	88.9
Visibility	0.072	0.015	0.13	2.2	97.8
Standing biomass of large fishes					
Intercept	-1.76	-1.99	-1.54	100	0
ln Human gravity	-0.31	-0.46	-0.15	100	0
ln Shark abundance	0.055	-0.16	0.27	33.3	66.7
Shark sanctuary	0.15	-0.23	0.52	23.2	76.8
Depth	0.0065	-0.053	0.066	43.2	56.8
Sea surface temperature	0.0042	-0.19	0.21	48.8	51.2
Visibility	0.088	0.021	0.16	1.60	98.4
Standing biomass of herbivorous fishes					
Intercept	-2.36	-2.51	-2.22	100	0
ln Human gravity	-0.16	-0.28	-0.037	98.3	1.70
ln Shark abundance	0.11	-0.068	0.29	14.8	85.2
Shark sanctuary	0.20	-0.087	0.50	12.3	87.7
Depth	-0.19	-0.25	-0.13	100	0
Sea surface temperature	-0.16	-0.31	-0.0086	95.9	4.10
Visibility	0.099	0.035	0.16	0.80	99.2
Abundance of all fishes					
Intercept	6.27	5.97	6.56	0	100
ln Human gravity	-0.17	-0.33	-0.020	96.5	3.50
ln Shark abundance	-0.23	-0.41	-0.051	98.4	1.60
Shark sanctuary	-0.10	-0.54	0.35	63.8	36.2
Depth	-0.011	-0.049	0.026	71.2	28.8
Sea surface temperature	0.56	0.36	0.77	100	0
Visibility	0.12	0.077	0.16	100	0
Abundance of large fishes					
Intercept	3.92	3.70	4.14	0	100
ln Human gravity	-0.27	-0.42	-0.12	99.9	0.10
ln Shark abundance	-0.026	-0.24	0.18	59.7	40.3
Shark sanctuary	0.30	-0.060	0.66	9.60	90.4
Depth	-0.012	-0.066	0.042	63.5	36.5

Sea surface temperature	-0.070	-0.26	0.13	72.5	27.5
Visibility	0.049	-0.012	0.11	10.1	89.9
Abundance of herbivorous fishes					
Intercept	4.54	4.34	4.72	0	100
ln Human gravity	-0.098	-0.23	0.033	88.5	11.5
ln Shark abundance	0.066	-0.11	0.24	26.5	73.5
Shark sanctuary	0.52	0.21	0.83	0.20	99.8
Depth	-0.31	-0.35	-0.28	100	0
Sea surface temperature	0.14	-0.024	0.31	7.20	92.8
Visibility	0.038	-0.0057	0.081	6.70	93.3
Body size of all fishes					
Intercept	2.56	2.51	2.61	0	100
ln Human gravity	-0.022	-0.052	0.0076	89.1	10.9
ln Shark abundance	0.020	-0.018	0.058	20.7	79.3
Shark sanctuary	0.079	-0.0024	0.16	4.9	95.1
Depth	0.023	0.013	0.033	0	100
Sea surface temperature	-0.042	-0.085	0.0037	92.8	7.2
Visibility	0.0081	-0.0028	0.019	10.5	89.5
Body size of large fishes					
Intercept	3.27	3.22	3.31	0	100
ln Human gravity	-0.018	-0.041	0.0047	90.2	9.8
ln Shark abundance	0.011	-0.018	0.039	26.2	73.8
Shark sanctuary	0.087	0.014	0.17	2.3	97.7
Depth	0.010	0.0013	0.019	3.6	96.4
Sea surface temperature	-0.020	-0.057	0.016	81.4	18.6
Visibility	0.010	-0.000040	0.020	4.7	95.3
Body size of herbivorous fishes					
Intercept	2.69	2.63	2.76	0	100
ln Human gravity	0.0042	-0.038	0.049	43.8	56.2
ln Shark abundance	0.044	-0.015	0.11	11.1	88.9
Shark sanctuary	0.030	-0.080	0.14	34.2	65.8
Depth	0.018	0.0036	0.031	2.0	98.0
Sea surface temperature	-0.024	-0.081	0.039	75.7	24.3
Visibility	0.020	0.0036	0.035	2.4	97.6

Fin.